University of Stavanger

Faculty of Science and Technology

MASTER'S THESIS

Study program/ Specialization: Master's Degree Program in Mechanical and Structural Engineering – Civil Engineering	Spring semester, 2011 Open
Writer: Ragnhild Opsahl Steigen	Ragnhild Opsahl Steigen (Writer's signature)
Faculty supervisor: Jasna Bogunovic Jakobsen External supervisor: Roger Guldvik Ebeltoft	
Title of thesis: Modeling and analyzing a suspension bridge in light of deterioration of the main cable wires	
Credits (ECTS): 30	
Key words: Suspension bridge Steel bridge Eigen value analysis Structural engineering	Pages: 89 + enclosure: 101 Stavanger, 14/6-2011 Date/year

Modeling and analyzing a suspension bridge in light of deterioration of the main cable wires

Ragnhild Opsahl Steigen

Master thesis in structural and material engineering

University of Stavanger, spring 2011

Preface

The master thesis is the final part of my Master degree in structural and material science at the University of Stavanger. The thesis consists of collecting and studying data for Lysefjord Bridge in light of the deterioration of the main cables, and to carry out some analysis for the bridge. Data is given from The Norwegian Public Roads Administration (Statens Vegvesen).

The data is used to make a finite element model (FEM) of the bridge in ABAQUS. The model is analyzed with emphasis on eigen frequencies and mode shapes. A brief analysis of the bridge behavior during wind loading is also carried out.

The wire fractures observed in the main cables are summarized and analyzed with respect to the weather conditions in the area in a period with many wire fractures. Data on the weather in the area is given from Lysefjord Weather Station, that was contacted during the work with this thesis.

The thesis consists of;

- a presentation of the static and dynamic characteristics of a suspension bridge
- a summary of the wire fractures in the main cables on Lysefjord Bridge
- a weather analysis for periods with many wire fractures
- the modeling of a finite element model in ABAQUS
- an eigen value analysis and a brief wind analysis of the finite element model in ABAQUS
- a verification of the finite element model in ABAQUS by theoretical calculations

Thanks to the thesis supervisor at University of Stavanger, Jasna Bogunovic Jakobsen, and to Ove Mikkelsen for help with building the finite element model in ABAQUS. I also want to thank Roger Guldvik Ebeltoft in The Norwegian Public Roads Administration for information around the problem, and Per Slyngstad, also in The Norwegian Public Roads Administration, for results of the bridge model and analysis in Alvsat, and for the information used to build the model of the bridge in ABAQUS. Thanks also to Ole Tom Guse in Lysefjord Weather station for data on the weather near Lysefjord Bridge.

Contents

List of Figures

List of Tables

Abstract

Lysefjord Suspension Bridge, with a main span of 446 meters, has had problems with wire fractures in the main cables. This is reducing the durability of the bridge. Since the opening of the bridge in December 1997, over 1400 outer wire fractures have been detected. No clear reason for the failure has been found, but some material defects in the wires could be part of the reason. If the wires continue to fracture with the same rate as today, the main cables have to be maintained more often, and maybe changed much earlier than they were planned for in the beginning. Therefore, the bridge should be further analyzed, to detect any other reasons for the wire fractures, and to determine how and when the main cables should be maintained or changed.

A new finite element model is created in ABAQUS, and an eigen value analysis of the bridge model is carried out. A brief analysis of the fractures in light of the weather around the bridge is given. The main components of a suspension bridge is described, and analytical calculations are done based on equations from Bleich and Steinman to verify the results from ABAQUS and Alvsat. The bridge behavior during wind loading was briefly checked, and the displacement from wind load, from a 50 year wind speed, on the bridge has been examined. The loading from this wind speed, with coefficients that take into account different angles of the bridge girder, has been created in ABAQUS, through several iterations.

The eigenfrequency analysis done in ABAQUS and the analytical calculations give results that are in the same range as the ones from the original analysis done in Alvsat. The results from the analysis of the weather around the bridge in a period with many wire fractures indicates that after a sudden drop in temperature, many wire fractures occur. The critical wind velocity in regard to vortex induced vibrations is 7.5 m/s for the first vertical symmetric mode, this is a wind speed that can occur around the bridge, and fatigue in the wires could be a part of the reason for the cable fractures. The demand/capacity rate for the main cables with dead load is 25.2%. The results from this work can be used when deciding what to emphasize in further analysis of Lysefjord Bridge.

Chapter 1

Introduction

Lysefjord Bridge is a suspension bridge with a total length of 637 m. The main span is 446 m, and the two side spans are 34.5 m and 156.5 m. The bridge is localized on Rd. 13 crossing Lysefjorden between Forsand and Oanes in Rogaland. The bridge was opened in December 18th 1997. There has been observed a number of wire fractures in the main cables of the bridge, and therefore, an updated analysis of the bridge will have to be carried out. In the work with this report, data from the original analysis, data from the observations of the wire fractures in the bridge and data from a weather station in the area around the bridge have been collected as a beginning of this new analysis. The bridge is modeled in a finite element program, ABAQUS, and the model can be employed for further analysis of the bridge under various load conditions. The new model is based on the same parameters as the old model, and on figures and details from The Norwegian Public Roads Administration. The ABAQUS model of Hardanger Suspension Bridge, created by Aleksander Kyte for The Norwegian Public Roads Administration, was available for the present study and was used as a basis for developing a similar model for Lysefjord Bridge.

A part of the thesis was to get familiar with the load carrying characteristics of a suspension bridge under static loading, and dynamical behavior through eigenfrequencies and modes of vibration. The eigen frequencies and modes in the new finite element model are analyzed, and to understand the effect of changing key parameters, some tests without the towers, and with a shear center modeled 0.704 m above the neutral axis is carried out. Some of the frequencies found differed relatively much with the results from Alvsat, and one reason could be the asymmetry in the model in ABAQUS reflecting difference in the bridge girder elevation at the two towers. This was investigated with a symmetric bridge configuration without towers. To understand and validate the calculations done by Alvsat and ABAQUS, some frequencies and modes were theoretically calculated based on simplified equations from Bleich and Steinman.

The bridge cables have been inspected visually since the opening in 1997. To have more accurate observations, the bridge has been monitored with an acoustic monitoring system since late 2009, and the wire fractures detected of the system are presented in chapter three. Wind speed and temperature data from a weather station close to the bridge is analyzed and connected to the periods with many wire fractures. Even with only one and a half year of monitoring, it can be seen that there are far more fractures in the winter than in the summer. The results also shows that after a sudden drop in the temperature late

December 2009, many wire fractures occurred. A comparison to December 2010 shows that when the weather is cold but steady, far less wire fractures occur. The monitoring system is important in the further analysis of the bridge, and after a few more years with monitoring data, it is expected to increase the understanding of the wire fracture occurrence.

Chapter four shows the modeling of a finite element model of Lysefjord Bridge in ABAQUS step by step. Since the bridge was built over ten years ago, it has not been so straight forward to collect all the input data needed for the model, like the weight and rigidity of the bridge girder alone. Possible errors from this lack of information are discussed in chapter four. The input used in the original analysis done in Alvsat is used in the finite element model in ABAQUS. The model is created so that further analyses of the effect of wind and other loads can be carried out later.

In chapter five, the geometry of the model when dead load is taken into consideration, is discussed. It is important for the analysis that the length of the main span, the sag of the main cables and the rest of the geometry are as close to the real bridge as possible. The vertical displacement in the bridge girder due to dead load is almost 3 m. To perform a brief wind analysis of the bridge for the 50 year wind speed in the area, wind loading is calculated to be 38 m/s, the same as in the original analysis. This loading, with form factors taken from the input file in Alvsat, is applied to the model in ABAQUS. The intention was to use a subroutine in Fortran to simulate the wind load, but after several attempts, the wind load is calculated by hand and applied directly in the input file. Five iterations were done to find the true wind force at the correct angle. The displacement in node 19, the center of the bridge girder, with a force from 38 m/s applied, is 0.86 m in horizontal direction, and the girder is lifted up 0.056 m in vertical direction from the equilibrium with the dead load. The bridge girder is rotated with an angle of 0.3° in the center node.

A brief analysis with the finite element model is done in chapter six. The eigen frequencies and the mode shapes of the bridge, and displacement from 50 years wind speed are found. The frequencies and the mode shapes found from the analysis are close to the ones found from the previous analysis in Alvsat. As an example, the vertical and horizontal frequencies have in general less than 2% difference, and a maximum difference of 6% in the first vertical symmetric mode. There is however some differences, for example in the torsion frequencies, where the differences are between 10% and 23%. The reason for this is discussed in chapter six.

To control the results from ABAQUS, theoretical calculations of a few eigen frequencies and mode shapes are done in chapter seven, with a satisfying result. The maximum difference in the results compared to Alvsat, except for the first vertical frequency with a difference of 12%, is 4%. Compared to ABAQUS, the difference in first vertical frequency is 17%, while the maximum difference of the rest of the results are 6% in vertical direction, and between 14% and 25% for the torsion frequencies. The theory used is from Bleich and Steinman, but the equations are simplified and fit to Lysefjord Bridge. The theoretical calculations should be done more accurately if they were to be used alone, without any finite element model analysis.

Chapter 2

Suspension bridges

The suspension bridge is a type of cable supported bridges. Suspension bridges are lighter per unit length than any other type of bridge form and they dominate the genre of long span bridges. In Norway, there are around 200 suspension bridges in different shapes and lengths. Norwegian engineers are known to master the aerodynamic challenges associated with long, narrow suspension bridges that rarely exceed two traffic lanes in width. The first recorded suspension bridge built in Norway, was the Bakke Bridge in Vest-Agder, built in 1842, and it remained standing for a 110 years after its opening in 1844 [24]. When the cable wire improved after 1900, suspension bridges became more common, and their size increased too. Atna Bridge, a truss-stiffened bridge, opened over Glomma River in 1923, and it spanned 150 m. The most famous suspension bridge in Norway at this time is Hardanger Bridge that currently is during construction. The bridge will be the longest suspension bridge in Norway, with a main span of 1310 m and a total length of 1380 m.

The structural system of a cable supported bridge consists of [9];

- Towers supporting the cable system
- Main cables supporting the stiffening girder
- Anchor bolts supporting the cable system vertically and horizontally at the extreme ends
- Hanger cables connecting the stiffening girder to the main cable
- Stiffening girder with bridge deck

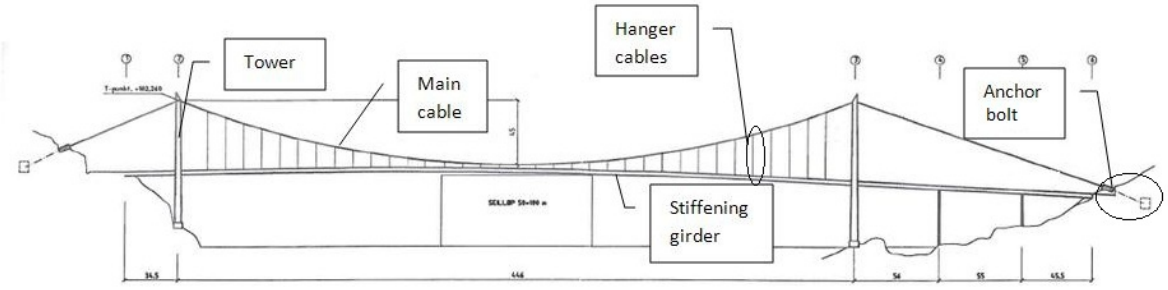

Figure 2.1: The main components of a suspension bridge shown on Lysefjord Bridge [7]

As can be seen in Figure 2.1 on the preceding page, the stiffening girder with the bridge deck is supported by two or more main cables with hanger cables attached regularly along the span. The main cables are hanging between the towers, and there are anchor bolts in each far end of the bridge where the main cables are fixed. An example of a suspension bridge is shown in figure 2.2. Akashi Kaikyo Bridge, also known as the Pearl Bridge in Japan, which opened in 1998, is the world's longest suspension bridge. The main span is 1991 m, and the towers are 288 m tall [6].

Figure 2.2: Akashi Kaikyo Bridge is the world's longest suspension bridge [6]

2.1 Stiffening girder

The stiffening girder main function is stiffening the roadway structure and carrying the traffic loading on the bridge. Large deformations caused by concentrated loads from e.g. one heavy trailer crossing the bridge are therefore avoided. The bridge girder is the element in the suspension bridge that will receive most of the external loading on the bridge. This loading will as mentioned come from traffic, wind and snow. The traffic and snow load will act directly on the top of the bridge girder, and as long as the bridge girder is rigid enough, it can take the concentrated loading from traffic. The wind exposed area is most commonly greater for the bridge girder than for the main cables.

To describe the general shape of the stiffening girder today, the collapse of Tacoma Narrows Bridge and the change in engineering practice that followed will be introduced in the following.

Tacoma Narrows Bridge had a main span of 853 m, and was at the time the third longest bridge in the world. It was called "Galloping Gertie"' due to its vertical rhythmic motion of the narrow two-lane solid plate girder immediately after the completion. This motion was not considered dangerous, and during the fatal day of November 7th 1940, some motion was expected. This day in November, the wind speed in the morning was around 18 m/s, and large vertical motion could be observed. After a while, the motion changed, and was dominated by an asymmetric torsion. The bridge survived this motion for about

one hour, but its lateral bracing system and some hangers was damaged, and collapse was inevitable [29].

Tacoma Narrows Bridge collapsed due to large forces caused by wind. It was the unfavorable shape of the girder combined with large slenderness, span to with ratio, which allowed this large dynamical vibration. The stiffening plate girder had sharp edges that caused the wind to make large curls above and under the plate that induced large dynamic torsion forces in the bridge. These curls became even stronger as the bridge started to twist, and this unfavorable interaction between the bridge motion and the airflow led to the bridge destruction. The bridge was built for a static force of 160 km/hr, but it collapsed at a much lower wind force [24, 9].

The bridge girder widely used today is narrow, like the one in Tacoma Narrows Bridge. However, the geometrical shape is changed, from a sharp edged plate girder, to a shape where the curls induced by twisting are decreased significantly, and torsion stiffeners are increased. This design comes from an improved understanding of the bridge girder aerodynamics that developed after the Tacoma Narrows collapse. In Lysefjord Bridge, the stiffening girder is a common box girder with stiffeners in trapezoidal shape, see Figure 2.3. The bridge girder is also stiffened by plate stiffeners at regular spacing along the span. The 13.6 m wide box girder features a typical Norwegian arrangement of two traffic lanes and a pedestrian sidewalk.

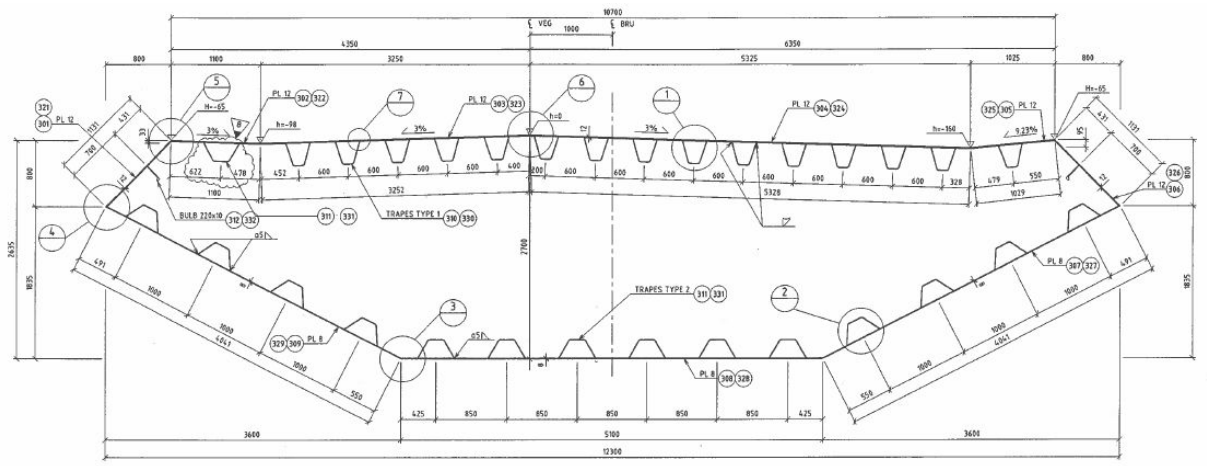

Figure 2.3: The cross section of the bridge girder in Lysefjord Bridge [7]

2.2 Main cables

The lightness of the suspension bridge is derived from the way the main cables are built, with their thousands of pencil-thin, but incredibly strong steel wires. All the tension forces from the girder are transferred to the main cables through the hangers. The cables have to support the stiffening girder, and live loads, without exceeding the capacity in any component. The suspension bridge is a flexible structure, due to almost zero bending stiffness in the cables. Since this structural shape depends on tension, the bridge appears beautiful and graceful, but in the same time, it is vulnerable to the dynamic forces of

wind. The cables need to allow for vibrations, and they should be corrosion resistant.

When steel is drawn (stretched) into wires, its strength increases; consequently, a relatively flexible bundle of steel wires is stronger than a solid steel bar of the same diameter. This is why steel cables are used to support suspension bridges. On some suspension bridges, like Lysefjord Bridge, the steel wires forming the cables have been galvanized. The main cables are described in greater detail under Chapter 3, Fracture of wires.

2.3 Hanger cables

The hanger cables are connected to the stiffening girder with a specific distance between them, and it is the girder that distributes the loading to this hanger cables. All the hanger cables are transferring forces as tension into the main cable.

2.4 Towers

A suspension bridge can have one or two towers. The far most common is two towers, each with two columns with two or more cross beams between them. The towers are exposed to compressive forces, transmitted by the main cables. They have to be thick enough to resist buckling, flexure and oscillation. The towers of most suspension bridges are made of steel, but quite a few bridges, including Lysefjord Bridge, have towers built of steel-reinforced concrete. Which of the materials that should be used depends on the conditions of each individual bridge. Steel-reinforced concrete will not buckle, and it will handle the large pressure from the main cables better than steel, it will also make the whole structure stiffer. Steel should be used in areas with potential risk of earthquake, since concrete will absorb less energy. There are other factors that should be taken into consideration as well, things like the geology of the site, the weather conditions in the area, what speed the building process should have, price, appearance and more. The depth and nature of the water the bridge is built over is also important, e.g. fresh or saltwater, and strength of currents is important factors. This may affect both the physical design and the choice of materials, e.g. if, and what kind of protective coatings that should be used.

The static conditions of the towers depend on whether the towers are anchored to the ground or not. E.g. Golden Gate Bridge is not anchored or fixed to the ground in any way, it is held in place by its weight. This means that if an earthquake occurs, the towers will rock on their base. The towers will not experience bending moment in the lower section in the same way as towers anchored to the ground. In Lysefjord Bridge, the towers are anchored to the ground, and they will therefore experience the largest moment in the lower section. This is why the towers are built with an increasing cross-section from top down. Wind load on the side of the cables can induce bending moment into the top of the towers perpendicular to the bridge span. The main cables will stiffen the towers in the direction of the bridge span, and moments in this direction will be small.

2.5 Anchor piers

Anchor piers pull the side spans to the ground and fix them in place. The anchor piers must be able to hold down the cable with its weight or by transferring the tension force

in the ropes to the ground. Norwegian suspension bridges are most commonly anchored in rock, this is also the case in Lysefjord Bridge. To be able to maintain the anchor bolts, tunnels have to be built to give access.

Chapter 3

Fracture of wires in the main cables

3.1 The main cables

In Chapter 1, the main cables were presented in general. Here, a more detailed presentation of the cables in Lysefjord Bridge is given. Cross section of the main cables is shown in Figure 3.1. The main cables are built with two collections of locked coil cables, 6 cables in each. The cables are built with a core of round wires, and with five outer layers of z-wires. Each of the cables are 713 m long before dead load is applied, and they consist of 279 wires, where 54 of them are z-wires in the outer layer [10].

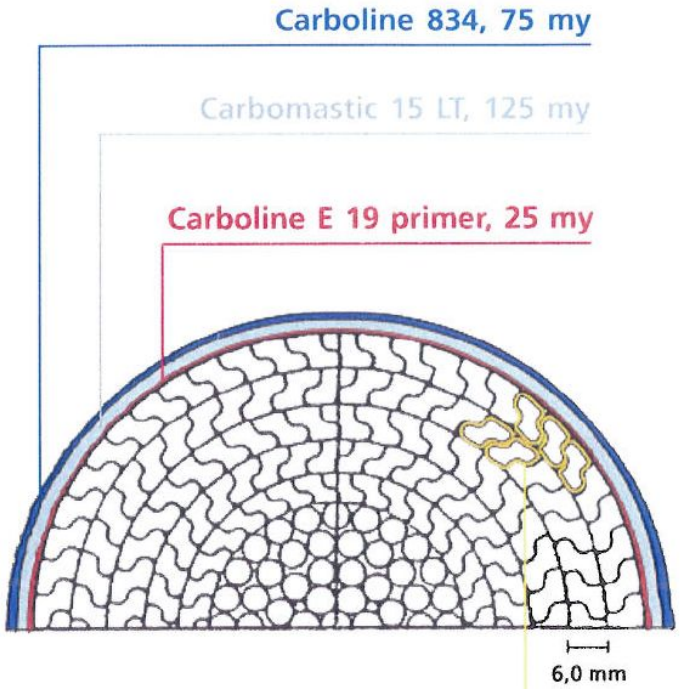

Figure 3.1: The cross section of the main cable in Lysefjord Bridge [7]

The process of making the cable is first to produce the wire, and then to make a cable out of a number of wires. The basis of the wire is a steel bar from a steel melt. This steel bar is rolled in a comprehensive process, and in the end, it is a round steel bar with a diameter of about 10 mm. This steel bar is then formed into a thin round steel wire,

or into a Z-formed wire by further rolling and forming. This cold rolling and forming process could create damage to the wires. This is likely to have happened to the wires in the main cables of Lysefjord Bridge, see Section 3.2. The rolling and forming process can also include different hardening faces. After this, the wire is hot-dip galvanized, where an outer layer of Zinc coating is applied to make the wire corrosion resistant. The wires are then spun into cables in a certain way.

It can be seen that the main cables are protected with different layers on the outside. The first layer is a 25 my thick layer of Carboline E 19 primer, and the second layer is a 125 my thick layer of Carbomastic 15 LT. On the outside, the third and last layer is a 75 my thick layer of Carboline 834. Carboline E 19 primer is a two-component epoxy polyamide primer that acts as corrosion resistance for the steel. Carbomastic 15 LT is a two-components, high build, and low temperature curing modified epoxy mastic that build coating with excellent adhesion to rusted steel and most aged coatings. The last and outer layer consists of Carboline 834, that also gives corrosion resistance [5]. The three different layers on the outside of the cable will protect the cable against corrosion as long as the coating is intact. It is however experienced corrosion on the cables, the impact of this is discussed in Section 3.2.

Wire fractures in the main cables of suspension bridges are not unusual, but the amount of fractures that can be seen in Lysefjord Bridge has not been seen on any other suspension bridge in Norway. Wire fractures are representing a maintenance issue, but only when a large amount of fractures happens on a relatively small area, the fractures weaken the load carrying capacity in the main cable. On Lysefjord Bridge, one wire fracture represents a weakening on the load carrying capacity of 0,4% in one cable [10]. Also, if the wire fractures happen with a certain distance, their weakening nature should not be summed up. This can be explained by the construction of the main cable, and the z-wires. The z-wires will lock in each other, and since the main cable is spun in spiral, the lost capacity in the cable will be maintained after 2-3 meters [10].

The wire fractures can be divided into two groups, where the first group is more or less randomly wire fractures along the cable. These fractures are often caused by the production, and the fractures will be spread out with a large distance between each fracture such that they do not interact. The other group is the fractures close to a mechanical link, like a clamp or over the tower, or into the anchor bolt. These fractures are caused by badly placed details, or by fatigue due to extra oscillations on these places. The fractures in group two can often be many and they often happen at the same place. These fractures represent a severe weakening of the capacity of the main cable. In Lysefjord Bridge, many fractures from group number one, randomly wire fractures spread out along the cables are the issue that needs to be analyzed.

3.2 Possible reasons for wire fractures

The reason for the wire fractures is probably a combination of more than one factor. Both the material properties, and stress inducing forces will have impact on the wire fractures. In this section, a summary of the reports from tests done by Sintef, DNV and Blom Bakke AS of the material properties of the main cable is presented. The reports were done in the

period directly after the bridge opening, when the first unusual number of wire fractures was observed during a guaranty related survey. The reasons for wire fractures found in the reports are imperfections on the surface of the Z-wires that initiate cracks, and reduce the cross section area of the wire.

As mentioned in Section 3.1 on page 9, the rolling process when manufacturing the wires could cause small defects in the surface of the wires. This is the case in the wires in the main cables in Lysefjord Bridge, where imperfections are observed at the edge of the Z-wires, see Figure 3.2. From a sample of wire fractures from the bridge that was examined, local defects along one profile edge was found. The sample shown in Figure 3.2, with this amount of defects could be a local occurrence, but defects have been found in inspection of other samples as well. These local defects are most likely caused by the manufacturing process, not from the legation of the steel.

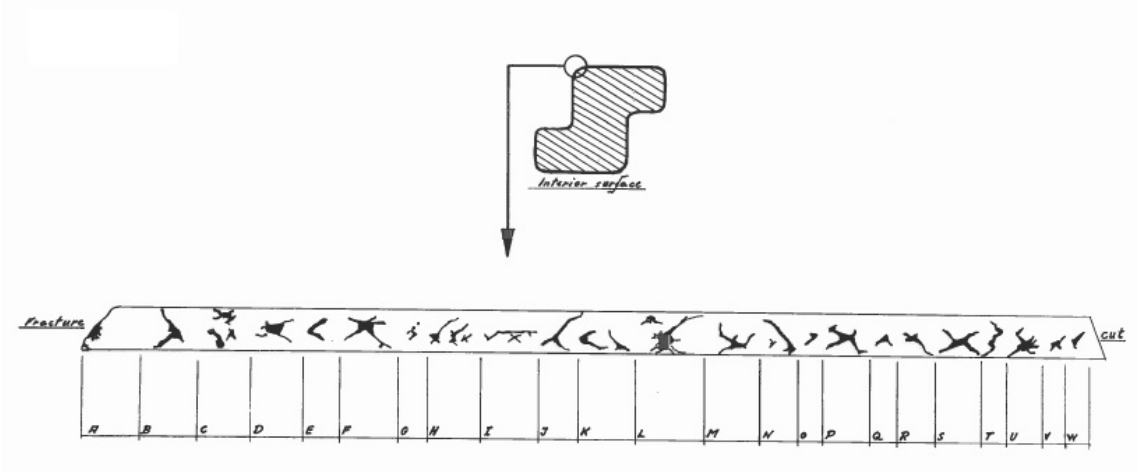

Figure 3.2: The surface defects detected on one examined Z-wire from Lysefjord Bridge [28]

At the location of the defect, the cross sectional area is reduced by one fourth, and the wire has suffered a tensile overload. The initial crack formation is suspected to be caused by fatigue, but it is not possible to establish the true mode of cracking, when the surface of the crack is mechanically deformed [28]. Figure 3.3 on the next page shows the fracture surface of the Z-wire. Fractures of brittle behavior may initiate in connection with defects of a certain size when the wire is exposed to bending stresses [20]. This can mean that forces that induce either bending stresses to the cables, or large axial stress or a combination will cause the wires to fracture.

The examination of samples from the main cables gave no indications suggesting that corrosion or fatigue has contributed to the fractures. There were found no deleterious material constituent or abnormalities other than the surface defects. This indicates that the reason for the wire fractures is the rolling and forming of the wires, and not the legation of the steel itself. There is a chance that hydrogen embrittlement has contributed to the fractures as a result of the cleaning process prior to the galvanizing of the wires. Before the wires are galvanized, they are normally cleaned in an acid solution. Atomic hydrogen may diffuse into the steel substrate during this cleaning process, and this could

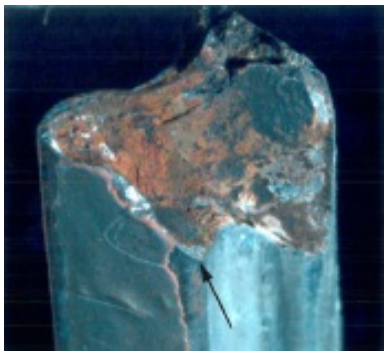

Figure 3.3: The fracture surface of one examined Z-wire from Lysefjord Bridge [28]

cause cracks of brittle nature. It is however not likely that hydrogen caused by corrosion due to reduction of oxygen has contributed to the fractures [19]. The effect of hydrogen embrittlement on the fracture toughness in general is significant. This explains why the wire fractures on Lysefjord Bridge occur in smaller and smaller defects in the surface. The fractures happen over many years due to the low diffusion rate of hydrogen [18].

It is clear that the defects found on the surface of the Z-wires are reducing the capacity of the wires, causing them to fracture at a lower stress-level than they are built for. It does not exist this kind of detailed documentation of testing on other suspension bridges main cables, therefore, it could be that it exist cables without fractures in other bridges, even though they have defects in the surface, see Section 3.8 on page 19. The model built in ABAQUS can be used for evaluation of stresses in the bridge cables due to traffic, wind and other types of loads. In connection with the wire fracture occurrence, weather in the area around the bridge has been examined in the following.

3.3 SoundPrint® acoustic monitoring

To detect wire fractures, a non destructive testing method with acoustic monitoring has been used on Lysefjord Bridge. The system is presented below, together with the results from the monitoring. The monitoring is a complement to the visual inspections. The monitoring system, SoundPrint®, was installed by Advitam, and it was operational from the 1st of October 2009. SoundPrint® is used to detect probable wire fractures on the main cables. An array of sensors are placed along the cables to measure the response of the cables caused by the energy released when the tensioned wires fractures [26]. In the central span, the system provides a longitudinal location of the wire fractures. During the monitoring period, the system showed a satisfying performance and reliability, and the monitoring is now working fine on the bridge [12]. The acoustic monitoring detects and locates failure of tensioned steel wires in Lysefjord Bridge. The monitoring system uses acoustic sensors distributed about the structure, and data is processed on site and transmitted over the Internet to a center that uses proprietary processing software to generate reports summarizing the time, location and classification of the recorded events [23]. The data from Lysefjord Bridge is sent to Advitam in France, and they make a summarizing report every third month, that is sent to The Norwegian Public Roads Administration.

Because the system is recording a change of the system, and not a condition, the monitoring has to be permanent. Monitoring during the whole service life is hardly ever affordable, and therefore the determination of the initial condition before the monitoring period is important. The application field of such monitoring will therefore concentrate on structures with problems of durability, where the service life may be extended by this kind of equipment. Though the system does not provide any information of deterioration that occurred before its implementation, acoustic monitoring can help the engineer to assess the present status of the bridge and can also assist in deciding whether costly maintenance is required or not [8].

There has been done testing with the monitoring system, and it has been concluded that continuous acoustic monitoring is able to record, analyze, classify and locate the wire fractures [8]. This test is done on grouted and partially grouted tendons. Irrelevant signals and ambient noises such as noises from traffic, construction activity and other ambient sources have to be filtered out from the events that are evident for the structural capacity of the bridge [8]. Advitam, that is monitoring Lysefjord Bridge needs to know when a visual inspection are carried out, or maintenance is done on the bridge, such that the notices not are registered as wire fractures. Another test of the system has been done on the Bronx Whitestone Bridge in New York City. This suspension bridge is 701 m long, and was opened for traffic in 1939. Here, the system correctly classified the events and located them longitudinally with errors raging from 0 to 0.7 m. The information from the system can be used to localize areas of deterioration in large structures like a suspension bridge, and can help determine where to focus the inspection [23].

It is important that the monitoring system is working properly, and that it monitors all the wire fractures. The trials done with the system seems to verify the monitoring system as a reliable system. There are however some issues and questions that can be raised around the system at Lysefjord Bridge. Since only the wire fractures that occurs on the outside of the cable can be seen on visual inspections, the acoustic monitoring should find more fractures than can be inspected, since there is likely to be inner fractures as well. On the inspections done after the monitoring however, most or all of the fractures has been found. This could mean that the acoustic monitoring do not register the inner fractures, or that there is almost only fractures in the outer wires. To verify the acoustic monitoring system on Lysefjord Bridge, a x-ray or magnetic inspection should be done, and the results should be compared to the results from SoundPrint®.

3.4 Wire fractures detected visually

The Norwegian Public Roads Administration and Mesta have done observations of the wire fractures since September 2001. Based on these observations, the average wire fracture rate per year can be found. It can also be seen where in the span the wire fractures occur, and if there are more fractures in the side spans or in the mid span. Which cable that has most wire fractures is shown in Figure 3.4 on the next page. Cable number 4 has the most fractures, with 252 fractures, while cable number 2 has the least number of fractures, with 30 fractures. As can be seen in Figure 3.5 on the following page, the cables in the middle of the main span has more wire fractures than the ones on the sides. If the fractures are summed up on each side, the number of fractures on west side of the

bridge is 753, and on the east side 650. This difference could be due to the load carrying characteristics in the bridge. There is also a possibility that the force from wind on the bridge more often comes from one side than the other, this could induce more stress in one side, that could cause more fractures in one side than in the other. The traffic loading could also be an explanation, since this is an asymmetric loading.

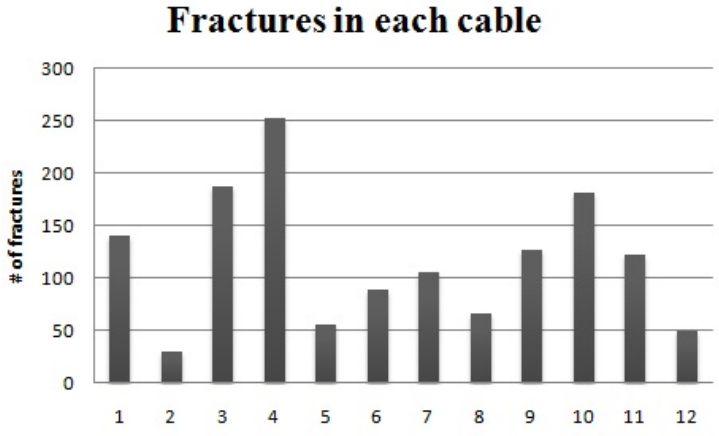

Figure 3.4: Amount of fractures in each of the twelve cables from the opening of the bridge Dec. 1997 to Oct. 2010

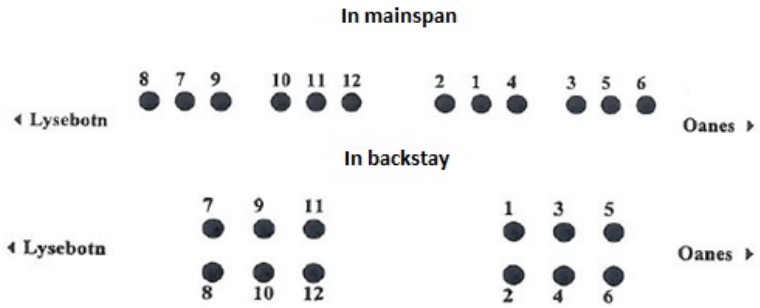

Figure 3.5: Cable arrangement in Lysefjord Bridge

Since the opening of the bridge in 1998, 1403 wire fractures have been detected visually in the main cables of Lysefjord Bridge. The last inspection of the cables was done by The Norwegian Public Roads Administration in October 2010, and based on all the inspections done since the opening of the bridge, an average of 116 wire fractures/year can be found [7]. It can be seen that the wire fracture rate has varied over the years, and that it is still high, but slowing down at the moment, this is shown in Figure 3.6 on the next page. The rate seen in Lysefjord Bridge is much higher than for any other bridge with similar problems in Norway, see Section 3.8 on page 19.

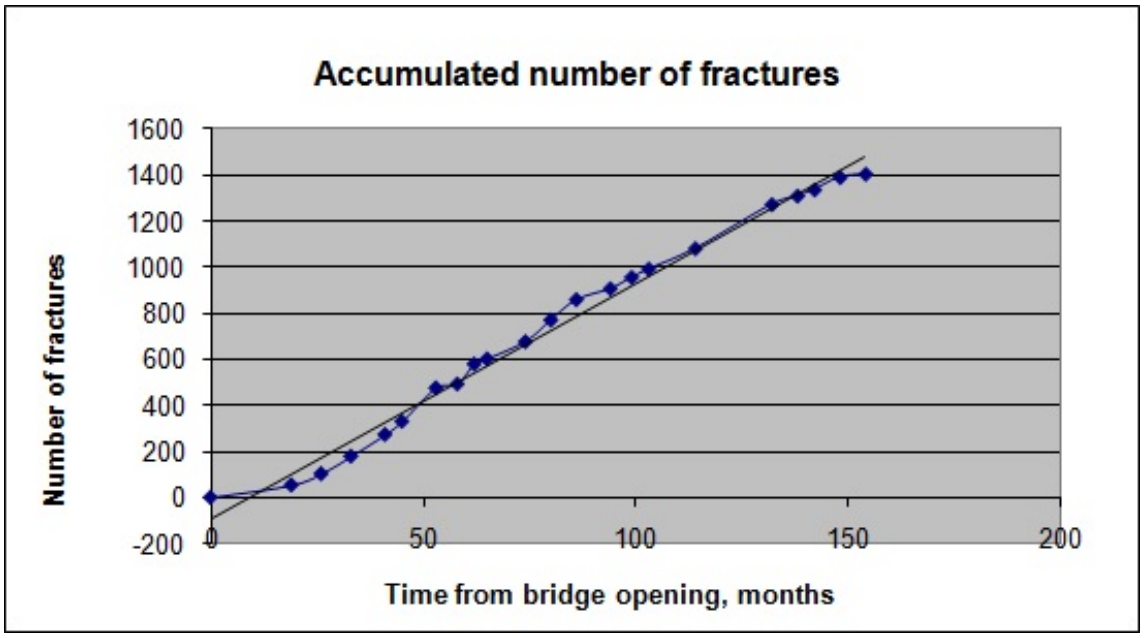

Figure 3.6: Accumulated wire fractures from the opening of the bridge Dec. 1997 to Oct. 2010

3.5 Monitored wire fractures

After the monitoring system was installed, a spatial and temporal distribution for the wire fractures can be found. This means that we can look closer into the weather at the time the fracture occurs. After analyzing the wire fractures and the monitoring reports from Advitam, a period with many wire fractures is chosen, and compared with the same period the year after. The data is analyzed to see if the weather was somehow different in the time period. To find a period with more wire fractures, the fractures in each month are summarized, and shown in Figure 3.7 on the next page. There is just one and a half year of monitored wire fractures, and to see clear results, a longer period would be preferred. Even with this short period of monitoring, some tendencies can be found, and these are presented and discussed in the following.

From this figure, it is clear that there is more wire fractures in the winter than in the summer. The reason for this could therefore be in the weather, since it could be that the amount of fractures follows the seasons. There is, however, a possibility that these differences have another explanation, for example that in the summer, the traffic is lower or at least different than in the rest of the year, and therefore, very few wire fractures happen in this period at the year. The reason is most likely a combination of the characteristics of the steel, and the loading on the bridge. To see which period in the winter months that has the most fractures, the two monitored winter periods in 2009 and 2010 are shown in Figure 3.8 on page 17. From the figure, December 2009 seems to be the month with the most wire fractures. Compared to the same period in 2010, there is a significant difference in the amount of wire fractures, and therefore this period has been analyzed and further discussed.

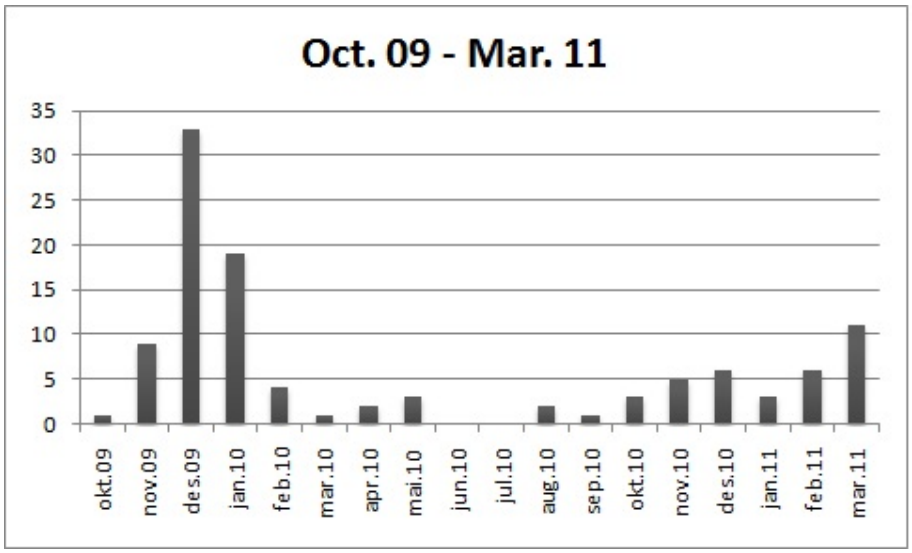

Figure 3.7: Amount of wire fractures recorded by Advitam Oct. 09 to Mar. 11 [2]

3.6 Weather around Lysefjord Bridge

To be able to look at the wire fractures related to weather in the area around the bridge before and during the fractures, data from a weather station at Forsand has been collected and used [21]. Lysefjord weather station has data from 2006 and up till today. The data are given from day to day, and as averages and min/max for each month and year. The data should be correct, but there has been some issues with the monitoring device, such that some measurements are wrong. There is always an uncertainty when it comes to collected data, and the data is used as they are here, since the error are considered to be relatively small if any.

Since the weather station is placed in Forsand, some kilometers further out in Lysefjord than the bridge, the data could differ a little from the real weather situation around the bridge, see figure 3.9 on page 18. The temperature should be about the same as around the bridge, but the wind speed and gust wind could be different due to different topography around the bridge.

From figure 3.7 and figure 3.8 on the next page, the amount of wire fractures are very high in December 2009. To see if there has been a weather situation that is somewhat unique in this period, the weather data for December 2009 and for December 2010 are analyzed and compared, see Figure 3.10 on page 20 and 3.11 on page 21. The weather data that is considered most important in this analysis is temperature and maximum wind speed over ten minutes period. To be able to make comparisons between the weather and the wire fractures, the three figures are placed directly under each other.

Wind

The wind in the area around Lysefjord Bridge could be a reason or a part of the reason for the fractures in the wires, see more discussion in Section 5.4 on page 36. The wind creates vibrations and oscillations through the bridge, and this can cause fatigue in the

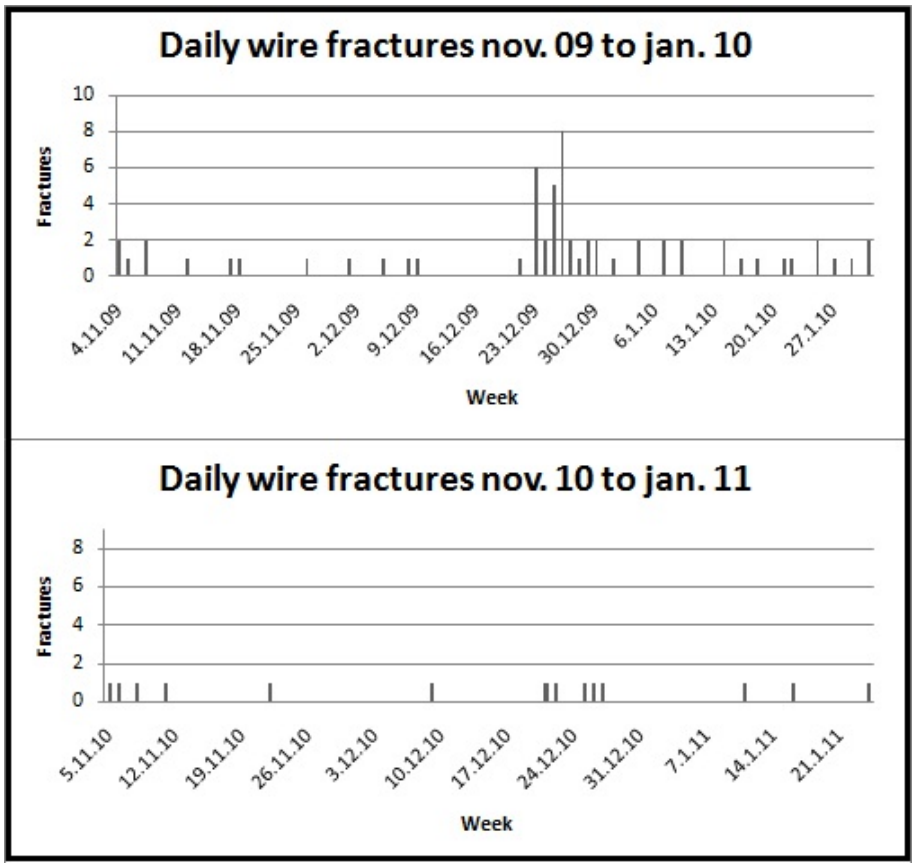

Figure 3.8: Daily fractures during the period from Oct. to Jan. 2009 and 2010 [2]

main cable wires. The beginning of Lysefjorden, where the bridge is located, is shielded from the open sea, and it is not known to have large wind forces. Wind is complex and it is not easy to determine the forces from wind on the bridge, it does not necessarily have to be high wind speed to create large movement in the bridge. The maximum wind speed over ten minutes duration during December 2009 and 2010 was about the same, around 20 m/s. The average wind speed over ten minutes during December 2009 and 2010 was 3.9 m/s and 2.3 m/s. No clear signs that the mean wind speed are a part of the reason for the wire fractures are found in this comparison. It could however be that vortex induced vibrations and such phenomena will occur with this wind speed, this is further discussed in Section 5.4 on page 36.

Temperature

Steel is known to expand when the temperature goes up by a specific temperature coefficient. It is also known to change its characteristics, and become more brittle when the temperature goes down and below a certain temperature. The cables can therefore become brittle in cold temperatures, and together with other factors that increase the stress in the cables, temperature can be a reason or part of the reason for the wire fractures. From Figure 3.10 on page 20 and 3.11 on page 21, it can be seen that the temperature in December 2009 was relatively high in the beginning, and then it was a sudden drop in temperature. A few days after this drop in temperature, very many wire fractures was monitored. In December 2010, the temperature was evenly cold during the entire month,

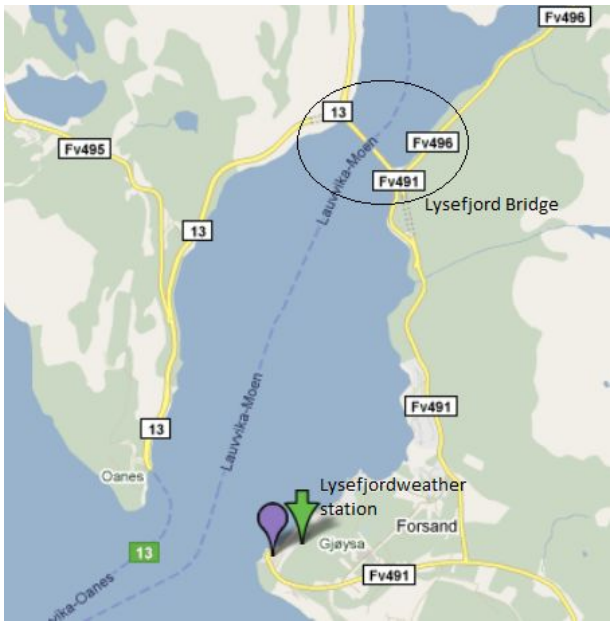

Figure 3.9: Lysefjord weather station is stationed in Forsand [11]

and it can be seen that there are only a few wire fractures during this month. This observation, done from only two periods during the monitoring period, indicated that the wire fractures can be caused by sudden changes in the temperature. To make this statement however, more monitoring should be done and compared to the weather in the area, and testing of the main cables should be done by a laboratory.

Rainfall and ice

The rainfall is ignored in this analysis, since it is considered to have a small impact on the bridge. The snow and ice is also considered relatively small to wind load, and is not included in this analysis.

3.7 Maintenance and replacement of cables

If the fracture rate continues like today, the main cables will have to be maintained and strengthened in the short term, and all the cables will need to be changed, or extra cables have to be introduced after 30-40 years. The fracture rate needs to decrease tremendously if this should be avoided. The wire fractures are repaired by sealing and covering the damage. If many fractures are found next to each other, it could be that the locking mechanism between the wires is destroyed, and the wires can bend out of the cables. In these incidents, the wires must be put in place, or the cable must be replaced or improved. This is not a common condition [10]. There should be done more monitoring, and also more testing of the cables before they are changed, such that the same problem does not occur in the new cables.

3.8 Wire fractures in similar bridges

The experience with suspension bridges and cables in Norway has mainly been good. In the more than 40 other suspension bridges in Norway, no bridge has been close to having this many wire fractures after such a short period of time. There are however three cases where problems in the main cables have occurred. These three bridges are presented here.

Kjerringstraumen Bridge, Nordland

Kjerringstraumen Bridge is a two span cable supported bridge, where the spans are 180 m and 200 m. The main cables consist of twelve 68 mm locked coil cables in two layers, it was delivered in 1967. Each of the cables are 495,3 m long. After the bridge was installed, 48 wire fractures was found in 11 of 24 cables, where some of the cables had 14 fractures alone. 27 fractures was found by a magnet inductive examination. There was defects and cracks in the surface of the wires, and the Zinc coating had a pore grip and had fallen off on some areas of the wires. The cables was dismantled and thrown away, and new cables had to be ordered and put in place [10].

Kjellingstraumen Bridge, Nordland

Kjellingstraumen Bridge is a suspension bridge with one main span with the length of 260 m. Each of the main cables consists of ten 72 mm locked coil cables in two layers. Each of the cables has a length of 491 m, they were delivered in 1974. After the installation of the bridge, 7 wire fractures were detected, and some places the wires came out of the cable. It was detected small defects in the surface of the wires where the fractures had occurred with examination, and it was concluded with too large bending during transportation. The wire fracture rate has been low, but there has been some wire fractures during the years, and in 2004 the number of wire fractures was 56. There is, however, some insecurity around the number, since there has been only a few observations of the cables [10].

Nærøysund Bridge, Nord-Trøndelag

Nærøysund Bridge is a suspension bridge with a main span of 325 m. The main cables are 608 m long, and each cable is built with twelve 72 mm locked coil cables in two layers. The bridge was opened in 1981, but the year before, directly after the installation of the main cables, 4 wire fractures were observed. After opening, the number of fractures had increased to 30. The fractures was spread out over the cables, and some of the fractures had occurred already during the production. The examination of the main cables showed internal cracks in the wires in the thinnest area of the Z. These cracks were parallel to the cable, and it was assumed that the cracks were enlarged in the production process. Hydrogen embrittlement from the cleaning of the wire was assumed to be the reason for the cracks. The last inspection of the cables was in 1999, and a total of 119 wire fractures spread out over the cable was found. The wire fracture rate was increasing the first two years, more than the rate at Lysefjord Bridge, but then it slowed down and stabilized [10].

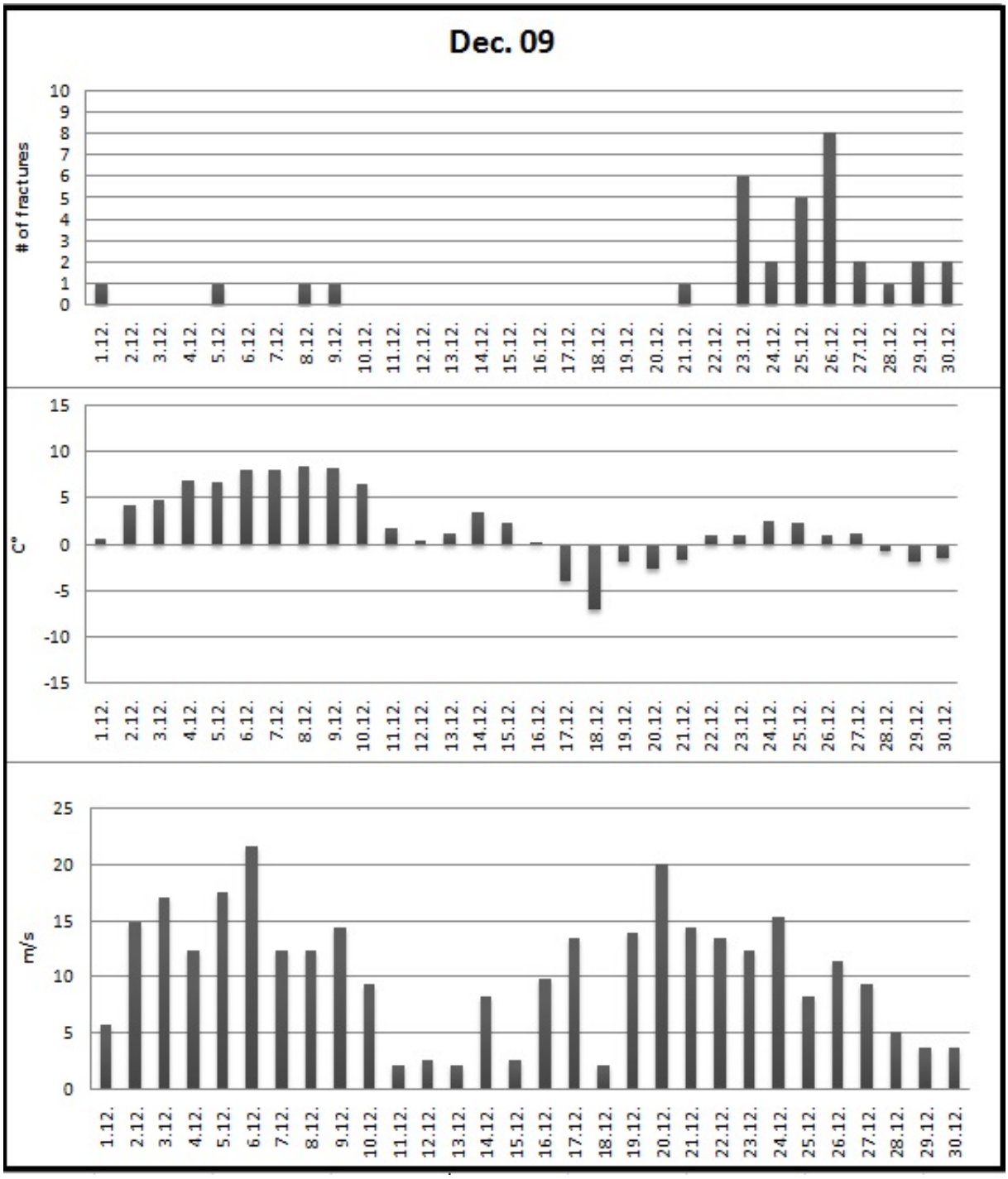

Figure 3.10: Amount of wire fractures, average temperature and maximum mean wind speed recorded Dec. 2009

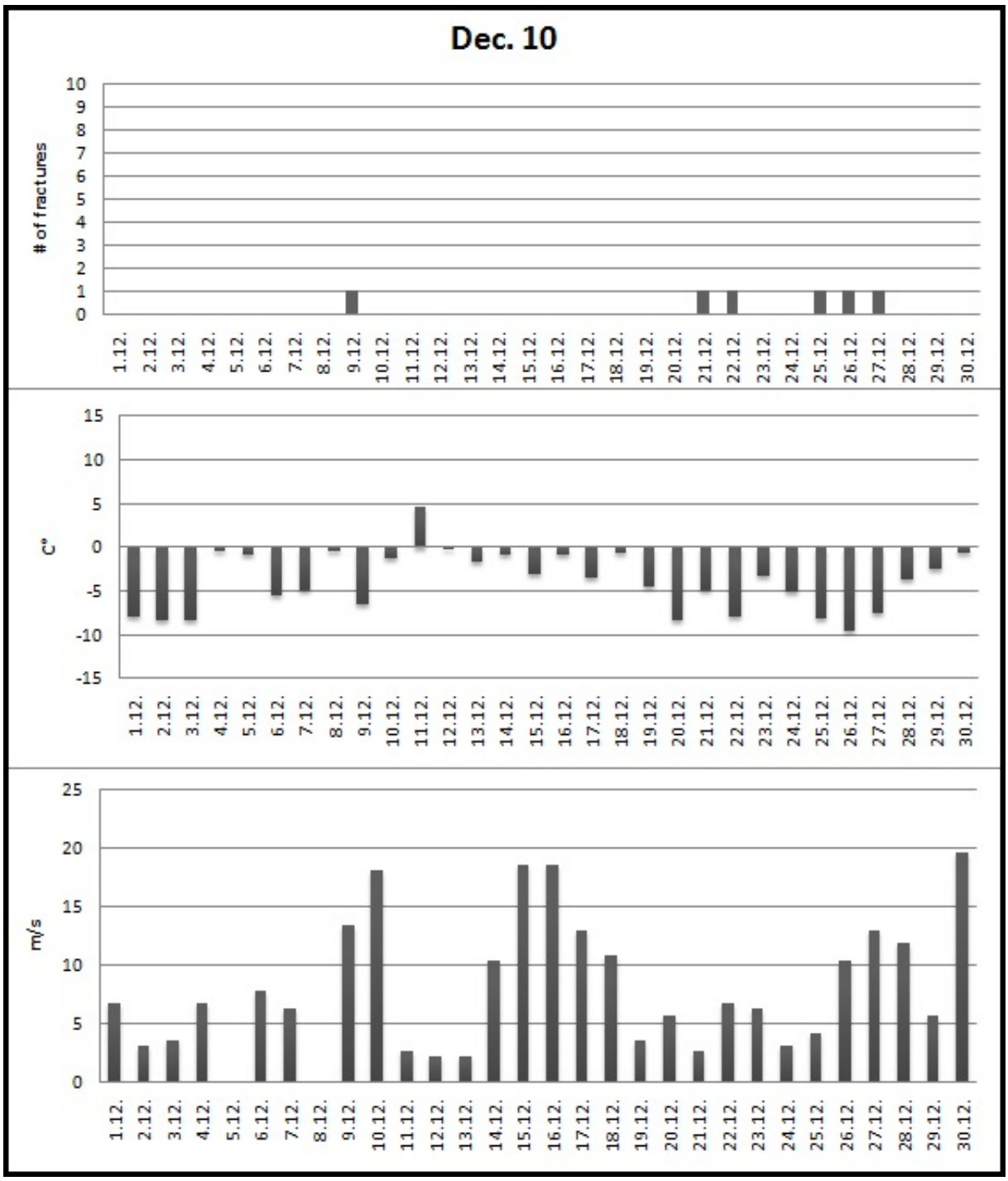

Figure 3.11: Amount of wire fractures, average temperature and maximum mean wind speed recorded Dec. 2010

Chapter 4

Finite element model of Lysefjord Bridge

The main purpose of building a finite element model of Lysefjord Bridge in ABAQUS, is to gain a direct insight into a finite element modeling of such a structure, as well as to provide a model suitable for further bridge analysis under various static and dynamic load conditions. The model is compared to the one previously established in Alvsat [1]. The model in Alvsat was also built by the finite element method [14], the input data used in Alvsat is used as a modeling base for the model in ABAQUS. The ABAQUS model of Hardanger Suspension Bridge, created by Aleksander Kyte for The Norwegian Public Roads Administration, was available for the present study and was used as a basis for developing a similar model for Lysefjord Bridge [17]. The explanation of the commands used in ABAQUS, is from the ABAQUS manual [15].

In this thesis the ABAQUS model is used for evaluation of eigenfrequencies, and displacement due to static wind loads is found and discussed in light of deterioration of the cable wires.

4.1 ABAQUS software

ABAQUS is a general purpose finite element program. The program is extensively used for advanced finite element analysis of non-linear problems. Many kind of structures or problems can be modeled in the program, it is made to solve many different non-linear static or dynamical problems. The most important non-linearity in the suspension bridge is the geometrical stiffness in the cable system. ABAQUS are updating the stiffness matrix continuously, like the real accumulated loading situation. Other non-linear effects that can be taken care of by the program is non-linear behavior of material and friction-problems [15]. For the bridge in question, the linear material behavior is assumed. Elements in the program can easily be removed from the model, and this makes the program suitable to analyze the redistribution of forces in the bridge if one or more hangers are broken, or during building, before all the elements are in place. This is not done here, since the bridge already is built, but it is possible to use the model to determine how much the capacity of the bridge is reduced with the fractures in the cable wires.

4.2 ABAQUS model

The model of Lysefjord Bridge is built with nodes and elements between them. The elements are given areas, rigidity and density to simulate the real bridge. All the different components of the bridge are built separately, as explained in the following. The units in ABAQUS are given from the International System of units (SI) as long as nothing else is given by a command. The model of Lysefjord Bridge has only SI-units.

4.2.1 Definition of directions

The elements in the model in ABAQUS have numbers from one and up, starting in the northern part of the bridge with the lowest number. The real and the fictive north in the bridge modeling is shown in Figure 4.1. Fictive north are given to the bridge such that the different elements of the model can be named by north, south, east and west, this simplifies the understanding of the model. The coordinates for the south and the west side of the bridge girder are defined positive, and the north and the east side is defined negative in the model in ABAQUS.

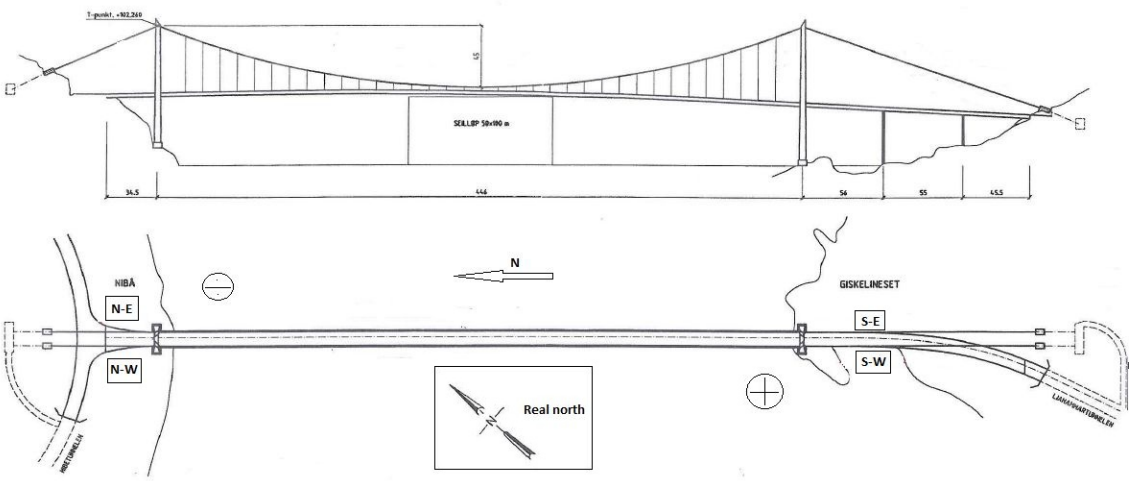

Figure 4.1: Real and fictive directions of the bridge [7]

The system of coordinates in the model in ABAQUS is shown in Figure 4.2 on the next page. X is the longitudinal axis of the bridge, often referred to as direction 1. Y is the horizontal axis, perpendicular to the longitudinal axis, often referred to as direction 2. Z is the vertical direction, often referred to as direction 3.

4.2.2 Elements

Bridge girder

Figure 4.3 on the following page shows how the bridge girder is built in ABAQUS. The numbers given in Figure 4.3 on the next page are listed in Section 4.2.3 on page 29. The chord that represents the bridge girder is modeled in the neutral axis of the bridge girder. The shear center does not necessarily coincide with the neutral axis, this is not taken into consideration in this model, see Section 6.2 on page 45. The bridge girder and the lower hanger link have a fixed connection. Hangers and cables are modeled as beam elements with a very small bending stiffness, see Section 4.2.5 on page 31. The tower is modeled

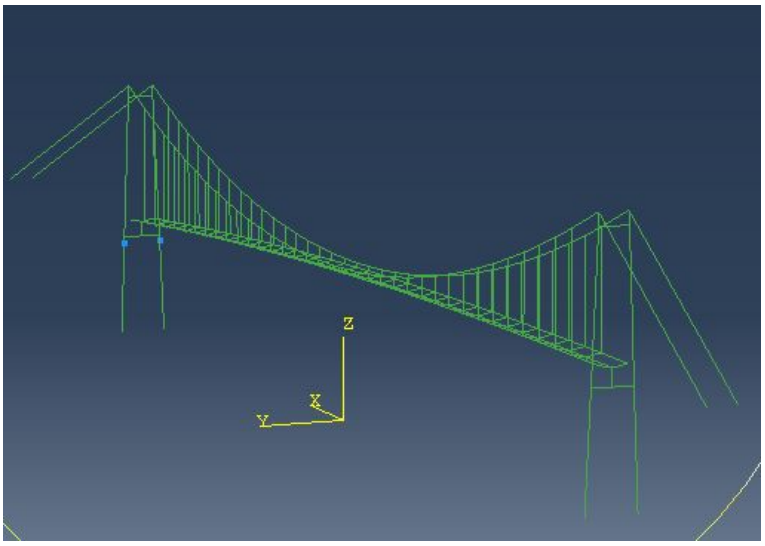

Figure 4.2: System of coordinates in ABAQUS

with low middle locking bar, which is the current design of the bridge.

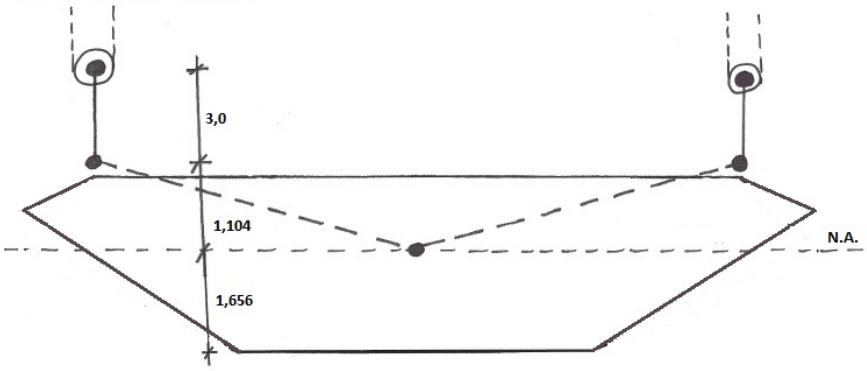

Figure 4.3: General ABAQUS model of the bridge girder

The main dimensions of the bridge girder is shown in Figure 4.4 on the next page

Definition of local directions in the bridge girder is shown in Figure 4.5 on the following page.

- V: Vertical direction
- H: Horizontal direction perpendicular to the direction of length
- T: Torsion

Note to H; H is the direction and displacement perpendicular to the bridge. Displacement in the longitudinal axis is also horizontal, but this will be specially described as the displacement along the span in the longitudinal axis.

The bridge girder is modeled with 36 members in the x-direction. The members are 12 m long, which is one member between each hanger. The first and the last member are 19 m long. To be able to put the hangers in vertical position, and not diagonally, dummy

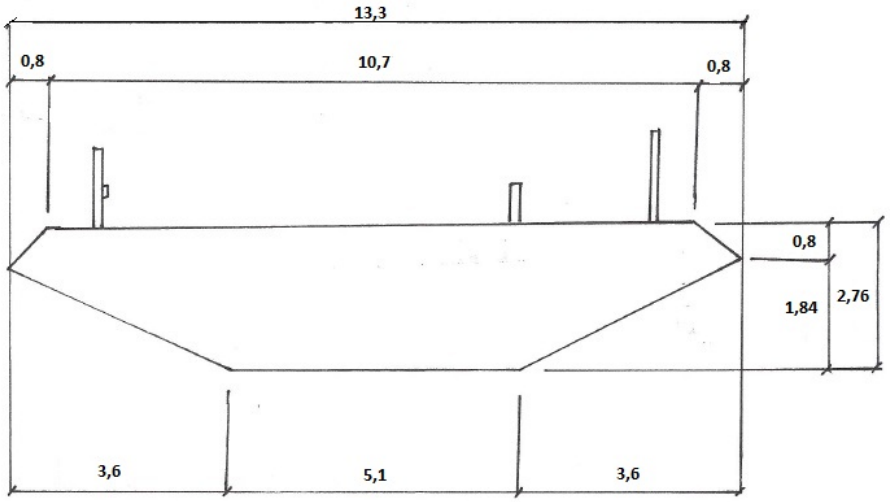

Figure 4.4: Bridge girder with dimensions

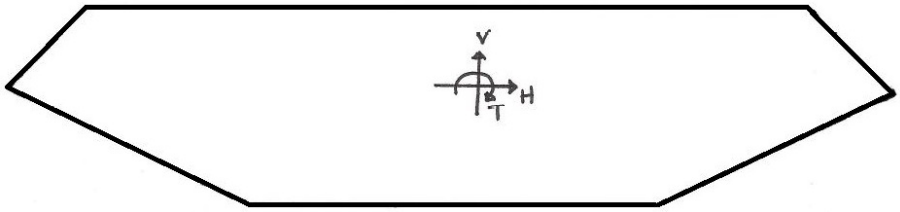

Figure 4.5: Directions in the model, seen from south

nodes were made on both sides of the girder to connect girder and hangers, see Figure 4.6 on the next page.
To model the bridge axis in vertical, z-direction, a second-degree polynomial was fitted to the three known points. At the connection with the northern tower, the elevation is 53.46 m, the midpoint elevation is 54.47 m, and the connection with the southern tower has the elevation of 46.00 m. To calculate an equation for the bridge girder shape, the three known points shown in Figure 4.7 on the following page is used.

Starting with the equation for a parable, and finding the parameters to determine the correct second-order equation for the bridge girder;

$$f(x) = ax^2 + bx + c \tag{4.1}$$

$$f(x) = y \tag{4.2}$$

Define x=0 to be in the center of the bridge girder in longitudinal direction, see Figure 4.7 on the next page. At the center of the bridge, y=1.007, but to achieve the correct shape when dead load is applied, the negative displacement has to be compensated, therefore, y(0);

$$y(0) = 1.007 + 1.5 = 2.507 \rightarrow c = 2.507 \tag{4.3}$$

Using the second known point, where x=-223;

$$(-223)^2 a - 223b + 2.507 = 0 \tag{4.4}$$

$$b = \frac{2.507 + (-223)^2 a}{223} = \frac{2.507}{223} + 223a \tag{4.5}$$

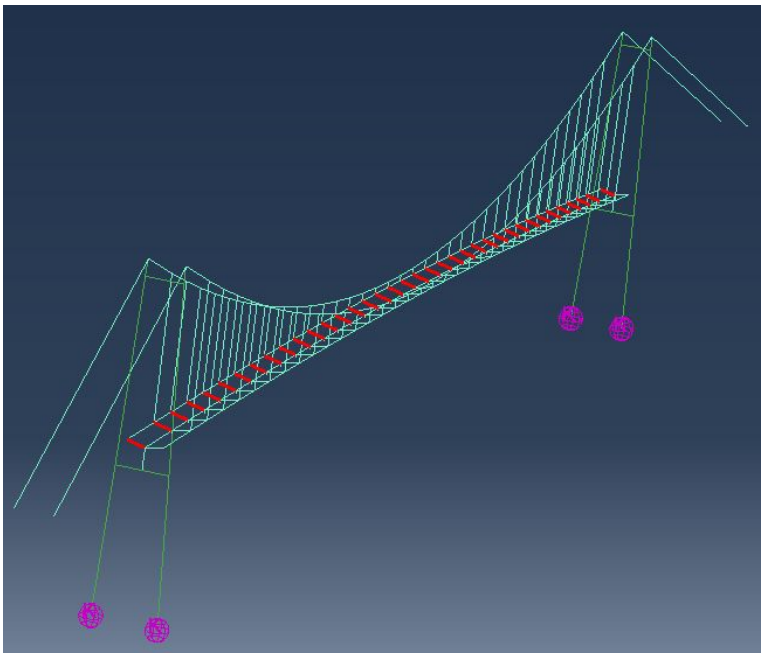

Figure 4.6: Dummy nodes to link the hangers to the bridge girder in ABAQUS

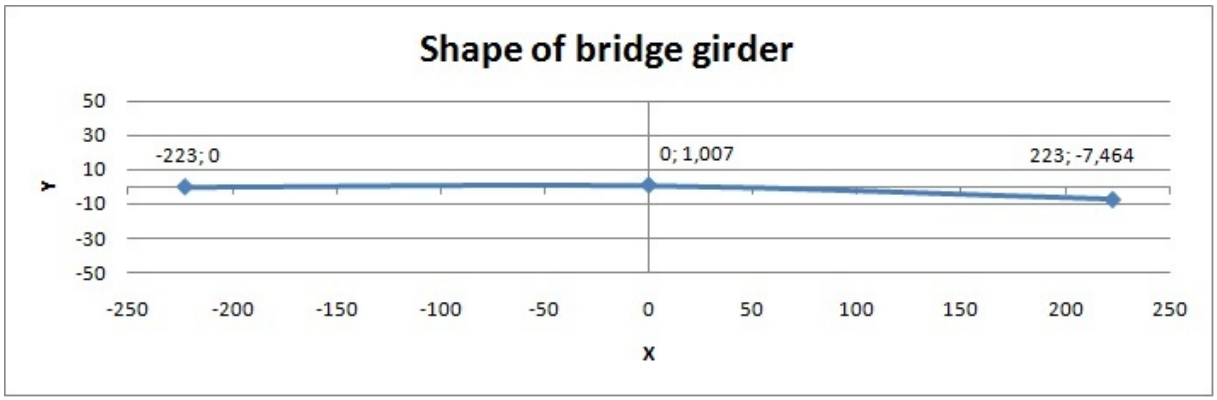

Figure 4.7: The shape of the bridge girder when dead load is applied

Using the third known point, where x=223;

$$223^2a + 223b + 2.507 = -7.464 \tag{4.6}$$

$$b = \frac{-9.971 - 223^2a}{223} = \frac{-9.971}{223} - 223a \tag{4.7}$$

Using the two equations 4.5 on the preceding page and 4.7 to determine a and b;

$$\frac{2.507}{223} + 223a = \frac{-9.971}{223} - 223a \tag{4.8}$$

$$a = -0.0001255 \tag{4.9}$$

$$b = -0.0167350 \tag{4.10}$$

The second-order equation for the bridge girder is found by substituting a,b and c;

$$f(x) = -0.0001255x^2 - 0.016735x + 2.507 \tag{4.11}$$

In theory, with this parable, the highest point of the bridge girder will be to the side of the middle, but the real top point of the bridge girder when it is hanging from the cables will probably be around the middle of the span. There are other perhaps more accurate ways to find this parable, but the method used here is considered close enough to the real structure. The shape of the bridge girder when it is loaded with dead load is discussed in Section 5.3 on page 35.

The type of element used for the bridge girder is B31, this is a 2-noded linear beam member with shear deformation. The main advantage of the beam element is that it is geometrically simple, and have few degrees of freedom. This simplicity is achieved by assuming that the member's deformation can be estimated entirely from the variables that are functions of position along the beam axis only. The beam theory is the one-dimensional approximation of a three-dimensional continuum. The reduction in dimensionality is a direct result of slenderness assumptions; that is, the dimensions of the cross-section are small compared to typical dimensions along the axis of the beam. The deformations in a beam element consists of axial deformation; bending; and, in space, torsion [15].

Main cables

The nodes for the connection between the hangers and the main cables was found by making a second-degree polynomial based on the top of the towers at 102.26 m, and the lowest point in the middle of the cable at 57.26 m, see Figure 4.8.

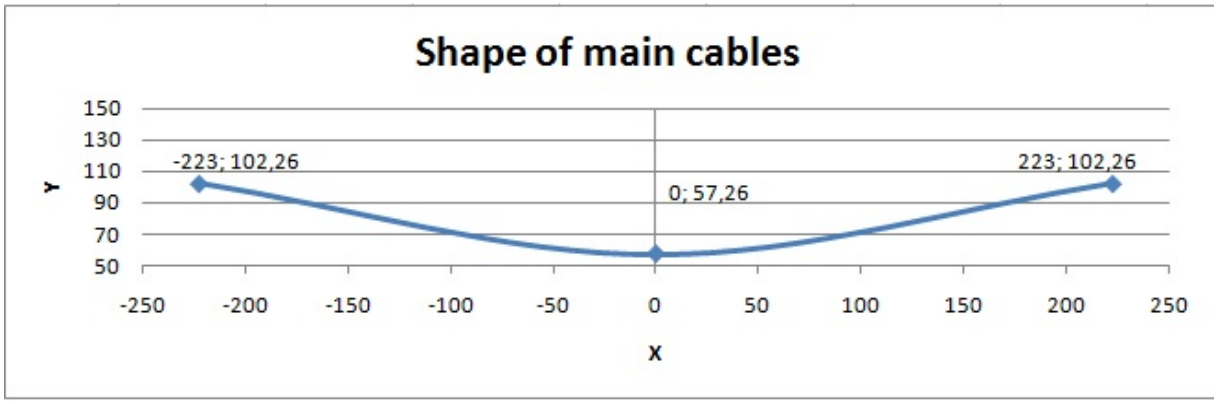

Figure 4.8: The shape of the main cables when the dead load is applied

Starting with the equation for a parable, Equation 4.5 on page 25 and 4.7 on the previous page, and finding the parameters to determine a second-order equation for the main cable. The sag is 45 m, and to obtain this when dead load is applied, a displacement of 2.8 m is included;

$$y(0) = -42.2 \rightarrow c = -42.2 \tag{4.12}$$

The cables have the same top points, and the minimum point is in the center.

$$b = 0 \tag{4.13}$$

Using the known point at the top of the tower, and determine a;

$$223^2 a - 42.2 = 0 \tag{4.14}$$

$$a = 0.00084860 \tag{4.15}$$

The second-order equation for the cables is found by substituting a, and c into the equation;

$$f(x) = 0.00084860x^2 - 42.2 \tag{4.16}$$

The main cables are modeled with one member between each hanger. The bending stiffness is set to 1 percent of a circular cross section with an outer diameter of 97 mm. This gives the member almost zero bending stiffness, and it will act like a jointed rod.

The main cables have an unusual cable configuration, a single row of 12 large locked-coil strands in the main span. This is not taken into consideration in this model, where the main cables are modeled as one main cable at each side of the bridge, with characteristics equivalent to those of the six cables.

Hangers

The hangers are modeled with one element for each hanger between the main cable and fictive points that simulates the bridge girder. The members are modeled in the same way as the main cable. Their bending stiffness is set to 1 percent of a circular cross section with an outer diameter of 48 mm, which is almost zero bending stiffness, and each hanger will act like a jointed rod. The hangers in the ABAQUS model are shown in Figure 4.9.

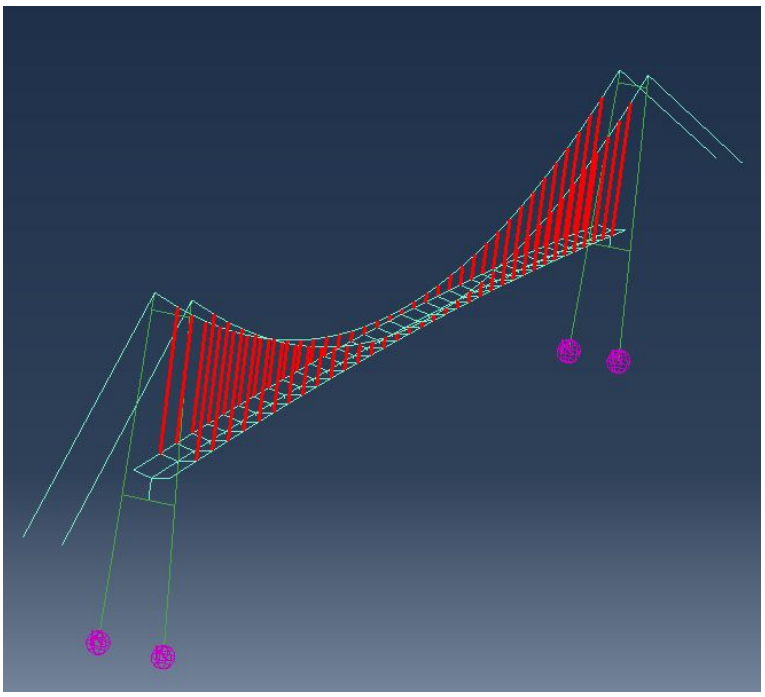

Figure 4.9: The hangers in the ABAQUS model

Towers

The towers are modeled with 29 members in each leg. The nodes that the members are attached to are placed such that the towers should be vertical when dead load is applied on the bridge. This is discussed in Section 5.3 on page 35. There is one cross beam below

the girder, and one in the top of the tower, these are modeled with 7 nodes, 6 elements each.

The tower legs are given names corresponding to their position in Figure 4.1 on page 23. The two towers are similar in height and in cross sectional areas, but there is a difference in the foundation, and in the height of the cross beam under the bridge girder. The differences in the two towers are reflected in the model, the cross beam under the bridge girder in the southern tower is around 7 m lower than in the northern tower, and the number of nodes under and over the lower cross beam is adjusted such that the element length over the height of the tower is almost equal.

The type of element used in the towers and the cross beams are FRAME3D. This is an element that is suitable for analysis of frame. The active degrees of freedom are displacement in X, Y, and Z, and rotation about the X-, Y-, and Z-axis. The frame elements are designed to be used for small-strain elastic or elastic-plastic analysis of frame-like structures composed of slender, initially straight beams. Typically, a single frame element will represent the entire structural member connecting two joints. A frame elements elastic response is governed by Euler-Bernoulli beam theory with fourth-order interpolations for the transverse displacement field, hence, the elements kinematics include the exact solution to concentrated end forces and moments and constant distributed loads. A frame elements plastic response is modeled with a lumped plasticity model at the elements ends that simulates the formation of plastic hinges. The elements can thus, be used for collapse load prediction based on the formation of plastic hinges [15]. This modeling capability is not used in the present analysis.

Rigidity, area and weight of the towers are calculated in Mathcad, and the numbers are interpolated in Excel to fit each of the 29 members in each tower. This calculations are shown in Appendix B. The element at the top of each tower leg is B31, this is a beam element, used to simulate the link to the cables.

4.2.3 Geometry

The geometry of the main components of the bridge is given in the following list.

- Main span: 446 m
- Sag: 45 m
- Distance between main cables: 10.25 m
- Length of back stay north: 73.906 m
- Length of back stay south: 166.046 m
- Cable slope of back stay north: 0.445°
- Cable slope of back stay south: 0.364°
- The shortest hanger: 3.0 m
- Distance from the lower hanger link to the neutral axis: 1,104 m
- Elevation of the top of the tower: + 102.260

- Elevation of the bottom of the tower foundation: + 6.500

Some of the values are visualized in Figure 4.3 on page 24 and 4.4 on page 25.

4.2.4 Conditions

- Side span: fixed in the point where the cables enters the rock
- Towers: All the tower legs are fixed in the foundation. All the tower top nodes linked to the cable is released
- Cross beams: fixed to the tower legs
- Girder end points: Simply supported, restrained sideways, supported against torsion and fixed in the longitudinal direction in the towers

The side span is fixed in the point where the cables enters the rock with the command BOUNDARY, and it is specified with 1,3,0, which represents the first degree of freedom constrained, the last degree of freedom constrained and the actual magnitude of the variable. The towers legs is fixed in the foundation, by use of the same command BOUNDARY as the side spans, but here, the specifying numbers is 1,5,0. This means that the nodes not only are fixed for displacement in X, Y, Z, but also rotation about X- and Y-axis. The nodes in the top of the towers are made hinged such that the cables only are held in place, and not fixed. This is done with the command RELEASE in ABAQUS, and its specified with S2, which refers to the top element end, and with ALLM, that represent a combination of all the rotational degrees of freedom (i.e., M1, M2, and T). The cross beams are linked to the tower legs using MPC. MPC stands for Multi-point constraints. They allow constraints to be imposed between different degrees of freedom of the model, and they can be quite general (nonlinear and non homogeneous). The bridge girder ends are simply supported, restrained sideways, supported against torsion and fixed in the longitudinal direction. The element used for the link is B33, which is a 2-node cubic beam. The element is released to act in the correct way, this is given in ABAQUS as RELEASE, and is specified with the end of the beam in the north of the bridge, S2. And with M2-T, that refers to a combination of rotational degrees of freedom about the n1-axis and the t-axis. In the south end of the bridge, the beam end S1 is the rotation about the n2-axis released. The beam end S2 is released in the same way as the beam on the north side of the bridge [15].

4.2.5 Stiffness properties

The rigidity of the bridge girder, the hangers, main cables and towers are given in Table 4.1.

Bridge girder	
A	0.343 m^2
I_1	0.429 m^4
I_2	4.952 m^4
I_T	0.929 m^4
C_w	4.762 m^6
E	210.000 N/mm^2
G	80.700 N/mm^2
Hangers	
A	0.0018 m^2
I	1 % of a circle with outer diameter 48 mm
E	180.000 N/mm^2
Main cable	
A (set of 6 cables)	0.044 m^2
I (one out of 12 cables)	1 % of a circle with outer diameter 97 mm
E	180.000 N/mm^2
Towers	
E_c	40.000 N/mm^2

Table 4.1: Stiffness properties for Lysefjord Bridge

The numbers given in the table are found from calculations done in Mathcad, see Appendix B. The area of the bridge girder given in ABAQUS is 5% higher than the area found from calculations. This is introduced to account for the stiffeners across the bridge girder. The area of the main cables is 12% higher, this is to reflect the clamps and the hanger links, that is stabilizing the cables. If the towers are notched, the modulus of elasticity of the concrete is expected to be considerably lower than 40.000 N/mm^2, this is not considered in this analysis.

4.2.6 Other parameters

- Temperature coefficient; $0.00001\frac{1}{^\circ C}$
- Gravity of acceleration; 9.81 m/s^2

Chapter 5

Applying load in the finite element model

5.1 Mass

The weight of the girder, hangers and main cables are taken from the input in Alvsat [1]. The mass of the towers are calculated based on their geometry. The calculations can be found in Appendix B.

Length of main span is 446 m. Weight of the girder is 5350 kg/m.
Weight of bridge girder $5350 \times 446 = 2386$ ton

Length of cable in main span is 458.89 m. Weight of the cable is 816 kg/m.
Mass of main cable in main span $2 \times 816 \times 458.89 = 749$ ton

The mass of the hangers and hanger links are included in the weight of the bridge girder and main cables. The same weight is used for the main cable in the back stay as in the main span, this gives a slightly higher weight than in the real bridge, but the error is considered small.

Length of back stay north is 87.55 m, length of back stay south is 174.51 m.
Mass of cable in back stay $816 \times 2 \times (87.55 + 174.51) = 428$ ton

Towers weight are 7919 ton.

The mass summarized is given in Figure 5.1.

Bridge girder	2386 ton
Main cable main span	364 ton
Mass in main span	2750 ton
Main cable back stay	181 ton
Mass in back stay	181 ton
Towers	7919 ton
Total mass	10850 ton

Table 5.1: Mass of Lysefjord Bridge

The mass in ABAQUS is 11030 ton, see Appendix C, this is 2% higher than the theoretical calculations. This difference could be caused by errors in the calculations of the mass. E.g. the weight of the towers and the cross beams are calculated based on an average cross section area, while in ABAQUS, each element weight is different. The most important is to see that the weight of the model in ABAQUS makes sense, and that it is in the same order of magnitude as the calculated weight.

5.2 Modeling of mass

To model the mass in the bridge girder, lower hanger link and half the hangers, the weight is distributed into 3 discrete points. This is showed in Figure 5.1.

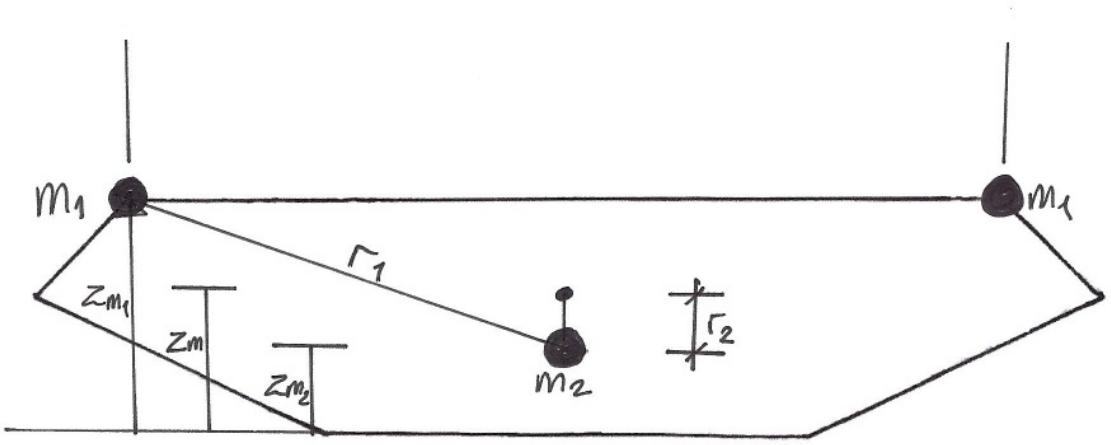

Figure 5.1: Modeling of mass of bridge girder in ABAQUS

From calculations in Mathcad;

- $m_1 = 1454\ kg/m$
- $m_2 = 2442\ kg/m$
- $r_1 = 5.267\ m$
- $r_2 = 0.85\ m$
- $Z_m = 1.656\ m$
- $Z_{m1} = 2.76\ m$
- $Z_{m2} = 0.806\ m$

The total mass is then;

$$M_{total} = 2 * m_1 + m_2 = 2 * 1454 + 2442 = 5350 kg/m$$

As can be seen in Figure 5.1, the lower mass point is placed 0,85 m under the neutral axis. This position is fitted such that the mass moment of inertia around the shear center, which here is placed in NA and the center of gravity is correct.
To sum up; the three different numbers, m_1, m_2 and r_2 are found from;

- Total mass of 5350 kg/m
- Mass moment of inertia 82430 kgm^2
- Center of gravity 0.12 m above N.A.

Note: The center of gravity is found from the Mathcad-calculations of the area of the bridge girder to be 0.12 m above N.A, see Appendix B. In the Mathcad-calculations to find the distribution of the load, the center of gravity is 0.21 m above N.A. The first calculation is done roughly, and without the weight of the hanger links and asphalt, that will bring the center of gravity higher up. One of the most important factor to obtain correct eigenfrequencies and displacements in the bridge is the mass moment of inertia, and in the calculations, this turns out as 82436 kgm^2, which is what was given in Alvsat.

To model the mass in ABAQUS, fictive nodes, or so-called dummy nodes have been used. These dummies are assigned mass in negative z-direction, to simulate dead load in the girder and hangers. The fictive nodes that are assigned $m_1 = 1454\ kg/m$, under the chord that is representing the bridge girder is shown in Figure 5.2.

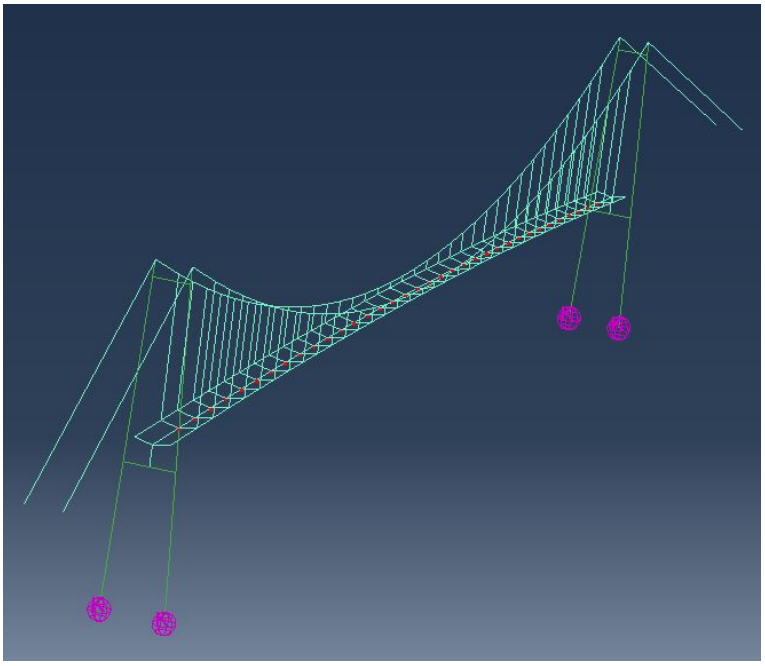

Figure 5.2: Fictive points to attach $m_1 = 1454\ kg/m$ under NA in ABAQUS

The mass of the hangers are evenly distributed, with 50% up to the upper hanger link, and 50% down to the lower hanger link. This distribution is chosen because this is how the mass was inserted into Alvsat.

The arrangement of the mass into 3 discrete points in the way it's been done here, is considered governing for eigenfrequencies and for static and dynamic wind analysis. If the bridge model later will be used in earthquake analysis, where the bending sideways between the hanger links is significant, this arrangement of mass should be calculated and distributed again. It is also important that the distribution of the mass in the longitudinal direction, and the element length is considered thoroughly in other analyses with this model.

5.3 Analysis of characteristic dead load

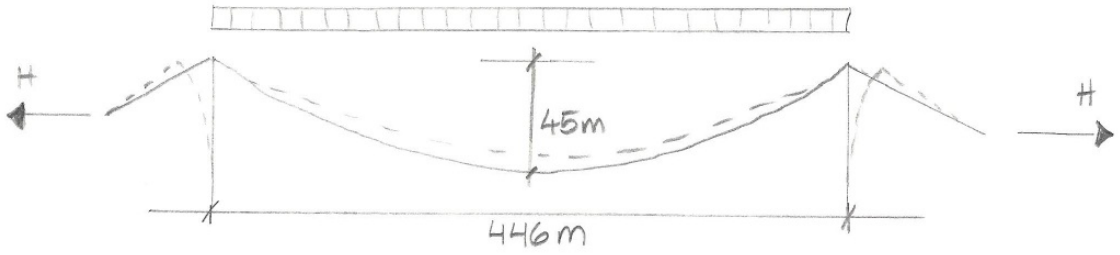

Figure 5.3: The model of the bridge with dead load applied

The dead load is based on a geometric non-linear analysis, the nodes are modeled with iterations such that after the model is loaded with dead load, the geometry should be correct, see Figure 5.3. There are however some differences between the loaded model and the real structure, but this is neglected. The model is modified several times to get the geometry as close to the real structure as possible. The parable for the bridge girder and the main cable is modified, such that with dead load on, the shortest hanger is 3 m, and the sag is 45 m. The equations for the parables are given in Section 4.2.2 on page 23.

Control of total horizontal force in both of the main cables;

$$M_{mainspan} = 2750ton = 26978kN$$

Theoretically;

$$H = \frac{F*L}{8*f} = \frac{26978*446}{8*45} = 33423kN$$

The analysis in ABAQUS;

$$H = 33731kN$$

Alvsat;

$$H = 33600kN$$

Difference between Alvsat and ABAQUS;

$33731kN - 33600kN = 131kN$ this is around 0.4%.

This should not affect the results to much, but could explain some of the differences in the results between ABAQUS and Alvsat. This constant loading in the main cables found from ABAQUS cause a stress of;

$$\sigma = \frac{H}{12A_c} = \frac{33731000\ N}{12{\cdot}0.0074\ m^2} = 380.4\ MPa$$

Where A_c is the cross section of one cable. The stress found here is, however, from the constant horizontal component of the force in the cables. The cables will have a maximum stress level where they are connected to the towers. To find the maximum stress level in the cables, the axial force in the element closest to the tower, 35110 kN, are used;

The true fore in the main cables close to the towers cause a stress of;

$$\sigma = \frac{F}{12A_c} = \frac{35110000\ N}{12 \cdot 0.0074\ m^2} = 395.4\ MPa$$

The cables used in suspension bridges in Norway today, included Lysefjord Bridge, has an ultimate tensile strength of 1570 MPa [18]. The stress from dead load on the bridge gives a demand/capacity rate in the cables of $\frac{395.4MPa}{1570MPa} = 25.2\%$.

5.4 Wind

The most complex loading on a suspension bridge is wind loading. Wind loading on the bridge girder can be divided into two different components, with static wind load that can be found from e.g. the mean characteristic wind speed, and dynamic wind load, that is induced by vortices, turbulence and due the movement of the bridge.

5.4.1 Static wind loading

The first group, the static wind velocity that is calculated from the mean wind speed, and the corresponding velocity pressure that is working on the bridge, is called static drag load and lift load. In addition, an overturning moment on the bridge will be generated. The load from drag forces acts in the direction of the wind. The lift force operate perpendicular to the direction of the wind, up or down on the bridge girder. The overturning moment acts around the bridge girders longitudinal axis. Mean value of these different forces, without turbulence and forces from movement of the bridge, can be calculated with the following equations:

Drag, force per length;

$$D = \frac{1}{2}\rho U^2 H C_D \tag{5.1}$$

Lift, force per length;

$$L = \frac{1}{2}\rho U^2 B C_L \tag{5.2}$$

Overturning moment, moment per length;

$$M = \frac{1}{2}\rho U^2 B^2 C_M \tag{5.3}$$

- ρ: air density
- U: the mean wind speed
- H: height of the bridge girder
- B: width of the bridge girder

C_D, C_L and C_M are parameters without dimension to reflect the wind load on the particular cross section geometry of the girder. These are usually found through tests in wind tunnels. They reflect all details on the bridge, e.g. railing. The parameters depend on the angle at which the wind acts on the bridge girder. Input data on Lysefjord Bridge is taken from the old analysis in Alvsat, this includes the wind load coefficients as well.

The coefficients are defined in the following.

Drag coefficient;

$$C_D = \frac{D}{qHl} \tag{5.4}$$

Lift coefficient;

$$C_L = \frac{L}{qBl} \tag{5.5}$$

Coefficient for overturning moment;

$$C_M = \frac{M}{qB^2l} \tag{5.6}$$

Where q is the mean velocity pressure $q = 0.5\rho U^2$, and l is the length of the bridge girder. Figure 5.4 shows the positive directions for the forces on the bridge girder. It also shows the angle of attack α.

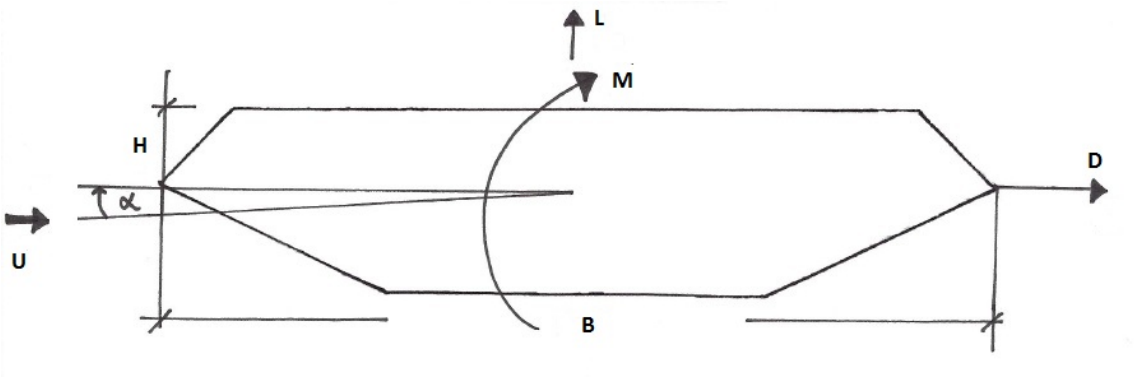

Figure 5.4: Positive directions for the forces, and the orientation of the wind.

The coefficients for Lysefjord Bridge found in Alvsat is simplified into linear functions of the angle of attack, based on the coefficient at $\alpha = 0$ and difference quotient for the tangent through this point. This gives us the following formulas for static drag, lift and overturning moment forces;

Drag;

$$D(\alpha) = \frac{1}{2}\rho U^2 h(C_D(\alpha = 0) + \alpha C_D'(\alpha = 0)) \tag{5.7}$$

Lift;

$$L(\alpha) = \frac{1}{2}\rho U^2 w(C_L(\alpha = 0) + \alpha C_L'(\alpha = 0)) \tag{5.8}$$

Overturning moment;

$$M(\alpha) = \frac{1}{2}\rho U^2 w^2(C_M(\alpha = 0) + \alpha C_M'(\alpha = 0)) \tag{5.9}$$

The wind load coefficients are shown in Table 5.2.

Drag coefficient	
C_D	1.00
$C_D^{'}$	0.00
Lift coefficient	
C_L	0.10
$C_L^{'}$	3.00
Moment coefficient	
C_M	0.10
$C_M^{'}$	3.00
Cable drag coefficient	
C_C	1.50

Table 5.2: Wind load coefficients

Since the quotient for the tangent of the drag coefficient is 0, drag force will be independent of the angle of attack. The drag load on the main cables is also assumed to be independent of the angle of attack, due to the round symmetric shape. In Lysefjord Bridge, the cable configuration, with six cables on each side, is different from the configuration with one main cable at each side, and this is considered to be taken into account by the drag coefficient used in Alvsat.

5.4.2 Mean wind speed

From Alvsat, the reference wind speed at the level of the bridge is given as 38.00 m/s. To calculate the wind speed around Lysefjord Bridge, the Norwegian Standard NS-EN 1991-1-4:2005+NA2009 is used [22].
The basic wind velocity is defined as middle wind speed in 10 minutes duration, 10 m above flat landscape for terrain category 2, and with a given return period of 50 years. The basic wind velocity for Forsand is 26 m/s. This basic wind velocity is then adjusted for different factors;

- Factor for wind directions; chosen for all directions; $C_{Direction} = 1.0$.
- Factor for season; chosen for the entire year; $C_{Season} = 1.0$.
- Factor for increasing wind speed with increasing height above sea level; ; $C_{HAS} = 1.0$.
- Factor for return period; chosen for a return period of 50 years; $C_{Returnperiod} = 1.0$.

The basic wind speed is then calculated to be;

$$W_{basic} = 1.0 * C_{Season} = 1.0 * C_{HAS} = 1.0 * C_{Returnperiod} = 1.0 * W_{Reference} = 26\ m/s \tag{5.10}$$

To take into account the terrain around the bridge, the place wind velocity is calculated. The place wind velocity is defined as the middle wind speed working on the bridge in 10 minutes. The height of the bridge, z, is set to 50 m above sea level, which is a mean value for the bridge girder. The reference height is $z_0 = 0.01\ m$, Terrain category 1 is chosen $k_T = 0.17$, this is for coastal sea, no trees. It could be discussed if this is the right terrain category, but it is considered to be the closest to the real terrain.

$$C_r = k_T ln(\frac{z}{z_0}) = 0.17 ln(\frac{50}{0.01}) = 1.448 \tag{5.11}$$

The topography factor, C_T is set to 1.0, since it is unclear if the terrain around the bridge will act reducing or increasing on the wind speed.

$$W_{place} = C_r C_T W_{basic} = 37.6 m/s \tag{5.12}$$

The place wind speed for the basic wind velocity and adjusted for terrain, topography and height, is 37.6 m/s, rounded up to 38 m/s. In the analysis, since the reference wind from Alvsat is the same as the one calculated, 38 m/s is used as the mean wind speed on the bridge.

It is also done some test analysis with higher wind speeds to see the movement of the bridge, and the displacement of the bridge girder. The results from these tests are described in Section 6.3 on page 64.

5.4.3 Simulated wind load in ABAQUS

To simulate the wind load on the bridge, distributed forces in horizontal and vertical direction as well as an overturning moment are applied to the model. The force in horizontal direction is drag, the force in vertical direction is lift, and the overturning moment is applied by a vertical force couple. The forces depend on the angle of attack, which again depend on the wind load. So an iterative approach is required. The plan was to simulate the wind with a subroutine in Fortran. This subroutine was originally developed for Hardanger Bridge by Jasna B. Jakobsen and Ingvild P. Bjørnsen, and it was modified to work on Lysefjord Bridge [3]. The routine in Fortran use parameters given in the ABAQUS input file, and with the form factors used in Alvsat. However, the subroutine would not work in the correct way, and in the end, the load was applied directly in the input file. The horizontal wind load is applied in positive direction, see directions in Figure 5.4 on page 37.

To simulate the wind on the bridge girder, dummy elements have been made in ABAQUS, see Figure 5.5 on the following page.

The wind load used in the analysis is for the wind velocity of 38 m/s. The drag force is applied on the bridge girder chord, and on the dummies on the side of the bridge girder, see Figure 5.5 on the next page. The lift force is applied on the bridge girder chord in a positive vertical direction. The overturning moment is applied as a vertical force couple on the bridge girder.

The forces are calculated and applied for 38 m/s with angle=0 in the first iteration. From the result file of this analysis, the rotation around length axis in the bridge girder, x-direction, is collected and used in a new calculation of the lift force and overturning moment. The new forces are applied to the bridge, and the procedure is repeated until the bridge twist converges. This takes 5 iterations. To see the displacement of the bridge girder for different wind forces, this procedure was also used for 20 m/s, 60 m/s and 80 m/s. The results are presented in Section 6.3 on page 64.

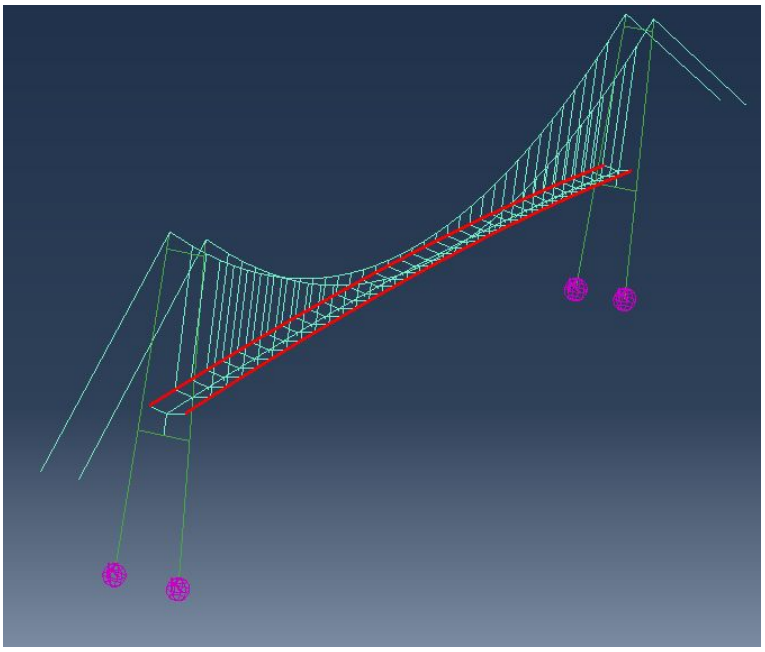

Figure 5.5: Dummy elements to simulate wind on the bridge girder in ABAQUS

In ABAQUS, a new step is created to apply wind loading. The AMPLITUDE=RAMP function is used, such that the load magnitude is to vary linearly over the step, from the value at the end of the previous step, to the value given on the loading option. It is used non-linear geometry in the loading, and 5000 increments. The option DLOAD is used to apply the load as a distributed load. The parameter OP=MOD is used, such that the existing loading from Step 1 remain. This option can be used to modify existing distributed loads, or defining additional distributed loads [15].

5.4.4 Dynamic wind loading

Suspension bridges with a certain length of the main span of the bridge are subjected to aerodynamic forces generated by structural motions. These self-excited motions are in turn excited and changed by the aerodynamic forces they generate. Aero elastic phenomena is interesting in suspension bridge design because of the shape of the bridge girder, the obstacles along the bridge girder such as hand railing, and because the wind flows around bridges often is turbulent [25]. On Lysefjord Bridge, the aero elastic behavior of vortex-induced oscillations is described qualitatively in the following.

Vortex-induced vibration

Vortex-induced vibrations on the bridge are motions in the structure excited by a force having the same frequency as the structure. In order to limit or prevent the vortex-induced vibration and the associated structural fatigue, there are several actions that can be taken. The eigen-frequency can be modified or increased, additional dampers can be installed on the bridge, or the generations of vortices can be disturbed by different obstacles that can be placed at the structure. The interference between an outer force exiting the bridge at the same wave-length as the bridge is called resonance. Resonance can be fatal to a bridge, as the vibrations created can be very large. These resonance vibrations

travel through the bridge like waves. When dampers or obstacles are introduced, they will interrupt the resonance, and prevent large vibrations. The obstacles can be placed all over the structure where needed [16].

The bridge girder have a bluff cross section, and the wind flow can experience separation and vorticity shed in the body wake. The flow around the bridge girder can depend on the Reynold number, R_e;

$$R_e = \frac{UD}{\upsilon} \tag{5.13}$$

- U: Wind speed
- D: Height of the bridge girder
- υ: Kinematic viscosity of air, 1.51E-5

For a wind speed of 38 m/s found in Section 5.4.2 on page 38, and a height of the bridge girder of 2.76 m.

$$R_e = \frac{38m/s \cdot 2.76m}{1.51E10 - 5} = 6.9E6 \tag{5.14}$$

For bodies with sharp corners, separation of the wind flow occurs at fixed points regardless of the value of R_e. The separation of the wind flow is also dependent on e.g. handrails. When the air flow is separated, vortices are induced alternately on the top and bottom of the bridge girder, and this induce a force in the vertical direction. The main pressure variations and fluctuating force associated are predominantly in the direction across the flow, see Figure 5.6 [16].

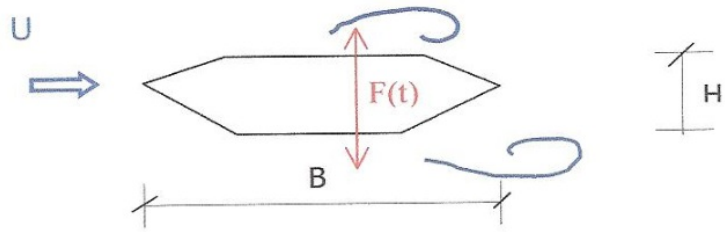

Figure 5.6: Vortex shedding around the bridge girder [16]

The shedding frequency is directly proportional to the wind speed U, inversely proportional to the reference dimension D, and depends on the cross sectional shape through a constant S_t called Strouhals number.

To find the critical wind speed at which the bridge will experience vortex-induced vibration;

$$f_s = \frac{S_t U}{D} \tag{5.15}$$

- S_t: Strouhals number
- U: Wind speed
- D: Height or width of the bridge girder

Strouhals number can be set to;

$$S_t = \frac{S_t U}{D} = 0.11 \tag{5.16}$$

... if the width over height ratio is close to 4.5, and height is used as D [13]. This was found from testing of an early design of Hardanger Suspension Bridge girder. From [22], Strouhals number for a rectangular box shape with the ratio around 4.5, is slightly higher than 0.11, but it is in the same order of magnitude. For Lysefjord Bridge;

$$\frac{w}{h} = \frac{12.3}{2.76} = 4.46 \tag{5.17}$$

and

$$S_t = 0.11 \tag{5.18}$$

The period of the first vertical symmetric mode shape is 3.29 seconds, and the frequency is then;

$$f_{vs1} = \frac{1}{3.29s} = 0.3Hz \tag{5.19}$$

To find the critical wind velocity, the vortex shedding in Equation 5.15 on the previous page is set equal to f_{vs1};

$$U_{cr} = \frac{f_{vs1} D}{S_t} = \frac{0.3Hz \cdot 2.76m}{0.11} = 7.5\ m/s \tag{5.20}$$

The wind velocity that can induce vertical symmetric mode shape 1 is 7.5 m/s. There is a fair chance that this is a common wind speed around the bridge, the average wind speed in 2010 was 2.3 m/s [21]. The critical wind velocity for vertical symmetric mode shape 2, calculated in the same way as for 1, is 10.2 m/s. The wire fractures in the main cables could therefore be partially caused also by fatigue from vortex-induced vibrations.

5.4.5 Non-linear geometric effects

The loading studied on this bridge model is dead load and wind load. In all the loading steps, ABAQUS is told that this is a non-linear geometry, by the command NLGEOM. This means that the deformations of the structure from loading are taken into consideration when more loading are applied. The effect from the extra loading caused by deformation is neglected if it is small, but in large deformations, this effects should be accounted for. Since Lysefjord Bridge is a suspension bridge, that is a relatively flexible construction, the loading is given as non-linear in all the steps in the model. This means that the analysis will take the non-linear geometric characteristics into consideration.

5.5 Other loads

There is also other loads and conditions that will excite the bridge, but these are not considered in this model and analysis in ABAQUS.

5.5.1 Earthquake

The model is not analyzed for earthquake in this thesis. If the model is to be used for this kind of analysis, it is important to consider the elements and the mass for the new analysis, see Section 5.2 on page 33.

5.5.2 Traffic

Traffic loading is an important loading to take into consideration when designing a bridge. In this thesis, the focus has been on building the finite element model in ABAQUS, and on some wind analysis. Traffic is therefore not a part of the analysis, but that should be done in a further analysis of the bridge in light of the deterioration of the main cables.

Chapter 6

Results from the analysis in ABAQUS

The purpose of the analysis of the model in ABAQUS, was to understand the bridge behavior during static loading, and to see how the bridge is deformed due to wind load from different wind speeds. The analysis is also done to see if the results differ from the previous analysis done in Alvsat. It is both the natural frequencies and the deformation and stresses from traffic, wind and other loads that is interesting to find. Since this finite element model is made based on numbers from the previous analysis in Alvsat, the input-data is as similar as possible. This does however not mean that the output-data will be similar, since the model in ABAQUS also includes the hangers and the towers. There is also a question about the geometry, and there could be some differences in the parable of the cable, the bridge girder, or the length of hangers. The effect of the towers are taken into consideration, and an analysis without them is also carried out. The effect of changing different parameters in the model is analyzed and described in the following.

The natural frequencies are outside the control of the designer once the sag of the cables has been selected. Further, the natural modes can be divided into shapes that are symmetric about the center, mid-span point, and shapes that are asymmetric. The cable tension are not changed in the asymmetric modes, these modes are associated with a longitudinal motion of the cable in the main span. This may be very important in the lowest asymmetric mode. The tension in the cables are however changed in the symmetric modes, with the associated cable length condition being satisfied over the aggregate length from anchorage to anchorage [29]. The sag in Lysefjord Bridge is 45 m, and there was done several iterations in the analysis to obtain the exact sag when the bridge was loaded with dead load. The bridge girder gives a significant contribution to the torsion stiffness of the bridge.

6.1 General

During the modeling process, different parameters in the model have been changed to see how this will influence the results from the analysis. The first results gave eigenfrequencies that did not match the results from Alvsat, even though the model should be built on the same input variables. The model in ABAQUS was less rigid than the one in Alvsat. This could be caused by very many things, such as errors in the input file, different shear and

mass center, different areas, and the fact that the model in ABAQUS directly includes the towers and the hangers. To see which input parameters that influenced the results most, the model was modified by changing one parameter at the time, and analyzed. The different analysis was then compared, to see how much the different results had changed. A presentation of the final model in ABAQUS, and of some of the tests that has been done to the model to understand the function of the parameters are given in the following.

6.2 Eigenfrequencies and eigenmodes

6.2.1 Eigenfrequencies

The frequencies of the eigen modes of a suspension bridge are important when dynamic response including the aerodynamic stability of the bridge is studied. The eigenfrequencies for the bridge are calculated about the center of gravity. In Appendix C, the first three eigenfrequencies are given in a cumulating list. The eigenfrequencies are found for the different types of modes. The first 3 modes are found of each type, this means that there is found 18 modes of vibration that is presented here;

- Group 1
  - HS-1: Horizontal symmetric, 1. mode
  - HS-2: Horizontal symmetric, 2. mode
  - HS-3: Horizontal symmetric, 3. mode
- Group 2
  - HA-1: Horizontal asymmetric, 1. mode
  - HA-2: Horizontal asymmetric, 2. mode
  - HA-3: Horizontal asymmetric, 3. mode
- Group 3
  - VS-1: Vertical symmetric, 1. mode
  - VS-2: Vertical symmetric, 2. mode
  - VS-3: Vertical symmetric, 3. mode
- Group 4
  - VA-1: Vertical asymmetric, 1. mode
  - VA-2: Vertical asymmetric, 2. mode
  - VA-3: Vertical asymmetric, 3. mode
- Group 5
  - TS-1: Torsion symmetric, 1. mode
  - TS-2: Torsion symmetric, 2. mode
  - TS-3: Torsion symmetric, 3. mode
- Group 6
  - TA-1: Torsion asymmetric, 1. mode
  - TA-2: Torsion asymmetric, 2. mode
  - TA-3: Torsion asymmetric, 3. mode

6.2.2 Comparison of the eigenfrequencies in Alvsat and ABAQUS

The eigenfrequencies from Alvsat, the original ABAQUS-model and the tests are shown in Table 6.1 on the next page.

ABAQUS original model compared to Alvsat

The original model of the bridge in ABAQUS is built on the same input parameters as the Alvsat model. There are however differences, explained in the beginning of the chapter, that will give results that differ from the original results. For the horizontal and vertical modes, the difference is around 0-6%, and for the torsion modes, the difference is from 10% to 23%. The higher mode, the larger difference between the results. Some of the differences in torsion modes can be caused by the fact that ABAQUS includes the strain in the hangers, while Alvsat does not.

Test 1

The shear center in the original model is assumed to be in the neutral axis. In Alvsat however, the shear center is set to be 0.4 m under the hanger link. This is included in test 1, where the option SHEAR CENTER is included in ABAQUS, and the shear center is set 0.704 m above the neutral axis of the bridge girder, see Figure 4.3 on page 24. Due to railing and asymmetric loading of the bridge, the shear center could be eccentric in horizontal, y-direction as well, but this is neglected in this model. The frequencies does not change when the shear center is included in this way in ABAQUS.

Test 2

Since the big difference between the model in Alvsat and ABAQUS is the presence of towers, this was expected to have impact on the results. To see how the modes are affected by the rigidity and mass of the towers, the towers was removed from the model. Instead of the towers, boundary conditions was induced. The main cables were fixed in vertical direction, and in the horizontal direction, y- direction, perpendicular to the length of the bridge in the top point. The bridge girder was fixed in the ends, instead of being coupled to the cross beams. The eigenfrequencies in ABAQUS were influenced by this to a different degree, when the tower was removed, some of the values were more equal to the results from Alvsat. No significant changes was found.

Test 3

The original model reflects the bridge asymmetry about the mid span. In test 3, a symmetric version of the model, where the north part of the bridge is mirrored to the south part is made. The towers are not included in this test. This is to see how symmetry alone changes the results, and if the asymmetry in the bridge can make the cables act in a different way. The results from test 3 show that the horizontal frequencies is closer to the results in Alvsat, with max difference of 2%. The mode shapes look more like the modes from Alvsat compared to the modes in the original model. If Alvsat calculates the model as symmetric, this is probably the explanation to this change. All the other

frequencies are about the same as in the original model, the values are higher except from the first torsion symmetric and asymmetric frequencies. This difference could be due to the change in boundary conditions for the cables in x-direction (length direction) in the top of the towers. Without the towers the cables are free to move over the top. It could also be due to the difference in hanger length on the south side, where the hangers in test 3 are shorter than in the original model.

	Alvsat	Original		Test 1		Test 2		Test 3	
	Period[s]	Period[s]		Period[s]		Period[s]		Period[s]	
HS-1	7,71	7,81	1 %	7,81	1 %	7,77	1 %	7,75	0 %
HS-2	1,80	1,88	5 %	1,88	5 %	1,86	4 %	1,78	-1 %
HS-3	1,20	1,21	0 %	1,21	0 %	1,23	2 %	1,21	0 %
HA-1	2,26	2,31	2 %	2,31	2 %	2,28	1 %	2,28	1 %
HA-2	1,67	1,71	2 %	1,71	2 %	1,70	2 %	1,68	0 %
HA-3	1,00	1,02	3 %	1,02	3 %	1,03	3 %	1,02	2 %
VS-1	3,49	3,29	-6 %	3,29	-6 %	3,28	-6 %	3,22	-9 %
VS-2	2,50	2,45	-2 %	2,45	-2 %	2,43	-3 %	2,40	-4 %
VS-3	1,15	1,16	0 %	1,16	0 %	1,16	1 %	1,16	1 %
VA-1	4,69	4,68	0 %	4,68	0 %	4,52	-4 %	4,42	-6 %
VA-2	1,70	1,72	1 %	1,72	1 %	1,71	1 %	1,71	1 %
VA-3	0,83	0,84	1 %	0,84	1 %	0,84	1 %	0,84	1 %
TS-1	0,87	0,96	10 %	0,96	10 %	0,97	11 %	0,94	8 %
TS-2	0,31	0,36	14 %	0,36	15 %	0,37	18 %	0,38	19 %
TS-3	0,18	0,23	19 %	0,23	19 %	0,20	7 %	0,23	19 %
TA-1	0,47	0,53	11 %	0,53	11 %	0,55	14 %	0,55	14 %
TA-2	0,23	0,28	18 %	0,28	18 %	0,28	16 %	0,27	15 %
TA-3	0,15	0,20	23 %	0,20	23 %	0,17	12 %	0,20	22 %

Table 6.1: Calculated eigenfrequencies in ABAQUS compared to Alvsat

Table 6.1 summarizes the results for the analyses with the following models;

- Original: Towers are included, shear center in N.A.
- Test 1: Shear center at 0.704 m above N.A.
- Test 2: Model without towers, shear center in N.A.
- Test 3: Symmetric model without towers, shear center in N.A.

6.2.3 Comparison of the eigenmodes in Alvsat and ABAQUS

The comparison of the 18 mode shapes from Alvsat and the original model in ABAQUS is shown in Figures 6.1 on page 49 to 6.6 on page 54.

All the mode shapes are presented for the bridge girder. In ABAQUS the nodal displacement of an eigenmode is normalized in such a way that the maximum displacement within the structure is set to 1. Where the modes shown have largest value lower than one, this means that the maximum displacement occurs in the towers or in the cables. A difference between Alvsat and ABAQUS is that in Alvsat, no coupled modes are given, while there are in ABAQUS. Therefore, the modes from ABAQUS are considered un-coupled as long as the coupling is insignificant. A pure torsion mode is equal to a vertical displacement

in the cables of +1. The mode shapes from Alvsat is found from the output file, and they are shown as the displacement along the length of the bridge girder.

The horizontal modes found in ABAQUS are similar to the ones found in Alvsat. Horizontal symmetric mode 2 is asymmetric in ABAQUS, this is most likely caused by the fact that the bridge is asymmetric, and the hangers are longer on the south side of the bridge than on the north side. Horizontal asymmetric mode 3 is really a symmetric mode in the bridge girder, while the cables has the asymmetric form, see Figure 6.8 on page 56. The vertical mode shapes have a similar shape, while some of the modes has relatively large differences in the frequencies, and this is reflected in the size of the amplitude. The torsion mode shapes are also similar, the differences are larger in the higher modes than in the lower. This differences can partially be explained by the strain in the hangers that are included in ABAQUS, but not in Alvsat.

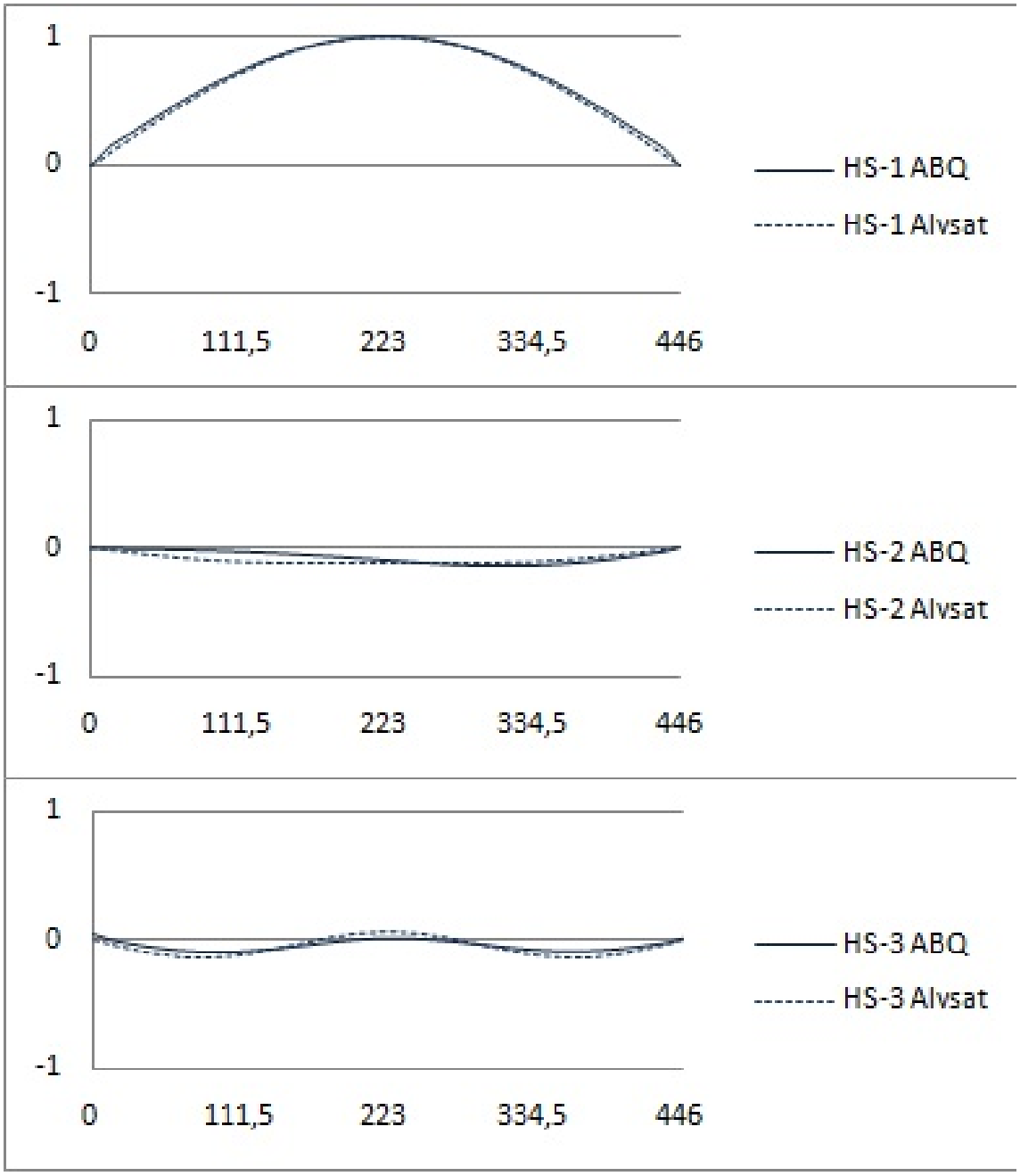

Figure 6.1: Horizontal symmetric modes

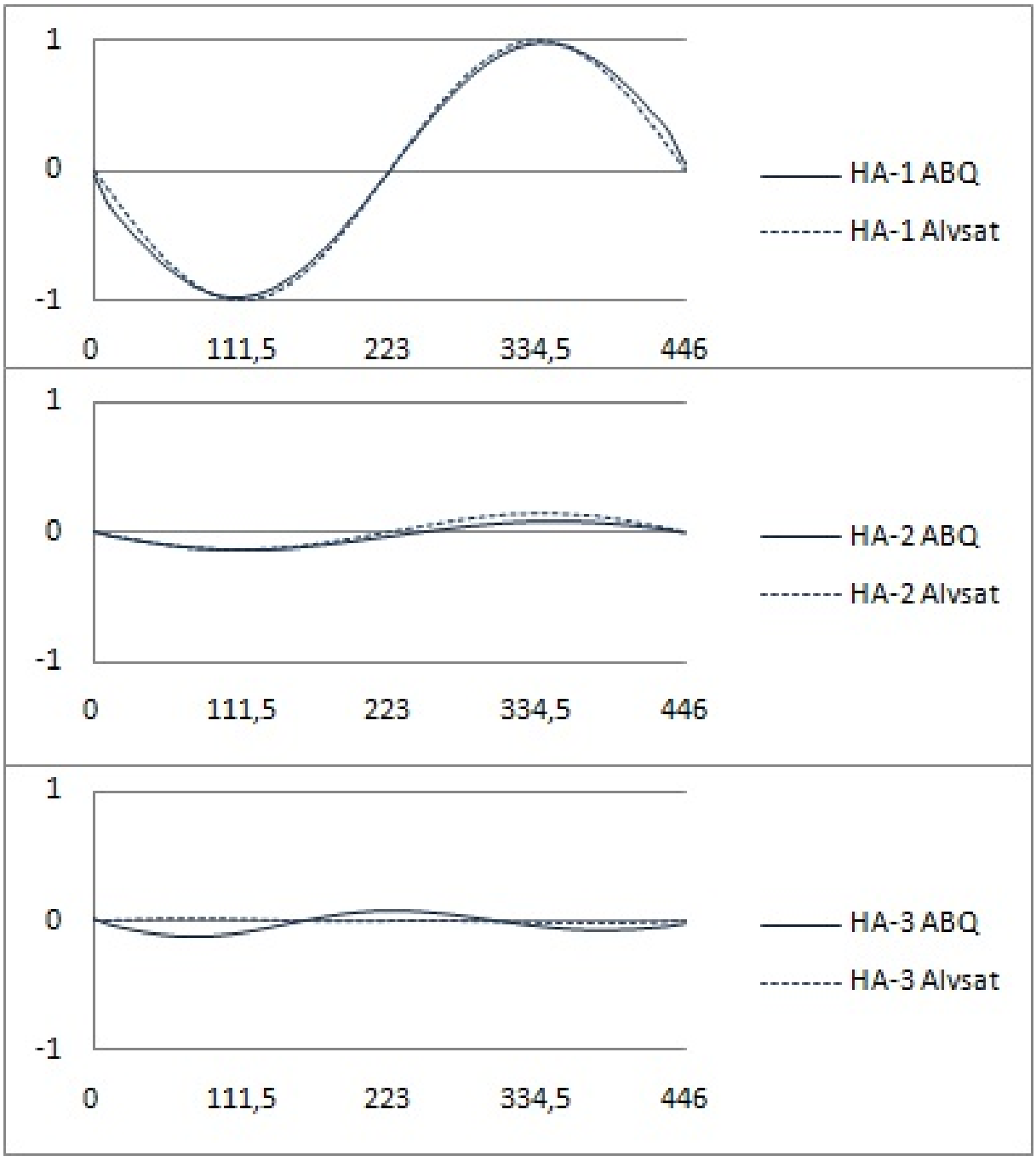

Figure 6.2: Horizontal asymmetric modes

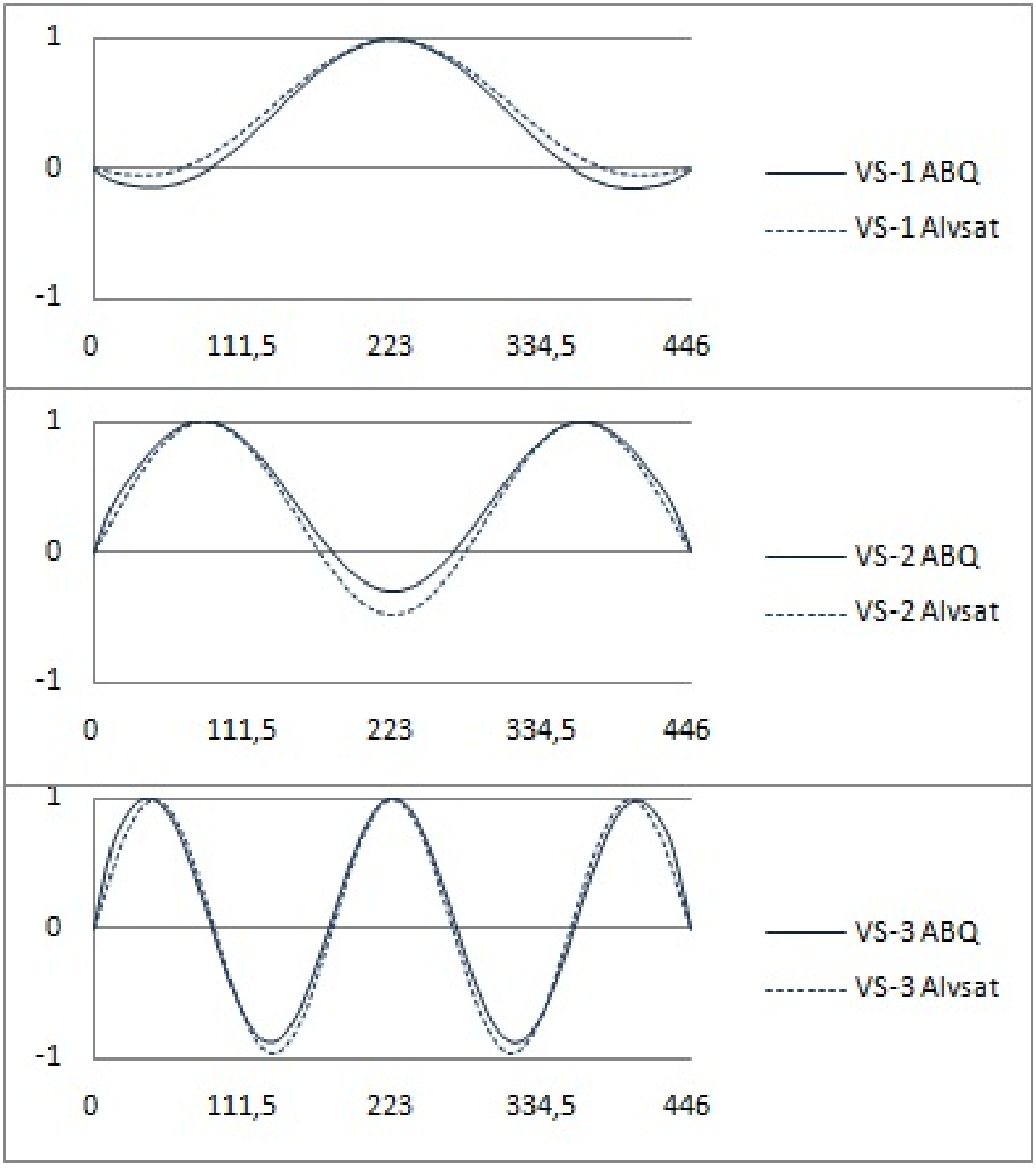

Figure 6.3: Vertical symmetric modes

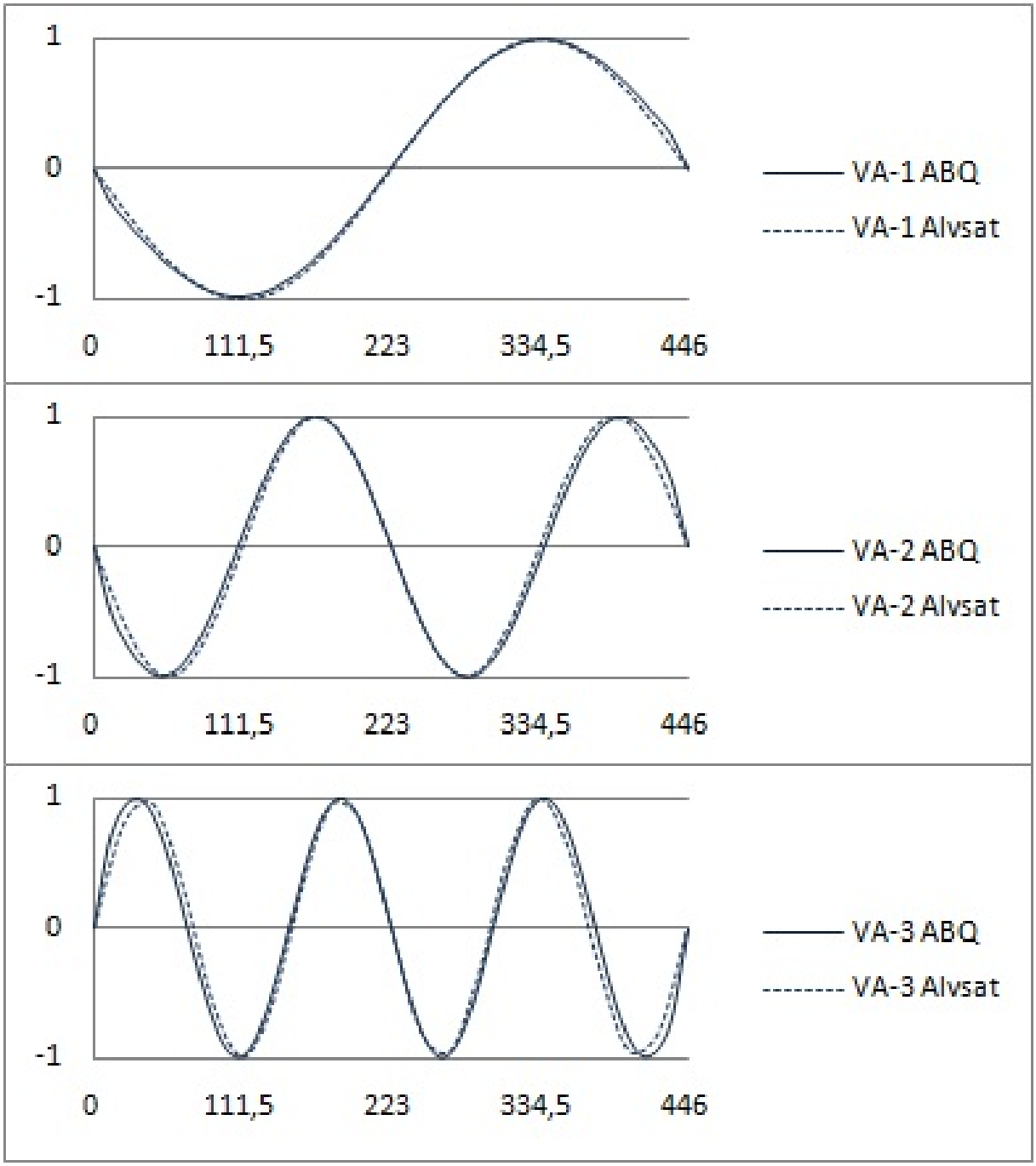

Figure 6.4: Vertical asymmetric modes

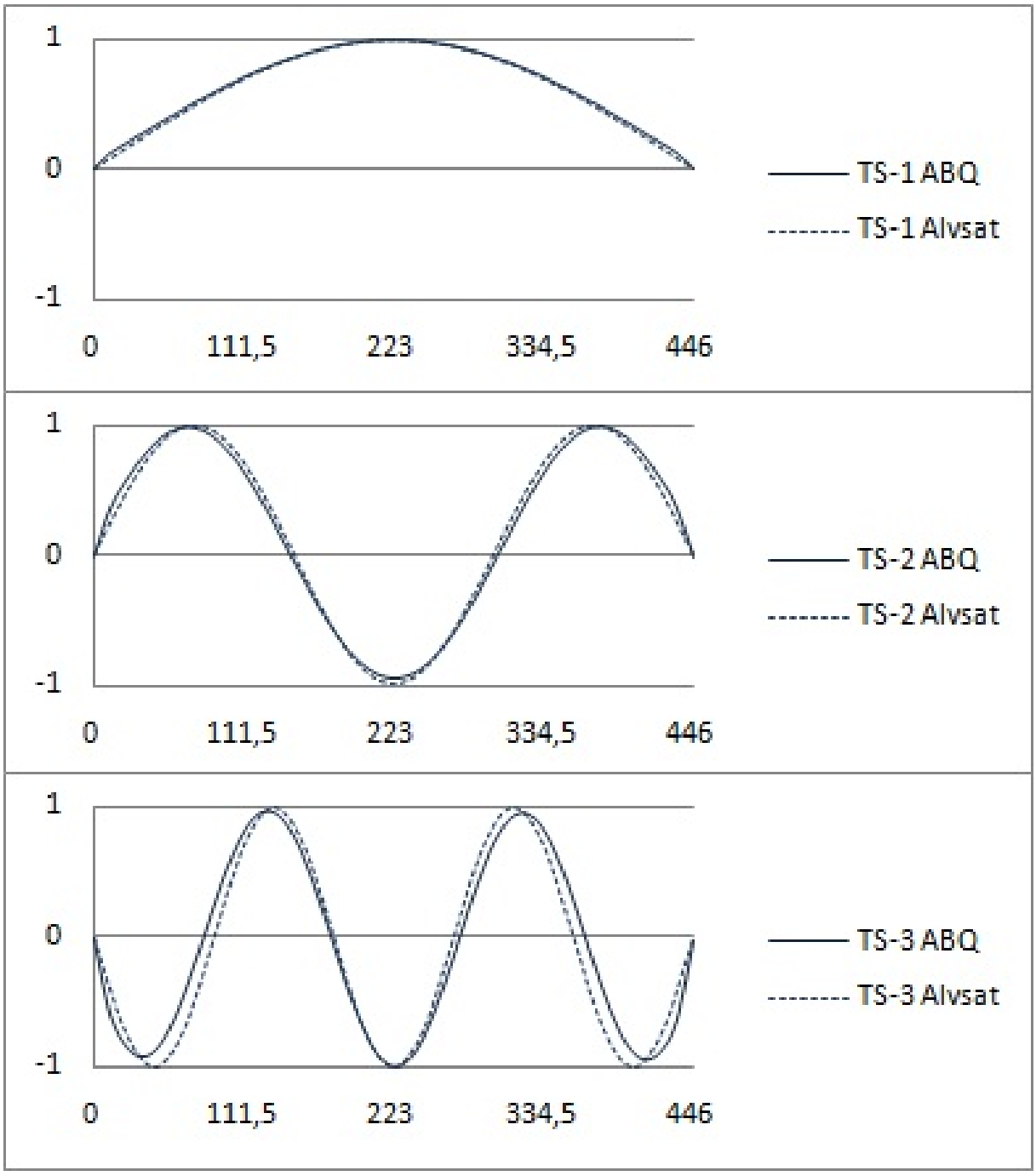

Figure 6.5: Torsional symmetric modes

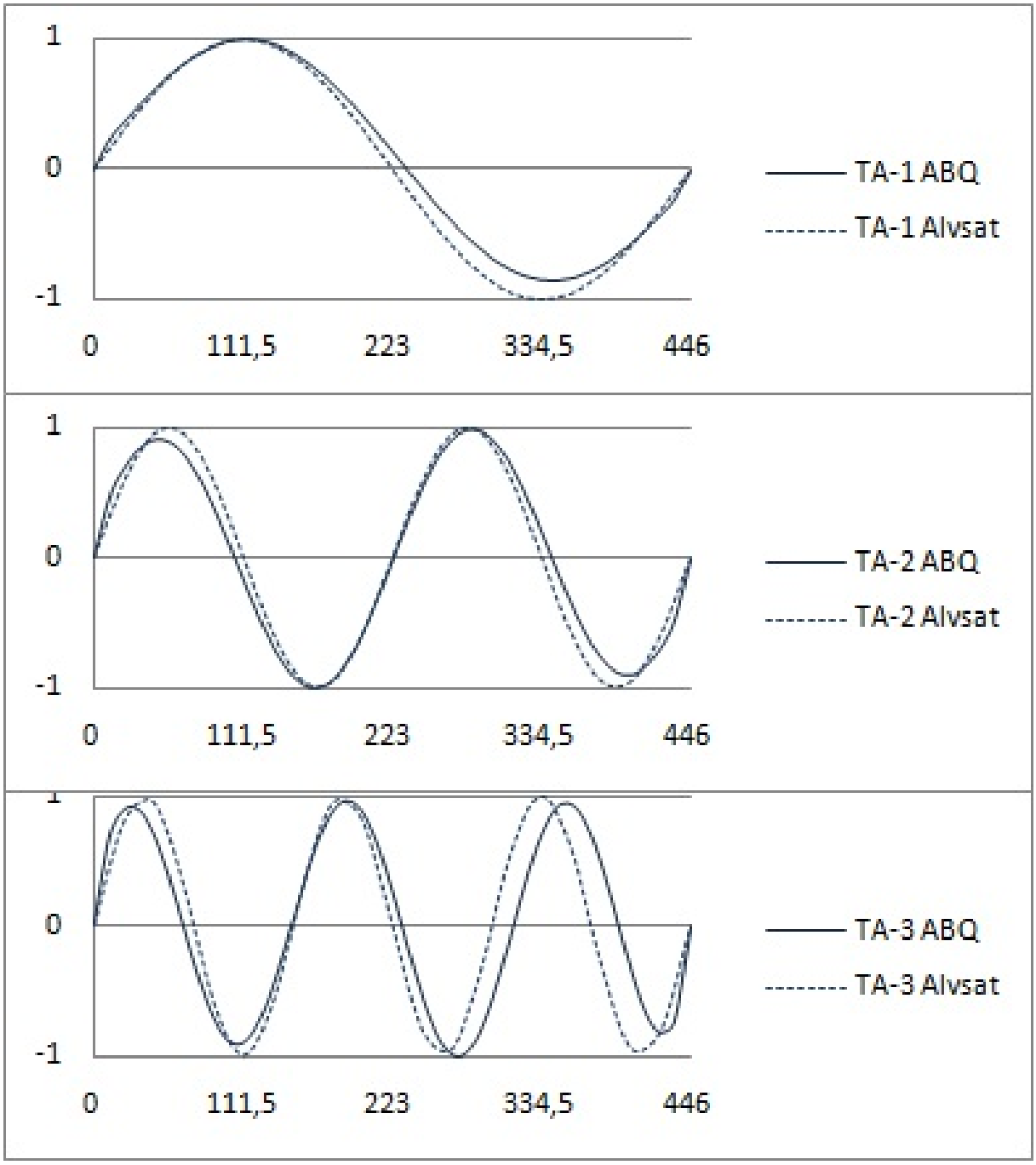

Figure 6.6: Torsional asymmetric modes

6.2.4 Horizontal displacement of the cables

This section refers to the horizontal displacement in the bridge only. The reason for this is to see the difference in displacement between the cables and the bridge girder. This is not a comparison between ABAQUS and Alvsat. There is a relative displacement between the bridge girder and the cables in the horizontal direction, and they are shown in Figures 6.7 and 6.8 on the following page. In the figures, the displacement of the bridge girder and cables are plotted on top of each other.

In all the modes except for the first symmetric one, the cables have the largest displacement. It is only in the 1. symmetric and asymmetric mode that the cables and the bridge girder have the same shape.

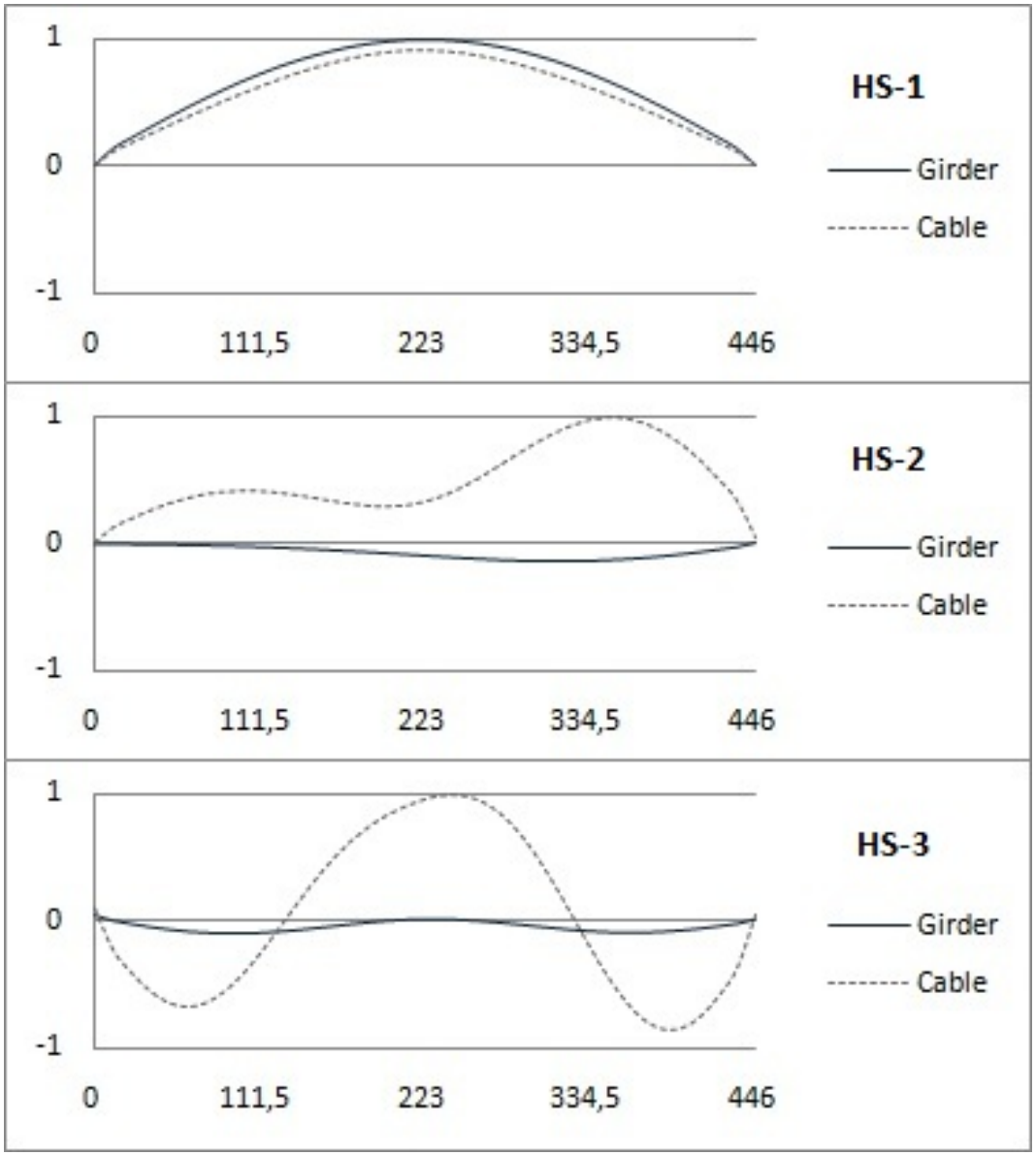

Figure 6.7: Horizontal symmetric modes, displacement in girder and cables

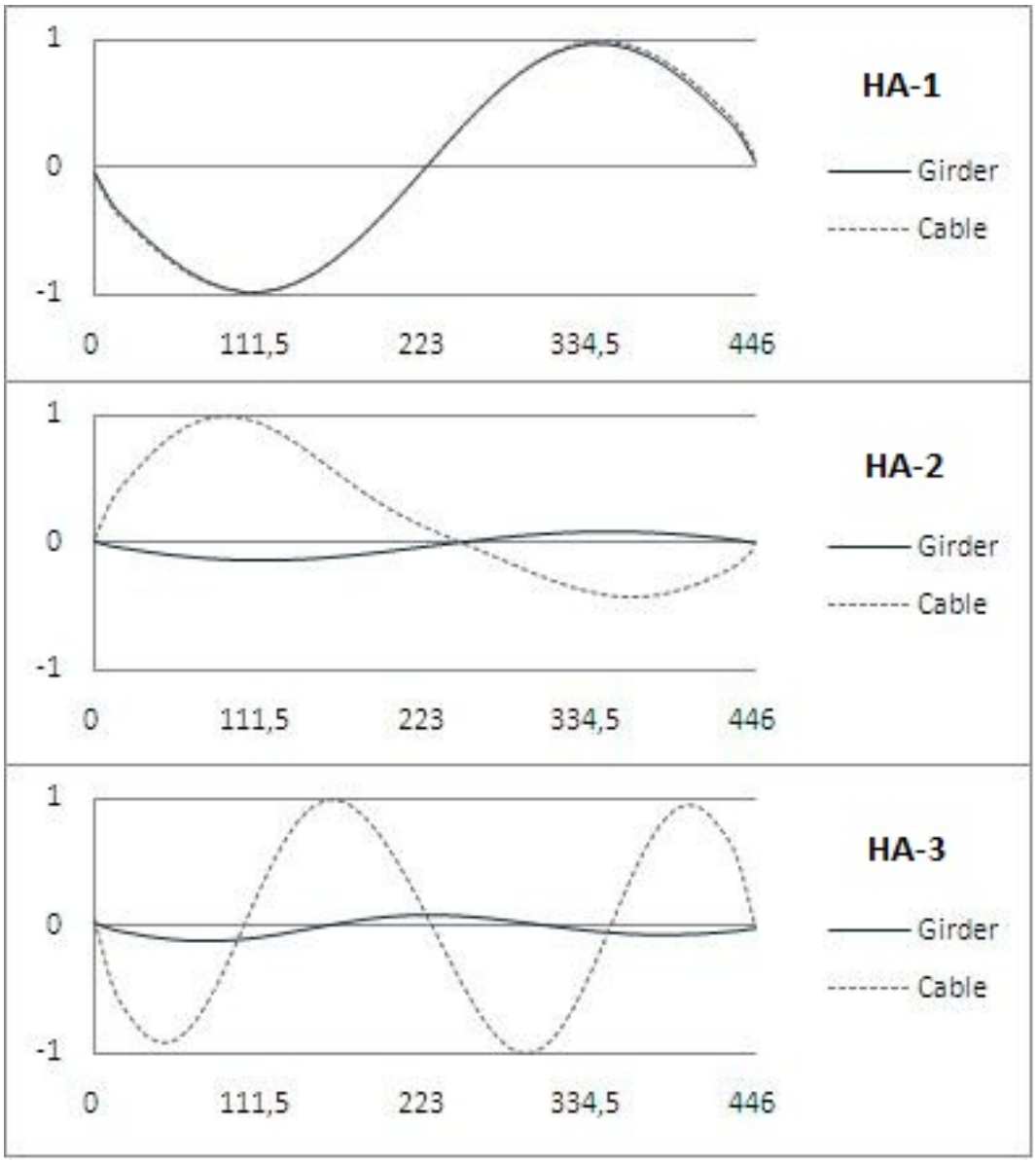

Figure 6.8: Horizontal asymmetric modes, displacement in girder and cables

6.2.5 Coupling of the directions

Alvsat is based on the uncoupled modes of vibration in the three directions, horizontal, vertical and torsion. The model in ABAQUS is used to see if this gives the correct results. In Figure 6.9 on the next page to 6.14 on page 63 the modes from ABAQUS is shown. In each diagram, the deformation along the bridge girder in the three different directions are drawn on top of each other. They are labeled;

- Y: Horizontal
- Z: Vertical
- T: Torsional

The bridge girder is fixed in the longitudinal direction, x, such that displacement is prohibited. The towers and the cables can move in this direction though.

The horizontal and vertical component are found directly from the output from ABAQUS. Torsional component are given as rotation in radians, and to plot the displacement from torsion, the rotation is multiplied by half the width of the bridge girder, and then normalized such that the largest displacement is set equal to +1.00.

Horizontal and vertical modes

Figure 6.9 on the next page to 6.12 on page 61 shows that the modes from ABAQUS are pure and uncoupled, similar to the mode shapes given in Alvsat. The maximum value in the second and third horizontal symmetric and asymmetric mode shapes are lower than 1. This does not mean that the mode is coupled to other directions, but it means that the maximum displacement appear in the cables, not in the bridge girder.

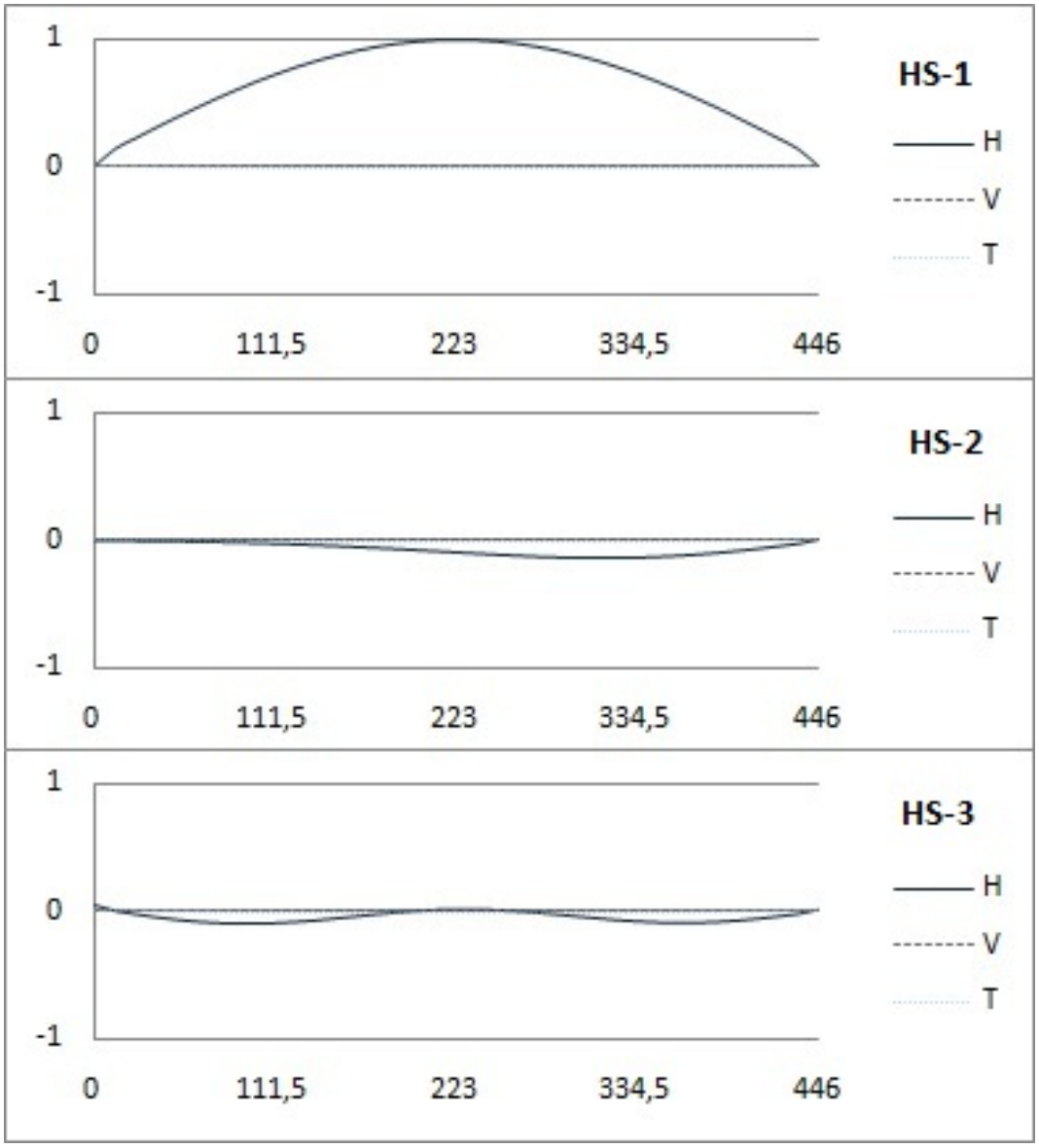

Figure 6.9: Horizontal symmetric mode, coupled

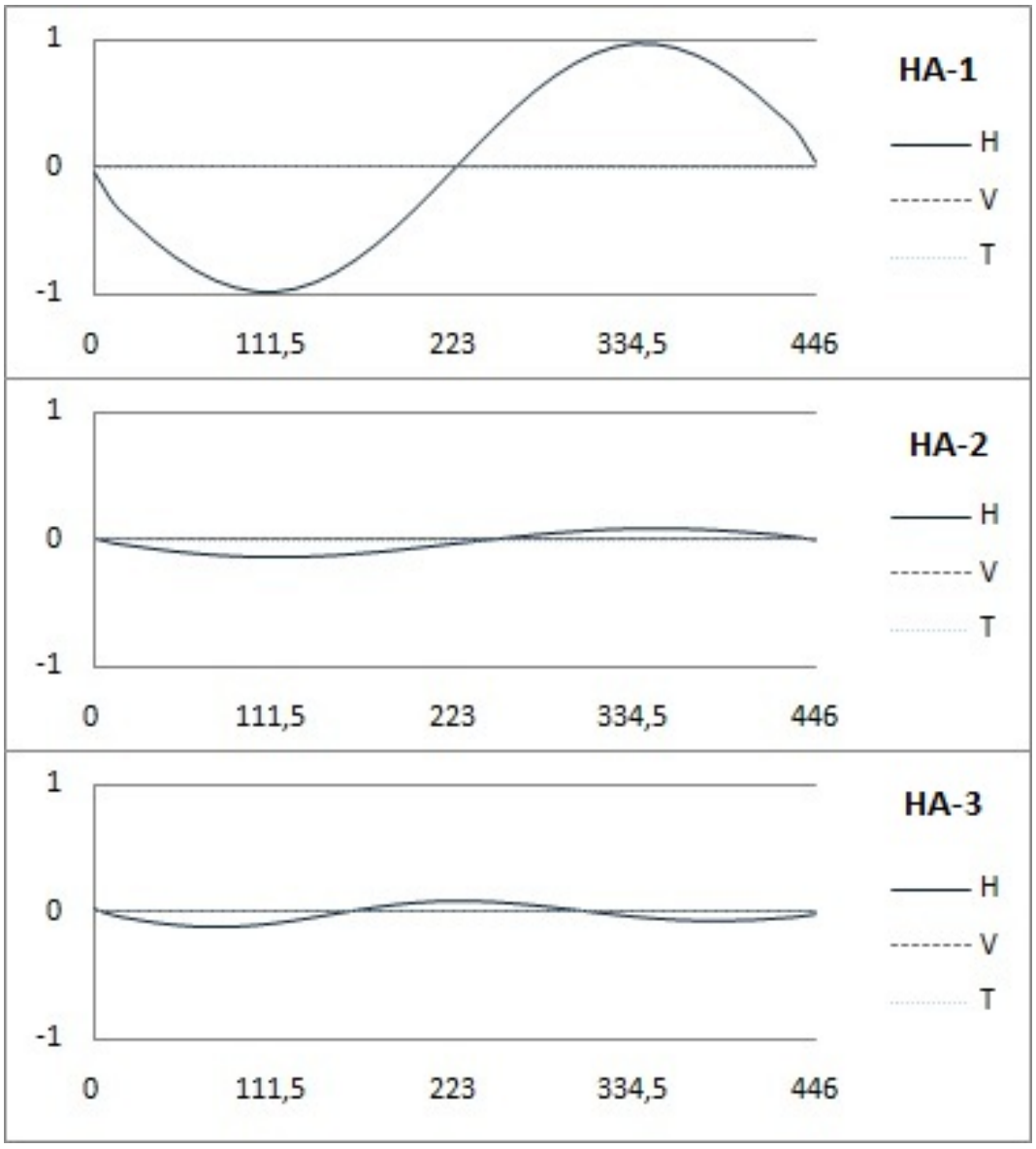

Figure 6.10: Horizontal asymmetric mode, coupled

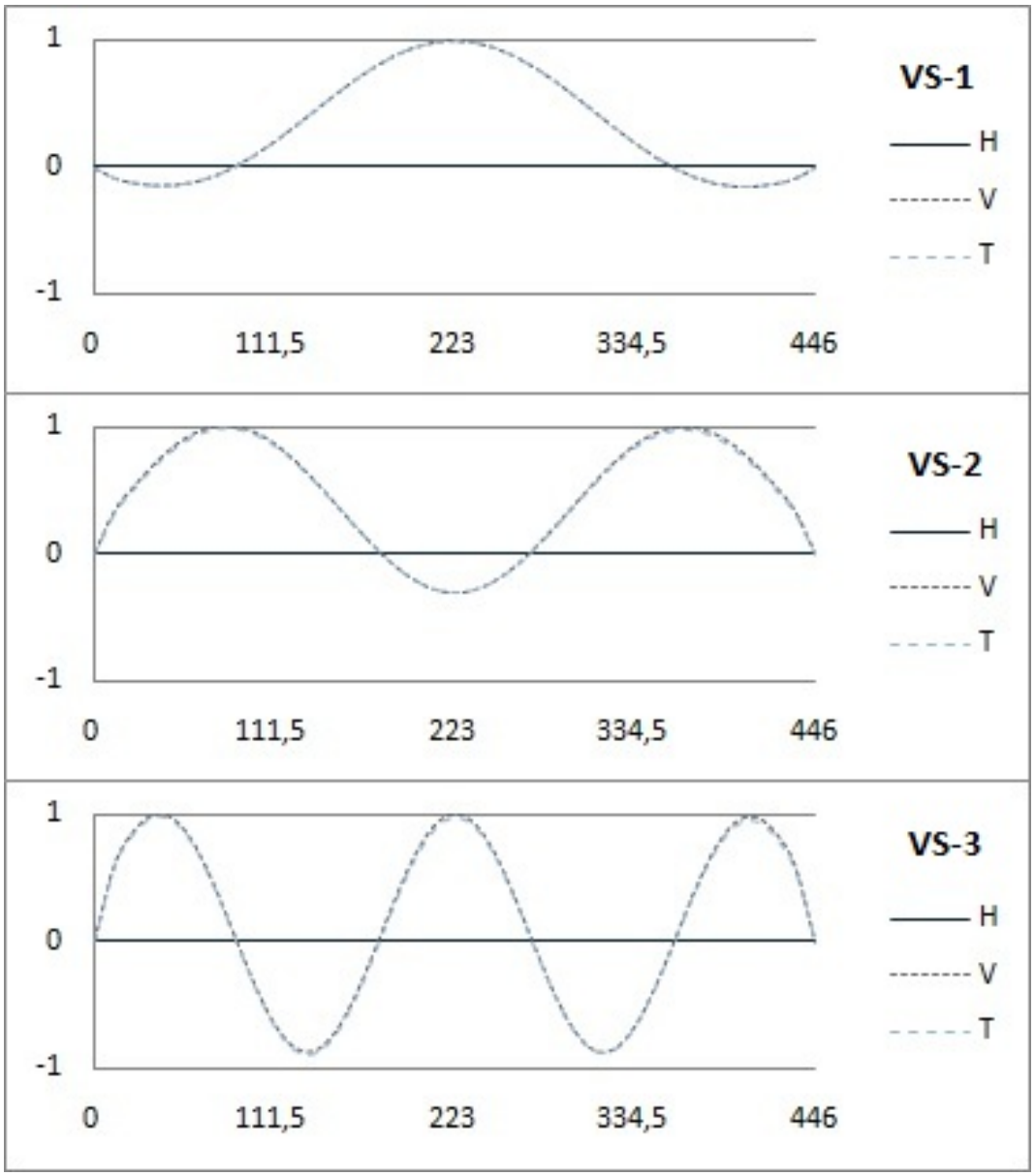

Figure 6.11: Vertical symmetric mode, coupled

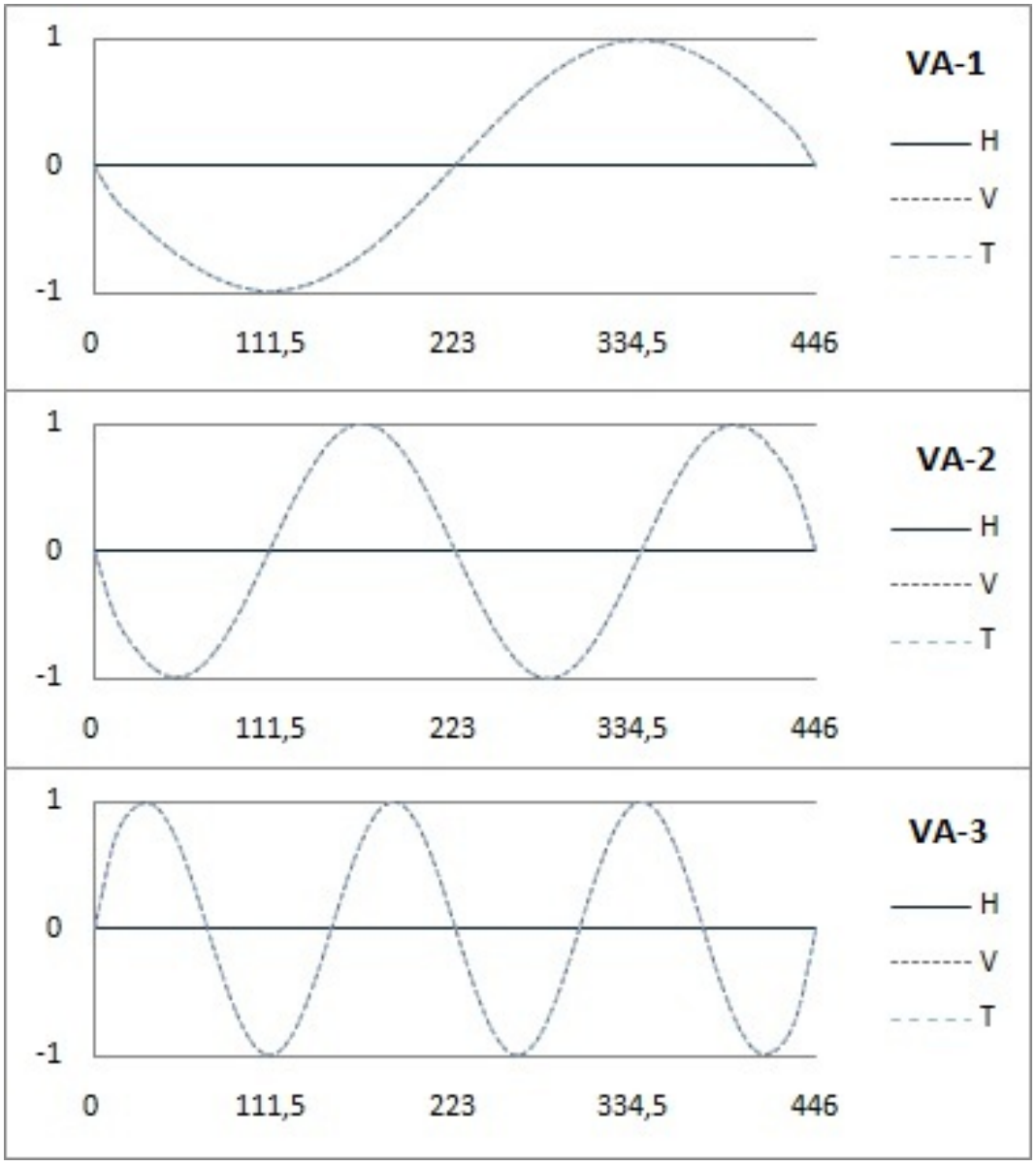

Figure 6.12: Vertical asymmetric mode, coupled

Torsional modes

Figure 6.13 and 6.14 on the following page shows that all the symmetric modes, and the first asymmetric mode is coupled to the horizontal direction.
There is a larger horizontal component in the first mode, than in the third mode. This could explain some of the differences in the frequencies between ABAQUS and Alvsat. Vertical displacement due to torsion refers to a point 5.125 m to the side of the centerline of the bridge girder.

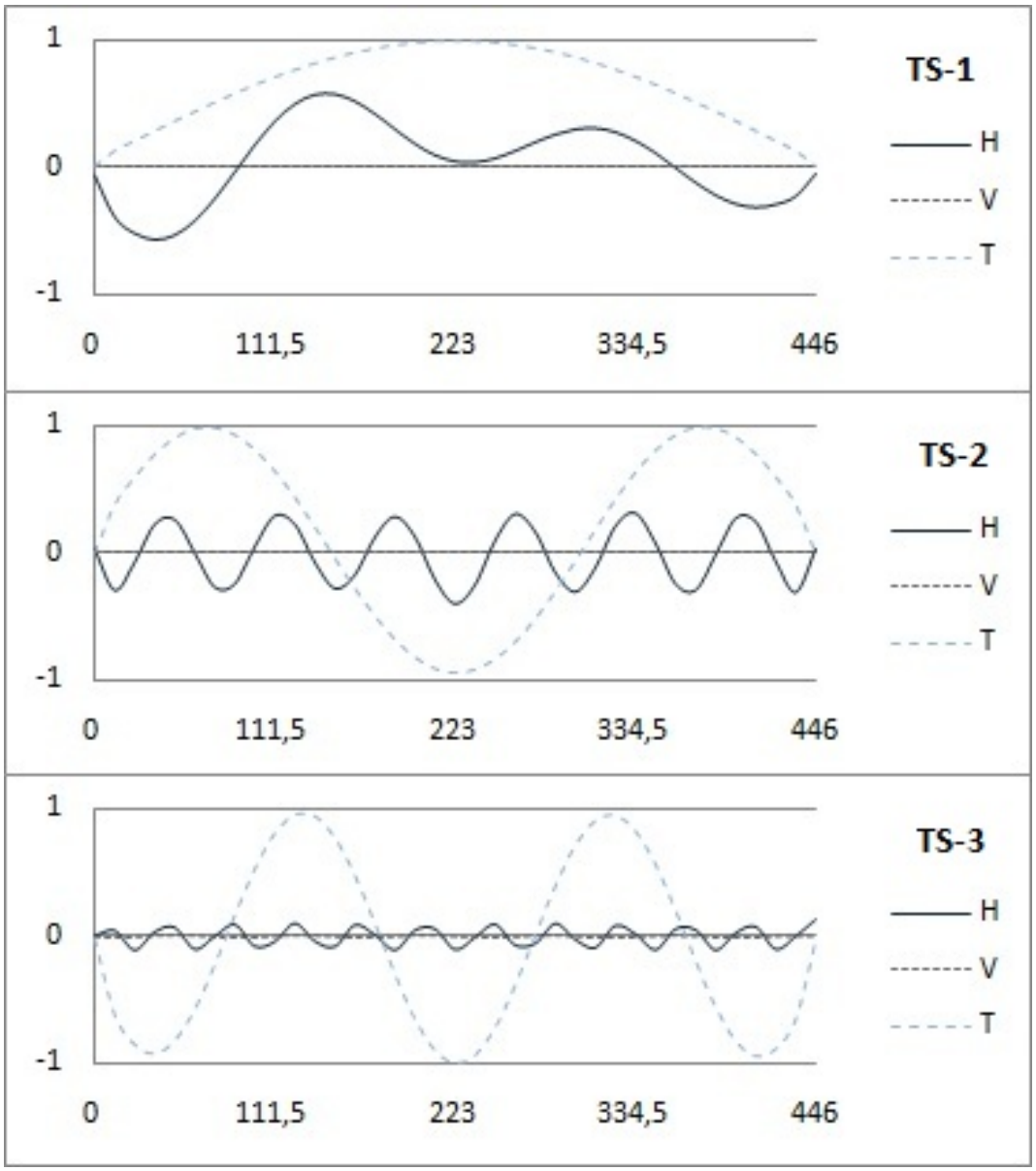

Figure 6.13: Torsional symmetric mode, coupled

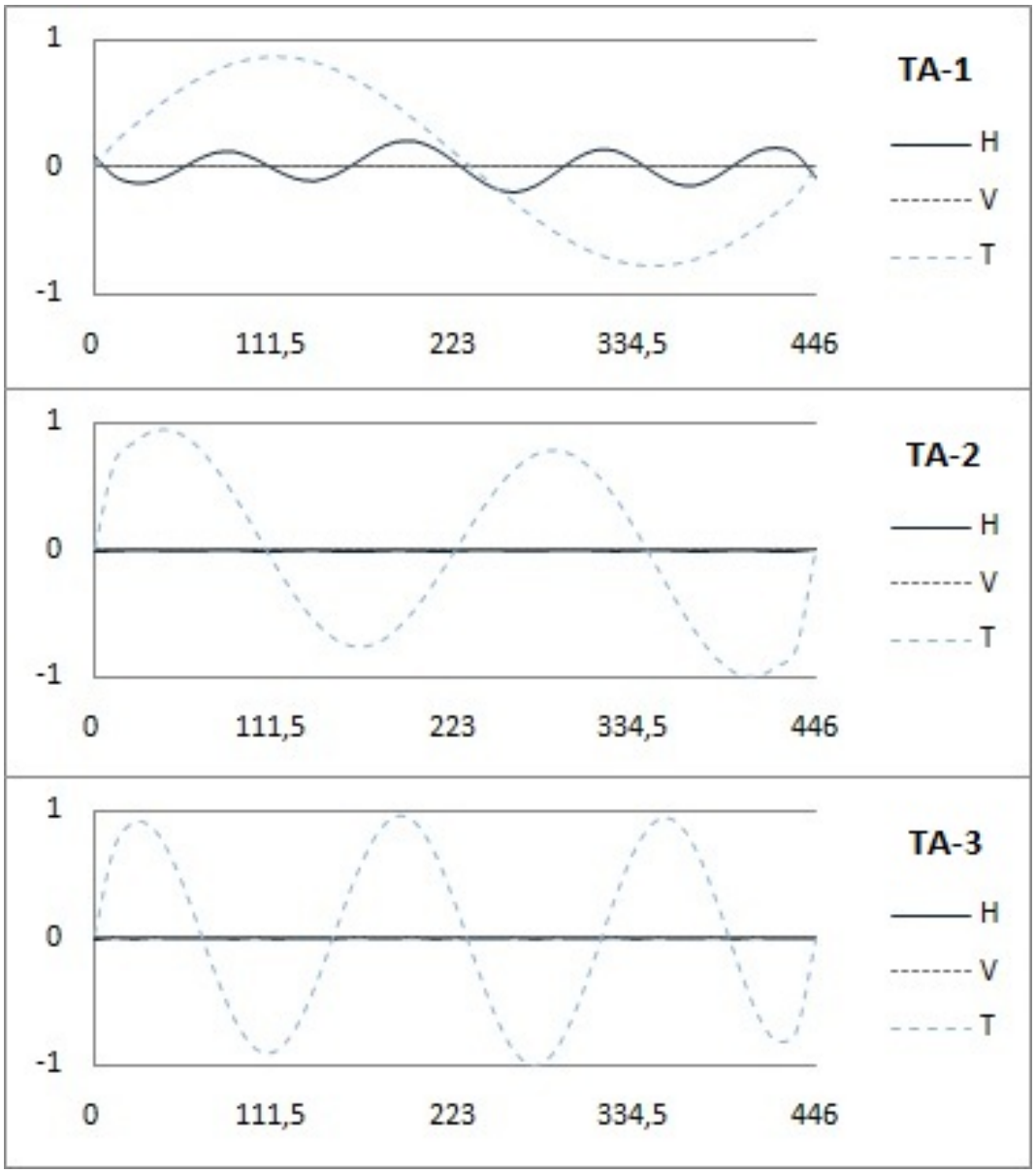

Figure 6.14: Torsional asymmetric mode, coupled

6.3 Displacement due to dead load

The displacement in the model in the center node of the bridge girder, node 19, caused by dead load is 2.85 m in negative z-direction. There is almost zero displacement in the x- and y-direction. This is expected, since the dead load only is working in negative z-direction. There is no rotation in the center node. The displacement in node 1019, which is the center node of the cable, has the same displacement as the bridge girder.

6.4 Displacement due to wind load

The directions of the wind loading on the bridge girder, together with the different axis is shown in Figure 6.15. This was also explained in Chapter 4 on page 22, but is given here as a clarifying remainder.

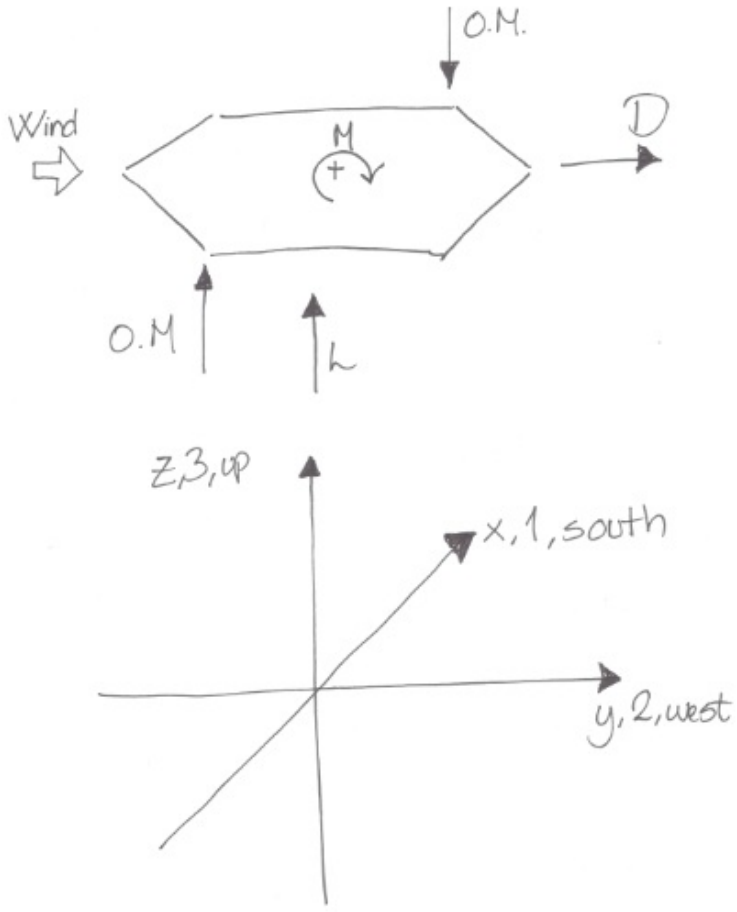

Figure 6.15: The directions of the wind loading on the bridge girder

The displacement of the bridge girder, caused by wind loading from a mean wind of 38 m/s, is 0.86 m in horizontal direction, in the center of the main span. In vertical, z-direction, the displacement in the center is 0.059 m. This means that the bridge is lifted a little bit, and it has a small bow in horizontal direction, see Figure 6.16 on the next page. There is as expected a very small displacement in x-direction, the length direction of the

bridge, due to the bending sideways. The angle in node 19 is 0.3°, this is not an large angle.

The displacement in the center of the bridge girder, for a mean wind speed, is shown in Table 6.2 on the following page and Figure 6.17 on page 67.The drag load is applied in positive direction, and the rotation in the results is defined positive in the same way it is shown in Figure 6.15 on the preceding page. This is deformation for static mean wind, without any dynamical factors.

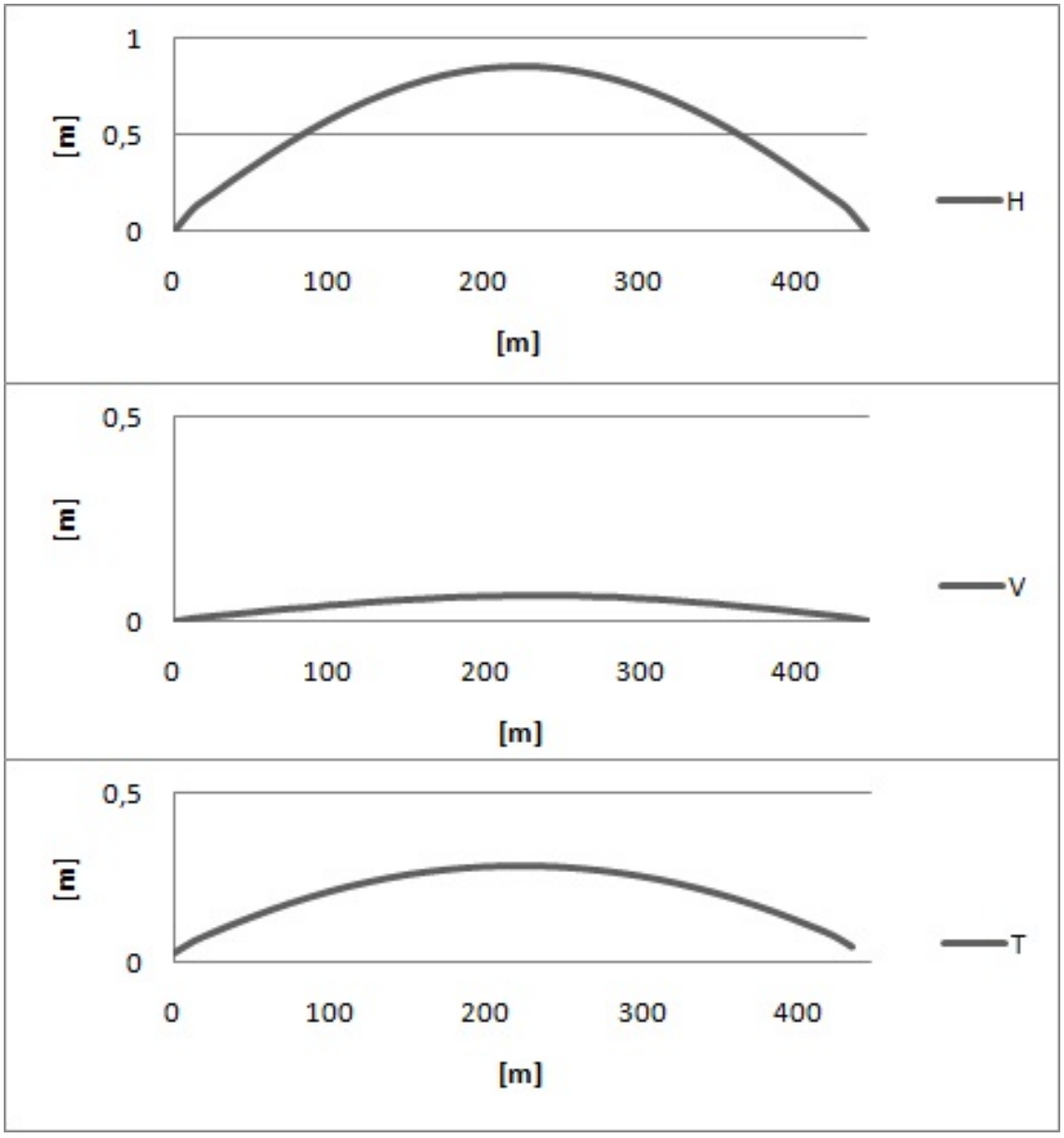

Figure 6.16: Displacement of the bridge girder when the loading from a mean wind speed of 38 m/s is applied, where H, V and T is horizontal, vertical and torsion respectively

U [m/s]	Y [m]	Z [m]	T [m]
0,00	0,000	0,000	0,0000
20,00	0,240	0,049	0,0040
38,00	0,860	0,059	0,0050
60,00	2,140	0,099	0,0070
80,00	3,796	0,189	0,0100

Table 6.2: The displacement of the bridge girder due to a mean wind in the center(node 19 at L/2)

6.5 Stress due to dead load and wind load

The stress in the cables caused by dead load and wind is shown in Figure 6.18 on the next page. It can be seen that the stress in the cables decrease when wind load is applied, this could be due to the lift load, that lift the bridge up. As the wind load is increased, the stress in the cables on the west side of the bridge increase, while the stress in the east side decrease. This is because the wind is applied from east on the bridge, such that the main span get an displacement against west. The maximum stress in the main cables from wind with a mean wind speed of 80 m/s;

$\sigma = \frac{F}{6A_c} = \frac{17621000\ N}{12 \cdot 0.0074\ m^2} = 396.9\ MPa$

The stress from dead load together with wind load on the bridge gives a demand/capacity rate in the cables of $\frac{396.9MPa}{1570MPa} = 25.3\%$. This is the same rate as for dead load alone.

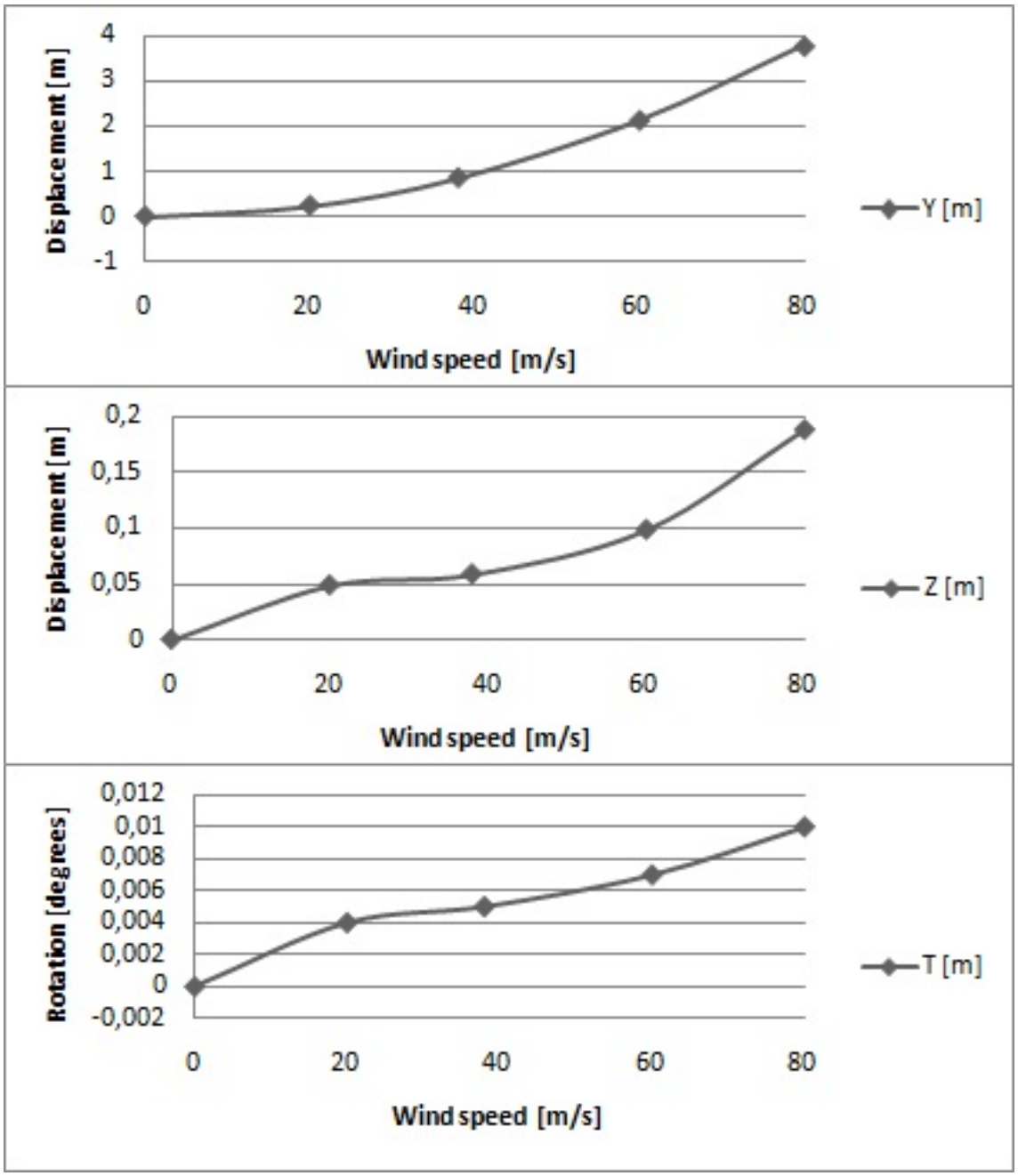

Figure 6.17: The displacement of the bridge girder due to a mean wind in the center(node 19 at L/2)

U [m/s]	σ NW [MPa]	σ SW [MPa]	σ NE [MPa]	σ SE [MPa]
0,00	395,4	391,0	395,4	391,0
20,00	392,0	387,7	384,0	379,8
38,00	392,8	388,6	383,0	378,7
60,00	394,4	390,5	380,8	376,8
80,00	396,9	393,7	378,8	375,3

Figure 6.18: Stress in the cables near the towers when dead load and wind load is applied

Chapter 7

Validation of eigenfrequencies and vibration modes

The eigenfrequenies and modes of a suspension bridge can as shown in the previous be found in finite element programs like ABAQUS and Alvsat. When using this kind of finite element programs, the geometry of the model, the rigidity and characteristics are given as input. There is always a possibility of errors in such input and there is a possibility that the program redefines, or read the input file in another way than the user expects.

To check the answers and output from these programs, some of the frequencies and vibration modes are found through calculations by hand. In this chapter, the six vertical eigen frequencies and modes, and the two first torsion symmetric and asymmetric eigen frequencies and modes are calculated by the use of Mathcad. The differences in the results are discussed. There has been used simplified equations from Bleich [4] and Steinman [27]. All details in the calculations are included in Appendix B.

The mode shapes from the calculations are shown in Figures 7.3 on page 72 to 7.7 on page 76. The mode shapes are nearly identical to the ones found from Alvsat and ABAQUS. This means that the programs has found the mode shapes in the way that was expected from the input.

7.1 Vertical eigenfrequencies and modes

The main reason for the calculations done by hand is to verify the output from ABAQUS and Alvsat. Therefore, the vertical eigen frequencies calculated here is some of the ones collected from the programs; VS-1, VS-2 and VS-3, and VA-1, VA-2 and VA-3. The eigen modes shown in Figure 7.1 on page 70 and 7.3 on page 72 are the first two vertical modes.

The theory and equations from Bleich is based on the following assumptions [4];

- Small amplitudes, and the extra force in the horizontal direction from inertia, is small relative to the horizontal force caused by dead load. This assumption is needed to be able to base the theory on the linear differential equation.
- The dead load and moment of inertia is constant within one span, but can change between the spans.

- The total mass of the bridge is considered to be concentrated along the centerline of the bridge girder, that is fixed in one direction.
- The hangers are considered to be infinite rigid, such that the vertical deformation of the bridge girder and the cables are considered equal. (This is the same as in Alvsat, while the hangers are allowed to deform in ABAQUS.)

Bleich use the linearized differential equation of the vibration problem with boundary conditions for suspension bridge to find the equations for circular frequencies. A full derivation can be found in his book. The equation used here is further written in a more convenient form.

7.1.1 Vertical asymmetric modes

To calculate the vertical asymmetric modes, the following differential equation is used;

$$m\frac{\partial^2\eta}{\partial t^2} + EI\frac{\partial^4\eta}{\partial x^4} - H_w\frac{\partial^2\eta}{\partial x^2} + \frac{w}{H_w}h = 0 \tag{7.1}$$

- m: mass of the main span
- w: Weight of the main span per meter
- g: Gravity load
- E: Modulus of elasticity for the bridge girder
- I: Moment of inertia around weak axis
- η: Amplitude at the distance x from the left point of attachment at time t
- H_w: The horizontal force in the cable caused by dead load
- h: Extra force in the cable

The equation for the vertical asymmetric modes of vibration is derived from Equation 7.1;

$$\omega(n) = \frac{n\pi}{l}\sqrt{\frac{g}{w}(H_w + n^2\lambda)} \tag{7.2}$$

- n: Number of sinusoidal half waves (n=2,4,6..)
- l: Length of the main span
- $\lambda = \frac{\pi^2 EI}{l^2}$

Equations from Steinman [27] is based on the fundamental equilibrium equation for a suspension bridge. The equations for the vertical asymmetric frequencies from Bleich and Steinman is identical, just presented in different forms;

$$w = -\frac{\partial^2}{\partial x^2}(H\eta + y\Delta H - EI\frac{\partial^2\eta}{\partial x^2}) \tag{7.3}$$

- H=H_w: Horizontal cable force
- ΔH: The increment produced by displacement

- E: Modulus of elasticity for the bridge girder
- I: Moment of inertia around weak axis
- η: Amplitude at the distance x from the left point of attachment at time t

The Coefficient of Rigidity, K(n), of the oscillating system is a significant criterion for aerodynamic stability;

$$K(n) = \frac{n^2\pi^2}{l^2}H_w + \frac{n^4\pi^4}{l^4}EI \tag{7.4}$$

$$\omega(n) = \sqrt{\frac{K(n)}{\frac{w}{g}}} \tag{7.5}$$

Figure 7.1 shows the first and second vertical asymmetric modes from analytical calculations, and these are compared to the first and second vertical asymmetric modes from ABAQUS and Alvsat, in Figure 7.2 on the following page. The first and second vertical asymmetric eigen modes has a similar shape, but they are laterally inversed.

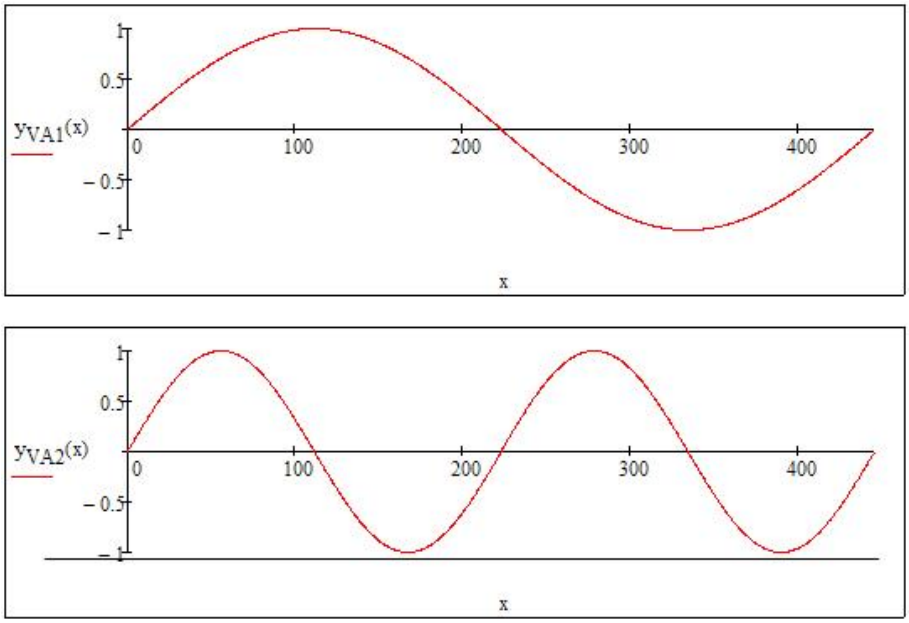

Figure 7.1: First and second vertical asymmetric modes from the analytical calculations

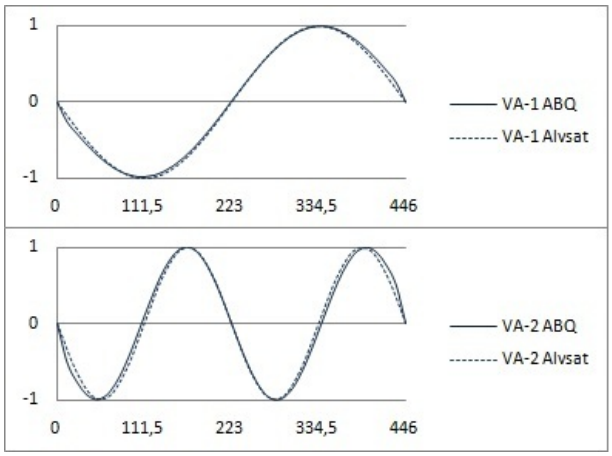

Figure 7.2: First and second vertical asymmetric modes from ABAQUS and Alvsat

7.1.2 Vertical symmetric modes

To compute the vertical symmetric mode, the energy equation valid for one span suspension bridges is used. The analysis is based upon the two equations [4];

$$T - V = \frac{1}{2}(\frac{w}{g}\omega^2 \int_0^1 \eta^2 dx - EI \int_0^1 \eta''^2 dx + H_w \int_0^1 \eta'' \eta dx - \frac{8f}{l^2} h \int_0^1 \eta dx) \tag{7.6}$$

and

$$\frac{8f}{l^2} \int_0^1 \eta dx - \frac{L_E h}{E_c A_c} = 0 \tag{7.7}$$

- T: Maximum kinetic energy in the construction as a function of η
- V:Maximum potential energy as a function of η(partly kept in the bridge span as elastic energy because of bending, and partly in the cables as elastic stress-strain energy and through increased potential of gravity)
- L_E: The length of the cable from hold-down to hold-down
- E_c: Modulus of elasticity for the cable
- A_c: Cross-section area for the cable

From the two energy equations 7.6 and 7.7, the following frequency equation for the 1. and 2. vertical symmetric mode is derived, for a more detailed derivation of the formulas, see [4];

$$A \cdot k + 9B(k - A \cdot p) = 0 \tag{7.8}$$

Where the two parameters A and B are given as;

$$A = s\omega^2 - H_w - \lambda \tag{7.9}$$

$$B = s\omega^2 - 9H_w - 91\lambda \tag{7.10}$$

and the parameters s, k and p are given as;

$$s = \frac{wl^2}{\pi^2 g} \tag{7.11}$$

$$k = \frac{32f}{\pi^3} \tag{7.12}$$

$$p = \frac{pil}{16f}\frac{L_E}{E_c A_c} \tag{7.13}$$

Solving the equation for ω, and find the frequencies. For n>3, the eigen frequencies can be found from;

$$\omega(n) = \sqrt{\frac{1}{s}(n^2 H_w + n^4\lambda + \frac{k}{n^2 p)}} \tag{7.14}$$

The equations from Steinman used to find vertical symmetric eigenfrequencies;

$$\sum_{n=1,3,5..} \frac{1}{n^2}\frac{C\frac{f}{l}}{K - K(n)} = 1 \tag{7.15}$$

K(n) is found from the first energy equation 7.6 on the previous page. Solving for C;

$$C = \frac{512}{pi^2}\frac{fE_c A_c}{l^2 L_E} \tag{7.16}$$

Finding the eigenfrequency;

$$\omega = \sqrt{\frac{K}{\frac{w}{g}}} \tag{7.17}$$

Where the stiffness parameter, K, is found from Equation 7.15. Figure 7.3 shows the first and second vertical symmetric modes from analytical calculations, and these are compared to the first and second vertical symmetric modes from ABAQUS and Alvsat, in Figure 7.4 on the following page. The first and second vertical symmetric eigen modes has a similar shape.

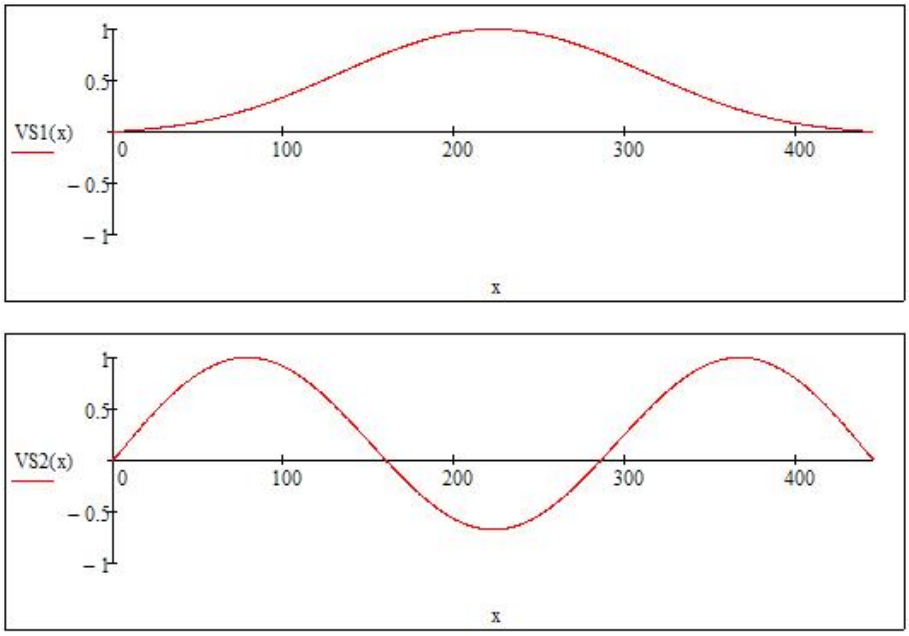

Figure 7.3: First and second vertical symmetric modes from the analytical calculations

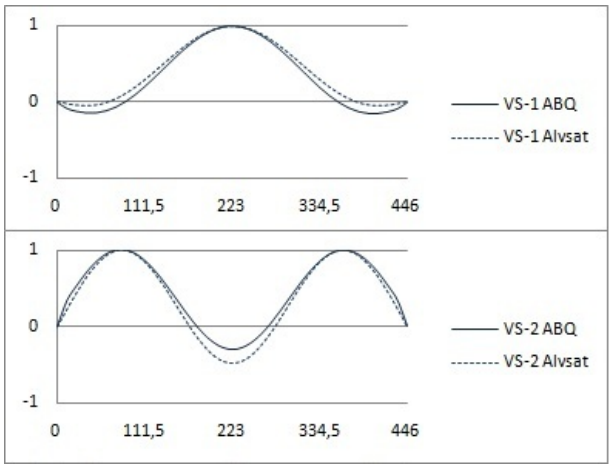

Figure 7.4: First and second vertical symmetric modes from ABAQUS and Alvsat

7.2 Torsion eigenfrequencies and modes

7.2.1 Torsion symmetric modes

The torsion symmetric modes are calculated based on Bleichs equations. The equations are simplified to fit the bridge girder that is used in Lysefjord Bridge, since the equations originally was derived for a rectangular girder. The bridge girder in Lysefjord Bridge is, like most bridge girders today a box with six corners, not a rectangular box shape. The eigen modes shown in Figure 7.7 on page 76 and 7.5 on page 75 are the first two torsion modes.

The 1. and 2. eigen frequency are derived from the following equation;

$$B \cdot (A - K) - \frac{A \cdot K}{9} = 0 \tag{7.18}$$

Where the two parameters A and B are given as;

$$A = s\omega^2 - \Lambda - R \tag{7.19}$$

$$B = s\omega^2 - 81\Lambda - 9R \tag{7.20}$$

$$K = \frac{E_c A_c}{L_E} \cdot \frac{64 f^2 w_h^2}{\pi^2} l^2 \tag{7.21}$$

Where;

$$s = M\frac{l}{4} \tag{7.22}$$

$$\Lambda = E \cdot Y \cdot \frac{\pi^4}{2l^3} \tag{7.23}$$

$$R = E \cdot \beta w_h \cdot h_{bg} + H_w \cdot \frac{w_h^2}{4}) \frac{\pi^2}{2l} \tag{7.24}$$

$$M = \frac{1}{g}(r^2 \cdot wght_{bg} + \frac{w_h^2}{4} \cdot wght_c) \tag{7.25}$$

$$Y = I_w \cdot \epsilon w^2 + I_h \cdot \epsilon h^2 \tag{7.26}$$

$$\epsilon w = \frac{w_{bg}}{2} - \frac{\mu w}{A_w}\beta h_{bg} \tag{7.27}$$

$$\epsilon h = \frac{l_{plates}}{2} - \frac{\mu h}{A_h}\beta w_{bg} \tag{7.28}$$

$$\frac{w_h h_{bg}}{\frac{\mu w \cdot h_{bg}^2}{A_w} + \frac{\mu h \cdot w_{bg}^2}{A_h}} \tag{7.29}$$

$$A_w = 1,09 t h_{bg}, A_h = 1,09 t w_{bg} \tag{7.30}$$

- l: Length of the bridge girder
- E: Modulus of elasticity for the bridge girder
- L_E: The length of the cable from hold-down to hold-down
- E_c: Modulus of elasticity for the cable
- A_c: Cross-section area for the cable
- f: Sag of the girder
- w_h: Width between the hangers
- h_{bg}: Height of bridge girder
- H_w: The horizontal force in the cable caused by dead load
- $wght_{bg}$: Weight of bridge girder
- $wght_c$: Weight of cable
- I_w: Area moment of inertia around the x-axis
- I_h: Area moment of inertia around the x-axis
- μw and μh: Factors that is put to $2\sqrt{2}$ to take into account the bridge girder shape
- L_E: The length of the cable from hold-down to hold-down
- E_c: Modulus of elasticity for the cable
- A_c: Cross-section area for the cable
- f: Sag of the cable

Figure 7.5 on the next page shows the first and second torsion symmetric modes from analytical calculations, and these are compared to the first and second torsion symmetric modes from ABAQUS and Alvsat, in Figure 7.4 on the preceding page. The first and second torsion symmetric eigen modes has a similar shape.

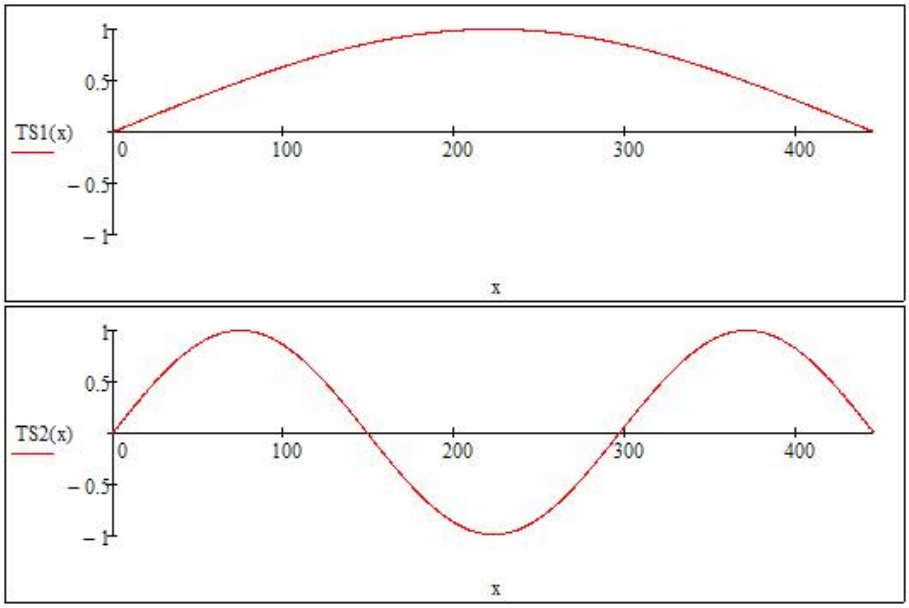

Figure 7.5: First and second torsion symmetric modes from the analytical calculations

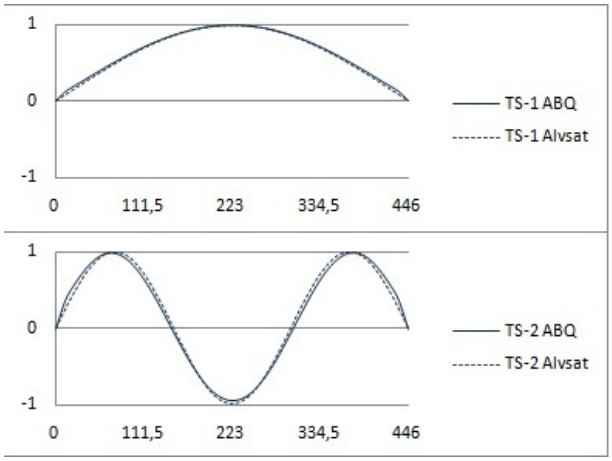

Figure 7.6: First and second torsion symmetric modes from ABAQUS and Alvsat

7.2.2 Torsion asymmetric modes

To find the torsion asymmetric modes, the following equation is used;

$$\omega = \sqrt{\frac{n^2}{s}(n^2 \cdot \Lambda + R)} \tag{7.31}$$

Where n is the number of sinusoidal half waves (2,4,6..)

Figure 7.7 on the next page shows the first and second torsion asymmetric modes from analytical calculations, and these are compared to the first and second torsion asymmetric modes from ABAQUS and Alvsat, in Figure 7.2 on page 71. The first and second torsion asymmetric eigen modes has a similar shape.

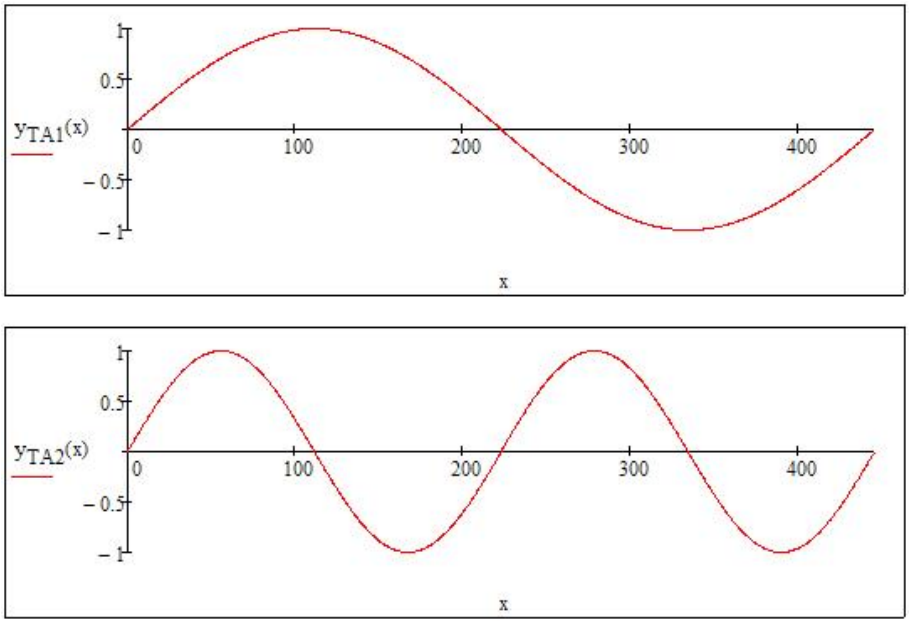

Figure 7.7: First and second torsion asymmetric modes from the analytical calculations

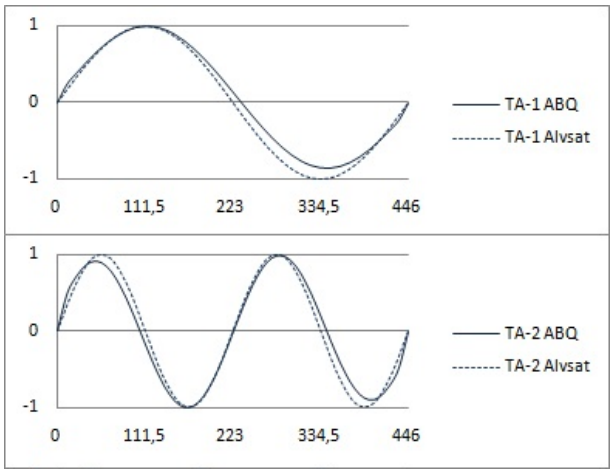

Figure 7.8: First and second torsion asymmetric modes from ABAQUS and Alvsat

7.3 Eigenfrequencies from calculations

A comparison between the calculated values, Alvsat and ABAQUS is shown in Table 7.1 on the next page. From the table, it can be seen that the vertical frequencies except VS-1 differs from Alvsat with maximum 4% and from ABAQUS with maximum 6%. The first vertical symmetric mode differs from Alvsat with 12% and from ABAQUS with 17%. The torsion frequencies differs from Alvsat with maximum 3% and from ABAQUS with maximum 24%. The torsion frequencies from ABAQUS differ relatively much from the Alvsat results, see the results and discussion in Section 6.2.2 on page 46. The difference could be caused by many factors, and one could be that the equations used in the calculations originally were made for another bridge girder shape than the one in Lysefjord Bridge. If the equations had been derived in a more accurate way, the results probably would have been closer than here. The results are however satisfyingly close to the ones found in the FEM programs as a verification, but the theoretical calculations should not be used alone

in an analysis of a suspension bridge.

	Alvsat	ABAQUS		Bleich/Steinman		
	Period[s]	Period[s]	Diff. From Alvsat	Period[s]	Diff. From Alvsat	Diff. From ABAQUS
VS-1	3,49	3,29	-6 %	3,974	12 %	17 %
VS-2	2,50	2,45	-2 %	2,607	4 %	6 %
VS-3	1,15	1,16	0 %	1,161	1 %	0 %
VA-1	4,69	4,68	0 %	4,890	4 %	4 %
VA-2	1,70	1,72	1 %	1,709	1 %	0 %
VA-3	0,83	0,84	1 %	0,837	0 %	0 %
TS-1	0,87	0,96	10 %	0,845	-3 %	-14 %
TS-2	0,31	0,36	14 %	0,305	-1 %	-18 %
TA-1	0,47	0,53	11 %	0,462	-2 %	-15 %
TA-2	0,23	0,28	18 %	0,227	-2 %	-24 %

Table 7.1: Eigenfrequencies from the original model in ABAQUS, Alvsat and calculations

Chapter 8

Conclusion

This thesis presents an analysis of Lysefjord Bridge in light of the deterioration of the main cables. The data given from The Norwegian Public Roads Administration in the work with this thesis are analyzed and a new finite element model is created. An analysis of the wire fractures in the main cables and a brief analysis of the fractures in relation to the weather around the bridge is also carried out. The main structural components of a suspension bridge are presented, and a brief introduction to the load carrying characteristics of the different components are given. This was done to understand more around this kind of bridges, and to understand the function of the main cables.

The conclusion of the work carried out is that there probably are more than one reason for the fractures of the wires in the main cables. There are more wire fractures in the winter than in the summer, and sudden temperature drops seems to induce more wire fractures. The critical wind speed of 7.5 m/s are found to excite the first vertical symmetric mode, and after studying the weather around the bridge, this seems to be a fairly common wind speed. This could cause wire fractures from fatigue over many years, and since there already are shown that small defects on the outside of the wires exists, cyclic load could make this defects grow and eventually fracture the wire. It is clear that more accurate parameter studies of the bridge should be carried out, due to a wire fracture rate of 116 fractures/year, that is much higher than any monitored bridge in Norway. Monitoring of the bridge response in different load situation would also be useful. More details from the work with the thesis are summarized in the following.

The main cables in Lysefjord Bridge has been inspected visually since the opening in 1997, and it has been monitored with an acoustic monitoring system since late 2009. There is also established a connection to a weather station stationed close to the bridge, that has provided data for wind speeds and temperatures. Even with only one and a half year of monitoring, it can be seen that there is far more fractures in the winter than in the summer. The results also shows that after a sudden drop in the temperature late December 2009, many wire fractures occurred. A comparison to December 2010 shows that when the weather is cold but steady, far less wire fractures occurs. The monitoring system is important in the new analysis of the bridge, and after a few more years, clear results are expected.

The finite element model in ABAQUS is based on data from the previous analysis in Alvsat, and the results from eigen frequencies and shapes are in the same order of mag-

nitude as from Alvsat. The modeling of element model of Lysefjord Suspension Bridge in ABAQUS was done and presented step by step. Since the bridge was built over ten years ago, there has been some challenges with collecting the data needed for the model. The input used in the original analysis done in Alvsat is used in the finite element model in ABAQUS. The model is built such that wind- and other analysis can be performed on the bridge later. The geometry of the model when dead load is taken into consideration is discussed and taken into consideration. It is important for the analysis that the length of the main span, the sag of the main cables and the rest of the geometry are as close to the real bridge as possible. The demand/capacity rate for the cables with dead load is 25.2%. The vertical displacement in the bridge girder due to dead load is almost 3 meter.

To perform a brief wind analysis of the bridge for 50 year wind speed in the area, wind loading is calculated to be 38 m/s, the same as in the original analysis. This loading, with form factors taken from the input file in Alvsat is applied to the model in ABAQUS. The intention was to use a subroutine in Fortran to simulate the wind load, but after several attempts, the wind load is calculated by iteration directly in the input file. Five iterations were done to find the true wind force in the correct angle. The displacement in node 19, the center of the bridge girder is then 0.86 meter in horizontal direction, and the girder is lifted up to 0.056 meter in vertical direction, measured from the equilibrium position with dead load. The bridge girder is rotated with an angle of 0.3° in the center node.

The frequencies and the mode shapes found from the finite element model in ABAQUS are in agreement with the values previously calculated in Alvsat. As an example, the vertical and horizontal frequencies has in general less than 2% difference, and a maximum difference of 6% in the first vertical symmetric mode. There are however some differences, for example in the torsion frequencies, where the differences is between 10% and 23%. There could be several reasons for this difference, but no obvious reason has been found. To verify the results from ABAQUS, theoretical calculations of some of the eigen frequencies and mode shapes are carried out, with a satisfying result. The maximum difference in the results, except for the first vertical frequency with a difference of 12%, compared to Alvsat is 4%. Compared to ABAQUS, the difference in first vertical frequency is 17%, while the maximum difference of the rest of the results are 6% in vertical direction, and between 14% and 25% for the torsion frequencies. The theory used is from Bleich and Steinman, but the equations are simplified and fit to Lysefjord Bridge. One of the big differences is the shape of the bridge girder, that in the equations are quadratic, while in Lysefjord Bridge is shaped with six corners. The theoretical calculations should be done more accurate if they were to be done alone, without any finite element model analysis.

Chapter 9

Further recommendations

If the bridge is to be analyzed for how many wire fractures the bridge can take before the capacity is lower than demanded, the bridge model can be modified in different ways. To see how the wire fractures impact on the capacity of the bridge, a method to model the fractures in the bridge model should be found. This could be done by dividing the different components of the bridge into smaller elements, and giving the elements where the fractures has occurred lower capacity than the other elements.

The monitoring system should be maintained and continued, and it is important that visual inspections are carried out for the bridge as a control of the monitoring device. After e.g. five years of monitoring, an analysis of the fractures compared to weather should be carried out. It should also be considered to use another type of inspection, e.g. x-ray, to control and find the accurate state of the wire fractures in the cables. Another monitoring system capturing bridge response (e.g. in terms of accelerations or strains) could provide additional data on possible special load situations associated with the wire fracture events.

A high rate of fractures per year has been seen since the opening of the bridge for over ten years ago. The main cables will have to be maintained or changed earlier than expected, and the work with planning how to maintain of change the cables should be started now, such that a good solution is found before it actually have to be done. Which kind of steel that should be used in the cables must be decided, and if possible and preferable, the cable configuration can be changed.

A finite element model of Lysefjord Bridge has been built in ABAQUS, and some wind analysis on the bridge is carried out. ABAQUS does however not have a module for moving traffic loading, or a module for building combinations in the different loading conditions. This is not necessarily limiting, but it makes it more time-consuming and complex to do this kind of analysis. NovaFrame is a program with this kind of modules. This is also a program built on the finite element method, but it is made for bridges only. NovaFrame, and also NovaDesign, that is a program for concrete structures analysis could be used to supplement the analysis in ABAQUS.

Bibliography

[1] AAJ. Beregninger av egenfrekvenser for lysefjordbrua. Tech. rep., Statens Vegvesen, 1999.

[2] Auvray, M. Lysefjord suspension bridge acoustic monitoring from 01/01/2011 to 31/03/2011. Tech. Rep. NOR0159 REP 404, Advitam, 2011.

[3] Bjørnsen, I. P. Static and dynamic analysis of a suspension bridge excited by wind load. Master's thesis, UiS, 2007.

[4] Bleich, F., McCullough, C., Rosecrans, R., and Vincent, G. S. *The mathematical theory of vibration in suspension bridges: a contribution to the work of the Advisory Board on the Investigation of Suspension Bridges.* Department of commerce, Bureau of public roads, 1950.

[5] Carboline. http://www.carboline.com, April 10th 2011.

[6] Øderud, H. T., and Nordahl, R. S. http://www.snl.no/bro. Web, November 2010.

[7] Ebeltoft, R. G. Lysefjord bridge, visual inspection of cable breakage. Tech. rep., Statens Vegvesen, 2008 - 2010.

[8] Fricker, S., and Vogel, T. Site installation and testing of a continuous acoustic monitoring. *Construction and Building Materials 21*, 3 (2007), 501 – 510. Fracture, Acoustic Emission and NDE in Concrete (KIFA-4).

[9] Gimsing, N. J. *Cable supported bridges, concept and design*, 2nd. ed. John Wiley and Sons, New York USA, 1997.

[10] Gjerding-Smith, K. Rv 13 lysefjordbrua, trådbrudd i kabler, konsekvenser og tiltak. Tech. Rep. 2001-06, Sivilingeniørene Haug og Blom-Bakke AS, 2004.

[11] Google. http://www.maps.google.com, April 25th 2011.

[12] Gourvellec, G. Lysefjord bridge soundprint acoustic monitoring. Tech. Rep. NOR0159 REP 402, Advitam, 2010.

[13] Hjorth-Hansen, Strømmen, E., Bogunovic Jakobsen, J., Brathaug, H.-P., and Solheim, E. Wind tunnel investigations for a proposed suspension bridge across the hardanger fjord. Tech. Rep. 3, Balkema, 1993. Moan et al., (eds.).

[14] Høyte, J., and Brathaug, F. *ALVSAT VERSJON 3.4, Usermanual*, 1990.

[15] Inc, A. *ABAQUS, Analysis users manual*, version 6.4 ed., 2003.

[16] Jakobsen, J. B. Lecture notes from environmental loads; wind load on structures, 2010.

[17] Kyte, A. G. Hardangerbrua: Abaqus bjelkemodell, dynamisk analyse. Tech. rep., Statens Vegvesen, 2006.

[18] Lange, H., Lange, T., Johnsen, R., Kongstein, O. E., and Nilsen, N. I. Høyfast kabeltråd med strekkfasthet 1570mpa og 1770mpa, måling av bruddseighet og effekt av hydrogensprøhet. Tech. Rep. 801059, SINTEF, 2010.

[19] Leinum, B. H. Examination of failed z-wire rods rv13, lysefjord. Tech. Rep. 53010498, DNV, 2000.

[20] Leinum, B. H. Examination of a 1.65 m spare main cable section rv13, lysefjord bridge. Tech. Rep. 53010389, DNV, 2001.

[21] LysefjordWeatherStation. http://www.lysefjordweather.com, April 16th 2011.

[22] Norway, S. *Norwegian Standard NS-EN 1991-1-4:2005+NA2009, Eurocode 1:Loads on structures, wind loading*, 2005/2009.

[23] Paulson, P., and Elliott, J. F. Soundprint acoustic monitoring system, http://www.ndt.net/article/wcndt00/papers/idn777/idn777.htm, October 2000.

[24] Scott, R. *In the wake of Tacoma, suspension bridges and the quest for aerodynamic stability.* American Society of Civil Engineers, 2001.

[25] Simiu, E., and Miyata, T. *Design of Buildings and Bridges for Wind A Practical Guide for ASCE-7 Standard Users and Designers of Special Structures.* John Wiley and Sons, New Jersey, 2006.

[26] SoundPrint®. http://www.soundprint.com, May 11th 2011.

[27] Steinman, D. B. Modes and natural frequencies of suspension bridge oscillations. *Journal of the Franklin Institute 268*, 3 (1959), 148 – 174.

[28] Strengelsrud, K. Examination of a fractured section of wire from a main cable of the lysefjord bridge. Tech. Rep. 53010389, DNV, 1999.

[29] Wyatt, T. A. Bridge aerodynamics 50 years after tacoma narrows - part 1: The tacoma narrows failure and after. *Journal of Wind Enigneering and Industrial Aerodynamics 40* (1992), 317–326.

Appendices

Appendix A

Figures

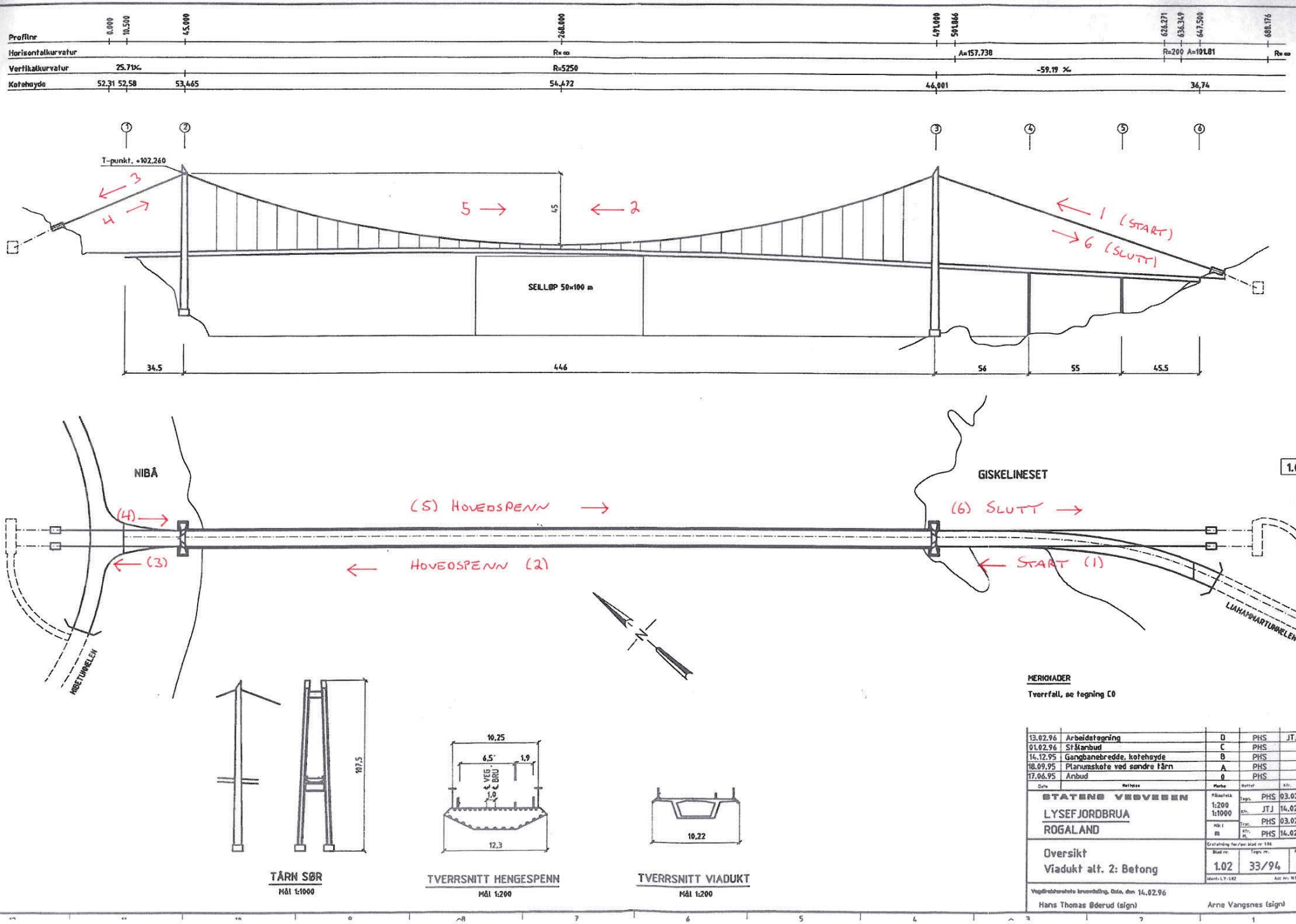

Appendix C - Figures

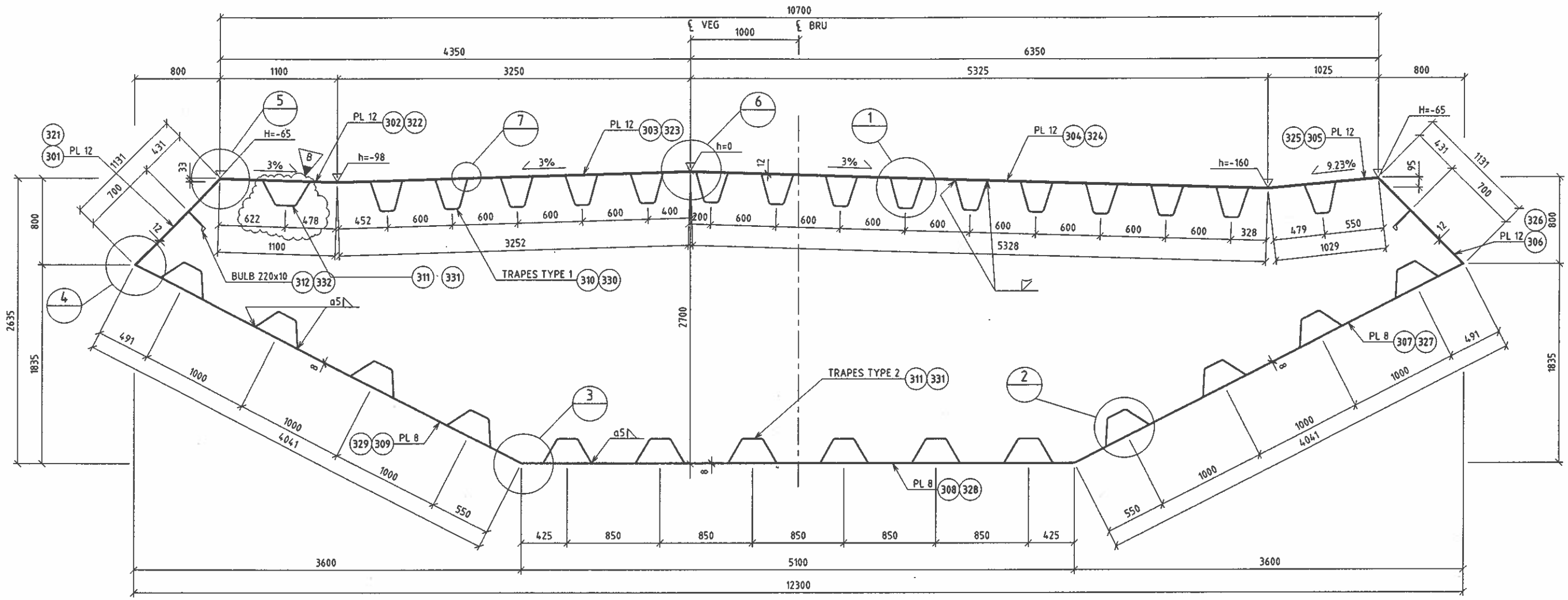

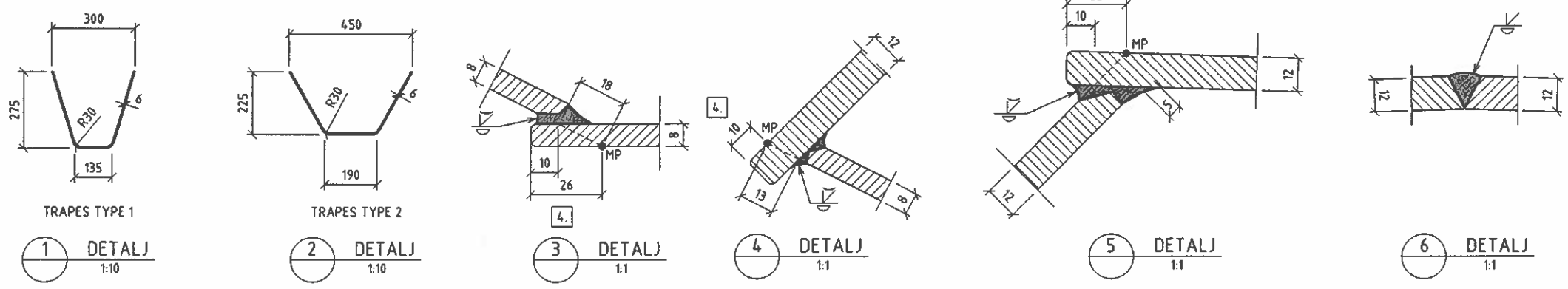

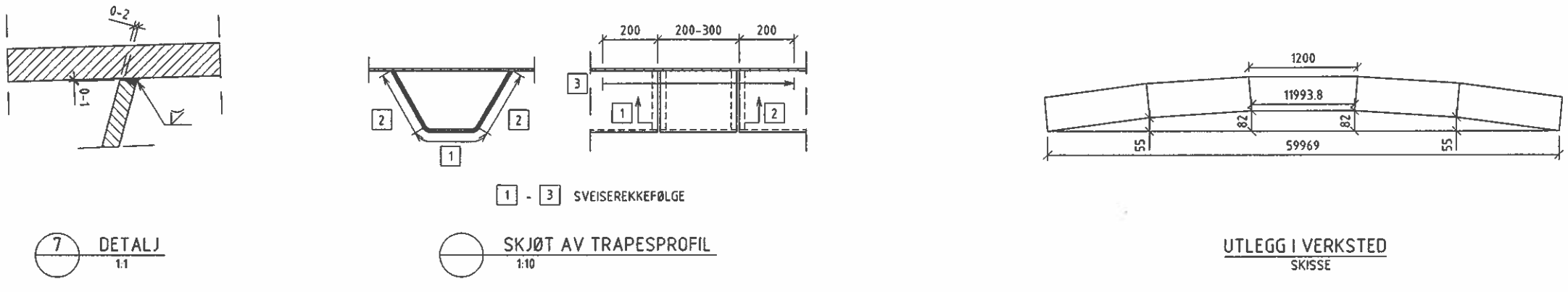

8.02

MERKNADER

1. MÅL ER GITT TIL MÅLEPUNKT, MP, YTTERKANT KASSE.
2. BUTTSVEISER, DETALJ 6, KAN ALTERNATIVT UTFØRES MOT KERAMISK BAKLEGG.
3. SKJØT AV TRAPESPROFILER UTFØRES MED BUTTSVEIS MED BAKLEGG. BAKLEGG HEFTES I SVEISEFUGEN.
4. OVERLENGDER PÅ PANELER BESTEMMES AV ENTREPRENØR I FORBINDELSE MED UTARBEIDELSE AV VERKSTEDTEGNINGER OG SVEISEPROSEDYRER.

Dato	Rettelse	Merke	Rettet	Kfr.
05.07.96	STIVER FLYTTET	B	DIY	LRE
02.07.96	ARBEIDSTEGNING	A	DIY	LRE
01.02.96	STÅLANBUD	0	GBJ	LRE

STATENS VEGVESEN

LYSEFJORDBRUA
ROGALAND

Målestokk: 1:20, 1:10, 1:1
Mål i mm

Tegn 10.95 LRE
Kfr. 07.96 DIY
Trac 10.95 GBJ
Kfr.pl. 07.96 PHS

STÅLKASSE
TYPISK TVERRSNITT

Bruer
Blad nr. 8.02
Tegn nr. 381/95
Rev B
Fdnavn S87118-02

Vegdirektoratets bruavdeling, Oslo den 02.07.96
Arne Vangsnes (sign.) Per Helge Styngstad (sign.)

AAS-JAKOBSEN
DRLMCA AAS-JAKOBSEN A.S
Løkenhaverveien 4, 0283 Oslo. Telefon 22505044

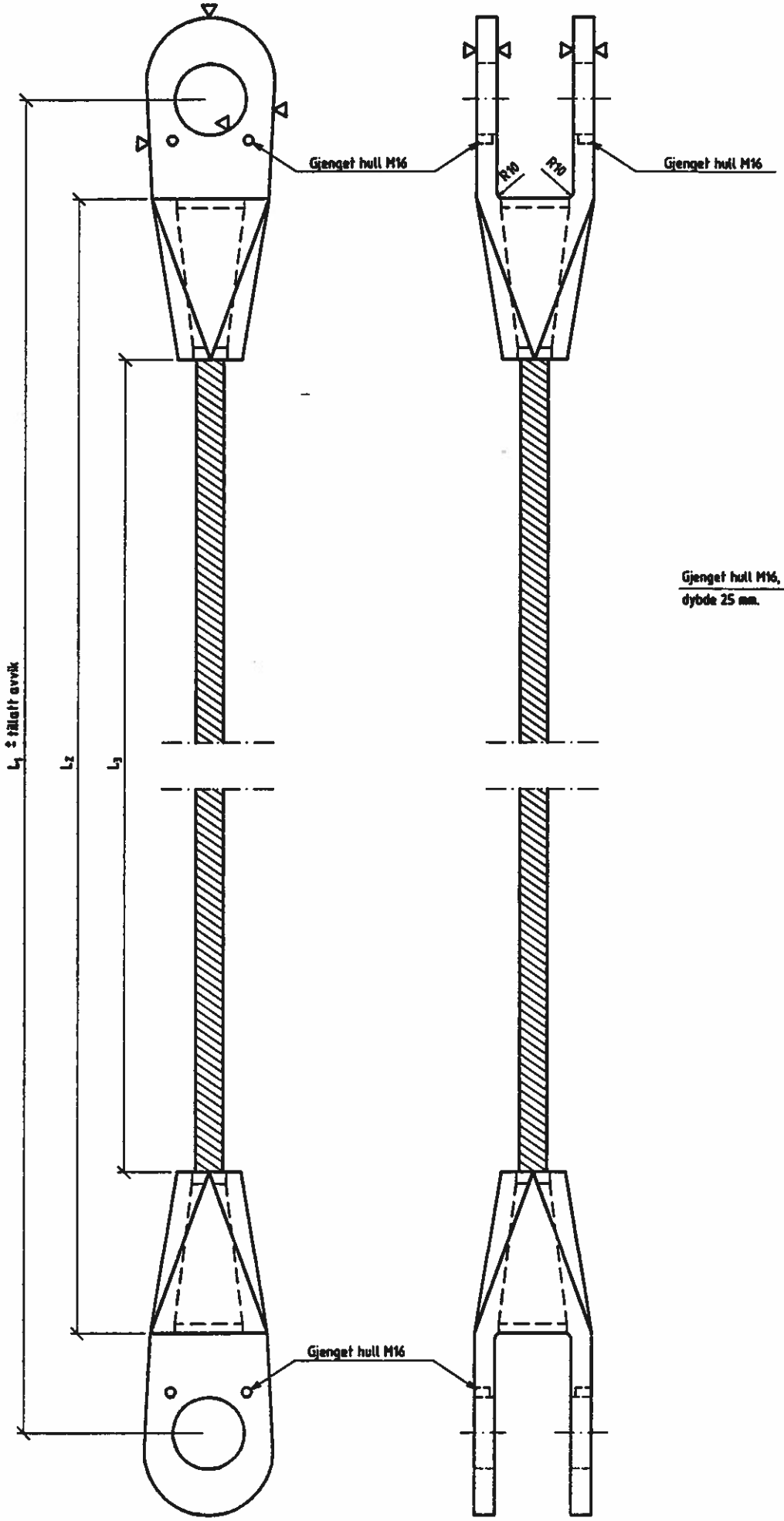

HENGESTANG

1:5

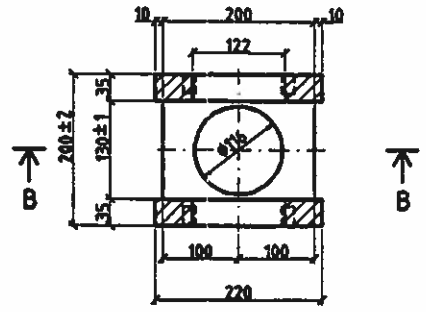

SNITT A-A

1:5

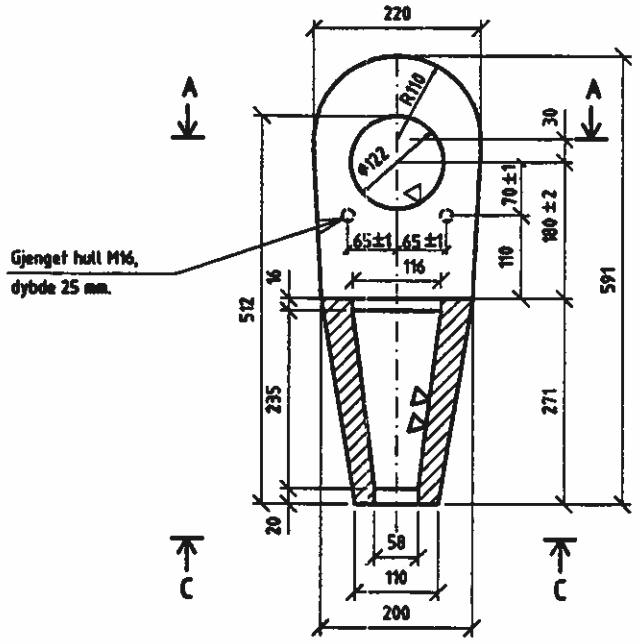

SNITT B-B

1:5

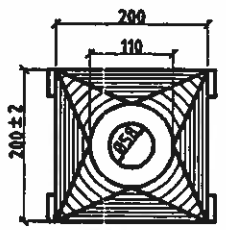

SNITT C-C

1:5

Hengestang nr.	Antall	L_1 (m)	L_2 (m)	L_3 (m)	Hengestangs-lengdene måles under gitt last (kN)
1	2	40,502	40,142	39,600	501
2	2	35,984	35,624	35,082	250
3	2	31,708	31,348	30,806	336
4	2	27,735	27,375	26,833	313
5	2	24,050	23,690	23,148	319
6	2	20,656	20,296	19,754	317
7	2	17,550	17,190	16,648	317
8	2	14,732	14,372	13,830	317
9	2	12,204	11,844	11,302	317
10	2	9,964	9,604	9,062	317
11	2	8,010	7,650	7,108	316
12	2	6,345	5,985	5,443	316
13	2	4,967	4,607	4,065	316
14	2	3,877	3,517	2,975	316
15	2	3,073	2,713	2,171	316
16	2	2,555	2,195	1,653	316
17	2	2,325	1,965	1,423	316
18	2	2,382	2,022	1,480	316
19	2	2,724	2,364	1,822	316
20	2	3,354	2,994	2,452	316
21	2	4,270	3,910	3,368	316
22	2	5,474	5,114	4,572	316
23	2	6,963	6,603	6,061	316
24	2	8,740	8,380	7,838	316
25	2	10,804	10,444	9,902	317
26	2	13,157	12,797	12,255	317
27	2	15,796	15,436	14,894	317
28	2	18,723	18,363	17,821	317
29	2	21,939	21,579	21,037	317
30	2	25,444	25,084	24,542	317
31	2	29,237	28,877	28,335	319
32	2	33,321	32,961	32,419	313
33	2	37,692	37,332	36,790	337
34	2	42,366	42,006	41,464	248
35	2	47,281	46,921	46,379	506
Summer	70	595,904	583,304	564,334	

6.02

MERKNADER

1. Det er i alt 70 hengestenger.
2. Total kabellengde er 1166,606 meter.
3. Kablene utføres spiralslått, lukket og fullgalvanisert.
4. Minste effektive bruddkapasitet per kabel er 2200 kN.
5. Temperatur under lengdemåling er forutsatt som +5 °C.
6. Kabelhodene utføres i støpestål med minimum strekk-fasthet f_y = 340 N/mm².
7. Mål som er angitt med toleranser, er faste i henhold til "Statens vegvesens håndbok 122. Utgave for Lysefjord-bru-1995", prosess 85.631 c) avsnitt Form og bearbeiding.

14.10.96	Korrigert ihht. leverandørens endringer	A	BI	PHS
01.02.96	Stålanbud	2	BI	
12.01.96	Rev. anbudstegning	1	BI	
14.12.95	Anbudstegning	0	BI	
Dato	Rettelse	Merke	Rettet	Ktr.

STATENS VEGVESEN

LYSEFJORDBRUA
ROGALAND

Kabler og hengestenger
Hengestenger

Målestokk 1:5
Mål i mm

Tegn. 12.95 BI
Ktr. 10.96 PHS
Trac. 12.95 IMJ
Ktr.fl. 10.96 PHS

Dwgs. 96-1789

Kont. nr. 6.02
Tegn. nr. 330/95
Rev. A

Filnavn LY-6-02

Vegdirektoratets bruavdeling, Oslo den 15/10-96

Arne Vangsnes (sign.) *Per Helge Slyngstad (sign.)*

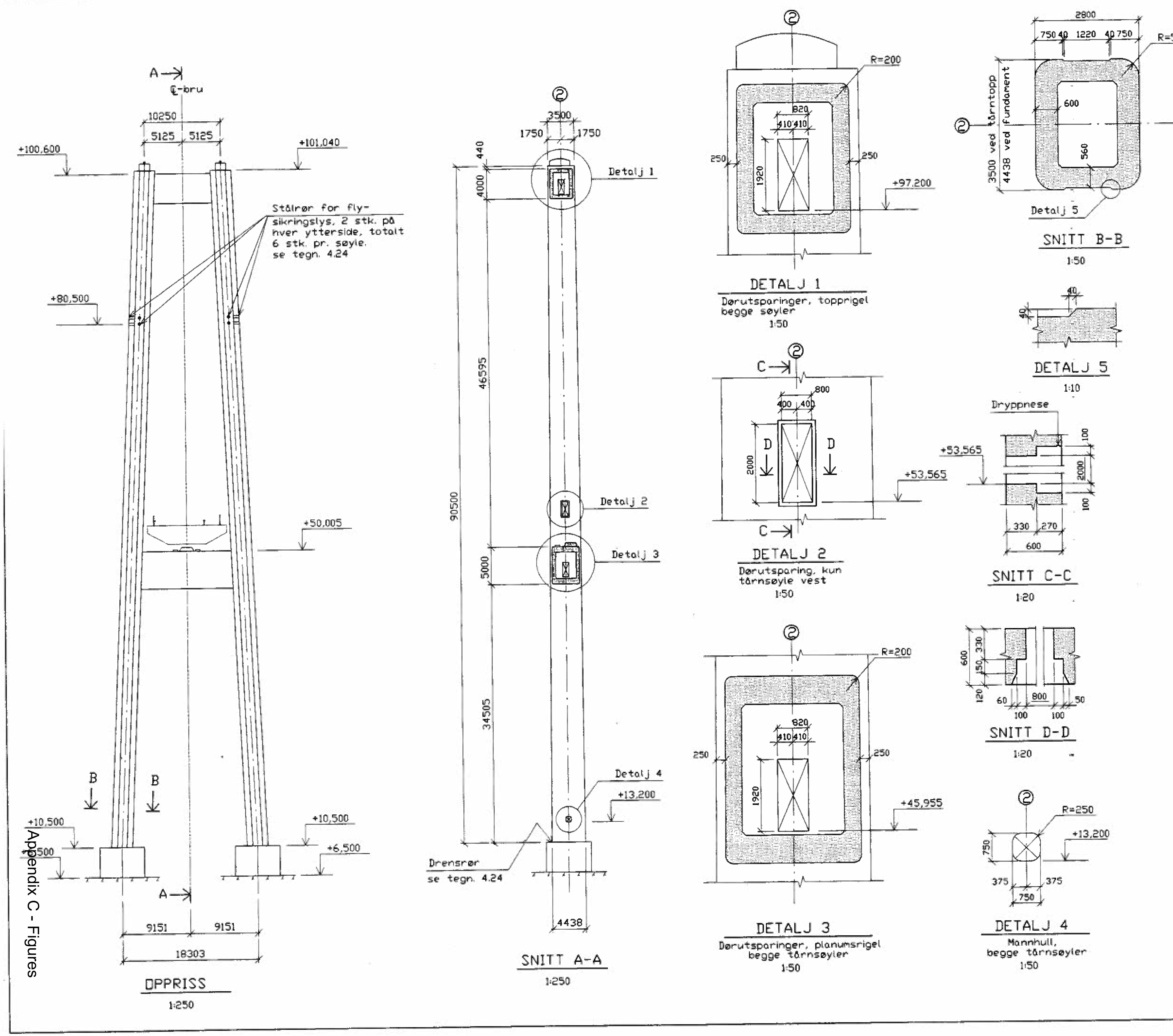

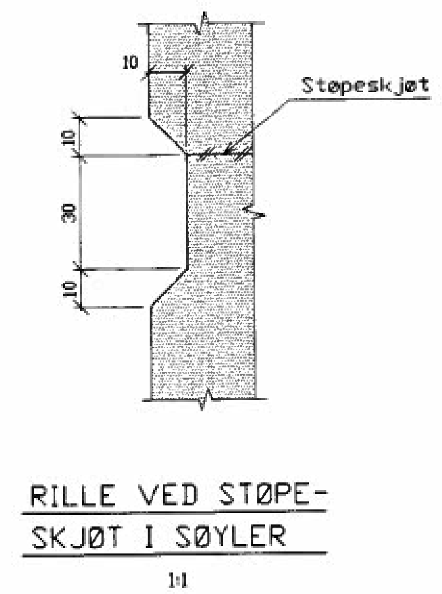

RILLE VED STØPE-SKJØT I SØYLER

1:1

MERKNADER

Miljøklasse MA NS 3473
Kontrollklasse Utvidet kontroll NS 3420

Utvendige hjørner på tårnsøyler avrundes med radius R=500 mm
Innvendig avfasing: 100 mm

Utvendige hjørner på rigler avrundes med radius R=200 mm
Innvendig avfasing 100 mm

Vertikale hjørner på fundament avrundes med R= 500 mm

BETONG

Fundament
Fasthetsklasse: C35
Masseforhold m≤0,50
D_{100} = 27 mm, D_{100} = 16 mm ved tett armering
Porevolum 5±1,5%

Søyler og rigler
Fasthetsklasse C55
Masseforhold m≤0,40
D_{100} = 27 mm, D_{100} = 16 mm ved tett armering
Porevolum 4±1,0%

ARMERING

Slakkarmering K500 TE

Spennarmering:
Flytekraft $F_{0,2}$ er den kraft i kabelen som tilsvarer flytespenning, eller den spenningen som gir 0,2 % permanent tøyning i stålet
Rigler: $F_{0,2}$= 2004 kN pr kabel
Oppspenningskraft 0,8xF
Fjellanker: $F_{0,2}$ = 3173 kN pr kabel
Oppspenningskraft 0,7xF

HENVISNINGER

Topp- og planumsrigel, se blad nr 4.07 og 4.08
Armering søyler, se blad nr 4.05, 4.06 og 4.11
Fundament, se blad nr 4.03
Innstøpingsgods, se teg 4.24

4.01

01 07 97	Som bygget	D	EL	LBB
23 05 96	Dørutsparing, Div rørutsp	C	EL	LBB
25 10 95	Arbeidstegning	B	SW	OK
18 09 95	Fundamentplassering Koteh pl rigel	A	PHS	
29 06 95	Anbud	0	PHS	
Dato	Rettelse	Merke	Rettet	Kfr

STATENS VEGVESEN

LYSEFJORDBRUA
ROGALAND

Tårn nord
Form

Målestokk 1:250, 1:50, 1:10, 1:1
Tegn 08 03 95 PHS
Kfr 10 95 OK
Trac 08 03 95 TOJ
Kfr 10 95 PHS
Bruer: 11-1737
Blad nr 4.01
Tegn nr 129/95
Rev D
Filnavn: LY-4-01

Vegdirektoratets bruavdeling, Oslo den 30/10_95
A. Vangsnes (sign.) P.H. Slyngstad (sign.)

HAUG OG BLOM-BAKKE A/S

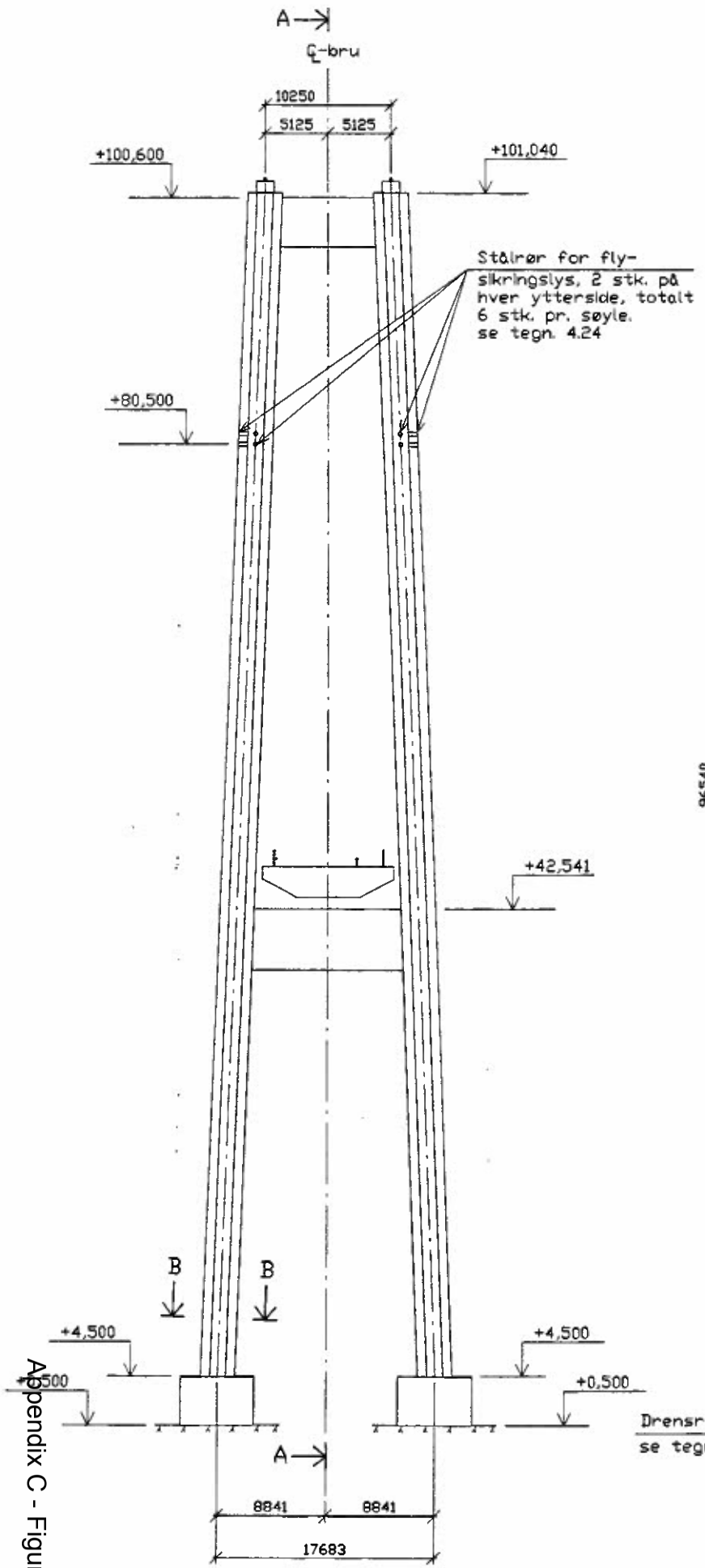

OPPRISS

1:250

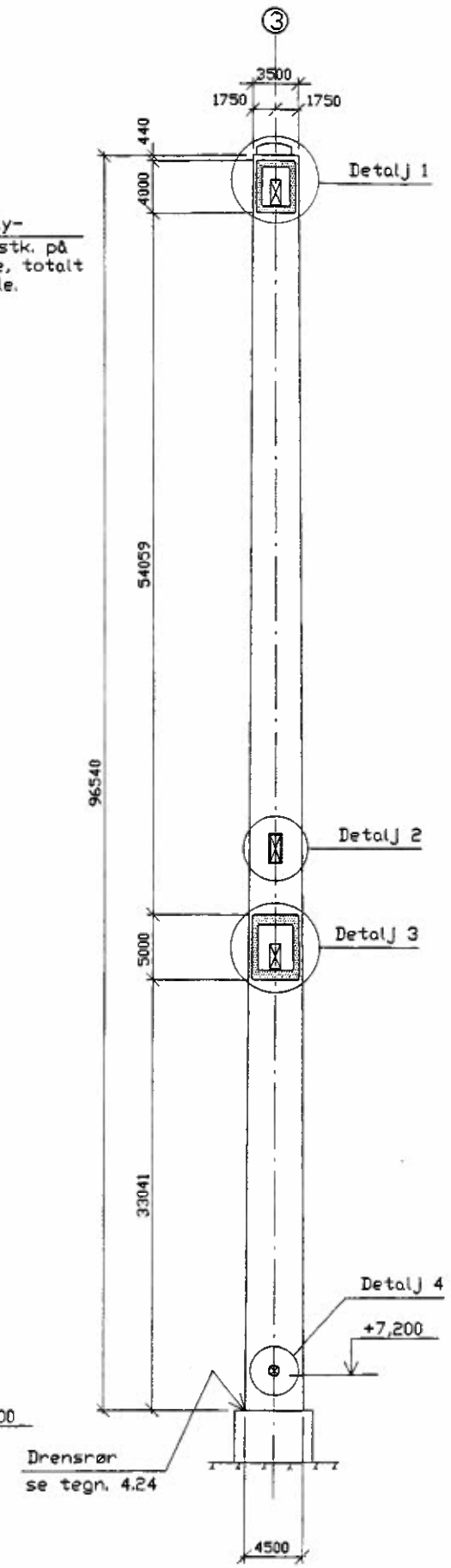

SNITT A-A

1:250

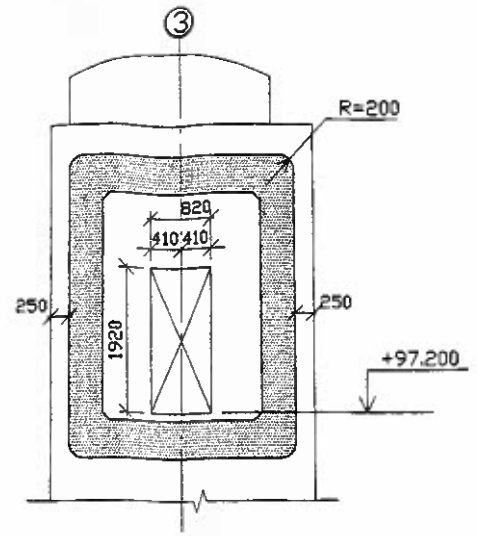

DETALJ 1

Dørutsparinger, topprigel
begge søyler

1:50

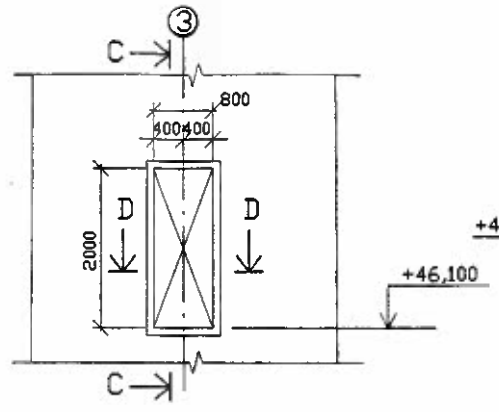

DETALJ 2

Dørutsparing, kun
tårnsøyle vest

1:50

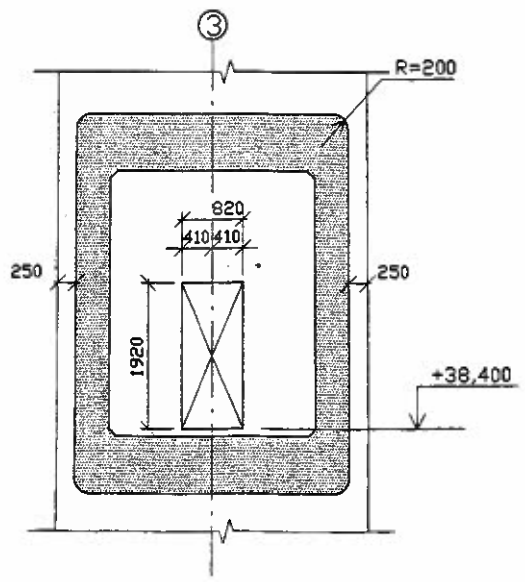

DETALJ 3

Dørutsparinger, planumsrigel
begge tårnsøyler

1:50

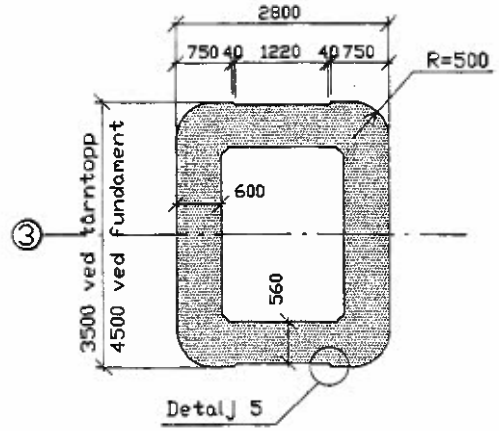

SNITT B-B

1:50

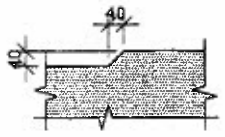

DETALJ 5

1:10

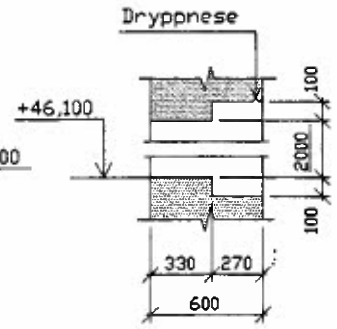

SNITT C-C

1:20

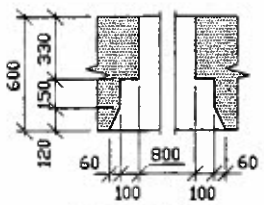

SNITT D-D

1:20

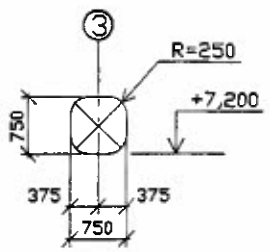

DETALJ 4

Mannhull,
begge tårnsøyler

1:50

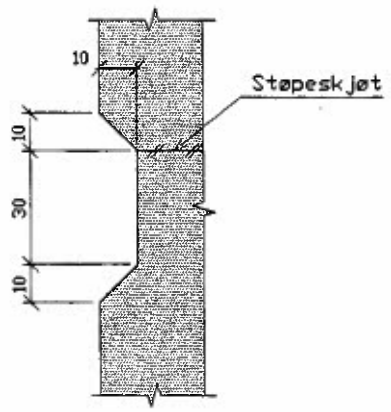

RILLE VED STØPE-
SKJØT I SØYLER

1:1

MERKNADER

Miljøklasse: MA NS 3473
Kontrollklasse: Utvidet kontroll NS 3420

Utvendige hjørner på tårnsøyler avrundes med radius R=500 mm.
Innvendig avfasing: 100 mm.

Utvendige hjørner på rigler avrundes med radius R=200 mm.
Innvendig avfasing: 100 mm.

Vertikale hjørner på fundament avrundes med R= 500 mm

BETONG

Fundament
- Fasthetsklasse: C35
- Masseforhold: m≤0,50
- D_{100} = 27 mm, D_{100} = 16 mm ved tett armering
- Porevolum: 5±1,5%

Søyler og rigler
- Fasthetsklasse: C55
- Masseforhold: m≤0,40
- D_{100} = 27 mm, D_{100} = 16 mm ved tett armering
- Porevolum: 4±1,0%

ARMERING

Slakkarmering K500 TE

Spennarmering:
Flytekraft $F_{0,2}$ er den kraft i kabelen som tilsvarer flytespenning, eller den spenningen som gir 0,2 % permanent tøyning i stålet.
- Rigler: $F_{0,2}$ = 2004 kN pr. kabel. Oppspenningskraft 0,8xF
- Fjellanker: $F_{0,2}$ = 3173 kN pr. kabel. Oppspenningskraft 0,7xF

HENVISNINGER

Rigler form, se blad 4.19
Topp- og planumsrigel, se blad nr. 4.21 og 4.22
Armering søyle, se blad nr. 4.16, 4.17 og 4.25
Fundament, se blad nr. 4.14

Dato	Revisjon	Merke	Rettet	Kontr.
01.07.97	Som bygget.	E	EL.	LBB
07.05.96	Dørutsparing, Flysikringslys	D	EL	LBB
29.01.96	Dørutsparing. Div. rørutsp.	C	LBB	OK
25.10.95	Arbeidstegning	B	SW	OK
18.09.95	Fundamentplassering	A	PHS	
29.06.95	Anbud	0	PHS	

STATENS VEGVESEN

LYSEFJORDBRUA
ROGALAND

Tårn sør
Form

Målestokk: 1:250, 1:50 1:20, 1:10 1:1, Mål i mm

Tegn. 08.03.95 PHS
Kontr. 10.95 OK
Godkj. 10.95 EL
Godkj. 10.95 PHS

Dwgnr. 11-1737
Bind nr. 4.12
Tegn. nr. 72/94
Rev. E
Filnavn: LY-4-12

Vegdirektoratets bruavdeling, Oslo den 30/10-95

A. Vangsnes (sign.) P.H. Slyngstad (sign.)

Entreprenør: AS VEIDEKKE OG OSLO-DØRKE A/S

4.12

Appendix B

Calculations

Analysis of vibration modes of Lysefjord Bridge

From the mathematical theory of vibration in suspension bridges by Freidrich Bleich and Modes and natural frequencies of suspension-bridge oscillations' by D. B. Steinman.

The calculations are presented here, both frequencies and Eigen modes. A presentation of the equations and the results are given and discussed in Chapter 7.

Length of the main span..... $l := 446m$

Cable sag..... $f := 45m$

Width of bridge girder..... $w_{bg} := 12.3m$

Height of bridge girder..... $h_{bg} := 2.76m$

Distance between hangers..... $w_h := 10.25m$

Thickness of plates in girder …….. $t_{bg} := \frac{8mm + 12mm}{2} = 0.01\,m$

Modulus of elasticity, girder..... $E := 210000 \frac{N}{mm^2}$

Modulus of elasticity, cable..... $Ec := 180000 \frac{N}{mm^2}$

Area of one main cable..... $Ac := 0.05m^2$

Moment of inertia, girder..... $I := 0.429m^4$

Mass of main span..... $m_{ms} := 2750000kg$

Weight of bridge girder..... $wght_{bg} := 5350 \frac{kg}{m} \cdot g$

$$wght_{bg} = 5.247 \times 10^4 \frac{kg}{s^2}$$

Weight of cable..... $wght_c := 408 \frac{kg}{m} \cdot g$

$$wght_c = 4.001 \times 10^3 \frac{kg}{s^2}$$

Mass moment of inertia..... $I_m := 82430 \frac{kg \cdot m^2}{m}$

Weight of main span per meter……. $w := \frac{m_{ms} \cdot g}{1}$

$$w = 6.047 \times 10^4 \frac{kg}{s^2}$$

Finding the horizontal cable force using the equation on page 70;

Cable force..... $H_w := \frac{w \cdot 1^2}{8f}$

$$H_w = 3.341 \times 10^7 N$$

Alvsat force..... $H := 2 \cdot 16.80 \cdot 10^6 N = 3.36 \times 10^7 N$

Bleich use the linearized differential equation of the vibration problem with boundary conditions for suspension bridge to find the equations for circular frequencies. A full derivation can be found in his book. The equation used here is further written in a more convenient form, where the following abbreviation is used;

Vertical asymmetric modes;

Abbreviation ..... $\lambda := \frac{\pi^2 \cdot E \cdot I}{1^2}$

$$\lambda = 4.47 \times 10^6 N$$

Circular frequencies (convenient form[3.2])..... $\omega_{BVA}(n) := \frac{n\pi}{1} \cdot \sqrt{\frac{g}{w}\left(H_w + n^2 \cdot \lambda\right)}$

Frequencies ..... $T_{BVA}(n) := \frac{2\pi}{\omega_{BVA}(n)}$

Number of half waves in the main span ..... $n := 2, 4 .. 6$

Vertical asymmetric frequencies and periods for n equal to 2, 4 and 6;

n =	$\omega_{BVA}(n)$ =		$T_{BVA}(n)$ =	
2	1.285	$\cdot\frac{rad}{sec}$	4.89	·s
4	3.676		1.709	
6	7.503		0.837	

The frequencies and periods are calculated when the bridge are vibrating with 2, 4 and 6 sinusoidal half waves. *This is corresponding to mode VA-1, VA-2 and VA-3 in the report from Abaqus.*

Modes and natural frequencies of suspension-bridge oscillations

By D.B. Steinman

Number of half waves in the main span ..... $n := 2,4..6$

The fundamental equilibrium equation for a suspension bridge is;

$$\Delta w := -\frac{d^2}{dx^2}\left(H_w\cdot\eta + y\cdot\Delta H - E\cdot I\cdot\frac{d^2}{dx^2}\eta\right)$$

Where H.w is the horizontal cable tension, ΔH is the increment produced by displacement, I is the moment of Inertia of the section of the stiffening truss, and E is the modulus of elasticity for the truss.

The coefficient of rigidity of the oscillating system is a significant criterion for aerodynamic stability. Formula 9 is the simplest and most useful formula for K, and it is exact for all even values of n, the so-called "anti symmetrical modes", since for these modes, ΔH=0.

Stiffness coefficient ..... $K_{SVA}(n) := \frac{\pi^2\cdot n^2}{l^2}\cdot H_w + \frac{\pi^4\cdot n^4}{l^4}\cdot E\cdot I$

Circular frequency ..... $\omega_{SVA}(n) := \sqrt{\frac{K_{SVA}(n)}{\frac{w}{g}}}$

Frequencies ..... $T_{SVA}(n) := \frac{2\cdot\pi}{\omega_{SVA}(n)}$

Vertical asymmetric frequencies and periods for n equal to 2, 4 and 6;

n =	$\omega_{SVA}(n)$ =		$T_{SVA}(n)$ =	
2	1.285	$\cdot\frac{rad}{sec}$	4.89	·s
4	3.676		1.709	
6	7.503		0.837	

The value of K(2) is the "Coefficient of Rigidity" of the suspension bridge, and this is a useful criterion for aerodynamic stability.

The frequencies and periods are calculated when the bridge are vibrating with 2, 4 and 6 sinusoidal half waves. *This is corresponding to mode VA-1, VA-2 and VA-3 in the report from Abaqus.*

Put $y0 := 1$

$$y_{VA}(x,\Omega) := y0 \cdot \sin\left(\Omega \cdot \frac{x}{1}\right)$$

$$\Omega := 2\pi 1..2$$

$$y_{VA1}(x) := y_{VA}(x, 2\cdot\pi\cdot 1)$$

$$y_{VA2}(x) := y_{VA}(x, 2\cdot\pi\cdot 2)$$

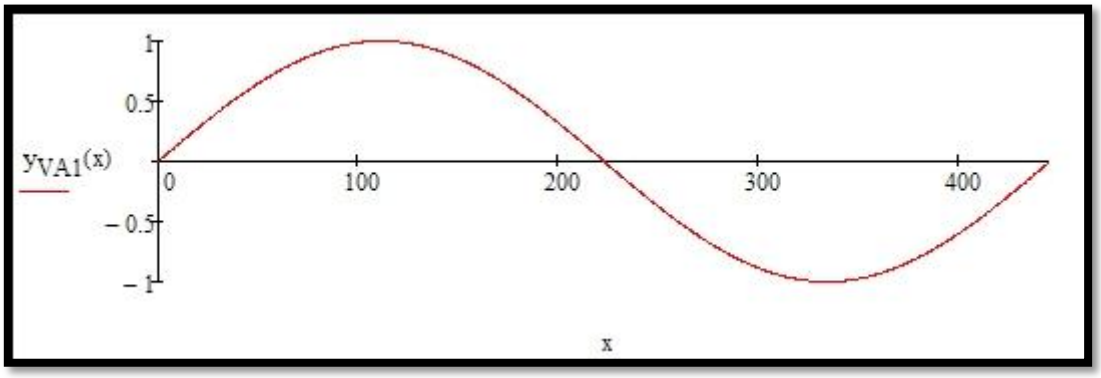

First vertical asymmetric mode from Bleich/Steinman calculations

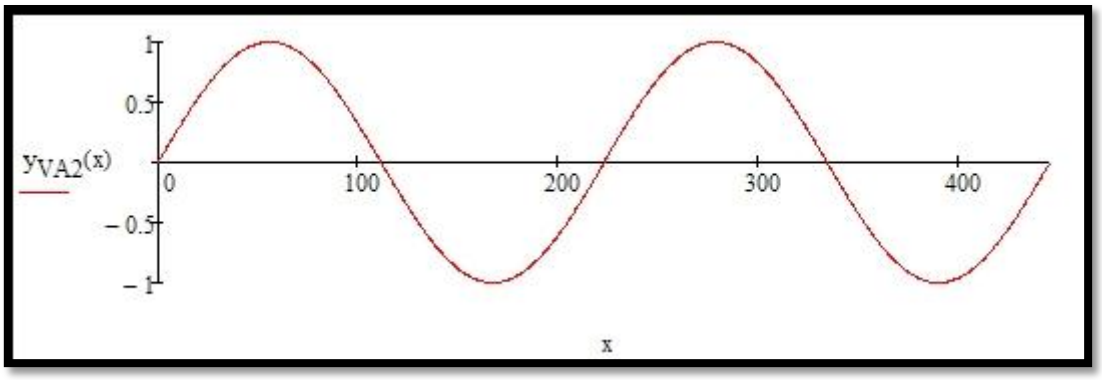

Second vertical asymmetric mode from Bleich/Steinman calculations

Vertical symmetric mode;

Article 7. - Suspension bridge with unloaded backstays

Using the energy equation valid for one span, then the analysis is based upon the two equations:

$$T - V := \frac{1}{2}\left(\frac{w}{g}\omega^2 \cdot \int_0^1 \eta^2\,dx - EI \cdot \int_0^1 \eta''^2\,dx + H_w \cdot \int_0^1 \eta'' \cdot \eta\,dx - \frac{8f}{1^2} \cdot h \cdot \int_0^1 \eta\,dx\right)$$

and

$$\frac{8f}{1^2} \cdot \int_0^1 \eta\,dx - \frac{L_E \cdot h}{E_c \cdot A_c} = \blacksquare \cdot 0$$

$$L_E := \int \left(\frac{ds}{dx}\right)^2 ds$$

Length .....

..... the integral extends from hold-down to hold-down of the cable. The hold-down is the anchor bolts in the far ends of the bridge.

$$L_E := \sum_1 \left[1 + \left(\frac{8f^2}{1}\right) \cdot \sec^3 \cdot \gamma\right]$$

Where γ is the inclination of the cable chord. AL.so, Σ denotes summations covering all similar expressions in all spans.

Cable length ..... $LE := 720m$

Equation of frequency (3.54):

$$A \cdot k + 9 \cdot B \cdot (k - A \cdot p) = 0$$

With the parameters ..... $A = s \cdot \omega^2 - H_w - \lambda$

$$B = s \cdot \omega^2 - 9H_w - 81\lambda$$

$s := \dfrac{w \cdot 1^2}{\pi^2 \cdot g}$ $\quad s = 1.243 \times 10^8 \, m \cdot kg$

$k := \dfrac{32f}{\pi^3}$ $\quad k = 46.442 \, m$

$p := \dfrac{\pi \cdot 1}{16f} \cdot \dfrac{LE}{Ec \cdot Ac}$ $\quad p = 1.557 \times 10^{-7} \, \dfrac{s^2}{kg}$

Substituting for A and B, and solving the equation;

$A(x) := s \cdot x^2 - H_w - \lambda$

$B(x) := \left(s \cdot x^2 - 9H_w - 81\lambda \right)$

This give the ω1 and ω2 ..... $\begin{pmatrix} 1.581 \\ 2.41 \\ -1.581 \\ -2.41 \end{pmatrix} \dfrac{1}{s}$

Higher symmetric modes can be determined based with a sufficient degree of accuracy upon a sine curve of n half waves (3.57);

$\omega_{BVS}(n) := \sqrt{\dfrac{1}{s} \cdot \left(n^2 \cdot H_w + n^4 \cdot \lambda + \dfrac{k}{n^2 \cdot p} \right)}$

$\omega_{BVS}(5) = 5.413 \cdot \dfrac{rad}{sec}$

$\omega 1_{BVS} := 1.581 \dfrac{rad}{sec}$ $T1_{BVS} := \dfrac{2\pi}{\omega 1_{BVS}} = 3.974 \, s$

$\omega 2_{BVS} := 2.41 \dfrac{rad}{sec}$ $T2_{BVS} := \dfrac{2\pi}{\omega 2_{BVS}} = 2.607 \, s$

$\omega 3_{BVS} := \omega_{BVS}(5) = 5.413 \cdot \dfrac{rad}{sec}$ $T3BVS := \dfrac{2\pi}{\omega 3_{BVS}} = 1.161 \, s$

D. B. Steinman;

Length ..... $L_s := \sum_1 \int_0^1 \frac{ds^2}{dx^2}\, ds$

..... the integral extends from hold-down to hold-down of the cable. The hold-down is the anchor bolts in the far ends of the bridge.

$$L_s := \sum_1 \left[1 + \left(\frac{8f^2}{1} \right) \cdot \sec^3 \cdot \gamma \right]$$

Length of cable ..... $L_s := 720m$

Dimensional constant for the structure .....

$$C := \frac{512}{\pi^2} \cdot \frac{f}{1^2} \cdot \frac{Ec \cdot Ac}{L_s}$$

$$C = 1.467 \times 10^5 \, Pa$$

$$\frac{C \cdot f}{1} = 1.48 \times 10^4 \, Pa$$

Equation 12 c:

$$\Sigma \left(\frac{1}{n^2} \cdot \frac{C \cdot \frac{f}{1}}{K - K_n} \right) = 1$$

$$n := 1, 3 .. 5$$

Kn is given from equation 9;

$$K(n) := \frac{\pi^2 \cdot n^2}{1^2} \cdot H_w + \frac{\pi^4 \cdot n^4}{1^4} \cdot E \cdot I$$

$$K_n = \left(K(n) := \frac{\pi^2 \cdot n^2}{1^2} \cdot H_w + \frac{\pi^4 \cdot n^4}{1^4} \cdot E \cdot I \right)$$

n =	K(n) =
1	$1.88 \cdot 10^3$ Pa
3	$3.288 \cdot 10^4$
5	$1.801 \cdot 10^5$

For symmetrical modes, and with the consistent relative amplitudes substituted it must yield the same value of K for each component mode. To satisfy this condition, the relationship under must be satisfied. Equation 12 c with n=1 and n=3;

This give the K1 and K2 .....

$$\begin{pmatrix} 1.541 \times 10^4 \\ 3.58 \times 10^4 \end{pmatrix} \text{Pa}$$

$K_{11} := 1.541 \times 10^4 \text{Pa}$

$K_{21} := 3.58\,10^4 \text{Pa}$

$\omega_{SVS11} := \sqrt{\frac{K_{11}}{\frac{w}{g}}} = 1.581 \cdot \frac{\text{rad}}{\text{sec}}$ $TS11 := \frac{2\pi}{\omega_{SVS11}} = 3.974\,\text{s}$

$\omega_{SVS21} := \sqrt{\frac{K_{21}}{\frac{w}{g}}} = 2.41 \cdot \frac{\text{rad}}{\text{sec}}$ $TS21 := \frac{2\pi}{\omega_{SVS21}} = 2.608\,\text{s}$

Solving the equation with n=3 and n=5;

$$q(x) := \frac{1}{3^2} \cdot \frac{C \cdot \frac{f}{1}}{x - K(3)} + \frac{1}{5^2} \cdot \frac{C \cdot \frac{f}{1}}{x - K(5)} - 1$$

This give the K1 and K2 ..... $\begin{pmatrix} 3.452 \times 10^4 \\ 1.807 \times 10^5 \end{pmatrix}$ Pa

$K_{22} := 3.452 \times 10^4 \text{Pa}$

$K_{32} := 1.807 \times 10^5 \cdot \text{Pa}$

$\omega_{SVS22} := \sqrt{\frac{K_{22}}{\frac{w}{g}}}$

$$\omega_{SVS32} := \sqrt{\frac{K_{32}}{\frac{w}{g}}}$$

$$\omega_{SVS22} = 2.366 \cdot \frac{rad}{sec} \quad T_{SVS22} := \frac{2\pi}{\omega_{SVS22}} = 2.655\,s$$

$$\omega_{SVS32} = 5.414 \cdot \frac{rad}{sec} \quad T_{SVS32} := \frac{2\pi}{\omega_{SVS32}} = 1.161\,s$$

Solving the equation with n=1, n=3 and n=5;

$$p(y) := \frac{1}{1^2} \cdot \frac{C \cdot \frac{f}{1}}{y - K(1)} + \frac{1}{3^2} \cdot \frac{C \cdot \frac{f}{1}}{y - K(3)} + \frac{1}{5^2} \cdot \frac{C \cdot \frac{f}{1}}{y - K(5)} - 1$$

$$p(y)\ \text{solve},y \rightarrow = \begin{pmatrix} 3.578 \times 10^4 \\ 1.537 \times 10^4 \\ 1.807 \times 10^5 \end{pmatrix} Pa$$

$$K_{13} := 1.537 \times 10^4 Pa$$

$$K_{23} := 3.578 \times 10^4 Pa$$

$$K_{33} := 1.807 \times 10^5 Pa$$

$$\omega_{SVS13} := \sqrt{\frac{K_{13}}{\frac{w}{g}}}$$

$$\omega_{SVS23} := \sqrt{\frac{K_{23}}{\frac{w}{g}}}$$

$$\omega_{SVS33} := \sqrt{\frac{K_{33}}{\frac{w}{g}}}$$

$$\omega_{SVS13} = 1.579 \cdot \frac{rad}{sec} \quad T_{SVS13} := \frac{2\pi}{\omega_{SVS13}} = 3.98\,s$$

$$\omega_{SVS23} = 2.409 \cdot \frac{rad}{sec} \quad T_{SVS23} := \frac{2\pi}{\omega_{SVS23}} = 2.608\,s$$

$$\omega_{SVS33} = 5.414 \cdot \frac{rad}{sec} \quad T_{SVS33} := \frac{2\pi}{\omega_{SVS33}} = 1.161\,s$$

The frequencies and periods are calculated when the bridge are vibrating with 1, 3 and 5 sinusoidal half waves. *This is corresponding to mode VS-1, VS-2 and VS-3 in the report from Abaqus.*

Vertical symmetric modes for Lysefjord bridge;

1. and 2. vertical symmetric mode shape

Equation 3.53 from Bleich yields;

$$a_3 = \frac{A}{3B} \cdot a_1$$

Equation 12d from Steinman;

$$na = \frac{1}{K - K_n}$$

The relative amplitudes can be found from this equation.

NOTE: To find a3/a1, put n=3 and Kn=k(3), while to find a3, put K=K1. To find a1, put n=1, Kn=K(1) and K=K1.

First vertical symmetric mode;

Using the lowest eigenfrequency from Bleich for vertical symmetric modes for A and B, and put a1=1;

$$\omega 1_{BVS} = 1.581 \cdot \frac{rad}{sec}$$

$$A(\omega 1_{BVS}) = 2.727 \times 10^8\,N$$

$$B(\omega 1_{BVS}) = -3.521 \times 10^8\,N$$

$$a_{11} := 1$$

$$a_{31} := \frac{A(\omega 1_{BVS})}{3 \cdot B(\omega 1_{BVS})} \cdot a_{11}$$

$$a_{31} = -0.258$$

$$y_{11}(x) := a_{11} \cdot \sin\left(\frac{\pi \cdot x}{1}\right)$$

$$y_{31}(x) := a_{31} \cdot \sin\left(\frac{3 \cdot \pi \cdot x}{1}\right)$$

$$y_{12}(x) := y_{11}(x) + y_{31}(x)$$

$$y_{12}(233m) = 1.25$$

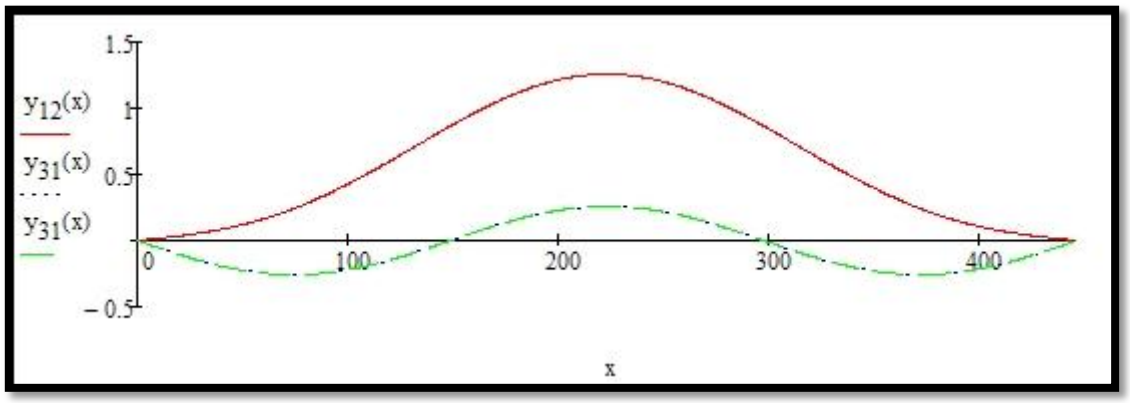

The green line shows VS-1, that is combined from the two lines that represent n=1 and n=3.

Using the equations from Steinman to control the mode shape of VS-1;

$$a_1 := \frac{1 \cdot Pa}{(K_{11} - K(1))}$$

$$a_1 = 7.391 \times 10^{-5}$$

$$a_3 := \frac{1 \cdot Pa}{3 \cdot (K_{11} - K(3))}$$

$$a_3 = -1.908 \times 10^{-5}$$

$$\frac{a_3}{a_1} = -0.258$$

This is the same result as from Bleich.

$$a_5 := \frac{1Pa}{5 \cdot (K_{11} - K(5))}$$

$$a_5 = -1.215 \times 10^{-6}$$

$$\frac{a_5}{a_1} = -0.016$$

Includes a5 to see if this has a big influence on the shape of VS-1;

$$y_{12}(x) := a_{11} \cdot \sin\left(\frac{\pi \cdot x}{1}\right)$$

$$y_{32}(x) := a_{31} \cdot \sin\left(\frac{3 \cdot \pi \cdot x}{1}\right)$$

$$y_{52}(x) := a_5 \cdot \sin\left(\frac{5 \cdot \pi \cdot x}{1}\right)$$

$$y_1(x) := y_{12}(x) + y_{32}(x) + y_{52}(x)$$

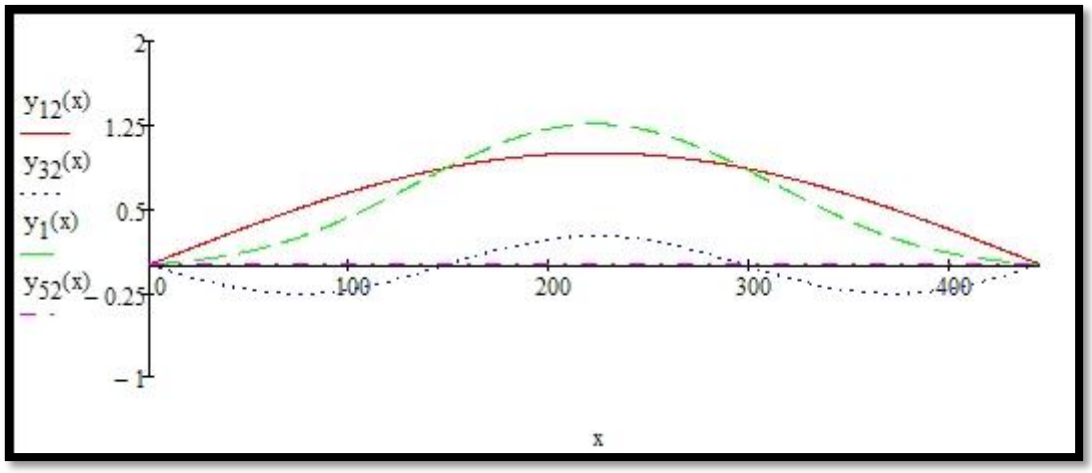

The green line shows VS-1 as a combination of n=1, n=3 and n=5.

It can be seen that as expected, a5 has very little impact on the mode shape.

Second vertical symmetric mode;

Using the second eigenfrequency from Bleich for vertical symmetric modes for A and B, and put a1=1;

$$A\left(\omega 2_{BVS}\right) = 6.839 \times 10^{8}\,N$$

$$B\left(\omega 2_{BVS}\right) = 5.901 \times 10^{7}\,N$$

$$\omega 2_{BVS} = 2.41 \cdot \frac{rad}{sec}$$

$$a_1 := 1$$

$$a_{32} := \frac{A\left(\omega 2_{BVS}\right)}{3 \cdot B\left(\omega 2_{BVS}\right)} \cdot a_1$$

$$a_{32} = 3.863$$

$$y_{13}(x) := a_1 \cdot \sin\left(\frac{\pi \cdot x}{1}\right)$$

$$y_{33}(x) := a_{32} \cdot \sin\left(\frac{3 \cdot \pi \cdot x}{1}\right)$$

$$y_{23}(x) := y_{12}(x) + y_{32}(x)$$

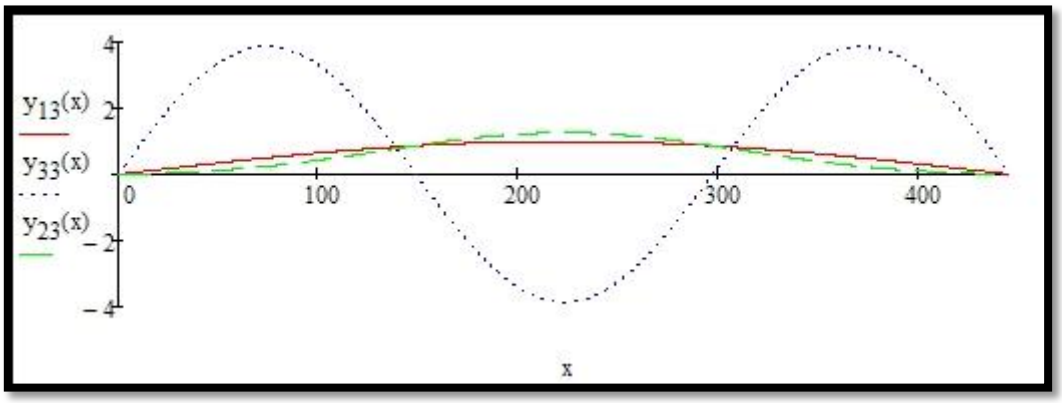

The green line shows VS-2, as a combination of n=1 and n=3.

Using the equations from Steinman to control the mode shape of VS-1;

$$a_{12} := \frac{1 \cdot Pa}{\left(K_{23} - K(1)\right)}$$

$$a_{12} = 2.95 \times 10^{-5}$$

$$a_{32} := \frac{1 \cdot Pa}{3 \cdot \left(K_{23} - K(3)\right)}$$

$$a_{32} = 1.151 \times 10^{-4}$$

$$\frac{a_{32}}{a_{12}} = 3.903$$

This is close to the same result from Bleich.

$$a_{52} := \frac{1 \cdot Pa}{5\left(K_{23} - K(5)\right)}$$

$$a_{52} = -1.386 \times 10^{-6}$$

$$\frac{a_{52}}{a_{12}} = -0.047$$

$$y_{123}(x) := a_{12} \cdot \sin\left(\frac{\pi \cdot x}{1}\right)$$

$$y_{323}(x) := a_{32} \cdot \sin\left(\frac{3 \cdot \pi \cdot x}{1}\right)$$

$$y_{523}(x) := a_{52} \cdot \sin\left(\frac{5 \cdot \pi \cdot x}{1}\right)$$

$$y_2(x) := y_{123}(x) + y_{323}(x) + y_{523}(x)$$

Includes a5 to see which impact this will have on the mode shape;

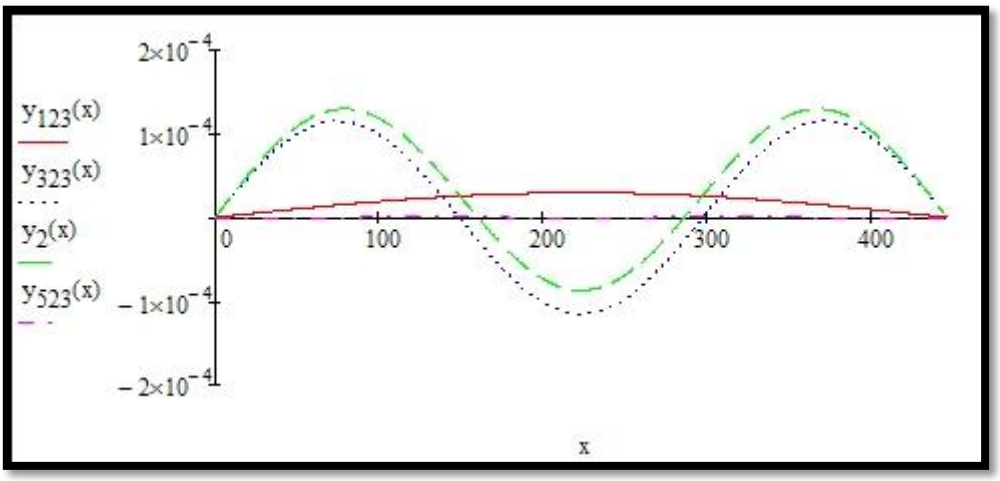

The green line shows VS-2, that is a combination of n=1, n=3 and n=5.

a5 has a very little impact on the mode shape also in mode 2.

Normalizing the modes, such that largest displacement is equal to +/- 1.0.

$$y_1(223 \cdot m) = 1.258$$

$$y_2(223 \cdot m) = -8.701 \times 10^{-5}$$

$$y_2(74.55 \cdot m) = 1.292 \times 10^{-4}$$

$$VS1(x) := \frac{y_1(x)}{y_1(223 \cdot m)}$$

$$VS2(x) := \frac{y_2(x)}{y_2(74.55 \cdot m)}$$

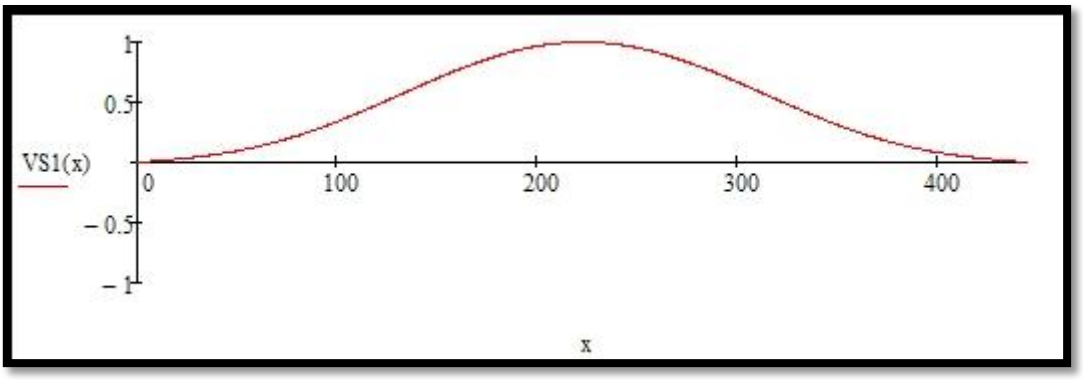

First vertical symmetric mode from Bleich/Steinman calculations

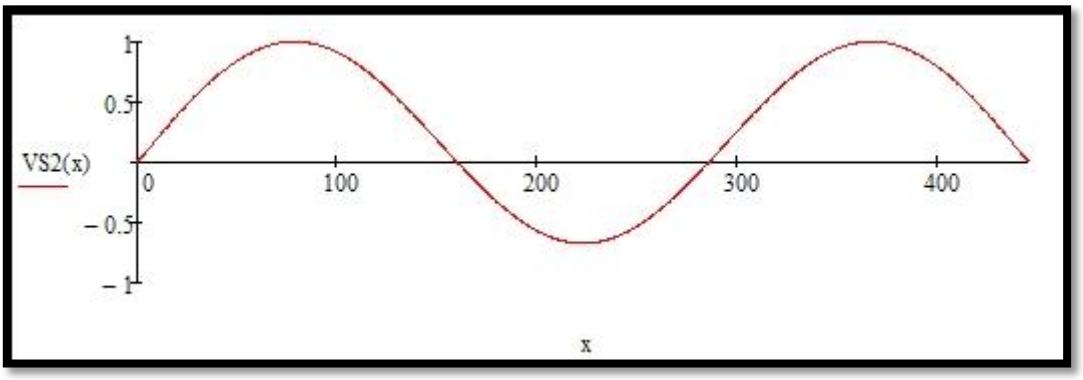

Second vertical symmetric mode from Bleich/Steinman calculations

Torsional vibration modes

$$w_{ms} := \frac{m_{ms}}{1}$$

$$w_{ms} = 6.166 \times 10^{3} \frac{kg}{m}$$

Weight of main span per meter .....

$$r^2 = \frac{\Sigma m_{ms} \cdot r^2}{\Sigma m_{ms}} = \frac{I_m}{w_{ms}}$$

$$r := \sqrt{\frac{I_m}{w_{ms}}}$$

$$r = 3.656\,m$$

$$\frac{w_{bg}}{2r} = 1.682$$

From chapter 5, Bleich;

Assume

$\mu w := 2\cdot\sqrt{2}$ and $\mu h := 2\sqrt{2}$

$A_w := 1.09\cdot t_{bg}\cdot h_{bg}$ $\quad A_w = 0.03\,m^2$

$A_h := 1.09\cdot t_{bg}\cdot w_h$ $\quad A_h = 0.112\,m^2$

$$\beta := \frac{w_h\cdot h_{bg}}{\left(\frac{\mu w\cdot h_{bg}^{\,2}}{A_w}\right)+\left(\frac{\mu h\cdot w_{bg}^{\,2}}{A_h}\right)} \qquad \beta = 6.223\times 10^{-3}\,m^2$$

$$R := \left(E\cdot\beta\cdot w_h\cdot h_{bg} + H_w\cdot\frac{w_h^{\,2}}{4}\right)\cdot\frac{\pi^2}{21} \qquad R = 4.188\times 10^{8}\cdot\frac{kg\cdot m^2}{sec^2}$$

Area moment of inertia around x-axis ..... $I_{w1} := t_{bg}\cdot w_{bg}\cdot\frac{h_{bg}^{\,2}}{2} = 0.468\,m^4$

Length of the side plates of the girder... $l_{plates} := 5.172m$

Area moment of inertia around y-axis ..... $I_{h1} := t_{bg}\cdot l_{plates}\cdot\frac{w_{bg}^{\,2}}{2} = 3.912\,m^4$

From Alvsat, where the stiffeners inside the bridge girder is taken into consideration, the area moments are (these will be used in the following calculations);

$I_w := 0.429m^4$

$I_h := 4.952m^4$

$$\varepsilon w := \frac{w_{bg}}{2} - \frac{\mu w}{A_w} \cdot \beta \cdot h_{bg} \qquad \varepsilon w = 4.535\,m$$

$$\varepsilon h := \frac{l_{plates}}{2} - \frac{\mu h}{A_h} \cdot \beta \cdot w_{bg} \qquad \varepsilon h = 0.648\,m$$

$$Y := I_w \cdot \varepsilon w^2 + I_h \cdot \varepsilon h^2 \qquad Y = 10.905 \cdot m^6$$

$$\Lambda := E \cdot Y \cdot \frac{\pi^4}{2 \cdot l^3} \qquad \Lambda = 1.257 \times 10^6 \cdot N \cdot m$$

$$M := \frac{1}{g} \cdot \left(r^2 \cdot wght_{bg} + \frac{w_h^2}{4} \cdot wght_c \right) \qquad M = 8.224 \times 10^4\, m \cdot kg$$

$$s := M \cdot \frac{1}{4} \qquad s = 9.17 \times 10^6\, m^2 \cdot kg$$

$$LE := 720m$$

$$K := \frac{Ec \cdot Ac}{LE} \cdot \frac{64 \cdot f^2 \cdot w_h^2}{\pi^2 \cdot l^2} \qquad K = 8.669 \times 10^7 \cdot N \cdot m$$

Equation of frequency (3.54):

$$B \cdot (A - K) - \frac{A \cdot K}{9} = p$$

With the parameters .....

$$A = s \cdot \omega^2 - R - \Lambda$$

$$B = s \cdot \omega^2 - 9R - 81\Lambda$$

Substituting for A and B, and solving the equation;

$$A(x) := s \cdot x^2 - \Lambda - R$$

$$B(x) := s \cdot x^2 - 81\Lambda - 9R$$

Where x=ω

Where x=ω

This give the ω1 and ω2 ..... $\begin{pmatrix} 7.432 \\ 20.572 \\ -7.432 \\ -20.572 \end{pmatrix}$

$$\omega 1_{BTS} := 7.432 \frac{rad}{sec} \quad T1_{BTS} := \frac{2\pi}{\omega 1_{BTS}} = 0.845\,s$$

$$\omega 2_{BTS} := 20.572 \frac{rad}{sec} \quad T2_{BTS} := \frac{2\pi}{\omega 2_{BTS}} = 0.305\,s$$

The frequencies and periods are calculated when the bridge are vibrating with 1 and 3 sinusoidal half waves. *This is corresponding to mode TS-1 and TS-2 in the report from Abaqus.*

1. and 2. torsional symmetric mode

Equation 3.53 from Bleich yields;

$$a_{1T1} := -1$$

$$a_{3T1} := \frac{A(\omega 1_{BTS})}{3B(\omega 1_{BTS})} \cdot a_{1T1}$$

$$a_{3T1} = 0.009$$

$$\frac{a_{3T1}}{a_{1T1}} = -0.009$$

$$y_{1T1}(x) := a_{1T1} \cdot \sin\left(\frac{\pi \cdot x}{1}\right)$$

$$y_{3T1}(x) := a_{3T1} \cdot \sin\left(\frac{3 \cdot \pi \cdot x}{1}\right)$$

$$y_{T1}(x) := y_{1T1}(x) + y_{3T1}(x)$$

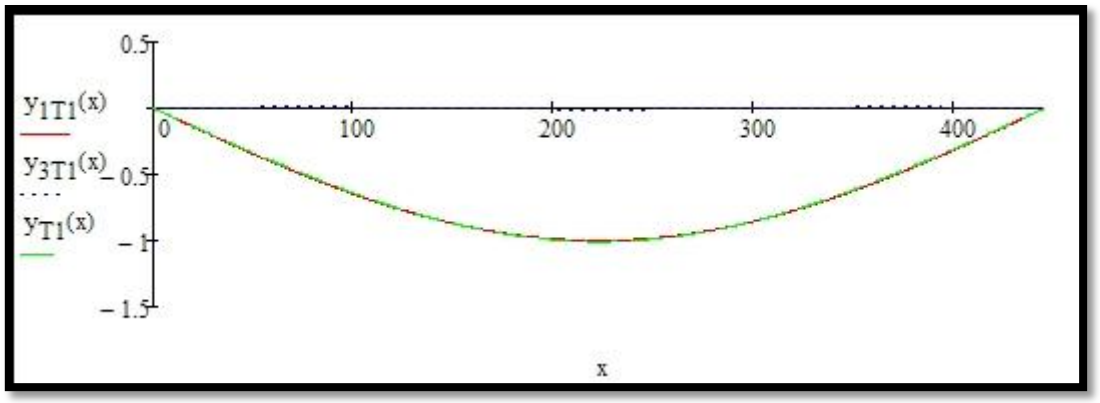

The green line shows TS-1, that is combined from the two lines that represent n=1 and n=3.

Second vertical symmetric mode;

Using the second eigenfrequency from Bleich for vertical symmetric modes for A and B, and put a1=1;

$$a_{1T2} := -1$$

$$a_{3T2} := \frac{A(\omega 2_{BTS})}{3B(\omega 2_{BTS})} \cdot a_{1T2}$$

$$a_{3T2} = -114.86$$

$$\frac{a_{3T2}}{a_{1T2}} = 114.86$$

$$y_{1T2}(x) := a_{1T2} \cdot \sin\left(\frac{\pi \cdot x}{1}\right)$$

$$y_{3T2}(x) := a_{3T2} \cdot \sin\left(\frac{3 \cdot \pi \cdot x}{1}\right)$$

$$y_{T2}(x) := y_{1T2}(x) + y_{3T2}(x)$$

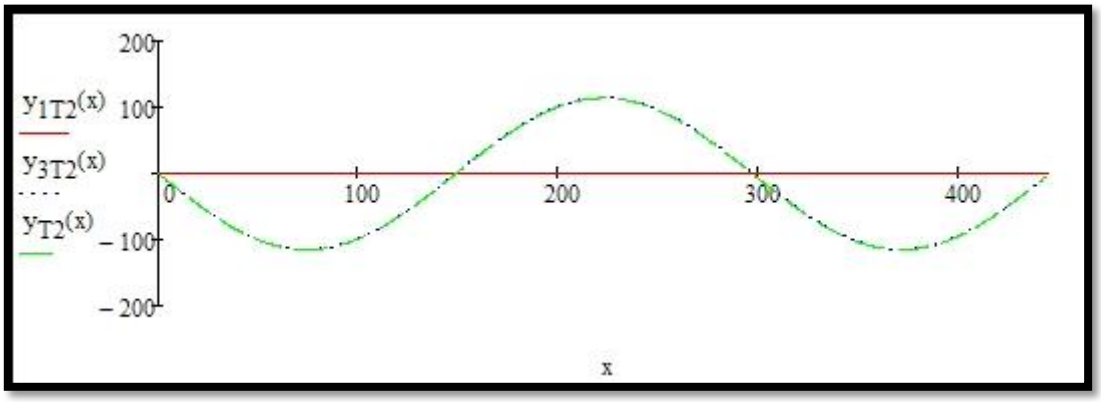

The green line shows VT-2, as a combination of n=1 and n=3.

Normalizing the modes, such that largest displacement is equal to +/- 1.0.

$y_{T1}(223 \cdot m) = -1.009$

$y_{T2}(223 \cdot m) = 113.86$

$y_{T2}(74.55 \cdot m) = -115.36$

$$TS1(x) := \frac{y_{T1}(x)}{y_{T1}(223 \cdot m)}$$

$$TS2(x) := \frac{y_{T2}(x)}{y_{T2}(74.55 \cdot m)}$$

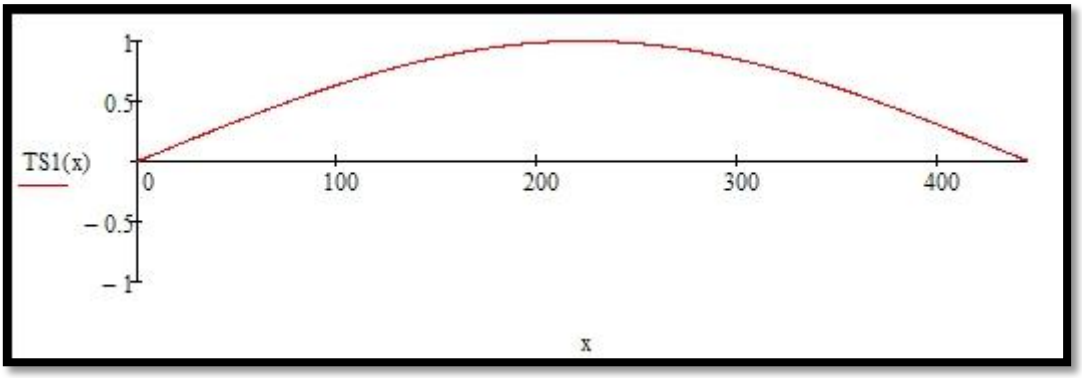

First torsional symmetric mode from Bleich/Steinman calculations

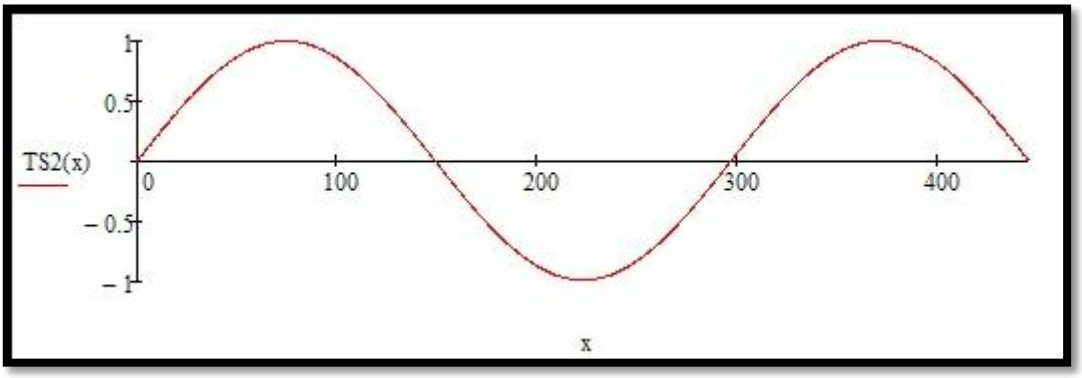

Second torsional symmetric mode from Bleich/Steinman calculations

Torsion asymmetric modes;

Equation 5.31, Bleich:

$$\omega 1_{BTA} := \sqrt{\frac{2^2}{s}\cdot\left(2^2\cdot\Lambda + R\right)} \qquad T1_{BTA} := \frac{2\pi}{\omega 1_{BTA}}$$

$$\omega 1_{BTA} = 13.596\cdot\frac{rad}{sec} \qquad T1_{BTA} = 0.462\,s$$

$$\omega 2_{BTA} := \sqrt{\frac{4^2}{s}\cdot\left(4^2\cdot\Lambda + R\right)} \qquad T2_{BTA} := \frac{2\pi}{\omega 2_{BTA}}$$

$$\omega 2_{BTA} = 27.673\,\frac{1}{s} \qquad T2_{BTA} = 0.227\,s$$

The frequencies and periods are calculated when the bridge are vibrating with 2 and 4 sinusoidal half waves. *This is corresponding to mode TA-1 and TA-2 in the report from Abaqus.*

Put

$$y0 := 1$$

$$y_{TA}(x,\Omega) := y0\cdot\sin\left(\Omega\cdot\frac{x}{1}\right)$$

$$\Omega := 2\pi 1..2$$

$$y_{TA1}(x) := y_{TA}(x, 2\cdot\pi\cdot 1)$$

$$y_{TA2}(x) := y_{TA}(x, 2\cdot\pi\cdot 2)$$

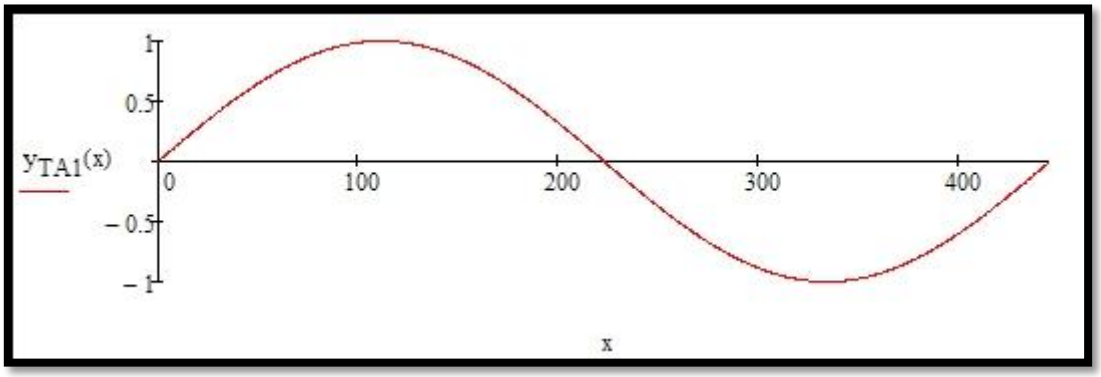

Second torsional asymmetric mode from Bleich/Steinman calculations

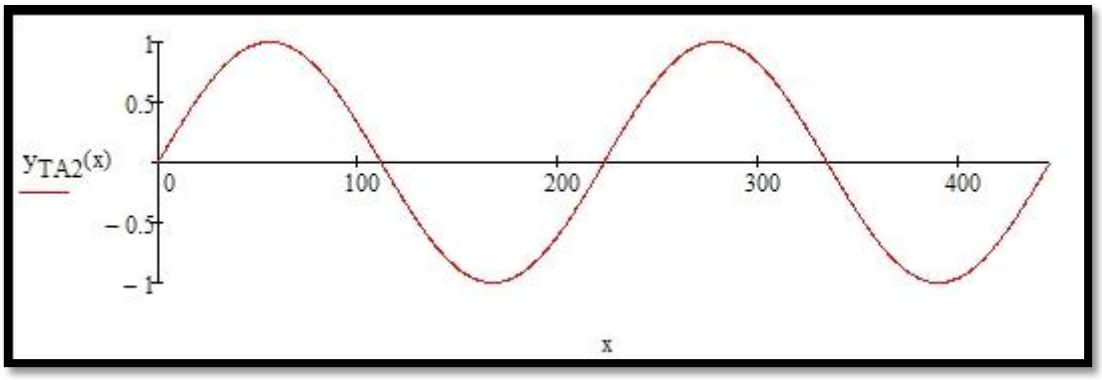

Second torsional asymmetric mode from Bleich/Steinman calculations

Lysefjord bridge girder – cross section area

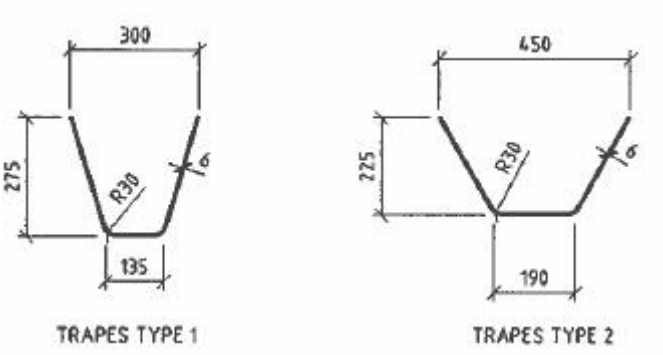

$t := 6mm$

Area of trapes type 1 .....

$b_{11} := 300mm$

$b_{21} := 135mm$

$h_{11} := 275mm$

$$l_{h1} := \sqrt{h_{11}^{2} + \left(\frac{b_{11} - b_{21}}{2}\right)^{2}} = 0.287\,m$$

$$a_1 := t \cdot \left(2 \cdot l_{h1} + b_{21}\right) = 4255 \cdot mm^{2}$$

Area of trapes type 2 .....

$b_{12} := 450mm$

$b_{22} := 190mm$

$h_{12} := 225mm$

$$l_{h2} := \sqrt{h_{12}^{2} + \left(\frac{b_{12} - b_{22}}{2}\right)^{2}} = 0.26\,m$$

$$a_2 := t \cdot \left(2 \cdot l_{h2} + b_{22}\right) = 4258 \cdot mm^{2}$$

Area of the plate in bridge girder .....

Top plate .....

$t_{tp} := 12mm$

$l_{tp} := 10700mm$

$$a_{tp} := t_{tp} \cdot l_{tp} = 0.13\,m^{2}$$

Upper sideplates ...

$t_{usp} := 12mm$

$l_{usp} := 1131mm$

$$a_{usp} := t_{usp} \cdot l_{usp} = 0.01\,m^{2}$$

Lower sideplates ...

$t_{lsp} := 8mm$

$l_{lsp} := 4041mm$

$$a_{lsp} := t_{lsp} \cdot l_{lsp} = 0.03\,m^{2}$$

Bottom plate .....

$t_{bp} := 8mm$

$l_{bp} := 5100mm$

$a_{bp} := t_{bp} \cdot l_{bp} = 0.04\,m^2$

Total area of the main plate .....

$a_{mp} := a_{tp} + a_{usp} + a_{lsp} + a_{bp} = 0.215\,m^2$

Total area of bridge girder .....

$a_{bg} := a_{mp} + (15 \cdot a_1) + (15 \cdot a_2)$

$a_{bg} = 0.343\,m^2$

This area is only the steel in the bridge girder, things like stiffeners and asphalt is not included.

Area of asphalt layer .....

$a_{asp} := 60mm \cdot l_{tp} = 0.642\,m^2$

Total area of bridge girder including asphalt .....

$a_{tot} := a_{bg} + a_{asp} = 0.985\,m^2$

The area included in ABAQUS does not include asphalt, but it is set to 0.36 m2 to include the effect from stiffeners along the span.

Calculation of weight to compare with the numbers given in Alvsat, this numbers are not used in the model.

Total weight of steel bridge girder .....

$w_{steel.bg} := a_{bg} \cdot 7800 \frac{kg}{m^3} = 2673.9 \frac{kg}{m}$

Weight from Alvsat.....

$w_{alvsat} := 5350 \frac{kg}{m}$

..... this weight includes stiffeners, railing, asphalt, lower hangerlink and half the hangerlink.

$w_{other.bg} := w_{alvsat} - w_{steel.bg} = 2676.132 \frac{kg}{m}$

Hangers are calculated in Excel .....

$w_{hangers} := \frac{23000kg}{446m} = 51.57 \frac{kg}{m}$

Mass centre of the bridge girder;

Masscentre of trapezoidal stiffners are set in the middle.

$z_{1.type1} := 2635mm - \frac{h_{11}}{3} = 2.543\,m$

$m_{1.type1} := a_1 \cdot 7800 \frac{kg}{m^3} = 33.191 \frac{kg}{m}$

$z_{1.type2} := 2635mm - \frac{h_{12}}{3} = 2.56\,m$

$m_{1.type2} := a_2 \cdot 7800 \frac{kg}{m^3} = 33.214 \frac{kg}{m}$

$$z_{2.type2} := \frac{2h_{12}}{3} = 0.15\,m$$

$$z_{4.type2} := \frac{1835mm}{2} + 2\frac{h_{12}}{3} = 1.067\,m$$

$$z_{3.type2} := 1835mm - \frac{h_{12}}{3} = 1.76\,m$$

$$z_{5.type2} := \frac{1835mm}{2} - \frac{h_{12}}{3} = 0.843\,m$$

$$z_{6.type2} := h_{12} = 0.225\,m$$

$$z_{type2} := z_{1.type2} + z_{2.type2}\cdot 6 + z_{3.type2}\cdot 2 + z_{4.type2}\cdot 2 + z_{5.type2}\cdot 2 + z_{6.type2}\cdot 2 = 11.25\,m$$

$$Stiff := z_{1.type1}\cdot m_{1.type1}\cdot 15 + m_{1.type2}\cdot z_{type2} = 1639.913\,kg$$

$$m_{tp} := a_{tp}\cdot 7800\frac{kg}{m^3} = 1001.52\frac{kg}{m}$$

$$z_{tp} := 2635mm$$

$$z_{usp} := 2635mm - 400mm = 2.235\,m$$

$$m_{usp} := a_{usp}\cdot 7800\frac{kg}{m^3} = 105.862\frac{kg}{m}$$

$$z_{lsp} := \frac{1835mm}{2} = 0.918\,m$$

$$m_{lsp} := a_{lsp}\cdot 7800\frac{kg}{m^3} = 252.158\frac{kg}{m}$$

$$z_{bp} := 4mm$$

$$m_{bp} := a_{bp}\cdot 7800\frac{kg}{m^3} = 318.24\frac{kg}{m}$$

$$Z_m := \frac{z_{bp}\cdot m_{bp} + z_{lsp}\cdot m_{lsp} + z_{usp}\cdot m_{usp} + z_{tp}\cdot m_{tp} + Stiff}{w_{steel.bg}} = 1.776\,m$$

Real distance from the bottom of the girder up to the centre of gravity is probably higher than 1,776m, since the weight of the hangerlinks and asphalt is above the top of the bridge girder. In calculations of the distribution of load into 3 discrete points, centre of gravity is found to be 1.868 meter above the bottom of the bridge girder. This difference therefore makes sence.

Modelling of mass in bridge girder

(Appendix to Section 5.2 Modelling of mass)

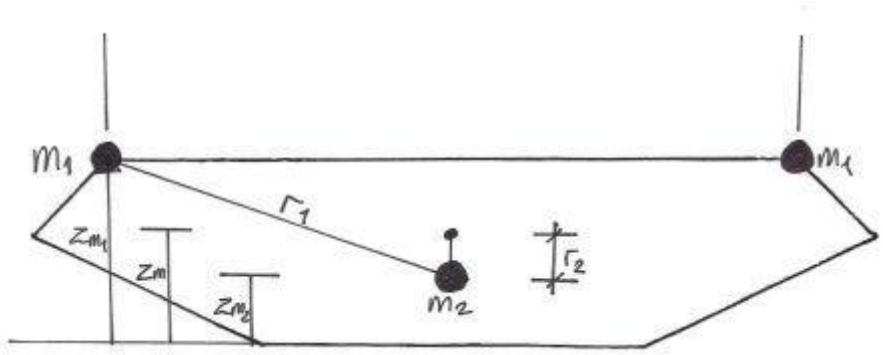

Given from Alvsat;

Distance from bottom plate in girder to mass center;

$Z_m := 1.776m$

Total mass in the bridge girder;

$M := 5350 \frac{kg}{m}$

Moment of inertia;

$I := 82430 \frac{kg \cdot m^2}{m}$

Find the distance from N.A. to the two masses m1 located close to the lower link of the hangers;

$r_1 := \sqrt{(1.104m)^2 + \left(\frac{10.3m}{2}\right)^2} = 5.267\,m$

$r_2 := 0.85m$

Distance from bottom plate in girder to mass 1;

$Z_{m1} := 2.76m$

Distance from bottom plate in girder to mass 2;

$Z_{m2} := Z_m - r_2 = 0.926\,m$

Mass 1;

$m_1 := 1454 \frac{kg}{m}$

Mass 2;

$m_2 := M - 2 \cdot m_1 = 2442 \frac{kg}{m}$

Distance from bottom plate in girder to mass center found;

$Z_{m.found} := \frac{2 \cdot Z_{m1} \cdot m_1 + Z_{m2} \cdot m_2}{2 \cdot m_1 + m_2} = 1.923\,m$

Moment of inertia found;

$$I_{found} := 2 \cdot m_1 \cdot r_1^{\,2} + m_2 \cdot r_2^{\,2} = 82436 \cdot \frac{kg \cdot m^2}{m}$$

Differences between the numbers given in Alvsat, and the ones found with the calculated mass configuration;

$$\Delta Z_m := Z_m - Z_{m.found} = -0.147\,m$$

$$\Delta I := I - I_{found} = -6.092\,m \cdot kg$$

Shear centre is given in Alvsat as 0.4 meter under lower hangerlinks, this means that they are;

$$Shearcentre := (2.76m - 0.4m) - 1.656m = 0.704\,m$$

…… above the defined neutral axis, this is taken into consideration in test 1 in the analysis of the eigen frequencies.

Moment of inertia for the towers

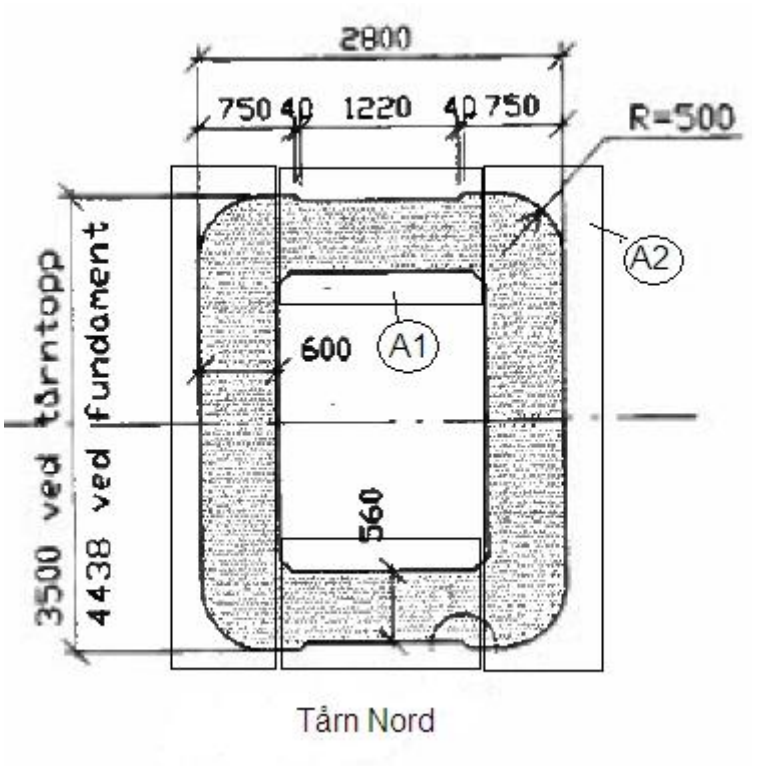

Geometry tower

To make the calculation easier to read and make, geometry is taken from the north tower.
This will be conservative.

Outer width .....

$w_{outer} := 4.438m$

Outer height .....

$h_{outer} := 2.800m$

Inner width .....

$w_{inner} := 4.438m - (0.560m \cdot 2) = 3.318\,m$

Inner height .....

$h_{inner} := 2.8m - 2 \cdot 0.6m = 1.6\,m$

Thickness 1 .....

$t_1 := 0.560m$

Thickness 2 .....

$t_2 := 0.600m$

Outer width top.....

$w_{outer.top} := 3.500m$

Outer height top .....

$h_{outer.top} := 2.800m$

Area 1 foundation.....

$A_1 := h_{inner} \cdot t_1 = 0.896\,m^2$

Area 2 foundation.....

$A_2 := w_{outer} \cdot t_2 = 2.6628\,m^2$

Surface inside the cetreline of the thin-walled section foundation

$A_{mf} := 2 \cdot (A_1 + A_2) = 7.1176\,m^2$

Area 1 top.....

$A_{1top} := h_{inner} \cdot t_1 = 0.896\,m^2$

Area 2 top.....

$A_{2top} := w_{outer.top} \cdot t_2 = 2.1\,m^2$

Surface inside the cetreline of the thin-walled section top

$A_{mt} := 2 \cdot (A_{1top} + A_{2top}) = 5.992\,m^2$

Area of foundation .....

$A_{foundation} := w_{outer} \cdot h_{outer} = 12.4264\,m^2$

Massmoment of inertia

Lengt of each section (30 sections in tower) ....

$l_{section} := 3.5m$

Mass density of concrete ...

$$\rho := 2500 \frac{kg}{m^3}$$

Mass 1 .....

$m_1 := l_{section} \cdot h_{inner} \cdot t_1 \cdot \rho = 7840\,kg$

Mass 2 .....

$m_2 := l_{section} \cdot w_{outer} \cdot t_2 \cdot \rho = 23299.5\,kg$

Mass 2 top.....

$m_{2.top} := l_{section} \cdot w_{outer.top} \cdot t_2 \cdot \rho = 18375\,kg$

Arm to centre of mass 1 .....

$$a_1 := \frac{w_{outer}}{2} - \frac{t_1}{2} = 1.939\,m$$

Arm to centre of mass 2 .....

$$a_2 := \frac{h_{inner}}{2} + \frac{t_2}{2} = 1.1\,m$$

Foundation

$$I_{ym.f} := 2 \cdot m_2 \cdot \left(\frac{t_2^2 + w_{outer}^2}{12} \right) + 2m_1 \cdot \left(\frac{t_1^2 + h_{inner}^2}{12} \right) + 2m_1 \cdot a_1^2$$

$I_{ym.f} = 140589.1\,m^2 \cdot kg$

$$I_{xm.f} := 2 \cdot m_2 \cdot \left(\frac{t_2^2 + w_{outer}^2}{12} \right) + 2m_1 \cdot \left(\frac{t_1^2 + h_{inner}^2}{12} \right) + 2m_2 \cdot a_2^2$$

$I_{xm.f} = 138021.5\,m^2 \cdot kg$

Top

$$I_{ym.t} := 2 \cdot m_{2.top} \cdot \left(\frac{t_2^2 + w_{outer.top}^2}{12} \right) + 2m_1 \cdot \left(\frac{t_1^2 + h_{inner}^2}{12} \right) + 2m_1 \cdot a_1^2$$

$I_{ym.t} = 101325.4\,m^2 \cdot kg$

$$I_{xm.top} := 2m_1 \cdot \left(\frac{t_1^2 + h_{inner}^2}{12} \right) + 2 \cdot m_{2.top} \cdot \left(\frac{t_2^2 + w_{outer.top}^2}{12} \right) + 2m_{2.top} \cdot a_2^2$$

$$I_{xm.top} = 86840.5\,m^2 \cdot kg$$

moment of inertia foundation

$$I_{x.outer} := \frac{w_{outer} \cdot h_{outer}^3}{12} = 8.1186\,m^4$$

$$I_{y.outer} := \frac{h_{outer} \cdot w_{outer}^3}{12} = 20.3957\,m^4$$

Second moment of inertia from foundation to top

Foundation;

$$I_{x.A1} := \frac{h_{inner} \cdot t_1^3}{12} = 0.0234\,m^4$$

$$I_{y.A1} := \frac{h_{inner}^3 \cdot t_1}{12} = 0.1911\,m^4$$

$$I_{x.A2} := \frac{w_{outer} \cdot t_2^3}{12} = 0.0799\,m^4$$

$$I_{y.A2} := \frac{w_{outer}^3 \cdot t_2}{12} = 4.3705\,m^4$$

$$d_1 := \frac{w_{outer}}{2} - \left(\frac{t_1}{2} \right) = 1.939\,m$$

$$d_2 := \frac{h_{inner}}{2} + \left(\frac{t_2}{2} \right) = 1.1\,m$$

$$I_{x.A1.merket} := 2I_{x.A1} + 2 \cdot \left(d_1^2 \cdot A_1 \right) = 6.7843\,m^4$$

$$I_{y.A2.merket} := 2I_{y.A2} + 2\left(d_2^2 \cdot A_2 \right) = 15.185\,m^4$$

$$I_{x.2nd.foundation} := I_{x.A1.merket} + 2I_{x.A2} = 6.944\,m^4$$

$$I_{y.2nd.foundation} := I_{y.A2.merket} + 2I_{y.A1} = 15.5673\,m^4$$

Top;

$$I_{x.A1.top} := \frac{h_{inner} \cdot t_1^3}{12} = 0.0234\,m^4$$

$$I_{y.A1.top} := \frac{h_{inner}^3 \cdot t_1}{12} = 0.1911\,m^4$$

$$I_{x.A2.top} := \frac{w_{outer.top} \cdot t_2^3}{12} = 0.063\,m^4$$

$$I_{y.A2.top} := \frac{w_{outer.top}^3 \cdot t_2}{12} = 2.1437\,m^4$$

$$d_{1.top} := \frac{w_{outer.top}}{2} - \left(\frac{t_1}{2}\right) = 1.47\,m$$

$$d_{2.top} := \frac{h_{inner}}{2} + \left(\frac{t_2}{2}\right) = 1.1\,m$$

$$I_{x.A1.merket.top} := 2I_{x.A1} + 2\cdot\left(d_{1.top}^{\ 2}\cdot A_{1top}\right) = 3.9192\,m^4$$

$$I_{y.A2.merket.top} := 2I_{y.A2} + 2\left(d_{2.top}^{\ 2}\cdot A_{2top}\right) = 13.823\,m^4$$

$$I_{x.2nd.top} := I_{x.A1.merket.top} + 2I_{x.A2.top} = 4.0452\,m^4$$

$$I_{y.2nd.top} := I_{y.A2.merket.top} + 2I_{y.A1.top} = 14.2053\,m^4$$

Torsional moment of inertia, It

For closed thin-walled cross-sections, (2nd formula of Bredt);
(This is probably not a thin-walled section, but this is conservative.
Foundation;

$$I_{T.foundation} := \frac{4\cdot A_{mf}^{\ 2}}{\left[\frac{\left(w_{outer} + h_{outer}\right)\cdot 2}{t_1 + t_2}\right]} = 16.2382\cdot m^4$$

Top;

$$I_{T.top} := \frac{4\cdot A_{mt}^{\ 2}}{\left[\frac{\left(w_{outer} + h_{outer}\right)\cdot 2}{t_1 + t_2}\right]} = 11.5083\cdot m^4$$

Second moment of inertia for the cross beams

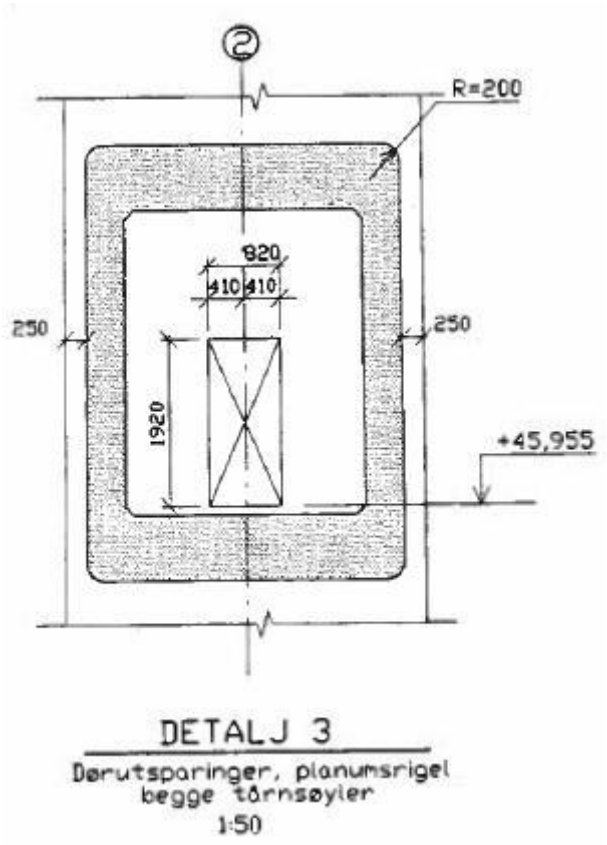

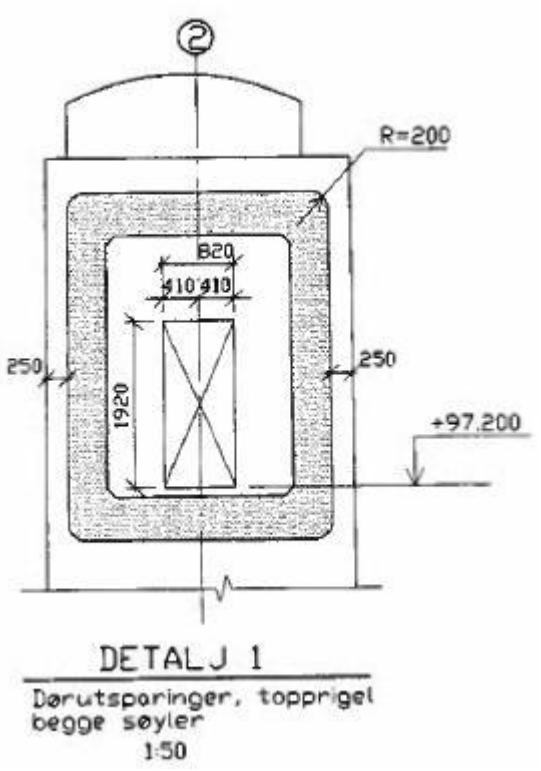

Geometry locking bar under bridge girder

Outer width girder bar.....

$w_{outer.girderbar} := 5m$

Outer height girder bar .....

$h_{outer.girderbar} := \frac{4.438m + 3.5m}{2} - 0.5m = 3.469\,m$

Inner width girder bar.....

$w_{inner.girderbar} := w_{outer.girderbar} - 1.2m = 3.8\,m$

Inner height girder bar .....

$h_{inner.girderbar} := h_{outer.girderbar} - 1m = 2.469\,m$

Thickness 1 girder bar .....

$t_{1girderbar} := 0.50m$

Thickness 2 girder bar .....

$t_{2girderbar} := 0.60m$

Outer width topbar.....

$w_{outer.topbar} := 4m$

Outer height topbar .....

$h_{outer.topbar} := 3.5m - 0.5m = 3\,m$

Inner width topbar.....

$w_{inner.topbar} := w_{outer.topbar} - 1m = 3\,m$

Inner height topbar .....

$h_{inner.topbar} := h_{outer.topbar} - 1m = 2\,m$

Thickness 1 topbar .....

$t_{1topbar} := 0.50m$

Thickness 2 topbar .....

$t_{2topbar} := 0.50m$

Area 1 girder bar.....

$A_{1girderbar} := h_{inner.girderbar} \cdot t_{1girderbar} = 1.2345\,m^2$

Area 2 girder bar.....

$A_{2girderbar} := w_{outer.girderbar} \cdot t_{2girderbar} = 3\,m^2$

Surface inside the cetreline of the thin-walled section girder bar

$A_{mgirderbar} := 2 \cdot \left(A_{1girderbar} + A_{2girderbar}\right) = 8.469\,m^2$

Area 1 topbar.....

$A_{1topbar} := h_{inner.topbar} \cdot t_{1topbar} = 1\,m^2$

Area 2 topbar.....

$A_{2topbar} := w_{outer.topbar} \cdot t_{2topbar} = 2\,m^2$

Surface inside the cetreline of the thin-walled section top bar

$A_{mtopbar} := 2 \cdot \left(A_{1topbar} + A_{2topbar}\right) = 6\,m^2$

Second moment of inertia

Under the bridge girder

$$I_{x.A1.girderbar} := \frac{h_{inner.girderbar} \cdot t_1^{\,3}}{12} = 0.0361\,m^4$$

$$I_{y.A1.girderbar} := \frac{h_{inner.girderbar}^{\,3} \cdot t_{1girderbar}}{12} = 0.6271\,m^4$$

$$I_{x.A2.girderbar} := \frac{w_{outer.girderbar} \cdot t_{2girderbar}^{\,3}}{12} = 0.09\,m^4$$

$$I_{y.A2.girderbar} := \frac{w_{outer.girderbar}^{\,3} \cdot t_{2girderbar}}{12} = 6.25\,m^4$$

$$d_{1.girderbar} := \frac{w_{outer.girderbar}}{2} - \left(\frac{t_{1girderbar}}{2}\right) = 2.25\,m$$

$$d_{2.girderbar} := \frac{h_{inner.girderbar}}{2} + \left(\frac{t_{2girderbar}}{2}\right) = 1.5345\,m$$

$$I_{x.A1.merket.girderbar} := 2I_{x.A1.girderbar} + 2 \cdot \left(d_{1.girderbar}^{\,2} \cdot A_{1girderbar}\right) = 12.5716\,m^4$$

$$I_{y.A2.merket.girderbar} := 2I_{y.A2.girderbar} + 2\left(d_{2.girderbar}^{\,2} \cdot A_{2girderbar}\right) = 26.6281\,m^4$$

$$I_{x.2nd.girderbar} := I_{x.A1.merket.girderbar} + 2I_{x.A2.girderbar} = 12.7516\,m^4$$

$$I_{y.2nd.girderbar} := I_{y.A2.merket.girderbar} + 2I_{y.A1.girderbar} = 27.8824\,m^4$$

Top;

$$I_{x.A1.topbar} := \frac{h_{inner.topbar} \cdot t_{1topbar}^{\,3}}{12} = 0.0208\,m^4$$

$$I_{y.A1.topbar} := \frac{h_{inner.topbar}^{3} \cdot t_{1topbar}}{12} = 0.3333\,m^4$$

$$I_{x.A2.topbar} := \frac{w_{outer.topbar} \cdot t_{2topbar}^{3}}{12} = 0.0417\,m^4$$

$$I_{y.A2.topbar} := \frac{w_{outer.topbar}^{3} \cdot t_{2topbar}}{12} = 2.6667\,m^4$$

$$d_{1.topbar} := \frac{w_{outer.topbar}}{2} - \left(\frac{t_{1topbar}}{2}\right) = 1.75\,m$$

$$d_{2.topbar} := \frac{h_{inner.topbar}}{2} + \left(\frac{t_{2topbar}}{2}\right) = 1.25\,m$$

$$I_{x.A1.merket.topbar} := 2I_{x.A1.topbar} + 2\cdot\left(d_{1.topbar}^{2} \cdot A_{1topbar}\right) = 6.1667\,m^4$$

$$I_{y.A2.merket.topbar} := 2I_{y.A2.topbar} + 2\left(d_{2.topbar}^{2} \cdot A_{2topbar}\right) = 11.5833\,m^4$$

$$I_{x.2nd.topbar} := I_{x.A1.merket.topbar} + 2I_{x.A2.topbar} = 6.25\,m^4$$

$$I_{y.2nd.topbar} := I_{y.A2.merket.topbar} + 2I_{y.A1.topbar} = 12.25\,m^4$$

Torsional moment of inertia, It

For closed thin-walled cross-sections, (2nd formula of Bredt);
Girder bar:

$$I_{T.girderbar} := \frac{4 \cdot A_{mgirderbar}^{2}}{\left[\frac{\left(w_{outer.girderbar} + h_{outer.girderbar}\right)\cdot 2}{t_{1girderbar} + t_{2girderbar}}\right]} = 18.6318\cdot m^4$$

Top;

$$I_{T.topbar} := \frac{4 \cdot A_{mtopbar}^{2}}{\left[\frac{\left(w_{outer.topbar} + h_{outer.topbar}\right)\cdot 2}{t_{1topbar} + t_{2topbar}}\right]} = 10.2857\cdot m^4$$

Weight of the towers and cross beams

$$w_{tower} := 4\cdot\left[\left(h_{inner}\cdot t_1\right) + \left(w_{outer}\cdot t_2\right) + A_{foundation}\right]\cdot\rho\cdot 101m = 17796.9\cdot ton$$

Weight of towers...
Weigth of lockig bars...

$$w_{bar} := 4\cdot\left(h_{inner.girderbar}\cdot t_{1girderbar} + w_{outer.girderbar}\cdot t_{2girderbar}\right)\cdot\rho\cdot 14m = 653.5\cdot ton$$

Total weigth. ..

$$w_{total} := w_{tower} + w_{bar} = 18450\cdot ton$$

$$w_{total} = 18450.4\cdot ton$$

Rigidity, areas and weight of the towers

The input data in the top of the sheet is taken from the Mathcad-sheet "Towers".
The numbers are interpolated to be inserted into ABAQUS for each element.

	A	I11	I12	Iw	Weight of tower
Foundation	7,1176	6,944	15,5673	16,2382	
Top	5,992	4,0452	14,2053	11,5083	
Difference	1,1256	2,8988	1,362	4,7299	Rho= 2500
Intervaldifferen	0,0417	0,1074	0,0504	0,1752	
Niva 2	7,1176	6,9440	15,5673	16,2382	55223
Niva 3	7,0759	6,8366	15,5169	16,0630	54899
Niva 4	7,0342	6,7293	15,4664	15,8878	54576
Niva 5	6,9925	6,6219	15,4160	15,7127	54252
Niva 6	6,9508	6,5145	15,3655	15,5375	53929
Niva 7	6,9092	6,4072	15,3151	15,3623	53606
Niva 8	6,8675	6,2998	15,2646	15,1871	53282
Niva 9	6,8258	6,1925	15,2142	15,0119	52959
Niva 10	6,7841	6,0851	15,1637	14,8367	52635
Niva 11	6,7424	5,9777	15,1133	14,6616	52312
Niva 12	6,7007	5,8704	15,0629	14,4864	51988
Niva 13	6,6590	5,7630	15,0124	14,3112	51665
Niva 14	6,6173	5,6556	14,9620	14,1360	51341
Niva 15	6,5756	5,5483	14,9115	13,9608	51018
Niva 16	6,5340	5,4409	14,8611	13,7857	50694
Niva 17	6,4923	5,3336	14,8106	13,6105	50371
Niva 18	6,4506	5,2262	14,7602	13,4353	50048
Niva 19	6,4089	5,1188	14,7097	13,2601	49724
Niva 20	6,3672	5,0115	14,6593	13,0849	49401
Niva 21	6,3255	4,9041	14,6089	12,9098	49077
Niva 22	6,2838	4,7967	14,5584	12,7346	48754
Niva 23	6,2421	4,6894	14,5080	12,5594	48430
Niva 24	6,2004	4,5820	14,4575	12,3842	48107
Niva 25	6,1588	4,4747	14,4071	12,2090	47783
Niva 26	6,1171	4,3673	14,3566	12,0338	47460
Niva 27	6,0754	4,2599	14,3062	11,8587	47137
Niva 28	6,0337	4,1526	14,2557	11,6835	46813
Niva 29	5,9920	4,0452	14,2053	11,5083	46490
Niva 30	5,9503	3,9378	14,1549	11,3331	46166
	Area	**Length**			**5880560 kg**
Area of foundat	**12,4264**	**3,1034483**			**385647 kg**
Area of crossbe	**8,469**	**14**			**592830 kg**
	6	**12**			**360000 kg**
Total weight					**7219037 kg**

Windload on Lysefjord bridge

NS-EN 3491-1-4
The basic wind velocity is defined as middle wind speed in 10 min, 10 m above flat landscape for terraincategory 2, and with a given return period.
Basic wind velocity;

$$v_{REF} := 26\frac{m}{s}$$

.... Reference wind for Forsand

$$c_{RET} := 1.0$$

.... Factor for wind directions, chosen for all directions

$$c_{ÅRS} := 1.0$$

.... Factor for season, chosen for the entire year

$$c_{HOH} := 1.0$$

.... Factor for height over sealevel

$$c_{SAN} := 1.0$$

.... Factor for return period, 50 years chosen

$$v_b := c_{RET} \cdot c_{ÅRS} \cdot c_{HOH} \cdot c_{SAN} \cdot v_{REF}$$

$$v_b = 26\frac{m}{s}$$

Basic wind pressure;

$$\rho := 1.25\frac{kg}{m^3}$$

.... Mass denisty of air

$$q_b := \frac{\rho}{2} \cdot v_b^2 = 422.5 \cdot \frac{N}{m^2}$$

Place wind velocity is defined as middle wind speed in 10 min.
Place wind velocity;

$$z := 50m$$

Terrain category 1; Coastal sea, no trees.

$$k_T := 0.17$$

$$z_0 := 0.01m$$

$$z_{min} := 2m$$

$$c_r := k_T \cdot \ln\left(\frac{z}{z_0}\right) = 1.448$$

.... Terrain factor

$$c_t := 1.0$$

.... Topography factor, set to 1, when it is un clear if the terrain around the bridge will give a reducing or increasing contribution

$$v_s := c_r \cdot c_t \cdot v_b$$

$$v_s = 37.6\frac{m}{s}$$

Place wind pressure;

$$q_s := \frac{\rho}{2} \cdot v_s^{\,2} = 885.763 \cdot \frac{N}{m^2}$$

Appendix C

ABAQUS

```
*HEADING
Analaysis of Lysefjord bridge
**********************************************************

**** Nodes                                                ****

**********************************************************

*NODE
**Bridge girder(modelled from north to south)

1    ,    -223.1014  ,    0.0000    ,    53.46490466
2    ,    -204.0000  ,    0.0000    ,    54.16479664
3    ,    -192.0000  ,    0.0000    ,    54.56016256
4    ,    -180.0000  ,    0.0000    ,    54.919396
5    ,    -168.0000  ,    0.0000    ,    55.24249696
6    ,    -156.0000  ,    0.0000    ,    55.52946544
7    ,    -144.0000  ,    0.0000    ,    55.78030144
8    ,    -132.0000  ,    0.0000    ,    55.99500496
9    ,    -120.0000  ,    0.0000    ,    56.173576
10   ,    -108.0000  ,    0.0000    ,    56.31601456
11   ,    -96.0000   ,    0.0000    ,    56.42232064
12   ,    -84.0000   ,    0.0000    ,    56.49249424
13   ,    -72.0000   ,    0.0000    ,    56.52653536
14   ,    -60.0000   ,    0.0000    ,    56.524444
15   ,    -48.0000   ,    0.0000    ,    56.48622016
16   ,    -36.0000   ,    0.0000    ,    56.41186384
17   ,    -24.0000   ,    0.0000    ,    56.30137504
18   ,    -12.0000   ,    0.0000    ,    56.15475376
19   ,    -0.0000    ,    0.0000    ,    55.972
20   ,    12.0000    ,    0.0000    ,    55.75311376
21   ,    24.0000    ,    0.0000    ,    55.49809504
22   ,    36.0000    ,    0.0000    ,    55.20694384
23   ,    48.0000    ,    0.0000    ,    54.87966016
24   ,    60.0000    ,    0.0000    ,    54.516244
25   ,    72.0000    ,    0.0000    ,    54.11669536
26   ,    84.0000    ,    0.0000    ,    53.68101424
27   ,    96.0000    ,    0.0000    ,    53.20920064
28   ,    108.0000   ,    0.0000    ,    52.70125456
29   ,    120.0000   ,    0.0000    ,    52.157176
30   ,    132.0000   ,    0.0000    ,    51.57696496
31   ,    144.0000   ,    0.0000    ,    50.96062144
32   ,    156.0000   ,    0.0000    ,    50.30814544
33   ,    168.0000   ,    0.0000    ,    49.61953696
34   ,    180.0000   ,    0.0000    ,    48.894796
35   ,    192.0000   ,    0.0000    ,    48.13392256
36   ,    204.0000   ,    0.0000    ,    47.33691664
37   ,    223.1276   ,    0.0000    ,    46.00109466
**Anchor bolt north-west
981  ,    -296.906   ,    5.1250    ,    53.4647
**West cable main span
1001 ,    -223.3363  ,    5.125,    102.26
```

```
1002 ,    -204.0000  ,    5.125,    95.3753
1003 ,    -192.0000  ,    5.125,    91.3427
1004 ,    -180.0000  ,    5.125,    87.5546
1005 ,    -168.0000  ,    5.125,    84.0108
1006 ,    -156.0000  ,    5.125,    80.7115
1007 ,    -144.0000  ,    5.125,    77.6565
1008 ,    -132.0000  ,    5.125,    74.8459
1009 ,    -120.0000  ,    5.125,    72.2798
1010 ,    -108.0000  ,    5.125,    69.9580
1011 ,    -96.0000   ,    5.125,    67.8806
1012 ,    -84.0000   ,    5.125,    66.0477
1013 ,    -72.0000   ,    5.125,    64.4591
1014 ,    -60.0000   ,    5.125,    63.1149
1015 ,    -48.0000   ,    5.125,    62.0151
1016 ,    -36.0000   ,    5.125,    61.1597
1017 ,    -24.0000   ,    5.125,    60.5487
1018 ,    -12.0000   ,    5.125,    60.1821
1019 ,    -0.0000    ,    5.125,    60.06
1020 ,    12.0000    ,    5.125,    60.1821
1021 ,    24.0000    ,    5.125,    60.5487
1022 ,    36.0000    ,    5.125,    61.1597
1023 ,    48.0000    ,    5.125,    62.0151
1024 ,    60.0000    ,    5.125,    63.1149
1025 ,    72.0000    ,    5.125,    64.4591
1026 ,    84.0000    ,    5.125,    66.0477
1027 ,    96.0000    ,    5.125,    67.8806
1028 ,    108.0000   ,    5.125,    69.9580
1029 ,    120.0000   ,    5.125,    72.2798
1030 ,    132.0000   ,    5.125,    74.8459
1031 ,    144.0000   ,    5.125,    77.6565
1032 ,    156.0000   ,    5.125,    80.7115
1033 ,    168.0000   ,    5.125,    84.0108
1034 ,    180.0000   ,    5.125,    87.5546
1035 ,    192.0000   ,    5.125,    91.3427
1036 ,    204.0000   ,    5.125,    95.3753
1037 ,    223.3363   ,    5.125,    102.26
**Anchor bolt south-west
1087 ,    389.0460   ,    5.1250    ,    46.0009
**Anchor bolt north-east
1981 ,    -296.906   ,    -5.125    ,    53.4647
**East cable main span
2001 ,    -223.3363  ,    -5.125    ,    102.26
2002 ,    -204.0000  ,    -5.125    ,    95.3753
2003 ,    -192.0000  ,    -5.125    ,    91.3427
2004 ,    -180.0000  ,    -5.125    ,    87.5546
2005 ,    -168.0000  ,    -5.125    ,    84.0108
2006 ,    -156.0000  ,    -5.125    ,    80.7115
2007 ,    -144.0000  ,    -5.125    ,    77.6565
2008 ,    -132.0000  ,    -5.125    ,    74.8459
2009 ,    -120.0000  ,    -5.125    ,    72.2798
2010 ,    -108.0000  ,    -5.125    ,    69.9580
2011 ,    -96.0000   ,    -5.125    ,    67.8806
```

```
2012 ,    -84.0000   ,    -5.125     ,    66.0477
2013 ,    -72.0000   ,    -5.125     ,    64.4591
2014 ,    -60.0000   ,    -5.125     ,    63.1149
2015 ,    -48.0000   ,    -5.125     ,    62.0151
2016 ,    -36.0000   ,    -5.125     ,    61.1597
2017 ,    -24.0000   ,    -5.125     ,    60.5487
2018 ,    -12.0000   ,    -5.125     ,    60.1821
2019 ,    -0.0000    ,    -5.125     ,    60.06
2020 ,    12.0000    ,    -5.125     ,    60.1821
2021 ,    24.0000    ,    -5.125     ,    60.5487
2022 ,    36.0000    ,    -5.125     ,    61.1597
2023 ,    48.0000    ,    -5.125     ,    62.0151
2024 ,    60.0000    ,    -5.125     ,    63.1149
2025 ,    72.0000    ,    -5.125     ,    64.4591
2026 ,    84.0000    ,    -5.125     ,    66.0477
2027 ,    96.0000    ,    -5.125     ,    67.8806
2028 ,    108.0000   ,    -5.125     ,    69.9580
2029 ,    120.0000   ,    -5.125     ,    72.2798
2030 ,    132.0000   ,    -5.125     ,    74.8459
2031 ,    144.0000   ,    -5.125     ,    77.6565
2032 ,    156.0000   ,    -5.125     ,    80.7115
2033 ,    168.0000   ,    -5.125     ,    84.0108
2034 ,    180.0000   ,    -5.125     ,    87.5546
2035 ,    192.0000   ,    -5.125     ,    91.3427
2036 ,    204.0000   ,    -5.125     ,    95.3753
2037 ,    223.3363   ,    -5.125     ,    102.26
**Anchor bolt south-east
2087 ,    389.0460   ,    -5.125     ,    46.0009
**Link between bridge girder and hanger west - hanger (1.104 above NA)

3001 ,    -223.0000  ,    5.125,    54.56890466
3002 ,    -204.0000  ,    5.125,    55.26879664
3003 ,    -192.0000  ,    5.125,    55.66416256
3004 ,    -180.0000  ,    5.125,    56.023396
3005 ,    -168.0000  ,    5.125,    56.34649696
3006 ,    -156.0000  ,    5.125,    56.63346544
3007 ,    -144.0000  ,    5.125,    56.88430144
3008 ,    -132.0000  ,    5.125,    57.09900496
3009 ,    -120.0000  ,    5.125,    57.277576
3010 ,    -108.0000  ,    5.125,    57.42001456
3011 ,    -96.0000   ,    5.125,    57.52632064
3012 ,    -84.0000   ,    5.125,    57.59649424
3013 ,    -72.0000   ,    5.125,    57.63053536
3014 ,    -60.0000   ,    5.125,    57.628444
3015 ,    -48.0000   ,    5.125,    57.59022016
3016 ,    -36.0000   ,    5.125,    57.51586384
3017 ,    -24.0000   ,    5.125,    57.40537504
3018 ,    -12.0000   ,    5.125,    57.25875376
3019 ,    -0.0000    ,    5.125,    57.076
3020 ,    12.0000    ,    5.125,    56.85711376
3021 ,    24.0000    ,    5.125,    56.60209504
3022 ,    36.0000    ,    5.125,    56.31094384
```

```
3023 ,     48.0000    ,     5.125,     55.98366016
3024 ,     60.0000    ,     5.125,     55.620244
3025 ,     72.0000    ,     5.125,     55.22069536
3026 ,     84.0000    ,     5.125,     54.78501424
3027 ,     96.0000    ,     5.125,     54.31320064
3028 ,     108.0000   ,     5.125,     53.80525456
3029 ,     120.0000   ,     5.125,     53.261176
3030 ,     132.0000   ,     5.125,     52.68096496
3031 ,     144.0000   ,     5.125,     52.06462144
3032 ,     156.0000   ,     5.125,     51.41214544
3033 ,     168.0000   ,     5.125,     50.72353696
3034 ,     180.0000   ,     5.125,     49.998796
3035 ,     192.0000   ,     5.125,     49.23792256
3036 ,     204.0000   ,     5.125,     48.44091664
3037 ,     223.0000   ,     5.125,     47.10509466
**Link between bridge girder and hanger east - hanger (1.104 above NA)

4001 ,     -223.0000  ,     -5.125     ,     54.56890466
4002 ,     -204.0000  ,     -5.125     ,     55.26879664
4003 ,     -192.0000  ,     -5.125     ,     55.66416256
4004 ,     -180.0000  ,     -5.125     ,     56.023396
4005 ,     -168.0000  ,     -5.125     ,     56.34649696
4006 ,     -156.0000  ,     -5.125     ,     56.63346544
4007 ,     -144.0000  ,     -5.125     ,     56.88430144
4008 ,     -132.0000  ,     -5.125     ,     57.09900496
4009 ,     -120.0000  ,     -5.125     ,     57.277576
4010 ,     -108.0000  ,     -5.125     ,     57.42001456
4011 ,     -96.0000   ,     -5.125     ,     57.52632064
4012 ,     -84.0000   ,     -5.125     ,     57.59649424
4013 ,     -72.0000   ,     -5.125     ,     57.63053536
4014 ,     -60.0000   ,     -5.125     ,     57.628444
4015 ,     -48.0000   ,     -5.125     ,     57.59022016
4016 ,     -36.0000   ,     -5.125     ,     57.51586384
4017 ,     -24.0000   ,     -5.125     ,     57.40537504
4018 ,     -12.0000   ,     -5.125     ,     57.25875376
4019 ,     -0.0000    ,     -5.125     ,     57.076
4020 ,     12.0000    ,     -5.125     ,     56.85711376
4021 ,     24.0000    ,     -5.125     ,     56.60209504
4022 ,     36.0000    ,     -5.125     ,     56.31094384
4023 ,     48.0000    ,     -5.125     ,     55.98366016
4024 ,     60.0000    ,     -5.125     ,     55.620244
4025 ,     72.0000    ,     -5.125     ,     55.22069536
4026 ,     84.0000    ,     -5.125     ,     54.78501424
4027 ,     96.0000    ,     -5.125     ,     54.31320064
4028 ,     108.0000   ,     -5.125     ,     53.80525456
4029 ,     120.0000   ,     -5.125     ,     53.261176
4030 ,     132.0000   ,     -5.125     ,     52.68096496
4031 ,     144.0000   ,     -5.125     ,     52.06462144
4032 ,     156.0000   ,     -5.125     ,     51.41214544
4033 ,     168.0000   ,     -5.125     ,     50.72353696
4034 ,     180.0000   ,     -5.125     ,     49.998796
4035 ,     192.0000   ,     -5.125     ,     49.23792256
```

```
4036 ,    204.0000   ,    -5.125     ,    48.44091664
4037 ,    223.0000   ,    -5.125     ,    47.10509466
**Fictitious mass point under the bridge girder (moment of inertia)

5002 ,    -204.0000  ,    0.0000     ,    53.0699
5003 ,    -192.0000  ,    0.0000     ,    53.322
5004 ,    -180.0000  ,    0.0000     ,    53.5466
5005 ,    -168.0000  ,    0.0000     ,    53.7437
5006 ,    -156.0000  ,    0.0000     ,    53.9134
5007 ,    -144.0000  ,    0.0000     ,    54.0557
5008 ,    -132.0000  ,    0.0000     ,    54.1705
5009 ,    -120.0000  ,    0.0000     ,    54.2579
5010 ,    -108.0000  ,    0.0000     ,    54.3178
5011 ,    -96.0000   ,    0.0000     ,    54.3503
5012 ,    -84.0000   ,    0.0000     ,    54.3553
5013 ,    -72.0000   ,    0.0000     ,    54.3329
5014 ,    -60.0000   ,    0.0000     ,    54.283
5015 ,    -48.0000   ,    0.0000     ,    54.2057
5016 ,    -36.0000   ,    0.0000     ,    54.101
5017 ,    -24.0000   ,    0.0000     ,    53.9687
5018 ,    -12.0000   ,    0.0000     ,    53.8091
5019 ,    -0.0000    ,    0.0000     ,    53.622
5020 ,    12.0000    ,    0.0000     ,    53.4075
5021 ,    24.0000    ,    0.0000     ,    53.1655
5022 ,    36.0000    ,    0.0000     ,    52.896
5023 ,    48.0000    ,    0.0000     ,    52.5991
5024 ,    60.0000    ,    0.0000     ,    52.2748
5025 ,    72.0000    ,    0.0000     ,    51.923
5026 ,    84.0000    ,    0.0000     ,    51.5438
5027 ,    96.0000    ,    0.0000     ,    51.1372
5028 ,    108.0000   ,    0.0000     ,    50.703
5029 ,    120.0000   ,    0.0000     ,    50.2415
5030 ,    132.0000   ,    0.0000     ,    49.7525
5031 ,    144.0000   ,    0.0000     ,    49.236
5032 ,    156.0000   ,    0.0000     ,    48.6921
5033 ,    168.0000   ,    0.0000     ,    48.1208
5034 ,    180.0000   ,    0.0000     ,    47.522
5035 ,    192.0000   ,    0.0000     ,    46.8957
5036 ,    204.0000   ,    0.0000     ,    46.2421
**Tower north, foot west
20001,    -223 ,    9.151,    6.5
20002,    -223.007803448276    ,    9.0122     ,    10.5
20003,    -223.015606896552    ,    8.8734     ,    13.5833
20004,    -223.023410344828    ,    8.7346     ,    16.6667
20005,    -223.031213793103    ,    8.5958     ,    19.75
20006,    -223.039017241379    ,    8.457,    22.8333
20007,    -223.046820689655    ,    8.3182     ,    25.9167
20008,    -223.054624137931    ,    8.1794     ,    29
20009,    -223.062427586207    ,    8.0406     ,    32.0833
20010,    -223.070231034483    ,    7.9018     ,    35.1667
20011,    -223.078034482759    ,    7.763,    38.25
20012,    -223.085837931035    ,    7.6242     ,    41.3333
```

```
20013,    -223.09364137931,    7.4854    ,    44.4167
20014,    -223.101444827586    ,    7.3466    ,    47.5
20015,    -223.109248275862    ,    7.2078    ,    50.8463
20016,    -223.117051724138    ,    7.069,    54.1925
20017,    -223.124855172414    ,    6.9302    ,    57.5388
20018,    -223.13265862069,    6.7914    ,    60.885
20019,    -223.140462068966    ,    6.6526    ,    64.2313
20020,    -223.148265517241    ,    6.5138    ,    67.5775
20021,    -223.156068965517    ,    6.375,    70.9237
20022,    -223.163872413793    ,    6.2362    ,    74.27
20023,    -223.171675862069    ,    6.0974    ,    77.6163
20024,    -223.179479310345    ,    5.9586    ,    80.9625
20025,    -223.187282758621    ,    5.8198    ,    84.3088
20026,    -223.195086206897    ,    5.681,    87.655
20027,    -223.202889655172    ,    5.5422    ,    91.0013
20028,    -223.210693103448    ,    5.4034    ,    94.3475
20029,    -223.218496551724    ,    5.2646    ,    97.6938
20030,    -223.2263  ,    5.1258    ,    101.04
**Tower north, foot east
20101,    -223 ,    -9.151    ,    6.5
20102,    -223.007803448276    ,    -9.0122    ,    10.5
20103,    -223.015606896552    ,    -8.8734    ,    13.5833
20104,    -223.023410344828    ,    -8.7346    ,    16.6667
20105,    -223.031213793103    ,    -8.5958    ,    19.75
20106,    -223.039017241379    ,    -8.457    ,    22.8333
20107,    -223.046820689655    ,    -8.3182    ,    25.9167
20108,    -223.054624137931    ,    -8.1794    ,    29
20109,    -223.062427586207    ,    -8.0406    ,    32.0833
20110,    -223.070231034483    ,    -7.9018    ,    35.1667
20111,    -223.078034482759    ,    -7.763    ,    38.25
20112,    -223.085837931035    ,    -7.6242    ,    41.3333
20113,    -223.09364137931,    -7.4854    ,    44.4167
20114,    -223.101444827586    ,    -7.3466    ,    47.5
20115,    -223.109248275862    ,    -7.2078    ,    50.8463
20116,    -223.117051724138    ,    -7.069    ,    54.1925
20117,    -223.124855172414    ,    -6.9302    ,    57.5388
20118,    -223.13265862069,    -6.7914    ,    60.885
20119,    -223.140462068966    ,    -6.6526    ,    64.2313
20120,    -223.148265517241    ,    -6.5138    ,    67.5775
20121,    -223.156068965517    ,    -6.375    ,    70.9237
20122,    -223.163872413793    ,    -6.2362    ,    74.27
20123,    -223.171675862069    ,    -6.0974    ,    77.6163
20124,    -223.179479310345    ,    -5.9586    ,    80.9625
20125,    -223.187282758621    ,    -5.8198    ,    84.3088
20126,    -223.195086206897    ,    -5.681    ,    87.655
20127,    -223.202889655172    ,    -5.5422    ,    91.0013
20128,    -223.210693103448    ,    -5.4034    ,    94.3475
20129,    -223.218496551724    ,    -5.2646    ,    97.6938
20130,    -223.2263  ,    -5.1258    ,    101.04
**cross beam under the bridge girder, tower north

20201,    -223.101444827586    ,    7.3466    ,    47.5
```

```
20202,    -223.101444827586    ,    4.9903    ,    47.5
20203,    -223.101444827586    ,    2.4952    ,    47.5
20204,    -223.101444827586    ,    0.0001    ,    47.5
20205,    -223.101444827586    ,    -2.495    ,    47.5
20206,    -223.101444827586    ,    -4.9901   ,    47.5
20207,    -223.101444827586    ,    -7.3466   ,    47.5
**cross beam top, tower north
20301,    -223.218496551724    ,    5.2646    ,    97.6938
20302,    -223.218496551724    ,    3.5097    ,    97.6938
20303,    -223.218496551724    ,    1.7548    ,    97.6938
20304,    -223.218496551724    ,    -0.0001   ,    97.6938
20305,    -223.218496551724    ,    -1.755    ,    97.6938
20306,    -223.218496551724    ,    -3.5099   ,    97.6938
20307,    -223.218496551724    ,    -5.2646   ,    97.6938
**Tower south, foot west
30001,    223   ,    9.151,    0.5
30002,    223.011596551724,    9.0122    ,    4.5
30003,    223.023193103448,    8.8734    ,    8.0541
30004,    223.034789655172,    8.7346    ,    11.6082
30005,    223.046386206896,    8.5958    ,    15.1623
30006,    223.057982758621,    8.457,    18.7164
30007,    223.069579310345,    8.3182    ,    22.2705
30008,    223.081175862069,    8.1794    ,    25.8246
30009,    223.092772413793,    8.0406    ,    29.3787
30010,    223.104368965517,    7.9018    ,    32.9328
30011,    223.115965517241,    7.763,    36.4869
30012,    223.127562068965,    7.6242    ,    40.041
30013,    223.139158620689,    7.4854    ,    43.4298
30014,    223.150755172414,    7.3466    ,    46.8187
30015,    223.162351724138,    7.2078    ,    50.2075
30016,    223.173948275862,    7.069,    53.5963
30017,    223.185544827586,    6.9302    ,    56.9852
30018,    223.19714137931 ,    6.7914    ,    60.374
30019,    223.208737931034,    6.6526    ,    63.7628
30020,    223.220334482758,    6.5138    ,    67.1517
30021,    223.231931034482,    6.375,    70.5405
30022,    223.243527586207,    6.2362    ,    73.9293
30023,    223.255124137931,    6.0974    ,    77.3182
30024,    223.266720689655,    5.9586    ,    80.707
30025,    223.278317241379,    5.8198    ,    84.0958
30026,    223.289913793103,    5.681,    87.4847
30027,    223.301510344827,    5.5422    ,    90.8735
30028,    223.313106896551,    5.4034    ,    94.2623
30029,    223.324703448275,    5.2646    ,    97.6512
30030,    223.3363   ,    5.1258    ,    101.04
**Tower south, foot east
30101,    223   ,    -9.151    ,    0.5
30102,    223.011596551724,    -9.0122   ,    4.5
30103,    223.023193103448,    -8.8734   ,    8.0541
30104,    223.034789655172,    -8.7346   ,    11.6082
30105,    223.046386206896,    -8.5958   ,    15.1623
30106,    223.057982758621,    -8.457    ,    18.7164
```

```
30107,    223.069579310345,    -8.3182    ,    22.2705
30108,    223.081175862069,    -8.1794    ,    25.8246
30109,    223.092772413793,    -8.0406    ,    29.3787
30110,    223.104368965517,    -7.9018    ,    32.9328
30111,    223.115965517241,    -7.763     ,    36.4869
30112,    223.127562068965,    -7.6242    ,    40.041
30113,    223.139158620689,    -7.4854    ,    43.4298
30114,    223.150755172414,    -7.3466    ,    46.8187
30115,    223.162351724138,    -7.2078    ,    50.2075
30116,    223.173948275862,    -7.069     ,    53.5963
30117,    223.185544827586,    -6.9302    ,    56.9852
30118,    223.19714137931 ,    -6.7914    ,    60.374
30119,    223.208737931034,    -6.6526    ,    63.7628
30120,    223.220334482758,    -6.5138    ,    67.1517
30121,    223.231931034482,    -6.375     ,    70.5405
30122,    223.243527586207,    -6.2362    ,    73.9293
30123,    223.255124137931,    -6.0974    ,    77.3182
30124,    223.266720689655,    -5.9586    ,    80.707
30125,    223.278317241379,    -5.8198    ,    84.0958
30126,    223.289913793103,    -5.681     ,    87.4847
30127,    223.301510344827,    -5.5422    ,    90.8735
30128,    223.313106896551,    -5.4034    ,    94.2623
30129,    223.324703448275,    -5.2646    ,    97.6512
30130,    223.3363   ,    -5.1258    ,    101.04
**cross beam under the bridge girder, tower south

30201,    223.127562068965,    7.6242     ,    40.041
30202,    223.127562068965,    5.1754     ,    40.041
30203,    223.127562068965,    2.5877     ,    40.041
30204,    223.127562068965,    0.0001     ,    40.041
30205,    223.127562068965,    -2.5877    ,    40.041
30206,    223.127562068965,    -4.1754    ,    40.041
30207,    223.127562068965,    -7.6242    ,    40.041
**cross beam top, tower south
30301,    223.324703448275,    5.2646     ,    97.6512
30302,    223.324703448275,    3.5097     ,    97.6512
30303,    223.324703448275,    1.7548     ,    97.6512
30304,    223.324703448275,    -0.0001    ,    97.6512
30305,    223.324703448275,    -1.755     ,    97.6512
30306,    223.324703448275,    -3.5099    ,    97.6512
30307,    223.324703448275,    -5.2646    ,    97.6512
**
**
************************************************************

**** Structural elements                                ****

************************************************************

**
**Bridge girder
**
```

```
*ELEMENT , TYPE = B31 , ELSET=GIRDER

1     ,     1     ,     2
2     ,     2     ,     3
3     ,     3     ,     4
4     ,     4     ,     5
5     ,     5     ,     6
6     ,     6     ,     7
7     ,     7     ,     8
8     ,     8     ,     9
9     ,     9     ,     10
10    ,     10    ,     11
11    ,     11    ,     12
12    ,     12    ,     13
13    ,     13    ,     14
14    ,     14    ,     15
15    ,     15    ,     16
16    ,     16    ,     17
17    ,     17    ,     18
18    ,     18    ,     19
19    ,     19    ,     20
20    ,     20    ,     21
21    ,     21    ,     22
22    ,     22    ,     23
23    ,     23    ,     24
24    ,     24    ,     25
25    ,     25    ,     26
26    ,     26    ,     27
27    ,     27    ,     28
28    ,     28    ,     29
29    ,     29    ,     30
30    ,     30    ,     31
31    ,     31    ,     32
32    ,     32    ,     33
33    ,     33    ,     34
34    ,     34    ,     35
35    ,     35    ,     36
36    ,     36    ,     37
**
**
**
**
** Cable in main span
**
*ELEMENT , TYPE = B31 , ELSET=MAINCABLE

1001  ,     1001  ,     1002
1002  ,     1002  ,     1003
1003  ,     1003  ,     1004
1004  ,     1004  ,     1005
1005  ,     1005  ,     1006
1006  ,     1006  ,     1007
```

```
1007 ,    1007 ,    1008
1008 ,    1008 ,    1009
1009 ,    1009 ,    1010
1010 ,    1010 ,    1011
1011 ,    1011 ,    1012
1012 ,    1012 ,    1013
1013 ,    1013 ,    1014
1014 ,    1014 ,    1015
1015 ,    1015 ,    1016
1016 ,    1016 ,    1017
1017 ,    1017 ,    1018
1018 ,    1018 ,    1019
1019 ,    1019 ,    1020
1020 ,    1020 ,    1021
1021 ,    1021 ,    1022
1022 ,    1022 ,    1023
1023 ,    1023 ,    1024
1024 ,    1024 ,    1025
1025 ,    1025 ,    1026
1026 ,    1026 ,    1027
1027 ,    1027 ,    1028
1028 ,    1028 ,    1029
1029 ,    1029 ,    1030
1030 ,    1030 ,    1031
1031 ,    1031 ,    1032
1032 ,    1032 ,    1033
1033 ,    1033 ,    1034
1034 ,    1034 ,    1035
1035 ,    1035 ,    1036
1036 ,    1036 ,    1037
**
2001 ,    2001 ,    2002
2002 ,    2002 ,    2003
2003 ,    2003 ,    2004
2004 ,    2004 ,    2005
2005 ,    2005 ,    2006
2006 ,    2006 ,    2007
2007 ,    2007 ,    2008
2008 ,    2008 ,    2009
2009 ,    2009 ,    2010
2010 ,    2010 ,    2011
2011 ,    2011 ,    2012
2012 ,    2012 ,    2013
2013 ,    2013 ,    2014
2014 ,    2014 ,    2015
2015 ,    2015 ,    2016
2016 ,    2016 ,    2017
2017 ,    2017 ,    2018
2018 ,    2018 ,    2019
2019 ,    2019 ,    2020
2020 ,    2020 ,    2021
2021 ,    2021 ,    2022
```

```
2022 ,     2022 ,     2023
2023 ,     2023 ,     2024
2024 ,     2024 ,     2025
2025 ,     2025 ,     2026
2026 ,     2026 ,     2027
2027 ,     2027 ,     2028
2028 ,     2028 ,     2029
2029 ,     2029 ,     2030
2030 ,     2030 ,     2031
2031 ,     2031 ,     2032
2032 ,     2032 ,     2033
2033 ,     2033 ,     2034
2034 ,     2034 ,     2035
2035 ,     2035 ,     2036
2036 ,     2036 ,     2037
**
**
**
**
** Cable in backstay
**
*ELEMENT , TYPE = B31 , ELSET=BACKSTAYCABLE

1000 ,     981  ,     1001
1037 ,     1037 ,     1087
2000    ,       1981    ,       2001

2037    ,       2037    ,       2087

**
**
**
** Fictitious element between bridge girder and lower hanger link

**
*ELEMENT , TYPE = B31 , ELSET=DUMMY1

3001 ,     1     ,     3001
3002 ,     2     ,     3002
3003 ,     3     ,     3003
3004 ,     4     ,     3004
3005 ,     5     ,     3005
3006 ,     6     ,     3006
3007 ,     7     ,     3007
3008 ,     8     ,     3008
3009 ,     9     ,     3009
3010 ,     10    ,     3010
3011 ,     11    ,     3011
3012 ,     12    ,     3012
3013 ,     13    ,     3013
3014 ,     14    ,     3014
3015 ,     15    ,     3015
```

```
3016 ,     16    ,     3016
3017 ,     17    ,     3017
3018 ,     18    ,     3018
3019 ,     19    ,     3019
3020 ,     20    ,     3020
3021 ,     21    ,     3021
3022 ,     22    ,     3022
3023 ,     23    ,     3023
3024 ,     24    ,     3024
3025 ,     25    ,     3025
3026 ,     26    ,     3026
3027 ,     27    ,     3027
3028 ,     28    ,     3028
3029 ,     29    ,     3029
3030 ,     30    ,     3030
3031 ,     31    ,     3031
3032 ,     32    ,     3032
3033 ,     33    ,     3033
3034 ,     34    ,     3034
3035 ,     35    ,     3035
3036 ,     36    ,     3036
3037 ,     37    ,     3037
**
**
**
*ELEMENT , TYPE = B31 , ELSET=DUMMY2

4001 ,     1     ,     4001
4002 ,     2     ,     4002
4003 ,     3     ,     4003
4004 ,     4     ,     4004
4005 ,     5     ,     4005
4006 ,     6     ,     4006
4007 ,     7     ,     4007
4008 ,     8     ,     4008
4009 ,     9     ,     4009
4010 ,     10    ,     4010
4011 ,     11    ,     4011
4012 ,     12    ,     4012
4013 ,     13    ,     4013
4014 ,     14    ,     4014
4015 ,     15    ,     4015
4016 ,     16    ,     4016
4017 ,     17    ,     4017
4018 ,     18    ,     4018
4019 ,     19    ,     4019
4020 ,     20    ,     4020
4021 ,     21    ,     4021
4022 ,     22    ,     4022
4023 ,     23    ,     4023
4024 ,     24    ,     4024
4025 ,     25    ,     4025
```

```
4026 ,     26    ,     4026
4027 ,     27    ,     4027
4028 ,     28    ,     4028
4029 ,     29    ,     4029
4030 ,     30    ,     4030
4031 ,     31    ,     4031
4032 ,     32    ,     4032
4033 ,     33    ,     4033
4034 ,     34    ,     4034
4035 ,     35    ,     4035
4036 ,     36    ,     4036
4037 ,     37    ,     4037
**
**
**
**Hangers
**
*ELEMENT , TYPE = B31 , ELSET=HANGERS

5002 ,     3002 ,     1002
5003 ,     3003 ,     1003
5004 ,     3004 ,     1004
5005 ,     3005 ,     1005
5006 ,     3006 ,     1006
5007 ,     3007 ,     1007
5008 ,     3008 ,     1008
5009 ,     3009 ,     1009
5010 ,     3010 ,     1010
5011 ,     3011 ,     1011
5012 ,     3012 ,     1012
5013 ,     3013 ,     1013
5014 ,     3014 ,     1014
5015 ,     3015 ,     1015
5016 ,     3016 ,     1016
5017 ,     3017 ,     1017
5018 ,     3018 ,     1018
5019 ,     3019 ,     1019
5020 ,     3020 ,     1020
5021 ,     3021 ,     1021
5022 ,     3022 ,     1022
5023 ,     3023 ,     1023
5024 ,     3024 ,     1024
5025 ,     3025 ,     1025
5026 ,     3026 ,     1026
5027 ,     3027 ,     1027
5028 ,     3028 ,     1028
5029 ,     3029 ,     1029
5030 ,     3030 ,     1030
5031 ,     3031 ,     1031
5032 ,     3032 ,     1032
5033 ,     3033 ,     1033
5034 ,     3034 ,     1034
```

```
5035 ,     3035 ,     1035
5036 ,     3036 ,     1036
**
6002 ,     4002 ,     2002
6003 ,     4003 ,     2003
6004 ,     4004 ,     2004
6005 ,     4005 ,     2005
6006 ,     4006 ,     2006
6007 ,     4007 ,     2007
6008 ,     4008 ,     2008
6009 ,     4009 ,     2009
6010 ,     4010 ,     2010
6011 ,     4011 ,     2011
6012 ,     4012 ,     2012
6013 ,     4013 ,     2013
6014 ,     4014 ,     2014
6015 ,     4015 ,     2015
6016 ,     4016 ,     2016
6017 ,     4017 ,     2017
6018 ,     4018 ,     2018
6019 ,     4019 ,     2019
6020 ,     4020 ,     2020
6021 ,     4021 ,     2021
6022 ,     4022 ,     2022
6023 ,     4023 ,     2023
6024 ,     4024 ,     2024
6025 ,     4025 ,     2025
6026 ,     4026 ,     2026
6027 ,     4027 ,     2027
6028 ,     4028 ,     2028
6029 ,     4029 ,     2029
6030 ,     4030 ,     2030
6031 ,     4031 ,     2031
6032 ,     4032 ,     2032
6033 ,     4033 ,     2033
6034 ,     4034 ,     2034
6035 ,     4035 ,     2035
6036 ,     4036 ,        2036

**
**
**
**Fictitious mass elements under the bridge girder (moment of inertia)

**
*ELEMENT , TYPE = B31 , ELSET=DUMMY3

7002 ,     2    ,     5002
7003 ,     3    ,     5003
7004 ,     4    ,     5004
7005 ,     5    ,     5005
7006 ,     6    ,     5006
```

```
7007 ,     7     ,     5007
7008 ,     8     ,     5008
7009 ,     9     ,     5009
7010 ,     10    ,     5010
7011 ,     11    ,     5011
7012 ,     12    ,     5012
7013 ,     13    ,     5013
7014 ,     14    ,     5014
7015 ,     15    ,     5015
7016 ,     16    ,     5016
7017 ,     17    ,     5017
7018 ,     18    ,     5018
7019 ,     19    ,     5019
7020 ,     20    ,     5020
7021 ,     21    ,     5021
7022 ,     22    ,     5022
7023 ,     23    ,     5023
7024 ,     24    ,     5024
7025 ,     25    ,     5025
7026 ,     26    ,     5026
7027 ,     27    ,     5027
7028 ,     28    ,     5028
7029 ,     29    ,     5029
7030 ,     30    ,     5030
7031 ,     31    ,     5031
7032 ,     32    ,     5032
7033 ,     33    ,     5033
7034 ,     34    ,     5034
7035 ,     35    ,     5035
7036 ,     36    ,      5036


**
**Fictitious mass elements to create windmoment

**
*ELEMENT , TYPE = B31 , ELSET=DUMMY4

12001,     3001 ,     3002
12002,     3002 ,     3003
12003,     3003 ,     3004
12004,     3004 ,     3005
12005,     3005 ,     3006
12006,     3006 ,     3007
12007,     3007 ,     3008
12008,     3008 ,     3009
12009,     3009 ,     3010
12010,     3010 ,     3011
12011,     3011 ,     3012
12012,     3012 ,     3013
12013,     3013 ,     3014
12014,     3014 ,     3015
```

```
12015,    3015 ,    3016
12016,    3016 ,    3017
12017,    3017 ,    3018
12018,    3018 ,    3019
12019,    3019 ,    3020
12020,    3020 ,    3021
12021,    3021 ,    3022
12022,    3022 ,    3023
12023,    3023 ,    3024
12024,    3024 ,    3025
12025,    3025 ,    3026
12026,    3026 ,    3027
12027,    3027 ,    3028
12028,    3028 ,    3029
12029,    3029 ,    3030
12030,    3030 ,    3031
12031,    3031 ,    3032
12032,    3032 ,    3033
12033,    3033 ,    3034
12034,    3034 ,    3035
12035,    3035 ,    3036
12036,    3036 ,    3037
**
13001,    4001 ,    4002
13002,    4002 ,    4003
13003,    4003 ,    4004
13004,    4004 ,    4005
13005,    4005 ,    4006
13006,    4006 ,    4007
13007,    4007 ,    4008
13008,    4008 ,    4009
13009,    4009 ,    4010
13010,    4010 ,    4011
13011,    4011 ,    4012
13012,    4012 ,    4013
13013,    4013 ,    4014
13014,    4014 ,    4015
13015,    4015 ,    4016
13016,    4016 ,    4017
13017,    4017 ,    4018
13018,    4018 ,    4019
13019,    4019 ,    4020
13020,    4020 ,    4021
13021,    4021 ,    4022
13022,    4022 ,    4023
13023,    4023 ,    4024
13024,    4024 ,    4025
13025,    4025 ,    4026
13026,    4026 ,    4027
13027,    4027 ,    4028
13028,    4028 ,    4029
13029,     4029 ,    4030
```

```
13030,     4030  ,     4031
13031,     4031  ,     4032
13032,     4032  ,     4033
13033,     4033  ,     4034
13034,     4034  ,     4035
13035,     4035  ,     4036
13036,     4036  ,     4037
**
**
**
**Tower north
**
*ELEMENT, TYPE=FRAME3D,ELSET=NIVA1

20001,     20001,     20002
20101,     20101,     20102
*ELEMENT, TYPE=FRAME3D,ELSET=NIVA2

20002,     20002,     20003
20102,     20102,     20103
*ELEMENT, TYPE=FRAME3D,ELSET=NIVA3

20003,     20003,     20004
20103,     20103,     20104
*ELEMENT, TYPE=FRAME3D,ELSET=NIVA4

20004,     20004,     20005
20104,     20104,     20105
*ELEMENT, TYPE=FRAME3D,ELSET=NIVA5

20005,     20005,     20006
20105,     20105,     20106
*ELEMENT, TYPE=FRAME3D,ELSET=NIVA6

20006,     20006,     20007
20106,     20106,     20107
*ELEMENT, TYPE=FRAME3D,ELSET=NIVA7

20007,     20007,     20008
20107,     20107,     20108
*ELEMENT, TYPE=FRAME3D,ELSET=NIVA8

20008,     20008,     20009
20108,     20108,     20109
*ELEMENT, TYPE=FRAME3D,ELSET=NIVA9

20009,     20009,     20010
20109,     20109,     20110
*ELEMENT, TYPE=FRAME3D,ELSET=NIVA10

20010,     20010,     20011
20110,     20110,     20111
```

```
*ELEMENT, TYPE=FRAME3D,ELSET=NIVA11

20011,    20011,    20012
20111,    20111,    20112
*ELEMENT, TYPE=FRAME3D,ELSET=NIVA12

20012,    20012,    20013
20112,    20112,    20113
*ELEMENT, TYPE=FRAME3D,ELSET=NIVA13

20013,    20013,    20014
20113,    20113,    20114
*ELEMENT, TYPE=FRAME3D,ELSET=NIVA14

20014,    20014,    20015
20114,    20114,    20115
*ELEMENT, TYPE=FRAME3D,ELSET=NIVA15

20015,    20015,    20016
20115,    20115,    20116
*ELEMENT, TYPE=FRAME3D,ELSET=NIVA16

20016,    20016,    20017
20116,    20116,    20117
*ELEMENT, TYPE=FRAME3D,ELSET=NIVA17

20017,    20017,    20018
20117,    20117,    20118
*ELEMENT, TYPE=FRAME3D,ELSET=NIVA18

20018,    20018,    20019
20118,    20118,    20119
*ELEMENT, TYPE=FRAME3D,ELSET=NIVA19

20019,    20019,    20020
20119,    20119,    20120
*ELEMENT, TYPE=FRAME3D,ELSET=NIVA20

20020,    20020,    20021
20120,    20120,    20121
*ELEMENT, TYPE=FRAME3D,ELSET=NIVA21

20021,    20021,    20022
20121,    20121,    20122
*ELEMENT, TYPE=FRAME3D,ELSET=NIVA22

20022,    20022,    20023
20122,    20122,    20123
*ELEMENT, TYPE=FRAME3D,ELSET=NIVA23

20023,    20023,    20024
20123,    20123,    20124
```

```
*ELEMENT, TYPE=FRAME3D,ELSET=NIVA24

20024,     20024,     20025
20124,     20124,     20125
*ELEMENT, TYPE=FRAME3D,ELSET=NIVA25

20025,     20025,     20026
20125,     20125,     20126
*ELEMENT, TYPE=FRAME3D,ELSET=NIVA26

20026,     20026,     20027
20126,     20126,     20127
*ELEMENT, TYPE=FRAME3D,ELSET=NIVA27

20027,     20027,     20028
20127,     20127,     20128
*ELEMENT, TYPE=FRAME3D,ELSET=NIVA28

20028,     20028,     20029
20128,     20128,     20129
*ELEMENT, TYPE=FRAME3D,ELSET=NIVA29

20029,     20029,     20030
20129,     20129,     20130
*ELEMENT, TYPE=B31,ELSET=NIVA30
20030,     20030,     1001
20130,     20130,     2001
*ELEMENT, TYPE=FRAME3D,ELSET=CROSSBEAM1

20201,     20201,     20202
20202,     20202,     20203
20203,     20203,     20204
20204,     20204,     20205
20205,     20205,     20206
20206,     20206,     20207
*ELEMENT, TYPE=FRAME3D,ELSET=CROSSBEAM2

20301,     20301,     20302
20302,     20302,     20303
20303,     20303,     20304
20304,     20304,     20305
20305,     20305,     20306
20306,     20306,     20307
**
**
**
**
**Tower south
**
*ELEMENT, TYPE=FRAME3D,ELSET=NIVA1

30001,     30001,     30002
```

```
30101,     30101,     30102
*ELEMENT, TYPE=FRAME3D,ELSET=NIVA2

30002,     30002,     30003
30102,     30102,     30103
*ELEMENT, TYPE=FRAME3D,ELSET=NIVA3

30003,     30003,     30004
30103,     30103,     30104
*ELEMENT, TYPE=FRAME3D,ELSET=NIVA4

30004,     30004,     30005
30104,     30104,     30105
*ELEMENT, TYPE=FRAME3D,ELSET=NIVA5

30005,     30005,     30006
30105,     30105,     30106
*ELEMENT, TYPE=FRAME3D,ELSET=NIVA6

30006,     30006,     30007
30106,     30106,     30107
*ELEMENT, TYPE=FRAME3D,ELSET=NIVA7

30007,     30007,     30008
30107,     30107,     30108
*ELEMENT, TYPE=FRAME3D,ELSET=NIVA8

30008,     30008,     30009
30108,     30108,     30109
*ELEMENT, TYPE=FRAME3D,ELSET=NIVA9

30009,     30009,     30010
30109,     30109,     30110
*ELEMENT, TYPE=FRAME3D,ELSET=NIVA10

30010,     30010,     30011
30110,     30110,     30111
*ELEMENT, TYPE=FRAME3D,ELSET=NIVA11

30011,     30011,     30012
30111,     30111,     30112
*ELEMENT, TYPE=FRAME3D,ELSET=NIVA12

30012,     30012,     30013
30112,     30112,     30113
*ELEMENT, TYPE=FRAME3D,ELSET=NIVA13

30013,     30013,     30014
30113,     30113,     30114
*ELEMENT, TYPE=FRAME3D,ELSET=NIVA14

30014,     30014,     30015
```

```
30114,    30114,    30115
*ELEMENT, TYPE=FRAME3D,ELSET=NIVA15

30015,    30015,    30016
30115,    30115,    30116
*ELEMENT, TYPE=FRAME3D,ELSET=NIVA16

30016,    30016,    30017
30116,    30116,    30117
*ELEMENT, TYPE=FRAME3D,ELSET=NIVA17

30017,    30017,    30018
30117,    30117,    30118
*ELEMENT, TYPE=FRAME3D,ELSET=NIVA18

30018,    30018,    30019
30118,    30118,    30119
*ELEMENT, TYPE=FRAME3D,ELSET=NIVA19

30019,    30019,    30020
30119,    30119,    30120
*ELEMENT, TYPE=FRAME3D,ELSET=NIVA20

30020,    30020,    30021
30120,    30120,    30121
*ELEMENT, TYPE=FRAME3D,ELSET=NIVA21

30021,    30021,    30022
30121,    30121,    30122
*ELEMENT, TYPE=FRAME3D,ELSET=NIVA22

30022,    30022,    30023
30122,    30122,    30123
*ELEMENT, TYPE=FRAME3D,ELSET=NIVA23

30023,    30023,    30024
30123,    30123,    30124
*ELEMENT, TYPE=FRAME3D,ELSET=NIVA24

30024,    30024,    30025
30124,    30124,    30125
*ELEMENT, TYPE=FRAME3D,ELSET=NIVA25

30025,    30025,    30026
30125,    30125,    30126
*ELEMENT, TYPE=FRAME3D,ELSET=NIVA26

30026,    30026,    30027
30126,    30126,    30127
*ELEMENT, TYPE=FRAME3D,ELSET=NIVA27

30027,    30027,    30028
```

```
30127,     30127,     30128
*ELEMENT, TYPE=FRAME3D,ELSET=NIVA28

30028,     30028,     30029
30128,     30128,     30129
*ELEMENT, TYPE=FRAME3D,ELSET=NIVA29

30029,     30029,     30030
30129,     30129,     30130
*ELEMENT, TYPE=B31,ELSET=NIVA30
30030,     30030,     1037
30130,     30130,     2037
*ELEMENT, TYPE=FRAME3D,ELSET=CROSSBEAM1

30201,     30201,     30202
30202,     30202,     30203
30203,     30203,     30204
30204,     30204,     30205
30205,     30205,     30206
30206,     30206,     30207
*ELEMENT, TYPE=FRAME3D,ELSET=CROSSBEAM2

30301,     30301,     30302
30302,     30302,     30303
30303,     30303,     30304
30304,     30304,     30305
30305,     30305,     30306
30306,     30306,     30307
**
**
**
************************************************************

**** Mass elements                                      ****

************************************************************

**
** Mass points at the lower hanger links, at each side of the
** bridge girder (Moment of inertia)
**
*ELEMENT , TYPE = MASS , ELSET=SIDE

18002,     3002
18003,     3003
18004,     3004
18005,     3005
18006,     3006
18007,     3007
18008,     3008
18009,     3009
18010,     3010
```

```
18011,    3011
18012,    3012
18013,    3013
18014,    3014
18015,    3015
18016,    3016
18017,    3017
18018,    3018
18019,    3019
18020,    3020
18021,    3021
18022,    3022
18023,    3023
18024,    3024
18025,    3025
18026,    3026
18027,    3027
18028,    3028
18029,    3029
18030,    3030
18031,    3031
18032,    3032
18033,    3033
18034,    3034
18035,    3035
18036,    3036
**
19002,    4002
19003,    4003
19004,    4004
19005,    4005
19006,    4006
19007,    4007
19008,    4008
19009,    4009
19010,    4010
19011,    4011
19012,    4012
19013,    4013
19014,    4014
19015,    4015
19016,    4016
19017,    4017
19018,    4018
19019,    4019
19020,    4020
19021,    4021
19022,    4022
19023,    4023
19024,    4024
19025,    4025
19026,    4026
```

```
19027,    4027
19028,    4028
19029,    4029
19030,    4030
19031,    4031
19032,    4032
19033,    4033
19034,    4034
19035,    4035
19036,       4036

**
**
**
** Mass points under the
** bridge girder (Moment of inertia)

**
*ELEMENT , TYPE = MASS , ELSET=UNDER

10002,    5002
10003,    5003
10004,    5004
10005,    5005
10006,    5006
10007,    5007
10008,    5008
10009,    5009
10010,    5010
10011,    5011
10012,    5012
10013,    5013
10014,    5014
10015,    5015
10016,    5016
10017,    5017
10018,    5018
10019,    5019
10020,    5020
10021,    5021
10022,    5022
10023,    5023
10024,    5024
10025,    5025
10026,    5026
10027,    5027
10028,    5028
10029,    5029
10030,    5030
10031,    5031
10032,    5032
10033,    5033
```

```
10034,     5034
10035,     5035
10036,     5036

**
**
**
** Mass points to attach the weigth of the girder ends

**
*ELEMENT , TYPE = MASS , ELSET=END
11001   ,       1
11037   ,       37
**
**
**
************************************************************

**** Dummy elements                                      ****

************************************************************

**
** Dummy gripping of tower leg
**
*ELEMENT, TYPE=SPRING1, ELSET=TOWERLEG

29001,20001
29101,20101
39001,30001
39101,30101
**
**
**
** Coupling between the cross beam under the bridge girder and
** the bridge girder
**
*ELEMENT, TYPE=B33, ELSET=BOUNDARY

29501,20204,1
39501,30204,37
**
**
**
************************************************************

**** Rigidity                                            ****

************************************************************

**
** Bridge girder
```

```
**
**Using the beam general section option, defined by
**A,I_11,I_12,I_22,J,,Warping constant(15.3.7-2).

**
*BEAM GENERAL SECTION, ELSET=GIRDER, SECTION=GENERAL, DENSITY=0.001

0.360, 0.429, 0.0, 4.952, 0.929, ,4.762

0,1,0
210000E6, 80700E6, 0.00001


**
**
** Coupling elements, very rigid, no mass

**
*BEAM GENERAL SECTION, ELSET=DUMMY1, SECTION=GENERAL, DENSITY=1E-12

1000,1000,0.0,1000,1000, ,
0,1,0
210000E6, 80700E6, 0.00001
*BEAM GENERAL SECTION, ELSET=DUMMY2, SECTION=GENERAL, DENSITY=1E-12

1000,1000,0.0,1000,1000, ,
0,1,0
210000E6, 80700E6, 0.00001
*BEAM GENERAL SECTION, ELSET=DUMMY3, SECTION=GENERAL, DENSITY=1E-12

1000,1000,0.0,1000,1000, ,
0,1,0
210000E6, 80700E6, 0.00001
**
**
**
** Elements for windmoment, low rigidity, no mass

**
*BEAM GENERAL SECTION, ELSET=DUMMY4, SECTION=GENERAL, DENSITY=0.00001

0.36, 0.429, 0.0, 4.952, 0.929, ,4.762

0,1,0
210000E1, 80700E1, 0.00001

**
**
** Hangers
**
*BEAM GENERAL SECTION, ELSET=HANGERS, SECTION=GENERAL, DENSITY=0.001
```

```
0.0018, 2.6E-9, 0, 2.6E-9, 5.2E-9

1,1,0
180000E6, 63077E6, 0.00001
**
**
**
** Cable in main span
**
** Cable weight+hangerlink+half the hanger = 408 kg/m

**
** RHO = 408kg/m / 0.05 m2 = 8160 kg/m3
**
*BEAM GENERAL SECTION, ELSET=MAINCABLE, SECTION=GENERAL, DENSITY=8160

0.05, 0.0000026,  0,  0.0000026,  0.0000052

0,1,0
180000E6, 80700E6, 0.00001
**
**
**
** Cable in backstay
**
** Cable weigth = 356 kg/m
**
** RHO = 356kg/m / 0.05m2 = 7120
**
*BEAM GENERAL SECTION, ELSET=BACKSTAYCABLE, SECTION=GENERAL,
DENSITY=7120
0.05, 0.0000026,  0,  0.0000026,  0.0000052

0,1,0
180000E6, 80700E6, 0.00001
**
**
**
** Towers (from foundation to top)

**
*FRAME SECTION,ELSET=NIVA1,SECTION=GENERAL,DENSITY=2500

12.4264    ,    8.1186    ,    0.1   ,    20.3957    ,    30
1,0,0
4E+10,1.67E+10
*FRAME SECTION,ELSET=NIVA2,SECTION=GENERAL,DENSITY=2500

7.1176    ,    6.9440    ,    0.1   ,    15.5673    ,    16.2382
1,0,0
4E+10,1.67E+10
```

```
*FRAME SECTION,ELSET=NIVA3,SECTION=GENERAL,DENSITY=2500

7.0759    ,    6.8366    ,    0.1   ,    15.5169    ,    16.0630
1,0,0
4E+10,1.67E+10
*FRAME SECTION,ELSET=NIVA4,SECTION=GENERAL,DENSITY=2500

7.0342    ,    6.7293    ,    0.1   ,    15.4664    ,    15.8878
1,0,0
4E+10,1.67E+10
*FRAME SECTION,ELSET=NIVA5,SECTION=GENERAL,DENSITY=2500

6.9925    ,    6.6219    ,    0.1   ,    15.4160    ,    15.7127
1,0,0
4E+10,1.67E+10
*FRAME SECTION,ELSET=NIVA6,SECTION=GENERAL,DENSITY=2500

6.9508    ,    6.5145    ,    0.1   ,    15.3655    ,    15.5375
1,0,0
4E+10,1.67E+10
*FRAME SECTION,ELSET=NIVA7,SECTION=GENERAL,DENSITY=2500

6.9092    ,    6.4072    ,    0.1   ,    15.3151    ,    15.3623
1,0,0
4E+10,1.67E+10
*FRAME SECTION,ELSET=NIVA8,SECTION=GENERAL,DENSITY=2500

6.8675    ,    6.2998    ,    0.1   ,    15.2646    ,    15.1871
1,0,0
4E+10,1.67E+10
*FRAME SECTION,ELSET=NIVA9,SECTION=GENERAL,DENSITY=2500

6.8258    ,     6.1925    ,    0.1   ,    15.2142    ,    15.0119
1,0,0
4E+10,1.67E+10
*FRAME SECTION,ELSET=NIVA10,SECTION=GENERAL,DENSITY=2500

6.7841    ,    6.0851    ,    0.1   ,    15.1637    ,    14.8367
1,0,0
4E+10,1.67E+10
*FRAME SECTION,ELSET=NIVA11,SECTION=GENERAL,DENSITY=2500

6.7424    ,    5.9777    ,    0.1   ,    15.1133    ,    14.6616
1,0,0
4E+10,1.67E+10
*FRAME SECTION,ELSET=NIVA12,SECTION=GENERAL,DENSITY=2500

6.7007    ,    5.8704    ,    0.1   ,    15.0629    ,    14.4864
1,0,0
4E+10,1.67E+10
*FRAME SECTION,ELSET=NIVA13,SECTION=GENERAL,DENSITY=2500
```

```
6.6590     ,     5.7630     ,     0.1   ,     15.0124    ,     14.3112
1,0,0
4E+10,1.67E+10
*FRAME SECTION,ELSET=NIVA14,SECTION=GENERAL,DENSITY=2500

6.6173     ,     5.6556     ,     0.1   ,     14.9620    ,     14.1360
1,0,0
4E+10,1.67E+10
*FRAME SECTION,ELSET=NIVA15,SECTION=GENERAL,DENSITY=2500

6.5756     ,     5.5483     ,     0.1   ,     14.9115    ,     13.9608
1,0,0
4E+10,1.67E+10
*FRAME SECTION,ELSET=NIVA16,SECTION=GENERAL,DENSITY=2500

6.5340     ,     5.4409     ,     0.1   ,     14.8611    ,     13.7857
1,0,0
4E+10,1.67E+10
*FRAME SECTION,ELSET=NIVA17,SECTION=GENERAL,DENSITY=2500

6.4923     ,     5.3336     ,     0.1   ,     14.8106    ,     13.6105
1,0,0
4E+10,1.67E+10
*FRAME SECTION,ELSET=NIVA18,SECTION=GENERAL,DENSITY=2500

6.4506     ,     5.2262     ,     0.1   ,     14.7602    ,     13.4353
1,0,0
4E+10,1.67E+10
*FRAME SECTION,ELSET=NIVA19,SECTION=GENERAL,DENSITY=2500

6.4089     ,     5.1188     ,     0.1   ,     14.7097    ,     13.2601
1,0,0
4E+10,1.67E+10
*FRAME SECTION,ELSET=NIVA20,SECTION=GENERAL,DENSITY=2500

6.3672     ,     5.0115     ,     0.1   ,     14.6593    ,     13.0849
1,0,0
4E+10,1.67E+10
*FRAME SECTION,ELSET=NIVA21,SECTION=GENERAL,DENSITY=2500

6.3255     ,     4.9041     ,     0.1   ,     14.6089    ,     12.9098
1,0,0
4E+10,1.67E+10
*FRAME SECTION,ELSET=NIVA22,SECTION=GENERAL,DENSITY=2500

6.2838     ,     4.7967     ,     0.1   ,     14.5584    ,     12.7346
1,0,0
4E+10,1.67E+10
*FRAME SECTION,ELSET=NIVA23,SECTION=GENERAL,DENSITY=2500

6.2421     ,     4.6894     ,     0.1   ,     14.5080    ,     12.5594
1,0,0
```

```
4E+10,1.67E+10
*FRAME SECTION,ELSET=NIVA24,SECTION=GENERAL,DENSITY=2500
6.2004     ,     4.5820     ,     0.1   ,     14.4575    ,     12.3842
1,0,0
4E+10,1.67E+10
*FRAME SECTION,ELSET=NIVA25,SECTION=GENERAL,DENSITY=2500
6.1588     ,     4.4747     ,     0.1   ,     14.4071    ,     12.2090
1,0,0
4E+10,1.67E+10
*FRAME SECTION,ELSET=NIVA26,SECTION=GENERAL,DENSITY=2500
6.1171     ,     4.3673     ,     0.1   ,     14.3566    ,     12.0338
1,0,0
4E+10,1.67E+10
*FRAME SECTION,ELSET=NIVA27,SECTION=GENERAL,DENSITY=2500
6.0754     ,     4.2599     ,     0.1   ,     14.3062    ,     11.8587
1,0,0
4E+10,1.67E+10
*FRAME SECTION,ELSET=NIVA28,SECTION=GENERAL,DENSITY=2500
6.0337     ,     4.1526     ,     0.1   ,      14.2557   ,     11.6835
1,0,0
4E+10,1.67E+10
*FRAME SECTION,ELSET=NIVA29,SECTION=GENERAL,DENSITY=2500
5.9920     ,     4.0452     ,     0.10  ,     14.2053    ,     11.5083
1,0,0
4E+10,1.67E+10
**
*BEAM GENERAL SECTION,ELSET=NIVA30,DENSITY=0.00001
5.9503     ,     3.9378     ,     0.10  ,     14.1549    ,     11.3331
1,0,0
4E+10,1.67E+10
**
*FRAME SECTION,ELSET=CROSSBEAM1,SECTION=GENERAL,DENSITY=2500
13.36,     12.7516    ,     0.10  ,     27.8824    ,     18.6318
1,0,0
4E+10,1.67E+10
*FRAME SECTION,ELSET=CROSSBEAM2,SECTION=GENERAL,DENSITY=2500
9.28  ,     6.2500     ,     0.10  ,     12.2500    ,     10.2875
1,0,0
4E+10,1.67E+10
**
** Dummy boundary towerleg, infinite rigid torsion spring
**
*SPRING, ELSET=TOWERLEG
6
1E+12
**
** Coupling between the cross beam under the bridge girder and
** the bridge girder, rigid element
**
*BEAM GENERAL SECTION,ELSET=BOUNDARY,DENSITY=0.000001
100   ,     1000  ,     0     ,     1000  ,     1000
1,0,0
```

```
4E+10,1.67E+10
**
**************************************************************
**** Assign lumped mass                                   ****
**************************************************************
**
** Lumped mass along the bridge girder
** From Mathcad, fit sutch that IM = 82436:
** "SIDE" = 1454 x 12 meter between hangers = 17448
** "UNDER" = 2442 x 12 = 29304
**
*MASS, ELSET=SIDE
17448
*MASS, ELSET=UNDER
29304
**
** Weight of the last 9,5 meters have to be added as a lumped mass
** at the end of the bridge girder.
** 9,5x5350=50825
**
*MASS, ELSET=END
50825
**
**************************************************************
**** Boundary conditions                                  ****
**************************************************************
**
** Nodes for boundary conditions
**
*NSET,NSET=ROCK
981,1087,1981,2087
*NSET,NSET=TOWER
1001,1037,2001,2037
*NSET,NSET=BOUNDARY
1,37
*NSET,NSET=ALL,GENERATE
1,50000,1
*NSET,NSET=TOWERLEG
20001,20101,30001,30101
**
** Boundary conditions
**
*BOUNDARY
ROCK,1,3,0
TOWERLEG,1,5,0
**1,1,1,0
**
**************************************************************
**** Couplings                                            ****
**************************************************************
**
** The nodes in the top of the towers are made hinged such that
```

```
** the cables not are rigid
**
*RELEASE
20030,S2,ALLM
20130,S2,ALLM
30030,S2,ALLM
30130,S2,ALLM
**
** Coupling between cross beams and towerlegs
*MPC
**Tower north
TIE,20201,20014
TIE,20207,20114
TIE,20301,20029
TIE,20307,20129
**Tower south
TIE,30201,30012
TIE,30207,30112
TIE,30301,30029
TIE,30307,30129
**
** The cross beam under the bridge girder, and
** the bridge girder:
** Fixed in the length direction in one side of the bridge
**
*RELEASE
29501,S2,M2-T
39501,S2,M2-T
39501,S1,M2
**
************************************************************
**** Elements                                           ****
************************************************************
**
*ELSET,ELSET=TOWER,GENERATE
20001,20030,1
20101,20130,1
20201,20206,1
20301,20306,1
30001,30030,1
30101,30130,1
30201,30206,1
30301,30306,1
**
*ELSET,ELSET=TOWERLEG1,GENERATE
20001,20030,1
30001,30030,1
*ELSET,ELSET=TOWERLEG2,GENERATE
20101,20130,1
30101,30130,1
**
*ELSET,ELSET=FRAME
```

```
20025,20048
20125,20148
20301,20306
**
************************************************************
**** Nodes to put on load                                ****
************************************************************
*NSET,NSET=WINDLOAD,GENERATE
2,36,1
*NSET,NSET=WINDCAB,GENERATE
1002,1036,1
2002,2036,1
**
*NSET,NSET=CENTRE
19
**
*NSET,NSET=GIRDER,GENERATE
1,37,1
*NSET,NSET=CABEL,GENERATE
1001,1037,1
2001,2037,1
*NSET,NSET=HLINK,GENERATE
3001,3037,1
4001,4037,1
**
************************************************************
**** Loading and analysis                                ****
************************************************************
**
** STEP1: DEADLOAD
** Deadload is given as static load, with non-linear geometry
**
*STEP,AMPLITUDE=RAMP,NAME=EGENVEKT,NLGEOM,INC=5000
*STATIC,STABILIZE=1E-10
1E-6,1E-6,1E-9,1E-6
**
** Cable

** Cable with half the hanger and hangerlink

** RHO-MED H.STENGER = 8524.2
** RHO-WITH HANGERS = 408kg/m / 0.0443 m2 = 9210
** RHO-WITHOUT HANGERS = 356kg/m / 0.0443m2 = 8036

** g = 9,81 x (8036/9210) = 8,5595

**
*DLOAD
MAINCABLE, GRAV, 8.5595, 0 , 0 , -1
BACKSTAYCABLE, GRAV, 9.810, 0 , 0 , -1
**
** Deadload bridge girder
```

```
** Deadload bridge girder included hangerlink and half the
** hanger = 5350 kg/m
**
** 5350 x 9,81 = 52483.5
**
*DLOAD
GIRDER, PZ, -52484
**
** Deadload tower
**
*DLOAD
TOWER, GRAV, 9.81, 0 , 0 , -1
**

*NODE PRINT, TOTALS=YES, FREQUENCY=100
RF
*NODE PRINT, TOTALS=YES, FREQUENCY=100
U
*EL PRINT, ELSET=MAINCABLE, FREQUENCY=100
SF
*EL PRINT, ELSET=GIRDER, FREQUENCY=100
SF

*END STEP
**
**
*STEP,NLGEOM
*FREQUENCY
110
**
*END STEP
```

Abaqus 6.10-1 Date 26-May-2011 Time 16:15:38
For use at University of Stavanger under license from Dassault Systemes or its subsidiary.

The Abaqus Software is a product of:

Dassault Systemes Simulia Corp.
Rising Sun Mills
166 Valley Street
Providence, RI 02909-2499, USA

Available for internal use at University of Stavanger.
The Abaqus Online Support System is accessible
through the "My Support" section of the SIMULIA
Home Page at http://www.simulia.com.

Support policies for academic licenses are described
on the SIMULIA web site at
http://www.simulia.com/academics/academic_support.html.

On machine D10430
you are authorized to run
Abaqus/Standard until 09-Dec-2011

Your site id is: 07STAVAN

For assistance or any other information you may
obtain contact information for your local office
from the world wide web at:

http://www.simulia.com/about/locations.html

```
* * * * * * * * * * * * * * * * * * * * * * * * * * * * * * * *
*                                                               *
*                   *****************                           *
*                   *  N O T I C E  *                           *
*                   *****************                           *
*                                                               *
*                                                               *
*                    Abaqus 6.10-1                              *
*                                                               *
*          BUILD ID: 2010_04_29-14.17.36 102575                 *
*                                                               *
*                                                               *
*  Please make sure you are using release 6.10manuals           *
*  plus the notes accompanying this release.                    *
*                                                               *
*                                                               *
*                                                               *
*                                                               *
*                                                               *
*   This program may not be used for commercial purposes        *
*           without payment of a commercial fee.                *
*                                                               *
* * * * * * * * * * * * * * * * * * * * * * * * * * * * * * * *
```

PROCESSING PART, INSTANCE, AND ASSEMBLY INFORMATION
****

END PROCESSING PART, INSTANCE, AND ASSEMBLY INFORMATION
****

OPTIONS BEING PROCESSED
****

```
*HEADING
        Analaysis of Lysefjord bridge
*NODE
*ELEMENT , TYPE = B31 , ELSET=GIRDER
*ELEMENT , TYPE = B31 , ELSET=MAINCABLE
*ELEMENT , TYPE = B31 , ELSET=BACKSTAYCABLE
*ELEMENT , TYPE = B31 , ELSET=DUMMY1
*ELEMENT , TYPE = B31 , ELSET=DUMMY2
*ELEMENT , TYPE = B31 , ELSET=HANGERS
*ELEMENT , TYPE = B31 , ELSET=DUMMY3
*ELEMENT , TYPE = B31 , ELSET=DUMMY4
*ELEMENT, TYPE=FRAME3D,ELSET=NIVA1
*ELEMENT, TYPE=FRAME3D,ELSET=NIVA2
*ELEMENT, TYPE=FRAME3D,ELSET=NIVA3
*ELEMENT, TYPE=FRAME3D,ELSET=NIVA4
*ELEMENT, TYPE=FRAME3D,ELSET=NIVA5
*ELEMENT, TYPE=FRAME3D,ELSET=NIVA6
*ELEMENT, TYPE=FRAME3D,ELSET=NIVA7
*ELEMENT, TYPE=FRAME3D,ELSET=NIVA8
*ELEMENT, TYPE=FRAME3D,ELSET=NIVA9
*ELEMENT, TYPE=FRAME3D,ELSET=NIVA10
*ELEMENT, TYPE=FRAME3D,ELSET=NIVA11
*ELEMENT, TYPE=FRAME3D,ELSET=NIVA12
*ELEMENT, TYPE=FRAME3D,ELSET=NIVA13
*ELEMENT, TYPE=FRAME3D,ELSET=NIVA14
*ELEMENT, TYPE=FRAME3D,ELSET=NIVA15
*ELEMENT, TYPE=FRAME3D,ELSET=NIVA16
*ELEMENT, TYPE=FRAME3D,ELSET=NIVA17
*ELEMENT, TYPE=FRAME3D,ELSET=NIVA18
*ELEMENT, TYPE=FRAME3D,ELSET=NIVA19
*ELEMENT, TYPE=FRAME3D,ELSET=NIVA20
*ELEMENT, TYPE=FRAME3D,ELSET=NIVA21
*ELEMENT, TYPE=FRAME3D,ELSET=NIVA22
*ELEMENT, TYPE=FRAME3D,ELSET=NIVA23
*ELEMENT, TYPE=FRAME3D,ELSET=NIVA24
*ELEMENT, TYPE=FRAME3D,ELSET=NIVA25
*ELEMENT, TYPE=FRAME3D,ELSET=NIVA26
*ELEMENT, TYPE=FRAME3D,ELSET=NIVA27
*ELEMENT, TYPE=FRAME3D,ELSET=NIVA28
*ELEMENT, TYPE=FRAME3D,ELSET=NIVA29
*ELEMENT, TYPE=B31,ELSET=NIVA30
*ELEMENT, TYPE=FRAME3D,ELSET=CROSSBEAM1
*ELEMENT, TYPE=FRAME3D,ELSET=CROSSBEAM2
*ELEMENT, TYPE=FRAME3D,ELSET=NIVA1
*ELEMENT, TYPE=FRAME3D,ELSET=NIVA2
*ELEMENT, TYPE=FRAME3D,ELSET=NIVA3
*ELEMENT, TYPE=FRAME3D,ELSET=NIVA4
*ELEMENT, TYPE=FRAME3D,ELSET=NIVA5
*ELEMENT, TYPE=FRAME3D,ELSET=NIVA6
*ELEMENT, TYPE=FRAME3D,ELSET=NIVA7
*ELEMENT, TYPE=FRAME3D,ELSET=NIVA8
*ELEMENT, TYPE=FRAME3D,ELSET=NIVA9
*ELEMENT, TYPE=FRAME3D,ELSET=NIVA10
*ELEMENT, TYPE=FRAME3D,ELSET=NIVA11
*ELEMENT, TYPE=FRAME3D,ELSET=NIVA12
*ELEMENT, TYPE=FRAME3D,ELSET=NIVA13
*ELEMENT, TYPE=FRAME3D,ELSET=NIVA14
*ELEMENT, TYPE=FRAME3D,ELSET=NIVA15
*ELEMENT, TYPE=FRAME3D,ELSET=NIVA16
*ELEMENT, TYPE=FRAME3D,ELSET=NIVA17
*ELEMENT, TYPE=FRAME3D,ELSET=NIVA18
*ELEMENT, TYPE=FRAME3D,ELSET=NIVA19
*ELEMENT, TYPE=FRAME3D,ELSET=NIVA20
*ELEMENT, TYPE=FRAME3D,ELSET=NIVA21
*ELEMENT, TYPE=FRAME3D,ELSET=NIVA22
*ELEMENT, TYPE=FRAME3D,ELSET=NIVA23
*ELEMENT, TYPE=FRAME3D,ELSET=NIVA24
*ELEMENT, TYPE=FRAME3D,ELSET=NIVA25
*ELEMENT, TYPE=FRAME3D,ELSET=NIVA26
*ELEMENT, TYPE=FRAME3D,ELSET=NIVA27
*ELEMENT, TYPE=FRAME3D,ELSET=NIVA28
*ELEMENT, TYPE=FRAME3D,ELSET=NIVA29
*ELEMENT, TYPE=B31,ELSET=NIVA30
*ELEMENT, TYPE=FRAME3D,ELSET=CROSSBEAM1
*ELEMENT, TYPE=FRAME3D,ELSET=CROSSBEAM2
*ELEMENT , TYPE = MASS , ELSET=SIDE
*ELEMENT , TYPE = MASS , ELSET=UNDER
*ELEMENT , TYPE = MASS , ELSET=END
*ELEMENT, TYPE=SPRING1, ELSET=TOWERLEG
*ELEMENT, TYPE=B33, ELSET=BOUNDARY
*NSET,NSET=ROCK
```

```
*NSET,NSET=TOWER
*NSET,NSET=BOUNDARY
*NSET,NSET=ALL,GENERATE
*NSET,NSET=TOWERLEG
*ELSET,ELSET=TOWER,GENERATE
*ELSET,ELSET=TOWERLEG1,GENERATE
*ELSET,ELSET=TOWERLEG2,GENERATE
*ELSET,ELSET=FRAME
*NSET,NSET=WINDLOAD,GENERATE
*NSET,NSET=WINDCAB,GENERATE
*NSET,NSET=CENTRE
*NSET,NSET=GIRDER,GENERATE
*NSET,NSET=CABEL,GENERATE
*NSET,NSET=HLINK,GENERATE
*BEAM GENERAL SECTION, ELSET=GIRDER, SECTION=GENERAL, DENSITY=0.001
*BEAM GENERAL SECTION, ELSET=DUMMY1, SECTION=GENERAL, DENSITY=1E-12
*BEAM GENERAL SECTION, ELSET=DUMMY2, SECTION=GENERAL, DENSITY=1E-12
*BEAM GENERAL SECTION, ELSET=DUMMY3, SECTION=GENERAL, DENSITY=1E-12
*BEAM GENERAL SECTION, ELSET=DUMMY4, SECTION=GENERAL, DENSITY=0.00001
*BEAM GENERAL SECTION, ELSET=HANGERS, SECTION=GENERAL, DENSITY=0.001
*BEAM GENERAL SECTION, ELSET=MAINCABLE, SECTION=GENERAL, DENSITY=8160
*BEAM GENERAL SECTION, ELSET=BACKSTAYCABLE, SECTION=GENERAL, DENSITY=7120
*BEAM GENERAL SECTION,ELSET=NIVA30,DENSITY=0.00001
*BEAM GENERAL SECTION,ELSET=BOUNDARY,DENSITY=0.000001
*FRAME SECTION,ELSET=NIVA1,SECTION=GENERAL,DENSITY=2500
*FRAME SECTION,ELSET=NIVA2,SECTION=GENERAL,DENSITY=2500
*FRAME SECTION,ELSET=NIVA3,SECTION=GENERAL,DENSITY=2500
*FRAME SECTION,ELSET=NIVA4,SECTION=GENERAL,DENSITY=2500
*FRAME SECTION,ELSET=NIVA5,SECTION=GENERAL,DENSITY=2500
*FRAME SECTION,ELSET=NIVA6,SECTION=GENERAL,DENSITY=2500
*FRAME SECTION,ELSET=NIVA7,SECTION=GENERAL,DENSITY=2500
*FRAME SECTION,ELSET=NIVA8,SECTION=GENERAL,DENSITY=2500
*FRAME SECTION,ELSET=NIVA9,SECTION=GENERAL,DENSITY=2500
*FRAME SECTION,ELSET=NIVA10,SECTION=GENERAL,DENSITY=2500
*FRAME SECTION,ELSET=NIVA11,SECTION=GENERAL,DENSITY=2500
*FRAME SECTION,ELSET=NIVA12,SECTION=GENERAL,DENSITY=2500
*FRAME SECTION,ELSET=NIVA13,SECTION=GENERAL,DENSITY=2500
*FRAME SECTION,ELSET=NIVA14,SECTION=GENERAL,DENSITY=2500
*FRAME SECTION,ELSET=NIVA15,SECTION=GENERAL,DENSITY=2500
*FRAME SECTION,ELSET=NIVA16,SECTION=GENERAL,DENSITY=2500
*FRAME SECTION,ELSET=NIVA17,SECTION=GENERAL,DENSITY=2500
*FRAME SECTION,ELSET=NIVA18,SECTION=GENERAL,DENSITY=2500
*FRAME SECTION,ELSET=NIVA19,SECTION=GENERAL,DENSITY=2500
*FRAME SECTION,ELSET=NIVA20,SECTION=GENERAL,DENSITY=2500
*FRAME SECTION,ELSET=NIVA21,SECTION=GENERAL,DENSITY=2500
*FRAME SECTION,ELSET=NIVA22,SECTION=GENERAL,DENSITY=2500
*FRAME SECTION,ELSET=NIVA23,SECTION=GENERAL,DENSITY=2500
*FRAME SECTION,ELSET=NIVA24,SECTION=GENERAL,DENSITY=2500
*FRAME SECTION,ELSET=NIVA25,SECTION=GENERAL,DENSITY=2500
*FRAME SECTION,ELSET=NIVA26,SECTION=GENERAL,DENSITY=2500
*FRAME SECTION,ELSET=NIVA27,SECTION=GENERAL,DENSITY=2500
*FRAME SECTION,ELSET=NIVA28,SECTION=GENERAL,DENSITY=2500
*FRAME SECTION,ELSET=NIVA29,SECTION=GENERAL,DENSITY=2500
*FRAME SECTION,ELSET=CROSSBEAM1,SECTION=GENERAL,DENSITY=2500
*FRAME SECTION,ELSET=CROSSBEAM2,SECTION=GENERAL,DENSITY=2500
*SPRING, ELSET=TOWERLEG
*MASS, ELSET=SIDE
*MASS, ELSET=UNDER
*MASS, ELSET=END
*BOUNDARY
*MPC
*RELEASE
*RELEASE
*BEAM GENERAL SECTION, ELSET=GIRDER, SECTION=GENERAL, DENSITY=0.001
*BEAM GENERAL SECTION, ELSET=DUMMY1, SECTION=GENERAL, DENSITY=1E-12
*BEAM GENERAL SECTION, ELSET=DUMMY2, SECTION=GENERAL, DENSITY=1E-12
*BEAM GENERAL SECTION, ELSET=DUMMY3, SECTION=GENERAL, DENSITY=1E-12
*BEAM GENERAL SECTION, ELSET=DUMMY4, SECTION=GENERAL, DENSITY=0.00001
*BEAM GENERAL SECTION, ELSET=HANGERS, SECTION=GENERAL, DENSITY=0.001
*BEAM GENERAL SECTION, ELSET=MAINCABLE, SECTION=GENERAL, DENSITY=8160
*BEAM GENERAL SECTION, ELSET=BACKSTAYCABLE, SECTION=GENERAL, DENSITY=7120
*BEAM GENERAL SECTION,ELSET=NIVA30,DENSITY=0.00001
*BEAM GENERAL SECTION,ELSET=BOUNDARY,DENSITY=0.000001
*FRAME SECTION,ELSET=NIVA1,SECTION=GENERAL,DENSITY=2500
*FRAME SECTION,ELSET=NIVA2,SECTION=GENERAL,DENSITY=2500
*FRAME SECTION,ELSET=NIVA3,SECTION=GENERAL,DENSITY=2500
*FRAME SECTION,ELSET=NIVA4,SECTION=GENERAL,DENSITY=2500
*FRAME SECTION,ELSET=NIVA5,SECTION=GENERAL,DENSITY=2500
*FRAME SECTION,ELSET=NIVA6,SECTION=GENERAL,DENSITY=2500
*FRAME SECTION,ELSET=NIVA7,SECTION=GENERAL,DENSITY=2500
*FRAME SECTION,ELSET=NIVA8,SECTION=GENERAL,DENSITY=2500
*FRAME SECTION,ELSET=NIVA9,SECTION=GENERAL,DENSITY=2500
```

```
 *FRAME SECTION,ELSET=NIVA10,SECTION=GENERAL,DENSITY=2500
 *FRAME SECTION,ELSET=NIVA11,SECTION=GENERAL,DENSITY=2500
 *FRAME SECTION,ELSET=NIVA12,SECTION=GENERAL,DENSITY=2500
 *FRAME SECTION,ELSET=NIVA13,SECTION=GENERAL,DENSITY=2500
 *FRAME SECTION,ELSET=NIVA14,SECTION=GENERAL,DENSITY=2500
 *FRAME SECTION,ELSET=NIVA15,SECTION=GENERAL,DENSITY=2500
 *FRAME SECTION,ELSET=NIVA16,SECTION=GENERAL,DENSITY=2500
 *FRAME SECTION,ELSET=NIVA17,SECTION=GENERAL,DENSITY=2500
 *FRAME SECTION,ELSET=NIVA18,SECTION=GENERAL,DENSITY=2500
 *FRAME SECTION,ELSET=NIVA19,SECTION=GENERAL,DENSITY=2500
 *FRAME SECTION,ELSET=NIVA20,SECTION=GENERAL,DENSITY=2500
 *FRAME SECTION,ELSET=NIVA21,SECTION=GENERAL,DENSITY=2500
 *FRAME SECTION,ELSET=NIVA22,SECTION=GENERAL,DENSITY=2500
 *FRAME SECTION,ELSET=NIVA23,SECTION=GENERAL,DENSITY=2500
 *FRAME SECTION,ELSET=NIVA24,SECTION=GENERAL,DENSITY=2500
 *FRAME SECTION,ELSET=NIVA25,SECTION=GENERAL,DENSITY=2500
 *FRAME SECTION,ELSET=NIVA26,SECTION=GENERAL,DENSITY=2500
 *FRAME SECTION,ELSET=NIVA27,SECTION=GENERAL,DENSITY=2500
 *FRAME SECTION,ELSET=NIVA28,SECTION=GENERAL,DENSITY=2500
 *FRAME SECTION,ELSET=NIVA29,SECTION=GENERAL,DENSITY=2500
 *FRAME SECTION,ELSET=CROSSBEAM1,SECTION=GENERAL,DENSITY=2500
 *FRAME SECTION,ELSET=CROSSBEAM2,SECTION=GENERAL,DENSITY=2500
 *SPRING, ELSET=TOWERLEG
 *MASS, ELSET=SIDE
 *MASS, ELSET=UNDER
 *MASS, ELSET=END
 *RELEASE
 *RELEASE
 *STEP,AMPLITUDE=RAMP,NAME=EGENVEKT,NLGEOM,INC=5000
 *STEP,NLGEOM
 *FREQUENCY
 *STEP,AMPLITUDE=RAMP,NAME=EGENVEKT,NLGEOM,INC=5000
 *STEP,NLGEOM
 *STEP,AMPLITUDE=RAMP,NAME=EGENVEKT,NLGEOM,INC=5000
 *STATIC,STABILIZE=1E-10
 *DLOAD
 *DLOAD
 *DLOAD
 *EL PRINT, ELSET=MAINCABLE, FREQUENCY=100
 *EL PRINT, ELSET=GIRDER, FREQUENCY=100
 *END STEP
 *STEP,NLGEOM
 *FREQUENCY
 *FREQUENCY
 *END STEP
 *BOUNDARY
 *STEP,AMPLITUDE=RAMP,NAME=EGENVEKT,NLGEOM,INC=5000
 *STATIC,STABILIZE=1E-10
 *NODE PRINT, TOTALS=YES, FREQUENCY=100
 *NODE PRINT, TOTALS=YES, FREQUENCY=100
 *END STEP
 *STEP,NLGEOM
 *FREQUENCY
 *FREQUENCY
 *END STEP

***WARNING: For 4 beam elements either the average curvature about the local
            1-direction differs by more than 0.1 degrees per unit length as
            compared to the default curvature or the approximate integrated
            curvature for the entire beam differs by more than 5 degrees as
            compared to the approximate integrated default curvature. This may
            be due to a user-specified normal or due to the nodal averaging
            routine used by Abaqus. This difference may cause unexpected
            behavior of the beam and you may want to verify that the beam
            normals are correct for your problem. The elements have been
            identified in element set WarnBeamCurvature1.


                          P R O B L E M   S I Z E


         NUMBER OF ELEMENTS IS                                    620
         NUMBER OF NODES IS                                       521
         NUMBER OF NODES DEFINED BY THE USER                      372
         NUMBER OF INTERNAL NODES GENERATED BY THE PROGRAM        149
         TOTAL NUMBER OF VARIABLES IN THE MODEL                  2677
         (DEGREES OF FREEDOM PLUS MAX NO. OF ANY LAGRANGE MULTIPLIER
          VARIABLES. INCLUDE *PRINT,SOLVE=YES TO GET THE ACTUAL NUMBER.)
```

END OF USER INPUT PROCESSING

JOB TIME SUMMARY
USER TIME (SEC) = 0.10000
SYSTEM TIME (SEC) = 0.10000
TOTAL CPU TIME (SEC) = 0.20000
WALLCLOCK TIME (SEC) = 1
1

Abaqus 6.10-1 Date 26-May-2011 Time 16:15:39
For use at University of Stavanger under license from Dassault Systemes or its subsidiary.

Analaysis of Lysefjord bridge STEP 1
INCREMENT 1
TIME COMPLETED IN
THIS STEP 0.00

S T E P 1 S T A T I C A N A L Y S I S

AUTOMATIC TIME CONTROL WITH -
A SUGGESTED INITIAL TIME INCREMENT OF 1.000E-06
AND A TOTAL TIME PERIOD OF 1.000E-06
THE MINIMUM TIME INCREMENT ALLOWED IS 1.000E-09
THE MAXIMUM TIME INCREMENT ALLOWED IS 1.000E-06

LINEAR EQUATION SOLVER TYPE DIRECT SPARSE

AUTOMATIC STABILIZATION WITH DISSIPATED ENERGY FRACTION = 1.000E-10

LARGE DISPLACEMENT THEORY WILL BE USED

TOTAL MASS OF MODEL

1.1029557E+07

LOCATION OF THE CENTER OF MASS OF THE MODEL

6.513760 5.7456290E-15 53.15018

MOMENTS OF INERTIA ABOUT THE ORIGIN

I(XX)	I(YY)	I(ZZ)
3.8766526E+10	5.0392696E+11	4.6603584E+11

PRODUCTS OF INERTIA ABOUT THE ORIGIN

I(XY)	I(XZ)	I(YZ)
-3.8553383E-06	-1.4072190E+07	-2.7400018E-06

MOMENTS OF INERTIA ABOUT THE CENTER OF MASS

I(XX)	I(YY)	I(ZZ)
7.6086718E+09	4.7230114E+11	4.6556787E+11

PRODUCTS OF INERTIA ABOUT THE CENTER OF MASS

I(XY)	I(XZ)	I(YZ)
-3.4425500E-06	3.8044435E+09	6.2821765E-07

M E M O R Y E S T I M A T E

PROCESS	FLOATING PT OPERATIONS PER ITERATION	MINIMUM MEMORY REQUIRED (MBYTES)	MEMORY TO MINIMIZE I/O (MBYTES)
1	2.44E+006	18	37

NOTE:
(1) SINCE ABAQUS DOES NOT PRE-ALLOCATE MEMORY AND ONLY ALLOCATES MEMORY AS NEEDED DURING THE ANALYSIS,

THE MEMORY REQUIREMENT PRINTED HERE CAN ONLY BE VIEWED AS A GENERAL GUIDELINE BASED ON THE BEST KNOWLEDGE AVAILABLE AT THE BEGINNING OF A STEP BEFORE THE SOLUTION PROCESS HAS BEGUN.

(2) THE ESTIMATE IS NORMALLY UPDATED AT THE BEGINNING OF EVERY STEP. IT IS THE MAXIMUM VALUE OF THE ESTIMATE FROM THE CURRENT STEP TO THE LAST STEP OF THE ANALYSIS, WITH UNSYMMETRIC SOLUTION TAKEN INTO ACCOUNT IF APPLICABLE.

(3) SINCE THE ESTIMATE IS BASED ON THE ACTIVE DEGREES OF FREEDOM IN THE FIRST ITERATION OF THE CURRENT STEP, THE MEMORY ESTIMATE MIGHT BE SIGNIFICANTLY DIFFERENT THAN ACTUAL USAGE FOR PROBLEMS WITH SUBSTANTIAL CHANGES IN ACTIVE DEGREES OF FREEDOM BETWEEN STEPS (OR EVEN WITHIN THE SAME STEP). EXAMPLES ARE: PROBLEMS WITH SIGNIFICANT CONTACT CHANGES, PROBLEMS WITH MODEL CHANGE, PROBLEMS WITH BOTH STATIC STEP AND STEADY STATE DYNAMIC PROCEDURES WHERE ACOUSTIC ELEMENTS WILL ONLY BE ACTIVATED IN THE STEADY STATE DYNAMIC STEPS.

(4) FOR MULTI-PROCESS EXECUTION, THE ESTIMATED VALUE OF FLOATING POINT OPERATIONS FOR EACH PROCESS IS BASED ON AN INITIAL SCHEDULING OF OPERATIONS AND MIGHT NOT REFLECT THE ACTUAL FLOATING POINT OPERATIONS COMPLETED ON EACH PROCESS. OPERATIONS ARE DYNAMICALY BALANCED DURING EXECUTION, SO THE ACTUAL BALANCE OF OPERATIONS BETWEEN PROCESSES IS EXPECTED TO BE BETTER THAN THE ESTIMATE PRINTED HERE.

(5) THE UPPER LIMIT OF MEMORY THAT CAN BE ALLOCATED BY ABAQUS WILL IN GENERAL DEPEND ON THE VALUE OF THE "MEMORY" PARAMETER AND THE AMOUNT OF PHYSICAL MEMORY AVAILABLE ON THE MACHINE. PLEASE SEE THE "ABAQUS ANALYSIS USER'S MANUAL" FOR MORE DETAILS. THE ACTUAL USAGE OF MEMORY AND OF DISK SPACE FOR SCRATCH DATA WILL DEPEND ON THIS UPPER LIMIT AS WELL AS THE MEMORY REQUIRED TO MINIMIZE I/O. IF THE MEMORY UPPER LIMIT IS GREATER THAN THE MEMORY REQUIRED TO MINIMIZE I/O, THEN THE ACTUAL MEMORY USAGE WILL BE CLOSE TO THE ESTIMATED "MEMORY TO MINIMIZE I/O" VALUE, AND THE SCRATCH DISK USAGE WILL BE CLOSE-TO-ZERO; OTHERWISE, THE ACTUAL MEMORY USED WILL BE CLOSE TO THE PREVIOUSLY MENTIONED MEMORY LIMIT, AND THE SCRATCH DISK USAGE WILL BE ROUGHLY PROPORTIONAL TO THE DIFFERENCE BETWEEN THE ESTIMATED "MEMORY TO MINIMIZE I/O" AND THE MEMORY UPPER LIMIT. HOWEVER ACCURATE ESTIMATE OF THE SCRATCH DISK SPACE IS NOT POSSIBLE.

(6) USING "*RESTART, WRITE" CAN GENERATE A LARGE AMOUNT OF DATA WRITTEN IN THE WORK DIRECTORY.

INCREMENT 1 SUMMARY

TIME INCREMENT COMPLETED 1.000E-06, FRACTION OF STEP COMPLETED 1.00
STEP TIME COMPLETED 1.000E-06, TOTAL TIME COMPLETED 1.000E-06

E L E M E N T O U T P U T

THE FOLLOWING TABLE IS PRINTED AT THE INTEGRATION POINTS FOR ELEMENT TYPE B31 AND ELEMENT SET MAINCABLE

ELEMENT	PT	FOOT-NOTE	SF1	SF2	SF3	SM1	SM2	SM3
1001	1		1.7555E+07	-16.05	-4.3362E-04	100.1	-7.1975E-04	6.8487E-03
1002	1		1.7447E+07	5.486	2.6293E-04	-28.14	1.9084E-03	6.7271E-03
1003	1		1.7332E+07	-4.843	-1.4304E-04	-21.54	9.3920E-04	6.5351E-03
1004	1		1.7221E+07	1.177	2.1346E-05	-41.90	1.5116E-03	6.3529E-03
1005	1		1.7115E+07	-1.100	-4.4290E-05	-38.04	1.4504E-03	6.1390E-03
1006	1		1.7015E+07	-0.1964	-1.7781E-05	-42.06	1.6315E-03	5.9025E-03
1007	1		1.6922E+07	-0.6528	-2.8288E-05	-42.31	1.7056E-03	5.6297E-03
1008	1		1.6834E+07	-0.6601	-2.3556E-05	-44.12	1.8081E-03	5.3125E-03
1009	1		1.6753E+07	-0.8490	-2.5278E-05	-45.33	1.8826E-03	4.9352E-03
1010	1		1.6678E+07	-1.076	-2.4559E-05	-46.59	1.9508E-03	4.4780E-03
1011	1		1.6608E+07	-1.458	-2.4657E-05	-48.00	1.9991E-03	3.9122E-03
1012	1		1.6545E+07	-1.932	-2.5570E-05	-49.47	2.0322E-03	3.1989E-03
1013	1		1.6487E+07	-2.692	-2.6954E-05	-51.02	2.0514E-03	2.2872E-03
1014	1		1.6434E+07	-3.710	-2.9889E-05	-52.85	2.0628E-03	1.1182E-03
1015	1		1.6387E+07	-4.995	-3.4461E-05	-54.74	2.0846E-03	-3.5286E-04
1016	1		1.6345E+07	-6.228	-3.9512E-05	-56.30	2.1446E-03	-2.1009E-03
1017	1		1.6311E+07	-6.704	-4.2536E-05	-56.59	2.2769E-03	-3.9500E-03
1018	1		1.6286E+07	-5.940	-3.6574E-05	-55.76	2.4817E-03	-5.5666E-03
1019	1		1.6271E+07	-4.203	-2.5233E-05	-55.16	2.7193E-03	-6.6506E-03
1020	1		1.6268E+07	-2.464	-9.6448E-06	-55.58	2.9238E-03	-7.1527E-03
1021	1		1.6276E+07	-1.172	1.2964E-06	-56.53	3.0521E-03	-7.2386E-03
1022	1		1.6294E+07	-0.4179	9.1038E-06	-57.24	3.1080E-03	-7.1064E-03
1023	1		1.6322E+07	-2.1683E-02	1.3693E-05	-57.57	3.1034E-03	-6.8911E-03
1024	1		1.6359E+07	0.1835	1.6352E-05	-57.43	3.0571E-03	-6.6630E-03
1025	1		1.6404E+07	0.2430	1.8298E-05	-57.06	2.9802E-03	-6.4522E-03
1026	1		1.6457E+07	0.3190	1.8750E-05	-56.34	2.8847E-03	-6.2691E-03
1027	1		1.6518E+07	0.2951	1.9605E-05	-55.35	2.7773E-03	-6.1145E-03
1028	1		1.6586E+07	0.3012	2.0703E-05	-54.32	2.6542E-03	-5.9863E-03
1029	1		1.6661E+07	0.3084	1.8368E-05	-53.00	2.5354E-03	-5.8815E-03
1030	1		1.6743E+07	0.3599	2.4261E-05	-51.09	2.3918E-03	-5.7960E-03
1031	1		1.6833E+07	0.1310	1.0712E-05	-50.04	2.2933E-03	-5.7284E-03
1032	1		1.6929E+07	0.7706	4.4035E-05	-46.22	2.0684E-03	-5.6727E-03
1033	1		1.7031E+07	-0.5831	-3.9535E-05	-46.69	2.1579E-03	-5.6348E-03

1034	1	1.7139E+07	3.374	1.7073E-04	-30.53	1.4421E-03	-5.5933E-03
1035	1	1.7251E+07	-1.710	-3.4672E-04	-21.41	2.6816E-03	-5.5959E-03
1036	1	1.7359E+07	9.673	5.8371E-04	66.07	-1.0232E-03	-5.5298E-03
2001	1	1.7555E+07	-16.05	4.3475E-04	100.1	7.2293E-04	-6.8683E-03
2002	1	1.7447E+07	5.486	-2.6360E-04	-28.14	-1.9121E-03	-6.7465E-03
2003	1	1.7332E+07	-4.843	1.4341E-04	-21.54	-9.4057E-04	-6.5542E-03
2004	1	1.7221E+07	1.177	-2.1394E-05	-41.90	-1.5145E-03	-6.3717E-03
2005	1	1.7115E+07	-1.100	4.4411E-05	-38.04	-1.4533E-03	-6.1575E-03
2006	1	1.7015E+07	-0.1964	1.7836E-05	-42.06	-1.6350E-03	-5.9207E-03
2007	1	1.6922E+07	-0.6528	2.8371E-05	-42.31	-1.7095E-03	-5.6475E-03
2008	1	1.6834E+07	-0.6601	2.3629E-05	-44.12	-1.8125E-03	-5.3299E-03
2009	1	1.6753E+07	-0.8490	2.5358E-05	-45.33	-1.8873E-03	-4.9521E-03
2010	1	1.6678E+07	-1.076	2.4640E-05	-46.59	-1.9560E-03	-4.4943E-03
2011	1	1.6608E+07	-1.458	2.4741E-05	-48.00	-2.0047E-03	-3.9279E-03
2012	1	1.6545E+07	-1.932	2.5662E-05	-49.47	-2.0381E-03	-3.2138E-03
2013	1	1.6487E+07	-2.692	2.7056E-05	-51.02	-2.0577E-03	-2.3009E-03
2014	1	1.6434E+07	-3.710	3.0006E-05	-52.85	-2.0694E-03	-1.1304E-03
2015	1	1.6387E+07	-4.995	3.4600E-05	-54.74	-2.0916E-03	3.4247E-04
2016	1	1.6345E+07	-6.228	3.9673E-05	-56.30	-2.1519E-03	2.0929E-03
2017	1	1.6311E+07	-6.704	4.2709E-05	-56.59	-2.2846E-03	3.9447E-03
2018	1	1.6286E+07	-5.940	3.6727E-05	-55.76	-2.4898E-03	5.5642E-03
2019	1	1.6271E+07	-4.203	2.5349E-05	-55.16	-2.7278E-03	6.6507E-03
2020	1	1.6268E+07	-2.464	9.7091E-06	-55.58	-2.9327E-03	7.1548E-03
2021	1	1.6276E+07	-1.172	-1.2697E-06	-56.53	-3.0613E-03	7.2424E-03
2022	1	1.6294E+07	-0.4179	-9.1058E-06	-57.24	-3.1173E-03	7.1115E-03
2023	1	1.6322E+07	-2.1683E-02	-1.3713E-05	-57.57	-3.1128E-03	6.8974E-03
2024	1	1.6359E+07	0.1835	-1.6386E-05	-57.43	-3.0664E-03	6.6704E-03
2025	1	1.6404E+07	0.2430	-1.8342E-05	-57.06	-2.9894E-03	6.4606E-03
2026	1	1.6457E+07	0.3190	-1.8800E-05	-56.34	-2.8937E-03	6.2784E-03
2027	1	1.6518E+07	0.2951	-1.9661E-05	-55.35	-2.7861E-03	6.1247E-03
2028	1	1.6586E+07	0.3012	-2.0766E-05	-54.32	-2.6627E-03	5.9974E-03
2029	1	1.6661E+07	0.3084	-1.8428E-05	-53.00	-2.5437E-03	5.8934E-03
2030	1	1.6743E+07	0.3599	-2.4342E-05	-51.09	-2.3997E-03	5.8088E-03
2031	1	1.6833E+07	0.1310	-1.0757E-05	-50.04	-2.3010E-03	5.7419E-03
2032	1	1.6929E+07	0.7706	-4.4178E-05	-46.22	-2.0755E-03	5.6870E-03
2033	1	1.7031E+07	-0.5831	3.9627E-05	-46.69	-2.1653E-03	5.6498E-03
2034	1	1.7139E+07	3.374	-1.7125E-04	-30.53	-1.4474E-03	5.6091E-03
2035	1	1.7251E+07	-1.710	3.4768E-04	-21.41	-2.6903E-03	5.6125E-03
2036	1	1.7359E+07	9.673	-5.8554E-04	66.07	1.0265E-03	5.5469E-03
MAXIMUM		1.7555E+07	9.673	5.8371E-04	100.1	3.1080E-03	7.2424E-03
ELEMENT		1001	2036	1036	1001	1022	2021
MINIMUM		1.6268E+07	-16.05	-5.8554E-04	-57.57	-3.1173E-03	-7.2386E-03
ELEMENT		1020	2001	2036	1023	2022	1021

THE FOLLOWING TABLE IS PRINTED AT THE INTEGRATION POINTS FOR ELEMENT TYPE B31 AND ELEMENT SET GIRDER

ELEMENT	PT	FOOT-NOTE	SF1	SF2	SF3	SM1	SM2	SM3
1	1		-3.4990E+05	-3.5496E+05	3.8455E-03	-3.3923E+06	-3.7593E-02	0.2650
2	1		-3.4560E+05	-5.0121E+04	4.8122E-03	-7.0738E+06	-0.1024	0.5836
3	1		-3.4471E+05	-2.9706E+04	4.4725E-03	-7.5385E+06	-0.1568	0.7503
4	1		-3.4280E+05	-2.4530E+04	4.0386E-03	-7.8485E+06	-0.2050	0.8973
5	1		-3.3955E+05	-2.2470E+04	3.5758E-03	-8.1142E+06	-0.2467	1.042
6	1		-3.3480E+05	-2.0892E+04	3.0974E-03	-8.3572E+06	-0.2813	1.187
7	1		-3.2835E+05	-2.0033E+04	2.5992E-03	-8.5843E+06	-0.3088	1.333
8	1		-3.1999E+05	-1.9799E+04	2.0789E-03	-8.8036E+06	-0.3288	1.478
9	1		-3.0942E+05	-1.9431E+04	1.5395E-03	-9.0176E+06	-0.3411	1.624
10	1		-2.9633E+05	-1.9534E+04	9.7478E-04	-9.2280E+06	-0.3455	1.770
11	1		-2.8028E+05	-2.0073E+04	3.8342E-04	-9.4399E+06	-0.3416	1.916
12	1		-2.6085E+05	-2.0262E+04	-2.2858E-04	-9.6533E+06	-0.3291	2.062
13	1		-2.3751E+05	-2.0770E+04	-8.6608E-04	-9.8674E+06	-0.3079	2.208
14	1		-2.0985E+05	-2.1318E+04	-1.5222E-03	-1.0084E+07	-0.2777	2.355
15	1		-1.7782E+05	-2.1818E+04	-2.1845E-03	-1.0303E+07	-0.2389	2.502
16	1		-1.4219E+05	-2.2044E+04	-2.8260E-03	-1.0523E+07	-0.1919	2.648
17	1		-1.0520E+05	-2.1447E+04	-3.3983E-03	-1.0741E+07	-0.1379	2.795
18	1		-7.0422E+04	-1.9547E+04	-3.8415E-03	-1.0947E+07	-7.8747E-02	2.941
19	1		-4.1499E+04	-1.5125E+04	-4.0939E-03	-1.1122E+07	-1.6363E-02	3.088
20	1		-2.0006E+04	-1.0473E+04	-4.1670E-03	-1.1252E+07	4.7405E-02	3.234
21	1		-5514.	-5540.	-4.0724E-03	-1.1334E+07	0.1111	3.382
22	1		3593.	-1118.	-3.8470E-03	-1.1366E+07	0.1735	3.530
23	1		9021.	2693.	-3.5191E-03	-1.1354E+07	0.2337	3.679
24	1		1.2146E+04	6000.	-3.1090E-03	-1.1303E+07	0.2906	3.828
25	1		1.3955E+04	8974.	-2.6303E-03	-1.1217E+07	0.3435	3.977
26	1		1.5112E+04	1.1993E+04	-2.0878E-03	-1.1096E+07	0.3917	4.127
27	1		1.6083E+04	1.4523E+04	-1.4985E-03	-1.0944E+07	0.4343	4.277
28	1		1.7139E+04	1.7415E+04	-8.5221E-04	-1.0760E+07	0.4709	4.428

29	1	1.8469E+04	2.0807E+04	-1.4872E-04	-1.0538E+07	0.5008	4.579
30	1	2.0215E+04	2.4250E+04	6.0121E-04	-1.0276E+07	0.5233	4.730
31	1	2.2426E+04	2.8607E+04	1.4149E-03	-9.9676E+06	0.5377	4.882
32	1	2.5136E+04	3.4161E+04	2.2998E-03	-9.5998E+06	0.5434	5.034
33	1	2.8364E+04	4.0983E+04	3.2597E-03	-9.1577E+06	0.5396	5.189
34	1	3.1967E+04	5.2095E+04	4.3755E-03	-8.6078E+06	0.5259	5.361
35	1	3.5284E+04	7.9622E+04	5.9895E-03	-7.8254E+06	0.5045	5.647
36	1	2.5338E+04	3.8358E+05	1.7879E-02	-3.6774E+06	0.4300	6.650
MAXIMUM		3.5284E+04	3.8358E+05	1.7879E-02	-3.3923E+06	0.5434	6.650
ELEMENT		35	36	36	1	32	36
MINIMUM		-3.4990E+05	-3.5496E+05	-4.1670E-03	-1.1366E+07	-0.3455	0.2650
ELEMENT		1	1	20	22	10	1

N O D E O U T P U T

THE FOLLOWING TABLE IS PRINTED FOR ALL NODES

NODE	FOOT-NOTE	RF1	RF2	RF3	RM1	RM2	RM3
981		-1.5860E+07	63.28	-1.0331E+07	0.000	0.000	0.000
1087		1.5631E+07	17.86	-4.9896E+06	0.000	0.000	0.000
1981		-1.5860E+07	-63.28	-1.0331E+07	0.000	0.000	0.000
2087		1.5631E+07	-17.86	-4.9896E+06	0.000	0.000	0.000
20001		-3.8903E+05	-1.5123E+06	3.6679E+07	7.7733E+05	-4.3218E+07	0.000
20101		-3.8903E+05	1.5123E+06	3.6679E+07	-7.7733E+05	-4.3218E+07	0.000
30001		6.1814E+05	-1.1944E+06	3.2706E+07	5.0430E+05	6.0741E+07	0.000
30101		6.1814E+05	1.1944E+06	3.2706E+07	-5.0430E+05	6.0741E+07	0.000
MAXIMUM		1.5631E+07	1.5123E+06	3.6679E+07	7.7733E+05	6.0741E+07	0.000
AT NODE		2087	20101	20101	20001	30101	1
MINIMUM		-1.5860E+07	-1.5123E+06	-1.0331E+07	-7.7733E+05	-4.3218E+07	0.000
AT NODE		1981	20001	1981	20101	20101	1
TOTAL		9.5121E-02	1.6840E-02	1.0813E+08	-0.3612	3.5046E+07	0.000

THE FOLLOWING TABLE IS PRINTED FOR ALL NODES

NODE	FOOT-NOTE	U1	U2	U3	UR1	UR2	UR3
1		6.4315E-02	-9.9990E-09	-4.9429E-03	5.2222E-09	2.2264E-02	1.8430E-10
2		7.4999E-02	-9.0514E-09	-0.4252	5.2898E-09	2.1544E-02	1.8346E-10
3		8.0611E-02	-8.2912E-09	-0.6782	5.3833E-09	2.0601E-02	1.8185E-10
4		8.5353E-02	-7.4178E-09	-0.9195	5.5036E-09	1.9597E-02	1.7969E-10
5		8.9278E-02	-6.4388E-09	-1.148	5.6474E-09	1.8551E-02	1.7691E-10
6		9.2447E-02	-5.3595E-09	-1.365	5.8144E-09	1.7470E-02	1.7345E-10
7		9.4920E-02	-4.1837E-09	-1.568	6.0046E-09	1.6356E-02	1.6928E-10
8		9.6761E-02	-2.9135E-09	-1.757	6.2180E-09	1.5213E-02	1.6436E-10
9		9.8039E-02	-1.5496E-09	-1.933	6.4547E-09	1.4040E-02	1.5863E-10
10		9.8820E-02	-9.1157E-11	-2.094	6.7147E-09	1.2839E-02	1.5208E-10
11		9.9176E-02	1.4640E-09	-2.241	6.9981E-09	1.1610E-02	1.4466E-10
12		9.9178E-02	3.1197E-09	-2.373	7.3048E-09	1.0352E-02	1.3633E-10
13		9.8902E-02	4.8811E-09	-2.489	7.6350E-09	9.0664E-03	1.2706E-10
14		9.8422E-02	6.7547E-09	-2.590	7.9885E-09	7.7520E-03	1.1683E-10
15		9.7817E-02	8.7486E-09	-2.675	8.3655E-09	6.4088E-03	1.0560E-10
16		9.7166E-02	1.0872E-08	-2.744	8.7660E-09	5.0365E-03	9.3337E-11
17		9.6551E-02	1.3137E-08	-2.796	9.1899E-09	3.6347E-03	8.0008E-11
18		9.6055E-02	1.5554E-08	-2.831	9.6373E-09	2.2040E-03	6.5563E-11
19		9.5761E-02	1.8137E-08	-2.849	1.0108E-08	7.4572E-04	4.9938E-11
20		9.5753E-02	2.0900E-08	-2.849	1.0602E-08	-7.3598E-04	3.3062E-11
21		9.6115E-02	2.3859E-08	-2.831	1.1120E-08	-2.2351E-03	1.4850E-11
22		9.6931E-02	2.7029E-08	-2.795	1.1661E-08	-3.7452E-03	-4.7926E-12
23		9.8283E-02	3.0429E-08	-2.741	1.2227E-08	-5.2598E-03	-2.5973E-11
24		0.1003	3.4077E-08	-2.669	1.2816E-08	-6.7728E-03	-4.8810E-11
25		0.1029	3.7992E-08	-2.578	1.3428E-08	-8.2793E-03	-7.3433E-11
26		0.1064	4.2194E-08	-2.470	1.4065E-08	-9.7743E-03	-9.9984E-11
27		0.1107	4.6705E-08	-2.344	1.4726E-08	-1.1254E-02	-1.2861E-10
28		0.1159	5.1545E-08	-2.200	1.5411E-08	-1.2713E-02	-1.5947E-10
29		0.1221	5.6738E-08	-2.039	1.6120E-08	-1.4147E-02	-1.9272E-10
30		0.1294	6.2305E-08	-1.860	1.6853E-08	-1.5553E-02	-2.2851E-10

31	0.1379	6.8272E-08	-1.665	1.7611E-08	-1.6923E-02	-2.6702E-10
32	0.1475	7.4663E-08	-1.454	1.8393E-08	-1.8253E-02	-3.0840E-10
33	0.1584	8.1506E-08	-1.227	1.9199E-08	-1.9534E-02	-3.5279E-10
34	0.1705	8.8829E-08	-0.9855	2.0030E-08	-2.0756E-02	-4.0035E-10
35	0.1840	9.6665E-08	-0.7293	2.0889E-08	-2.1904E-02	-4.5128E-10
36	0.1989	1.0505E-07	-0.4599	2.1794E-08	-2.2949E-02	-5.0650E-10
37	0.2250	1.1957E-07	-1.1252E-02	2.3492E-08	-2.3732E-02	-6.0613E-10
981	0.000	0.000	0.000	6.1555E-06	-8.6799E-03	4.4750E-07
1001	0.2297	-2.9443E-04	-8.8181E-03	6.6010E-06	1.6374E-02	-1.4979E-07
1002	0.1312	-2.5107E-04	-0.3938	6.9058E-06	2.0771E-02	-2.8015E-07
1003	6.9938E-02	-2.2532E-04	-0.6449	7.1147E-06	2.0009E-02	-3.0070E-07
1004	1.5588E-02	-2.0096E-04	-0.8895	7.3091E-06	1.9428E-02	-3.3969E-07
1005	-3.0486E-02	-1.7802E-04	-1.122	7.5022E-06	1.8306E-02	-3.6059E-07
1006	-6.8442E-02	-1.5653E-04	-1.342	7.6881E-06	1.7292E-02	-3.7719E-07
1007	-9.8646E-02	-1.3652E-04	-1.549	7.8676E-06	1.6177E-02	-3.8417E-07
1008	-0.1215	-1.1799E-04	-1.742	8.0390E-06	1.5061E-02	-3.8391E-07
1009	-0.1376	-1.0097E-04	-1.920	8.2010E-06	1.3902E-02	-3.7589E-07
1010	-0.1473	-8.5482E-05	-2.085	8.3516E-06	1.2716E-02	-3.6080E-07
1011	-0.1511	-7.1549E-05	-2.234	8.4885E-06	1.1501E-02	-3.3883E-07
1012	-0.1497	-5.9196E-05	-2.368	8.6084E-06	1.0254E-02	-3.1058E-07
1013	-0.1435	-4.8445E-05	-2.487	8.7070E-06	8.9721E-03	-2.7653E-07
1014	-0.1332	-3.9322E-05	-2.590	8.7784E-06	7.6532E-03	-2.3724E-07
1015	-0.1193	-3.1848E-05	-2.676	8.8153E-06	6.2899E-03	-1.9331E-07
1016	-0.1025	-2.6033E-05	-2.746	8.8091E-06	4.8801E-03	-1.4523E-07
1017	-8.3366E-02	-2.1871E-05	-2.798	8.7517E-06	3.4320E-03	-9.3319E-08
1018	-6.2674E-02	-1.9319E-05	-2.832	8.6404E-06	1.9777E-03	-3.7547E-08
1019	-4.1116E-02	-1.8299E-05	-2.849	8.4816E-06	5.4536E-04	2.1794E-08
1020	-1.9414E-02	-1.8697E-05	-2.847	8.2904E-06	-8.7169E-04	8.3750E-08
1021	1.7122E-03	-2.0396E-05	-2.828	8.0832E-06	-2.3000E-03	1.4658E-07
1022	2.1536E-02	-2.3289E-05	-2.791	7.8719E-06	-3.7541E-03	2.0831E-07
1023	3.9317E-02	-2.7294E-05	-2.735	7.6626E-06	-5.2283E-03	2.6744E-07
1024	5.4307E-02	-3.2345E-05	-2.662	7.4580E-06	-6.7133E-03	3.2284E-07
1025	6.5760E-02	-3.8396E-05	-2.570	7.2583E-06	-8.1978E-03	3.7378E-07
1026	7.2943E-02	-4.5407E-05	-2.459	7.0634E-06	-9.6764E-03	4.1970E-07
1027	7.5133E-02	-5.3350E-05	-2.331	6.8726E-06	-1.1140E-02	4.6028E-07
1028	7.1635E-02	-6.2200E-05	-2.184	6.6852E-06	-1.2583E-02	4.9529E-07
1029	6.1775E-02	-7.1937E-05	-2.020	6.5006E-06	-1.4005E-02	5.2438E-07
1030	4.4906E-02	-8.2544E-05	-1.839	6.3184E-06	-1.5397E-02	5.4767E-07
1031	2.0432E-02	-9.4006E-05	-1.641	6.1382E-06	-1.6745E-02	5.6458E-07
1032	-1.2210E-02	-1.0631E-04	-1.427	5.9593E-06	-1.8071E-02	5.7614E-07
1033	-5.3526E-02	-1.1944E-04	-1.196	5.7825E-06	-1.9303E-02	5.7932E-07
1034	-0.1039	-1.3338E-04	-0.9506	5.6049E-06	-2.0554E-02	5.8175E-07
1035	-0.1634	-1.4813E-04	-0.6916	5.4334E-06	-2.1376E-02	5.6414E-07
1036	-0.2307	-1.6365E-04	-0.4246	5.2499E-06	-2.1956E-02	5.7561E-07
1037	-0.3418	-1.8972E-04	-7.7565E-03	5.0103E-06	-1.9053E-02	4.4734E-07
1087	0.000	0.000	0.000	4.4795E-06	1.1953E-02	-1.0657E-06
1981	0.000	0.000	0.000	-6.1568E-06	-8.6799E-03	-4.4896E-07
2001	0.2297	2.9447E-04	-8.8181E-03	-6.6035E-06	1.6374E-02	1.5024E-07
2002	0.1312	2.5110E-04	-0.3938	-6.9091E-06	2.0771E-02	2.8106E-07
2003	6.9938E-02	2.2535E-04	-0.6449	-7.1187E-06	2.0009E-02	3.0170E-07
2004	1.5588E-02	2.0098E-04	-0.8895	-7.3136E-06	1.9428E-02	3.4084E-07
2005	-3.0486E-02	1.7804E-04	-1.122	-7.5073E-06	1.8306E-02	3.6183E-07
2006	-6.8442E-02	1.5655E-04	-1.342	-7.6937E-06	1.7292E-02	3.7851E-07
2007	-9.8646E-02	1.3653E-04	-1.549	-7.8738E-06	1.6177E-02	3.8554E-07
2008	-0.1215	1.1800E-04	-1.742	-8.0457E-06	1.5061E-02	3.8531E-07
2009	-0.1376	1.0098E-04	-1.920	-8.2082E-06	1.3902E-02	3.7729E-07
2010	-0.1473	8.5490E-05	-2.085	-8.3593E-06	1.2716E-02	3.6217E-07
2011	-0.1511	7.1556E-05	-2.234	-8.4967E-06	1.1501E-02	3.4017E-07
2012	-0.1497	5.9202E-05	-2.368	-8.6171E-06	1.0254E-02	3.1185E-07
2013	-0.1435	4.8452E-05	-2.487	-8.7161E-06	8.9721E-03	2.7771E-07
2014	-0.1332	3.9330E-05	-2.590	-8.7880E-06	7.6532E-03	2.3831E-07
2015	-0.1193	3.1856E-05	-2.676	-8.8252E-06	6.2899E-03	1.9425E-07
2016	-0.1025	2.6043E-05	-2.746	-8.8193E-06	4.8801E-03	1.4603E-07
2017	-8.3366E-02	2.1882E-05	-2.798	-8.7622E-06	3.4320E-03	9.3944E-08
2018	-6.2674E-02	1.9333E-05	-2.832	-8.6510E-06	1.9777E-03	3.7987E-08
2019	-4.1116E-02	1.8316E-05	-2.849	-8.4923E-06	5.4536E-04	-2.1552E-08
2020	-1.9414E-02	1.8717E-05	-2.847	-8.3011E-06	-8.7169E-04	-8.3720E-08
2021	1.7122E-03	2.0419E-05	-2.828	-8.0938E-06	-2.3000E-03	-1.4677E-07
2022	2.1536E-02	2.3315E-05	-2.791	-7.8824E-06	-3.7541E-03	-2.0872E-07
2023	3.9317E-02	2.7323E-05	-2.735	-7.6730E-06	-5.2283E-03	-2.6807E-07
2024	5.4307E-02	3.2377E-05	-2.662	-7.4681E-06	-6.7133E-03	-3.2368E-07
2025	6.5760E-02	3.8430E-05	-2.570	-7.2682E-06	-8.1978E-03	-3.7483E-07
2026	7.2943E-02	4.5443E-05	-2.459	-7.0730E-06	-9.6764E-03	-4.2095E-07
2027	7.5133E-02	5.3388E-05	-2.331	-6.8819E-06	-1.1140E-02	-4.6171E-07
2028	7.1635E-02	6.2240E-05	-2.184	-6.6942E-06	-1.2583E-02	-4.9689E-07
2029	6.1775E-02	7.1978E-05	-2.020	-6.5093E-06	-1.4005E-02	-5.2613E-07
2030	4.4906E-02	8.2586E-05	-1.839	-6.3266E-06	-1.5397E-02	-5.4955E-07
2031	2.0432E-02	9.4047E-05	-1.641	-6.1460E-06	-1.6745E-02	-5.6657E-07
2032	-1.2210E-02	1.0635E-04	-1.427	-5.9667E-06	-1.8071E-02	-5.7822E-07
2033	-5.3526E-02	1.1948E-04	-1.196	-5.7894E-06	-1.9303E-02	-5.8146E-07
2034	-0.1039	1.3342E-04	-0.9506	-5.6114E-06	-2.0554E-02	-5.8395E-07
2035	-0.1634	1.4816E-04	-0.6916	-5.4393E-06	-2.1376E-02	-5.6632E-07

2036	-0.2307	1.6368E-04	-0.4246	-5.2553E-06	-2.1956E-02	-5.7785E-07
2037	-0.3418	1.8974E-04	-7.7565E-03	-5.0150E-06	-1.9053E-02	-4.4917E-07
2087	0.000	0.000	0.000	-4.4826E-06	1.1953E-02	1.0687E-06
3001	8.8867E-02	-1.5737E-08	-7.4738E-03	5.2219E-09	2.2264E-02	1.8653E-10
3002	9.8782E-02	-2.7964E-08	-0.4255	2.1629E-08	2.1544E-02	3.4843E-10
3003	0.1034	-2.9820E-08	-0.6784	2.4862E-08	2.0601E-02	4.0097E-10
3004	0.1070	-2.9468E-08	-0.9197	2.5468E-08	1.9597E-02	4.3329E-10
3005	0.1098	-2.8726E-08	-1.149	2.5709E-08	1.8551E-02	4.6475E-10
3006	0.1117	-2.7843E-08	-1.365	2.5891E-08	1.7470E-02	4.9904E-10
3007	0.1130	-2.6895E-08	-1.568	2.6103E-08	1.6356E-02	5.3836E-10
3008	0.1136	-2.5876E-08	-1.757	2.6336E-08	1.5213E-02	5.8380E-10
3009	0.1135	-2.4771E-08	-1.933	2.6569E-08	1.4040E-02	6.3643E-10
3010	0.1130	-2.3612E-08	-2.094	2.6845E-08	1.2839E-02	6.9908E-10
3011	0.1120	-2.2382E-08	-2.241	2.7143E-08	1.1610E-02	7.7349E-10
3012	0.1106	-2.1058E-08	-2.373	2.7441E-08	1.0352E-02	8.6085E-10
3013	0.1089	-1.9672E-08	-2.489	2.7785E-08	9.0664E-03	9.6363E-10
3014	0.1070	-1.8194E-08	-2.590	2.8144E-08	7.7520E-03	1.0781E-09
3015	0.1049	-1.6619E-08	-2.675	2.8524E-08	6.4088E-03	1.1932E-09
3016	0.1027	-1.4936E-08	-2.744	2.8922E-08	5.0365E-03	1.2819E-09
3017	0.1006	-1.3124E-08	-2.796	2.9325E-08	3.6347E-03	1.2985E-09
3018	9.8488E-02	-1.1172E-08	-2.831	2.9735E-08	2.2040E-03	1.1992E-09
3019	9.6584E-02	-9.0461E-09	-2.849	3.0128E-08	7.4572E-04	9.8356E-10
3020	9.4940E-02	-6.8232E-09	-2.849	3.0614E-08	-7.3598E-04	7.1497E-10
3021	9.3647E-02	-4.4284E-09	-2.831	3.1122E-08	-2.2351E-03	4.5867E-10
3022	9.2796E-02	-1.8677E-09	-2.795	3.1679E-08	-3.7452E-03	2.5185E-10
3023	9.2477E-02	8.9324E-10	-2.741	3.2263E-08	-5.2598E-03	9.7815E-11
3024	9.2777E-02	3.8781E-09	-2.669	3.2868E-08	-6.7728E-03	-1.3889E-11
3025	9.3783E-02	7.1077E-09	-2.578	3.3493E-08	-8.2793E-03	-9.5717E-11
3026	9.5579E-02	1.0607E-08	-2.470	3.4130E-08	-9.7743E-03	-1.5780E-10
3027	9.8246E-02	1.4375E-08	-2.344	3.4808E-08	-1.1254E-02	-2.0748E-10
3028	0.1019	1.8467E-08	-2.200	3.5485E-08	-1.2713E-02	-2.4960E-10
3029	0.1065	2.2887E-08	-2.039	3.6181E-08	-1.4147E-02	-2.8756E-10
3030	0.1123	2.7645E-08	-1.861	3.6916E-08	-1.5553E-02	-3.2373E-10
3031	0.1192	3.2796E-08	-1.666	3.7648E-08	-1.6923E-02	-3.5947E-10
3032	0.1273	3.8352E-08	-1.454	3.8396E-08	-1.8253E-02	-3.9595E-10
3033	0.1368	4.4334E-08	-1.228	3.9167E-08	-1.9534E-02	-4.3397E-10
3034	0.1476	5.0847E-08	-0.9857	3.9866E-08	-2.0756E-02	-4.7375E-10
3035	0.1598	5.8152E-08	-0.7296	4.0204E-08	-2.1904E-02	-5.1506E-10
3036	0.1736	6.7821E-08	-0.4602	3.8260E-08	-2.2949E-02	-5.5614E-10
3037	0.1988	9.3757E-08	-1.4591E-02	2.3491E-08	-2.3732E-02	-6.0826E-10
4001	8.8867E-02	-1.5737E-08	-7.4739E-03	5.2224E-09	2.2264E-02	1.8208E-10
4002	9.8782E-02	-1.8129E-09	-0.4255	-1.1049E-08	2.1544E-02	1.8478E-11
4003	0.1034	1.3561E-09	-0.6784	-1.4095E-08	2.0601E-02	-3.7267E-11
4004	0.1070	2.4852E-09	-0.9197	-1.4460E-08	1.9597E-02	-7.3897E-11
4005	0.1098	3.3838E-09	-1.149	-1.4415E-08	1.8551E-02	-1.1093E-10
4006	0.1117	4.2898E-09	-1.365	-1.4262E-08	1.7470E-02	-1.5214E-10
4007	0.1130	5.2733E-09	-1.568	-1.4094E-08	1.6356E-02	-1.9980E-10
4008	0.1136	6.3234E-09	-1.757	-1.3900E-08	1.5213E-02	-2.5509E-10
4009	0.1135	7.4225E-09	-1.933	-1.3659E-08	1.4040E-02	-3.1916E-10
4010	0.1130	8.6063E-09	-2.094	-1.3415E-08	1.2839E-02	-3.9491E-10
4011	0.1120	9.8608E-09	-2.241	-1.3147E-08	1.1610E-02	-4.8418E-10
4012	0.1106	1.1170E-08	-2.373	-1.2832E-08	1.0352E-02	-5.8819E-10
4013	0.1089	1.2578E-08	-2.489	-1.2515E-08	9.0664E-03	-7.0950E-10
4014	0.1070	1.4066E-08	-2.590	-1.2167E-08	7.7520E-03	-8.4443E-10
4015	0.1049	1.5646E-08	-2.675	-1.1793E-08	6.4088E-03	-9.8203E-10
4016	0.1027	1.7326E-08	-2.744	-1.1390E-08	5.0365E-03	-1.0952E-09
4017	0.1006	1.9106E-08	-2.796	-1.0946E-08	3.6347E-03	-1.1384E-09
4018	9.8488E-02	2.1000E-08	-2.831	-1.0461E-08	2.2040E-03	-1.0681E-09
4019	9.6584E-02	2.3001E-08	-2.849	-9.9113E-09	7.4572E-04	-8.8368E-10
4020	9.4940E-02	2.5213E-08	-2.849	-9.4096E-09	-7.3598E-04	-6.4885E-10
4021	9.3647E-02	2.7592E-08	-2.831	-8.8818E-09	-2.2351E-03	-4.2897E-10
4022	9.2796E-02	3.0177E-08	-2.795	-8.3557E-09	-3.7452E-03	-2.6144E-10
4023	9.2477E-02	3.2969E-08	-2.741	-7.8097E-09	-5.2598E-03	-1.4976E-10
4024	9.2777E-02	3.5979E-08	-2.669	-7.2372E-09	-6.7728E-03	-8.3730E-11
4025	9.3783E-02	3.9227E-08	-2.578	-6.6361E-09	-8.2793E-03	-5.1149E-11
4026	9.5579E-02	4.2727E-08	-2.470	-5.9996E-09	-9.7743E-03	-4.2172E-11
4027	9.8246E-02	4.6522E-08	-2.344	-5.3567E-09	-1.1254E-02	-4.9738E-11
4028	0.1019	5.0600E-08	-2.200	-4.6630E-09	-1.2713E-02	-6.9339E-11
4029	0.1065	5.5000E-08	-2.039	-3.9411E-09	-1.4147E-02	-9.7871E-11
4030	0.1123	5.9760E-08	-1.861	-3.2099E-09	-1.5553E-02	-1.3330E-10
4031	0.1192	6.4871E-08	-1.666	-2.4270E-09	-1.6923E-02	-1.7458E-10
4032	0.1273	7.0372E-08	-1.454	-1.6112E-09	-1.8253E-02	-2.2086E-10
4033	0.1368	7.6297E-08	-1.228	-7.6896E-10	-1.9534E-02	-2.7162E-10
4034	0.1476	8.2597E-08	-0.9857	1.9456E-10	-2.0756E-02	-3.2694E-10
4035	0.1598	8.9069E-08	-0.7296	1.5736E-09	-2.1904E-02	-3.8750E-10
4036	0.1736	9.4178E-08	-0.4602	5.3275E-09	-2.2949E-02	-4.5686E-10
4037	0.1988	9.3756E-08	-1.4591E-02	2.3492E-08	-2.3732E-02	-6.0400E-10
5002	5.1412E-02	-3.2622E-09	-0.4249	5.2898E-09	2.1544E-02	1.8346E-10
5003	5.5105E-02	-1.6285E-09	-0.6780	5.3833E-09	2.0601E-02	1.8185E-10
5004	5.8452E-02	1.3456E-10	-0.9192	5.5036E-09	1.9597E-02	1.7969E-10
5005	6.1476E-02	2.0225E-09	-1.148	5.6474E-09	1.8551E-02	1.7691E-10
5006	6.4216E-02	4.0339E-09	-1.364	5.8144E-09	1.7470E-02	1.7345E-10

5007	6.6712E-02	6.1689E-09	-1.567	6.0046E-09	1.6356E-02	1.6928E-10
5008	6.9007E-02	8.4286E-09	-1.757	6.2180E-09	1.5213E-02	1.6436E-10
5009	7.1144E-02	1.0813E-08	-1.933	6.4547E-09	1.4040E-02	1.5863E-10
5010	7.3166E-02	1.3324E-08	-2.094	6.7147E-09	1.2839E-02	1.5208E-10
5011	7.5121E-02	1.5962E-08	-2.241	6.9981E-09	1.1610E-02	1.4466E-10
5012	7.7054E-02	1.8730E-08	-2.372	7.3048E-09	1.0352E-02	1.3633E-10
5013	7.9014E-02	2.1628E-08	-2.489	7.6350E-09	9.0664E-03	1.2706E-10
5014	8.1046E-02	2.4659E-08	-2.590	7.9885E-09	7.7520E-03	1.1683E-10
5015	8.3201E-02	2.7825E-08	-2.675	8.3655E-09	6.4088E-03	1.0560E-10
5016	8.5528E-02	3.1129E-08	-2.744	8.7660E-09	5.0365E-03	9.3337E-11
5017	8.8073E-02	3.4574E-08	-2.796	9.1899E-09	3.6347E-03	8.0008E-11
5018	9.0885E-02	3.8160E-08	-2.831	9.6373E-09	2.2040E-03	6.5563E-11
5019	9.4008E-02	4.1891E-08	-2.849	1.0108E-08	7.4572E-04	4.9938E-11
5020	9.7479E-02	4.5769E-08	-2.849	1.0602E-08	-7.3598E-04	3.3062E-11
5021	0.1013	4.9797E-08	-2.831	1.1120E-08	-2.2351E-03	1.4850E-11
5022	0.1056	5.3978E-08	-2.795	1.1661E-08	-3.7452E-03	-4.7926E-12
5023	0.1103	5.8312E-08	-2.741	1.2227E-08	-5.2598E-03	-2.5973E-11
5024	0.1154	6.2801E-08	-2.669	1.2816E-08	-6.7728E-03	-4.8810E-11
5025	0.1211	6.7448E-08	-2.578	1.3428E-08	-8.2793E-03	-7.3433E-11
5026	0.1273	7.2253E-08	-2.470	1.4065E-08	-9.7743E-03	-9.9984E-11
5027	0.1340	7.7215E-08	-2.344	1.4726E-08	-1.1254E-02	-1.2861E-10
5028	0.1413	8.2337E-08	-2.200	1.5411E-08	-1.2713E-02	-1.5947E-10
5029	0.1492	8.7614E-08	-2.039	1.6120E-08	-1.4147E-02	-1.9272E-10
5030	0.1578	9.3049E-08	-1.860	1.6853E-08	-1.5553E-02	-2.2851E-10
5031	0.1670	9.8639E-08	-1.665	1.7611E-08	-1.6923E-02	-2.6702E-10
5032	0.1770	1.0438E-07	-1.454	1.8393E-08	-1.8253E-02	-3.0840E-10
5033	0.1876	1.1027E-07	-1.227	1.9199E-08	-1.9534E-02	-3.5279E-10
5034	0.1990	1.1632E-07	-0.9852	2.0030E-08	-2.0756E-02	-4.0035E-10
5035	0.2111	1.2252E-07	-0.7290	2.0889E-08	-2.1904E-02	-4.5128E-10
5036	0.2240	1.2890E-07	-0.4596	2.1794E-08	-2.2949E-02	-5.0650E-10
20001	0.000	0.000	0.000	0.000	0.000	1.2099E-06
20002	4.2096E-04	2.0996E-05	-2.8934E-04	-3.3293E-06	2.0890E-04	6.1493E-06
20003	1.3851E-03	4.5197E-05	-6.6819E-04	-1.6716E-06	4.1456E-04	7.2062E-06
20004	2.9771E-03	6.7490E-05	-1.0422E-03	-2.0657E-06	6.1606E-04	7.9817E-06
20005	5.1837E-03	9.2991E-05	-1.4113E-03	-3.7224E-06	8.1325E-04	8.4688E-06
20006	7.9914E-03	1.2434E-04	-1.7754E-03	-5.8208E-06	1.0060E-03	8.6613E-06
20007	1.1386E-02	1.6157E-04	-2.1348E-03	-7.5019E-06	1.1941E-03	8.5529E-06
20008	1.5354E-02	2.0203E-04	-2.4896E-03	-7.8705E-06	1.3775E-03	8.1358E-06
20009	1.9879E-02	2.4025E-04	-2.8402E-03	-5.9934E-06	1.5560E-03	7.4032E-06
20010	2.4947E-02	2.6780E-04	-3.1871E-03	-8.9538E-07	1.7295E-03	6.3481E-06
20011	3.0542E-02	2.7318E-04	-3.5309E-03	8.4400E-06	1.8979E-03	4.9622E-06
20012	3.6648E-02	2.4172E-04	-3.8724E-03	2.3073E-05	2.0611E-03	3.2380E-06
20013	4.3248E-02	1.5538E-04	-4.2125E-03	4.4111E-05	2.2188E-03	1.1675E-06
20014	5.0326E-02	-7.3719E-06	-4.5521E-03	7.2710E-05	2.3711E-03	-1.2581E-06
20015	5.8536E-02	-2.3375E-04	-4.8831E-03	6.9902E-05	2.5339E-03	2.3936E-06
20016	6.7273E-02	-4.4245E-04	-5.2086E-03	6.2188E-05	2.6865E-03	5.5830E-06
20017	7.6505E-02	-6.1866E-04	-5.5282E-03	5.0539E-05	2.8289E-03	8.3067E-06
20018	8.6197E-02	-7.5092E-04	-5.8413E-03	3.5983E-05	2.9610E-03	1.0559E-05
20019	9.6313E-02	-8.3131E-04	-6.1476E-03	1.9605E-05	3.0826E-03	1.2337E-05
20020	0.1068	-8.5565E-04	-6.4471E-03	2.5557E-06	3.1935E-03	1.3633E-05
20021	0.1177	-8.2371E-04	-6.7396E-03	-1.3952E-05	3.2937E-03	1.4444E-05
20022	0.1289	-7.3942E-04	-7.0254E-03	-2.8634E-05	3.3831E-03	1.4765E-05
20023	0.1403	-6.1118E-04	-7.3047E-03	-4.0129E-05	3.4616E-03	1.4589E-05
20024	0.1520	-4.5202E-04	-7.5780E-03	-4.7000E-05	3.5290E-03	1.3913E-05
20025	0.1639	-2.7996E-04	-7.8461E-03	-4.7722E-05	3.5853E-03	1.2729E-05
20026	0.1760	-1.1828E-04	-8.1098E-03	-4.0679E-05	3.6304E-03	1.1034E-05
20027	0.1882	4.2029E-06	-8.3703E-03	-2.4152E-05	3.6641E-03	8.8227E-06
20028	0.2005	5.2703E-05	-8.6290E-03	3.6833E-06	3.6865E-03	6.0900E-06
20029	0.2129	-1.3853E-05	-8.8875E-03	4.4773E-05	3.6974E-03	2.8322E-06
20030	0.2252	-2.0902E-04	-9.1289E-03	6.9592E-05	3.6967E-03	3.6165E-06
20101	0.000	0.000	0.000	0.000	0.000	-1.2099E-06
20102	4.2096E-04	-2.0996E-05	-2.8934E-04	3.3293E-06	2.0890E-04	-6.1493E-06
20103	1.3851E-03	-4.5197E-05	-6.6819E-04	1.6716E-06	4.1456E-04	-7.2061E-06
20104	2.9771E-03	-6.7489E-05	-1.0422E-03	2.0656E-06	6.1606E-04	-7.9816E-06
20105	5.1837E-03	-9.2990E-05	-1.4113E-03	3.7224E-06	8.1325E-04	-8.4686E-06
20106	7.9914E-03	-1.2434E-04	-1.7754E-03	5.8207E-06	1.0060E-03	-8.6611E-06
20107	1.1386E-02	-1.6157E-04	-2.1348E-03	7.5018E-06	1.1941E-03	-8.5526E-06
20108	1.5354E-02	-2.0203E-04	-2.4896E-03	7.8704E-06	1.3775E-03	-8.1354E-06
20109	1.9879E-02	-2.4025E-04	-2.8402E-03	5.9933E-06	1.5560E-03	-7.4028E-06
20110	2.4947E-02	-2.6779E-04	-3.1871E-03	8.9528E-07	1.7295E-03	-6.3476E-06
20111	3.0542E-02	-2.7318E-04	-3.5309E-03	-8.4400E-06	1.8979E-03	-4.9617E-06
20112	3.6648E-02	-2.4172E-04	-3.8724E-03	-2.3073E-05	2.0611E-03	-3.2374E-06
20113	4.3248E-02	-1.5537E-04	-4.2125E-03	-4.4111E-05	2.2188E-03	-1.1669E-06
20114	5.0326E-02	7.3747E-06	-4.5521E-03	-7.2710E-05	2.3711E-03	1.2587E-06
20115	5.8536E-02	2.3376E-04	-4.8831E-03	-6.9902E-05	2.5339E-03	-2.3928E-06
20116	6.7273E-02	4.4245E-04	-5.2086E-03	-6.2188E-05	2.6865E-03	-5.5822E-06
20117	7.6506E-02	6.1866E-04	-5.5282E-03	-5.0539E-05	2.8289E-03	-8.3058E-06
20118	8.6197E-02	7.5092E-04	-5.8413E-03	-3.5982E-05	2.9610E-03	-1.0558E-05
20119	9.6313E-02	8.3131E-04	-6.1476E-03	-1.9605E-05	3.0826E-03	-1.2336E-05
20120	0.1068	8.5565E-04	-6.4471E-03	-2.5556E-06	3.1935E-03	-1.3632E-05
20121	0.1177	8.2371E-04	-6.7396E-03	1.3952E-05	3.2937E-03	-1.4443E-05
20122	0.1289	7.3942E-04	-7.0254E-03	2.8634E-05	3.3831E-03	-1.4764E-05

20123	0.1403	6.1118E-04	-7.3047E-03	4.0129E-05	3.4616E-03	-1.4588E-05
20124	0.1520	4.5202E-04	-7.5780E-03	4.7000E-05	3.5290E-03	-1.3911E-05
20125	0.1639	2.7996E-04	-7.8461E-03	4.7723E-05	3.5853E-03	-1.2728E-05
20126	0.1760	1.1828E-04	-8.1098E-03	4.0679E-05	3.6304E-03	-1.1033E-05
20127	0.1882	-4.2036E-06	-8.3703E-03	2.4152E-05	3.6641E-03	-8.8211E-06
20128	0.2005	-5.2704E-05	-8.6290E-03	-3.6833E-06	3.6865E-03	-6.0884E-06
20129	0.2129	1.3852E-05	-8.8875E-03	-4.4773E-05	3.6974E-03	-2.8305E-06
20130	0.2252	2.0901E-04	-9.1289E-03	-6.9592E-05	3.6967E-03	-3.6148E-06
20201	5.0326E-02	-7.3719E-06	-4.5521E-03	7.2710E-05	2.3711E-03	-1.2581E-06
20202	5.0322E-02	-5.0046E-06	-4.7253E-03	6.9890E-05	2.3634E-03	-1.7651E-06
20203	5.0318E-02	-2.5000E-06	-4.8698E-03	4.2567E-05	2.3552E-03	-1.3643E-06
20204	5.0316E-02	1.3055E-09	-4.9251E-03	1.8948E-09	2.3470E-03	2.6163E-10
20205	5.0318E-02	2.5026E-06	-4.8698E-03	-4.2564E-05	2.3552E-03	1.3649E-06
20206	5.0322E-02	5.0072E-06	-4.7253E-03	-6.9889E-05	2.3634E-03	1.7658E-06
20207	5.0326E-02	7.3747E-06	-4.5521E-03	-7.2710E-05	2.3711E-03	1.2587E-06
20301	0.2129	-1.3853E-05	-8.8875E-03	4.4773E-05	3.6974E-03	2.8322E-06
20302	0.2129	-9.2350E-06	-8.9619E-03	3.8048E-05	3.6974E-03	1.8888E-06
20303	0.2129	-4.6173E-06	-9.0153E-03	2.1484E-05	3.6974E-03	9.4488E-07
20304	0.2129	-2.7292E-10	-9.0345E-03	-1.2544E-09	3.6974E-03	8.1491E-10
20305	0.2129	4.6168E-06	-9.0153E-03	-2.1486E-05	3.6974E-03	-9.4325E-07
20306	0.2129	9.2345E-06	-8.9619E-03	-3.8050E-05	3.6974E-03	-1.8871E-06
20307	0.2129	1.3852E-05	-8.8875E-03	-4.4773E-05	3.6974E-03	-2.8305E-06
30001	0.000	0.000	0.000	0.000	0.000	-1.5424E-06
30002	-5.9051E-04	1.9059E-05	-2.5646E-04	-4.4065E-06	-2.9286E-04	-7.1879E-06
30003	-2.2227E-03	5.4746E-05	-6.4020E-04	-7.3413E-06	-6.2257E-04	-9.3149E-06
30004	-5.0094E-03	1.0194E-04	-1.0150E-03	-1.0826E-05	-9.4242E-04	-1.0940E-05
30005	-8.9150E-03	1.6061E-04	-1.3812E-03	-1.3739E-05	-1.2521E-03	-1.2051E-05
30006	-1.3903E-02	2.2668E-04	-1.7394E-03	-1.4914E-05	-1.5514E-03	-1.2639E-05
30007	-1.9935E-02	2.9182E-04	-2.0903E-03	-1.3139E-05	-1.8400E-03	-1.2690E-05
30008	-2.6974E-02	3.4331E-04	-2.4348E-03	-7.1480E-06	-2.1176E-03	-1.2194E-05
30009	-3.4979E-02	3.6385E-04	-2.7738E-03	4.3739E-06	-2.3840E-03	-1.1138E-05
30010	-4.3910E-02	3.3135E-04	-3.1084E-03	2.2796E-05	-2.6389E-03	-9.5085E-06
30011	-5.3726E-02	2.1878E-04	-3.4400E-03	4.9545E-05	-2.8821E-03	-7.2937E-06
30012	-6.4386E-02	-6.0958E-06	-3.7700E-03	8.6105E-05	-3.1135E-03	-4.4800E-06
30013	-7.5296E-02	-2.9506E-04	-4.0437E-03	9.0050E-05	-3.3229E-03	-8.6082E-06
30014	-8.6898E-02	-5.8630E-04	-4.3120E-03	8.7465E-05	-3.5217E-03	-1.2233E-05
30015	-9.9156E-02	-8.5918E-04	-4.5744E-03	7.9261E-05	-3.7096E-03	-1.5350E-05
30016	-0.1120	-1.0963E-03	-4.8301E-03	6.6400E-05	-3.8866E-03	-1.7955E-05
30017	-0.1255	-1.2836E-03	-5.0787E-03	4.9897E-05	-4.0525E-03	-2.0045E-05
30018	-0.1395	-1.4105E-03	-5.3197E-03	3.0825E-05	-4.2071E-03	-2.1614E-05
30019	-0.1540	-1.4702E-03	-5.5529E-03	1.0314E-05	-4.3503E-03	-2.2658E-05
30020	-0.1690	-1.4599E-03	-5.7782E-03	-1.0440E-05	-4.4820E-03	-2.3173E-05
30021	-0.1844	-1.3808E-03	-5.9957E-03	-3.0171E-05	-4.6021E-03	-2.3153E-05
30022	-0.2002	-1.2388E-03	-6.2055E-03	-4.7545E-05	-4.7105E-03	-2.2592E-05
30023	-0.2163	-1.0440E-03	-6.4082E-03	-6.1149E-05	-4.8071E-03	-2.1485E-05
30024	-0.2327	-8.1191E-04	-6.6041E-03	-6.9484E-05	-4.8917E-03	-1.9827E-05
30025	-0.2494	-5.6299E-04	-6.7942E-03	-7.0966E-05	-4.9643E-03	-1.7612E-05
30026	-0.2664	-3.2329E-04	-6.9794E-03	-6.3909E-05	-5.0248E-03	-1.4833E-05
30027	-0.2835	-1.2478E-04	-7.1609E-03	-4.6521E-05	-5.0731E-03	-1.1487E-05
30028	-0.3007	-5.6852E-06	-7.3402E-03	-1.6896E-05	-5.1090E-03	-7.5679E-06
30029	-0.3181	-1.0895E-05	-7.5191E-03	2.7002E-05	-5.1326E-03	-3.0708E-06
30030	-0.3355	-1.3520E-04	-7.6799E-03	4.4629E-05	-5.1437E-03	-2.9675E-06
30101	0.000	0.000	0.000	0.000	0.000	1.5424E-06
30102	-5.9051E-04	-1.9059E-05	-2.5646E-04	4.4066E-06	-2.9286E-04	7.1879E-06
30103	-2.2227E-03	-5.4746E-05	-6.4020E-04	7.3414E-06	-6.2257E-04	9.3148E-06
30104	-5.0094E-03	-1.0194E-04	-1.0150E-03	1.0826E-05	-9.4242E-04	1.0940E-05
30105	-8.9150E-03	-1.6061E-04	-1.3812E-03	1.3739E-05	-1.2521E-03	1.2051E-05
30106	-1.3903E-02	-2.2668E-04	-1.7394E-03	1.4915E-05	-1.5514E-03	1.2639E-05
30107	-1.9935E-02	-2.9182E-04	-2.0903E-03	1.3139E-05	-1.8400E-03	1.2690E-05
30108	-2.6974E-02	-3.4331E-04	-2.4348E-03	7.1482E-06	-2.1176E-03	1.2194E-05
30109	-3.4979E-02	-3.6385E-04	-2.7738E-03	-4.3738E-06	-2.3840E-03	1.1137E-05
30110	-4.3910E-02	-3.3136E-04	-3.1084E-03	-2.2796E-05	-2.6389E-03	9.5082E-06
30111	-5.3726E-02	-2.1878E-04	-3.4400E-03	-4.9545E-05	-2.8821E-03	7.2934E-06
30112	-6.4386E-02	6.0926E-06	-3.7700E-03	-8.6105E-05	-3.1135E-03	4.4796E-06
30113	-7.5296E-02	2.9506E-04	-4.0437E-03	-9.0050E-05	-3.3229E-03	8.6077E-06
30114	-8.6898E-02	5.8629E-04	-4.3120E-03	-8.7465E-05	-3.5217E-03	1.2232E-05
30115	-9.9156E-02	8.5918E-04	-4.5744E-03	-7.9262E-05	-3.7096E-03	1.5349E-05
30116	-0.1120	1.0963E-03	-4.8301E-03	-6.6401E-05	-3.8866E-03	1.7954E-05
30117	-0.1255	1.2836E-03	-5.0787E-03	-4.9897E-05	-4.0525E-03	2.0044E-05
30118	-0.1395	1.4105E-03	-5.3197E-03	-3.0825E-05	-4.2071E-03	2.1613E-05
30119	-0.1540	1.4702E-03	-5.5529E-03	-1.0314E-05	-4.3503E-03	2.2657E-05
30120	-0.1690	1.4599E-03	-5.7782E-03	1.0440E-05	-4.4820E-03	2.3172E-05
30121	-0.1844	1.3808E-03	-5.9957E-03	3.0170E-05	-4.6021E-03	2.3152E-05
30122	-0.2002	1.2388E-03	-6.2055E-03	4.7545E-05	-4.7105E-03	2.2591E-05
30123	-0.2163	1.0440E-03	-6.4082E-03	6.1149E-05	-4.8071E-03	2.1484E-05
30124	-0.2327	8.1191E-04	-6.6041E-03	6.9484E-05	-4.8917E-03	1.9826E-05
30125	-0.2494	5.6299E-04	-6.7942E-03	7.0966E-05	-4.9643E-03	1.7610E-05
30126	-0.2664	3.2329E-04	-6.9794E-03	6.3909E-05	-5.0248E-03	1.4832E-05
30127	-0.2835	1.2478E-04	-7.1609E-03	4.6521E-05	-5.0731E-03	1.1486E-05
30128	-0.3007	5.6870E-06	-7.3402E-03	1.6896E-05	-5.1090E-03	7.5665E-06
30129	-0.3181	1.0897E-05	-7.5191E-03	-2.7002E-05	-5.1326E-03	3.0693E-06
30130	-0.3355	1.3521E-04	-7.6799E-03	-4.4629E-05	-5.1437E-03	2.9660E-06

30201	-6.4386E-02	-6.0958E-06	-3.7700E-03	8.6105E-05	-3.1135E-03	-4.4800E-06
30202	-6.4395E-02	-4.1348E-06	-3.9811E-03	8.1315E-05	-3.1135E-03	-3.1603E-06
30203	-6.4401E-02	-2.0659E-06	-4.1547E-03	4.9128E-05	-3.1135E-03	-1.6437E-06
30204	-6.4403E-02	-1.6980E-09	-4.2207E-03	2.0515E-09	-3.1135E-03	-2.5810E-10
30205	-6.4401E-02	2.0627E-06	-4.1547E-03	-4.9128E-05	-3.1135E-03	1.6433E-06
30206	-6.4397E-02	3.3315E-06	-4.0579E-03	-7.1595E-05	-3.1135E-03	2.5888E-06
30207	-6.4386E-02	6.0926E-06	-3.7700E-03	-8.6105E-05	-3.1135E-03	4.4796E-06
30301	-0.3181	-1.0895E-05	-7.5191E-03	2.7002E-05	-5.1326E-03	-3.0708E-06
30302	-0.3181	-7.2629E-06	-7.5676E-03	2.6201E-05	-5.1326E-03	-2.0479E-06
30303	-0.3181	-3.6308E-06	-7.6053E-03	1.5560E-05	-5.1326E-03	-1.0244E-06
30304	-0.3181	1.1273E-09	-7.6194E-03	-9.1735E-10	-5.1326E-03	-7.1094E-10
30305	-0.3181	3.6330E-06	-7.6053E-03	-1.5562E-05	-5.1326E-03	1.0230E-06
30306	-0.3181	7.2652E-06	-7.5676E-03	-2.6202E-05	-5.1326E-03	2.0465E-06
30307	-0.3181	1.0897E-05	-7.5191E-03	-2.7002E-05	-5.1326E-03	3.0693E-06
MAXIMUM	0.2297	1.4702E-03	0.000	9.0050E-05	2.2264E-02	2.3172E-05
AT NODE	2001	30119	981	30013	1	30120
MINIMUM	-0.3418	-1.4702E-03	-2.849	-9.0050E-05	-2.3732E-02	-2.3173E-05
AT NODE	2037	30019	2019	30113	37	30020
TOTAL	9.642	4.1774E-06	-416.0	1.1095E-05	-6.7499E-02	-5.7404E-07

1

Abaqus 6.10-1 Date 26-May-2011 Time 16:15:40
For use at University of Stavanger under license from Dassault Systemes or its subsidiary.

Analaysis of Lysefjord bridge STEP 2
INCREMENT 1
TIME COMPLETED IN
THIS STEP 0.00

S T E P 2 C A L C U L A T I O N O F E I G E N V A L U E S

F O R N A T U R A L F R E Q U E N C I E S

THE LANCZOS EIGENSOLVER IS USED FOR THIS ANALYSIS
Abaqus WILL COMPUTE UNCOUPLED
STRUCTURAL AND ACOUSTIC MODES
NUMBER OF EIGENVALUES 110
HIGHEST FREQUENCY OF INTEREST 1.00000E+18
MAXIMUM NUMBER OF STEPS WITHIN RUN 35
BLOCK SIZE FOR LANCZOS PROCEDURE 7
THE EIGENVECTORS ARE SCALED SO THAT
THE LARGEST DISPLACEMENT ENTRY IN EACH VECTOR
IS UNITY
INITIAL STRESS AND DISPLACEMENT EFFECTS ARE
INCLUDED IN THE STIFFNESS MATRIX

THIS IS A LINEAR PERTURBATION STEP.
ALL LOADS ARE DEFINED AS CHANGE IN LOAD TO THE REFERENCE STATE

LARGE DISPLACEMENT THEORY WILL BE USED

M E M O R Y E S T I M A T E

PROCESS	FLOATING PT OPERATIONS PER ITERATION	MINIMUM MEMORY REQUIRED (MBYTES)	MEMORY TO MINIMIZE I/O (MBYTES)
1	2.44E+006	18	37

NOTE:
(1) SINCE ABAQUS DOES NOT PRE-ALLOCATE MEMORY AND ONLY ALLOCATES MEMORY AS NEEDED DURING THE ANALYSIS, THE MEMORY REQUIREMENT PRINTED HERE CAN ONLY BE VIEWED AS A GENERAL GUIDELINE BASED ON THE BEST KNOWLEDGE AVAILABLE AT THE BEGINNING OF A STEP BEFORE THE SOLUTION PROCESS HAS BEGUN.
(2) THE ESTIMATE IS NORMALLY UPDATED AT THE BEGINNING OF EVERY STEP. IT IS THE MAXIMUM VALUE OF THE ESTIMATE FROM THE CURRENT STEP TO THE LAST STEP OF THE ANALYSIS, WITH UNSYMMETRIC SOLUTION TAKEN INTO ACCOUNT IF APPLICABLE.
(3) SINCE THE ESTIMATE IS BASED ON THE ACTIVE DEGREES OF FREEDOM IN THE FIRST ITERATION OF THE CURRENT STEP, THE MEMORY ESTIMATE MIGHT BE SIGNIFICANTLY DIFFERENT THAN ACTUAL USAGE FOR PROBLEMS WITH SUBSTANTIAL CHANGES IN ACTIVE DEGREES OF FREEDOM BETWEEN STEPS (OR EVEN WITHIN THE SAME STEP). EXAMPLES ARE: PROBLEMS WITH SIGNIFICANT CONTACT CHANGES, PROBLEMS WITH MODEL CHANGE, PROBLEMS WITH BOTH STATIC STEP AND STEADY STATE DYNAMIC PROCEDURES WHERE ACOUSTIC ELEMENTS WILL ONLY BE ACTIVATED IN THE STEADY STATE DYNAMIC STEPS.
(4) FOR MULTI-PROCESS EXECUTION, THE ESTIMATED VALUE OF FLOATING POINT OPERATIONS FOR EACH PROCESS IS BASED ON AN INITIAL SCHEDULING OF OPERATIONS AND MIGHT NOT REFLECT THE ACTUAL FLOATING

POINT OPERATIONS COMPLETED ON EACH PROCESS. OPERATIONS ARE DYNAMICALY BALANCED DURING EXECUTION, SO THE ACTUAL BALANCE OF OPERATIONS BETWEEN PROCESSES IS EXPECTED TO BE BETTER THAN THE ESTIMATE PRINTED HERE.

(5) THE UPPER LIMIT OF MEMORY THAT CAN BE ALLOCATED BY ABAQUS WILL IN GENERAL DEPEND ON THE VALUE OF THE "MEMORY" PARAMETER AND THE AMOUNT OF PHYSICAL MEMORY AVAILABLE ON THE MACHINE. PLEASE SEE THE "ABAQUS ANALYSIS USER'S MANUAL" FOR MORE DETAILS. THE ACTUAL USAGE OF MEMORY AND OF DISK SPACE FOR SCRATCH DATA WILL DEPEND ON THIS UPPER LIMIT AS WELL AS THE MEMORY REQUIRED TO MINIMIZE I/O. IF THE MEMORY UPPER LIMIT IS GREATER THAN THE MEMORY REQUIRED TO MINIMIZE I/O, THEN THE ACTUAL MEMORY USAGE WILL BE CLOSE TO THE ESTIMATED "MEMORY TO MINIMIZE I/O" VALUE, AND THE SCRATCH DISK USAGE WILL BE CLOSE-TO-ZERO; OTHERWISE, THE ACTUAL MEMORY USED WILL BE CLOSE TO THE PREVIOUSLY MENTIONED MEMORY LIMIT, AND THE SCRATCH DISK USAGE WILL BE ROUGHLY PROPORTIONAL TO THE DIFFERENCE BETWEEN THE ESTIMATED "MEMORY TO MINIMIZE I/O" AND THE MEMORY UPPER LIMIT. HOWEVER ACCURATE ESTIMATE OF THE SCRATCH DISK SPACE IS NOT POSSIBLE.

(6) USING "*RESTART, WRITE" CAN GENERATE A LARGE AMOUNT OF DATA WRITTEN IN THE WORK DIRECTORY.

E I G E N V A L U E O U T P U T

MODE NO	EIGENVALUE	FREQUENCY (RAD/TIME)	FREQUENCY (CYCLES/TIME)	GENERALIZED MASS	COMPOSITE MODAL DAMPING
1	0.64582	0.80363	0.12790	1.34328E+06	0.0000
2	1.7997	1.3415	0.21351	1.37956E+06	0.0000
3	3.6521	1.9111	0.30415	7.46303E+05	0.0000
4	6.5644	2.5621	0.40777	1.11456E+06	0.0000
5	7.3748	2.7157	0.43221	1.37513E+06	0.0000
6	10.497	3.2399	0.51565	1.32619E+05	0.0000
7	11.138	3.3374	0.53116	1.37938E+05	0.0000
8	12.833	3.5823	0.57014	1.16536E+05	0.0000
9	13.407	3.6616	0.58276	1.39775E+06	0.0000
10	13.435	3.6654	0.58337	1.23925E+05	0.0000
11	16.872	4.1076	0.65375	1.16603E+06	0.0000
12	21.715	4.6600	0.74166	1.06445E+06	0.0000
13	26.445	5.1425	0.81845	1.54061E+05	0.0000
14	27.009	5.1970	0.82714	1.76394E+05	0.0000
15	28.645	5.3521	0.85182	3.15770E+06	0.0000
16	29.425	5.4245	0.86333	2.14454E+06	0.0000
17	37.258	6.1039	0.97147	1.58722E+05	0.0000
18	37.605	6.1323	0.97599	1.94764E+05	0.0000
19	38.490	6.2040	0.98740	7.44144E+05	0.0000
20	42.639	6.5298	1.0393	1.08759E+06	0.0000
21	52.127	7.2199	1.1491	2.08638E+06	0.0000
22	54.898	7.4093	1.1792	1.57226E+05	0.0000
23	55.651	7.4600	1.1873	1.56880E+05	0.0000
24	55.838	7.4725	1.1893	1.36752E+06	0.0000
25	74.181	8.6128	1.3708	1.84232E+05	0.0000
26	74.587	8.6364	1.3745	1.74510E+05	0.0000
27	87.282	9.3425	1.4869	2.43575E+06	0.0000
28	96.891	9.8433	1.5666	2.32451E+05	0.0000
29	98.214	9.9103	1.5773	1.71453E+05	0.0000
30	98.914	9.9455	1.5829	1.37112E+06	0.0000
31	103.20	10.159	1.6168	6.49174E+05	0.0000
32	124.10	11.140	1.7730	2.58917E+05	0.0000
33	124.79	11.171	1.7779	1.88221E+05	0.0000
34	126.77	11.259	1.7920	7.36930E+05	0.0000
35	133.96	11.574	1.8421	2.07122E+06	0.0000
36	140.56	11.856	1.8869	2.71012E+06	0.0000
37	154.50	12.430	1.9782	1.77753E+05	0.0000
38	154.77	12.440	1.9800	1.79061E+05	0.0000
39	162.71	12.756	2.0301	1.53812E+06	0.0000
40	169.86	13.033	2.0743	1.70564E+06	0.0000
41	182.96	13.526	2.1528	2.01781E+06	0.0000
42	187.09	13.678	2.1769	1.80232E+05	0.0000
43	187.29	13.685	2.1781	1.80954E+05	0.0000
44	222.44	14.915	2.3737	1.79553E+05	0.0000
45	222.60	14.920	2.3745	1.79819E+05	0.0000
46	249.09	15.783	2.5119	2.33872E+06	0.0000
47	256.20	16.006	2.5475	1.27046E+06	0.0000
48	260.39	16.137	2.5682	1.84007E+05	0.0000
49	260.51	16.140	2.5688	1.84190E+05	0.0000
50	284.17	16.857	2.6829	1.13776E+06	0.0000
51	300.71	17.341	2.7599	1.79376E+05	0.0000
52	300.74	17.342	2.7601	1.84832E+05	0.0000
53	303.14	17.411	2.7710	1.21502E+06	0.0000
54	343.15	18.524	2.9482	1.80703E+05	0.0000
55	343.21	18.526	2.9485	1.80748E+05	0.0000
56	383.10	19.573	3.1151	9.09114E+05	0.0000
57	387.42	19.683	3.1326	1.79040E+05	0.0000
58	387.47	19.684	3.1329	1.78917E+05	0.0000
59	397.75	19.944	3.1741	8.09367E+05	0.0000
60	405.38	20.134	3.2045	2.26056E+06	0.0000

61	433.22	20.814	3.3126	1.78783E+05	0.0000
62	433.24	20.815	3.3127	1.78809E+05	0.0000
63	447.51	21.154	3.3668	13.332	0.0000
64	447.51	21.154	3.3668	13.332	0.0000
65	480.20	21.913	3.4876	1.78188E+05	0.0000
66	480.21	21.914	3.4877	1.78232E+05	0.0000
67	498.70	22.332	3.5542	6.09952E+05	0.0000
68	527.94	22.977	3.6569	1.75782E+05	0.0000
69	527.94	22.977	3.6569	1.75853E+05	0.0000
70	551.18	23.477	3.7365	5.90213E+05	0.0000
71	576.08	24.002	3.8200	1.72536E+05	0.0000
72	576.08	24.002	3.8200	1.72473E+05	0.0000
73	584.02	24.167	3.8462	1.22390E+06	0.0000
74	624.23	24.985	3.9764	1.74549E+05	0.0000
75	624.23	24.985	3.9764	1.74488E+05	0.0000
76	647.64	25.449	4.0503	5.22676E+05	0.0000
77	652.55	25.545	4.0656	7.14583E+05	0.0000
78	671.97	25.922	4.1257	1.78236E+05	0.0000
79	671.99	25.923	4.1257	1.78293E+05	0.0000
80	718.91	26.812	4.2673	1.74020E+05	0.0000
81	718.95	26.813	4.2674	1.73897E+05	0.0000
82	754.65	27.471	4.3721	2.89504E+05	0.0000
83	762.26	27.609	4.3941	2.89788E+05	0.0000
84	764.53	27.650	4.4007	1.74386E+05	0.0000
85	764.70	27.653	4.4012	1.70577E+05	0.0000
86	773.82	27.818	4.4273	1.22189E+06	0.0000
87	808.88	28.441	4.5265	1.71491E+05	0.0000
88	808.92	28.442	4.5266	1.71576E+05	0.0000
89	829.95	28.809	4.5851	5.36716E+05	0.0000
90	851.10	29.174	4.6431	1.74745E+05	0.0000
91	851.12	29.174	4.6432	1.74839E+05	0.0000
92	891.00	29.850	4.7507	1.73453E+05	0.0000
93	891.01	29.850	4.7507	1.73480E+05	0.0000
94	906.43	30.107	4.7917	1.45535E+06	0.0000
95	928.24	30.467	4.8490	1.62896E+05	0.0000
96	928.25	30.467	4.8490	1.62933E+05	0.0000
97	962.48	31.024	4.9376	1.51753E+05	0.0000
98	962.48	31.024	4.9376	1.51749E+05	0.0000
99	970.56	31.154	4.9583	23.664	0.0000
100	970.56	31.154	4.9583	23.664	0.0000
101	991.68	31.491	5.0119	58672.	0.0000
102	993.46	31.519	5.0164	1.53194E+05	0.0000
103	993.46	31.519	5.0164	1.53298E+05	0.0000
104	1008.4	31.755	5.0539	1.17749E+05	0.0000
105	1020.9	31.951	5.0851	1.32281E+05	0.0000
106	1020.9	31.951	5.0851	1.32284E+05	0.0000
107	1044.6	32.321	5.1440	1.32455E+05	0.0000
108	1044.6	32.321	5.1440	1.32454E+05	0.0000
109	1049.1	32.390	5.1551	7.25876E+05	0.0000
110	1064.8	32.631	5.1934	87182.	0.0000

P A R T I C I P A T I O N F A C T O R S

MODE NO	X-COMPONENT	Y-COMPONENT	Z-COMPONENT	X-ROTATION	Y-ROTATION	Z-ROTATION
1	-1.04500E-04	1.3212	-2.80900E-06	-71.642	-6.60238E-03	0.84838
2	-4.13485E-02	3.63881E-05	1.54094E-02	-1.57288E-03	-141.88	-1.40823E-02
3	3.53013E-03	-8.97548E-05	1.1463	6.72729E-03	3.0560	-8.15231E-02
4	-1.33061E-02	-1.41472E-04	1.1237	1.00382E-02	1.1045	-0.19957
5	3.28117E-04	3.22889E-02	5.23562E-04	-0.12510	1.76499E-02	198.90
6	-5.33633E-06	1.08609E-06	-1.09526E-04	-1.01516E-04	1.14616E-03	-1.07650E-05
7	-1.64846E-03	1.2377	3.07977E-04	-111.51	-0.10805	110.01
8	-1.22485E-04	1.28237E-06	-3.66479E-05	-8.98373E-05	-1.68716E-02	-1.40944E-04
9	-1.06899E-02	-3.40578E-05	2.07511E-03	1.36212E-03	-68.152	-1.35474E-03
10	4.09405E-04	0.14020	-3.24019E-04	-16.313	5.40786E-02	-205.53
11	4.76238E-03	-1.6435	-4.76201E-04	117.02	0.28680	-292.08
12	1.66329E-02	-1.4072	8.63911E-04	98.356	0.96085	373.31
13	2.37797E-04	2.36177E-06	5.32175E-05	-1.77262E-04	1.11866E-02	-3.17037E-04
14	-6.18190E-02	1.5202	-9.70032E-04	-108.13	-3.5948	-157.35
15	1.0444	7.06913E-03	-7.45676E-02	-0.57487	60.441	-1.2263
16	1.1270	5.90249E-03	0.20900	-0.50211	65.533	-0.99369
17	-1.19919E-04	1.51575E-06	-3.23319E-05	-7.35043E-05	-7.13018E-03	-6.95178E-04
18	8.79557E-03	4.50105E-02	-2.90452E-04	-13.424	0.49982	-146.66
19	-3.24317E-03	-0.24757	-3.88050E-04	0.40066	-0.22174	-20.209
20	2.38374E-04	8.52501E-02	2.34899E-04	7.2038	2.54988E-02	9.5490
21	1.1561	-1.26559E-03	-0.11457	-8.02956E-02	71.924	-0.49815
22	1.62954E-04	-1.32418E-06	-3.95913E-05	4.04548E-05	1.65274E-02	-2.75547E-04
23	-7.71174E-03	-0.24000	5.37221E-04	14.029	-0.64858	16.254
24	-4.94541E-02	7.63597E-05	6.08180E-03	8.98688E-03	40.133	5.87626E-02
25	4.65817E-03	0.16204	-1.07847E-03	-2.4080	0.34228	148.80
26	-1.22936E-04	2.36479E-06	-2.42466E-05	-3.38850E-05	-6.50306E-03	9.15672E-04

27	-5.20400E-03	-0.43253	9.50352E-04	7.3670	-0.45544	-140.92
28	1.02730E-02	0.94904	6.11697E-05	-12.941	0.85632	-121.84
29	3.41718E-05	5.38222E-06	-4.48537E-04	-1.03099E-04	1.12786E-02	-7.51217E-04
30	-7.30359E-03	-2.93957E-04	0.16901	4.88785E-03	-0.45402	-0.11375
31	-1.06924E-02	-1.0220	-2.32807E-04	12.596	-0.97990	68.752
32	4.80082E-04	5.17581E-02	4.35205E-04	-0.91278	1.12068E-02	-80.497
33	1.87621E-05	1.70127E-06	5.42959E-05	-2.15129E-06	-1.49303E-02	7.79182E-05
34	-9.19391E-04	-6.00809E-02	-3.48725E-04	0.53815	-5.89096E-02	64.472
35	-6.44730E-04	-3.71014E-02	-3.70865E-04	0.18647	-1.88452E-02	53.587
36	-2.11289E-04	-1.29148E-02	-3.37357E-05	0.36954	-2.27283E-02	23.729
37	-4.30497E-05	2.55016E-06	-9.34962E-05	4.98880E-05	9.89938E-03	3.19722E-03
38	1.65470E-03	7.83367E-02	-7.53477E-05	-0.73548	0.32132	-5.2842
39	-6.89070E-02	2.68736E-03	6.25900E-03	-3.03246E-02	-39.131	0.18032
40	0.17774	-6.63538E-03	-1.62543E-02	7.10689E-02	23.257	-0.45127
41	2.62577E-05	3.71345E-03	1.17041E-05	-7.11822E-02	-1.44701E-02	-7.2806
42	-1.23737E-04	7.10928E-06	-9.78199E-05	-6.96306E-05	5.28653E-03	-8.03076E-03
43	4.45917E-04	2.10316E-03	1.38541E-04	0.26078	1.08014E-02	-10.101
44	9.33078E-06	-6.11508E-07	2.51698E-04	-3.89576E-06	-3.70994E-02	-9.96024E-04
45	2.28733E-04	-3.04119E-02	-3.01895E-05	0.55260	2.22242E-02	7.15614E-02
46	-0.22860	-1.64953E-03	-6.19671E-02	5.39730E-02	-6.8595	-0.54767
47	-2.84628E-02	-2.04613E-04	0.11884	6.79304E-03	-0.91776	-7.29830E-02
48	1.11434E-04	3.00668E-07	1.49332E-04	7.46089E-06	-6.21181E-02	-3.99788E-04
49	-1.35916E-03	9.51240E-04	-2.12169E-04	0.16036	-4.06679E-02	-4.9902
50	-4.85186E-04	-5.61500E-02	-1.02647E-04	-1.8489	-1.26936E-02	0.98748
51	3.24061E-05	-3.31344E-07	-4.90215E-04	8.48134E-05	9.17636E-02	9.80686E-04
52	2.42177E-04	4.58085E-03	8.28710E-06	-0.31218	7.55636E-03	-0.47127
53	-1.98671E-04	-6.02969E-02	-5.78731E-05	1.6630	-8.43158E-03	0.96399
54	-3.92616E-05	2.52591E-07	-8.16504E-04	7.29208E-06	0.23483	1.28776E-03
55	9.31623E-05	8.57512E-04	9.20791E-06	-0.11336	3.52346E-03	2.9263
56	-5.45979E-04	4.88836E-05	3.31754E-03	-4.86889E-03	-29.034	-6.40881E-02
57	-2.73408E-05	-6.52769E-06	5.48008E-03	2.20927E-04	-0.53016	-2.21766E-03
58	1.80018E-04	-1.15519E-02	-6.27959E-06	0.42039	-6.95672E-03	-0.30617
59	-4.95288E-04	-2.74227E-05	7.33830E-02	2.15364E-04	-13.685	-3.33538E-02
60	-5.11261E-02	-1.28779E-03	1.79053E-02	4.56363E-02	-4.7446	0.49586
61	-1.38029E-05	-1.68826E-06	-1.90395E-03	9.54792E-05	0.33231	7.06862E-05
62	9.19334E-05	-1.67697E-03	-3.15176E-05	9.75720E-02	5.24356E-03	-2.1479
63	-5.08449E-05	-5.46540E-06	-1.13451E-02	3.51013E-04	2.1079	4.19788E-03
64	1.01569E-03	-1.64270E-02	-1.76068E-04	1.0274	2.59823E-02	-12.265
65	8.92979E-06	1.06304E-05	5.62811E-04	-4.46354E-04	-0.22801	5.26690E-04
66	-2.22868E-04	9.05131E-03	6.20620E-06	-0.37481	1.63698E-03	0.39862
67	-8.94049E-05	2.49431E-03	-3.17962E-05	-6.23430E-02	3.43969E-02	2.2754
68	3.01807E-06	-8.29289E-06	-1.03636E-03	3.64996E-04	3.89989E-02	-5.29329E-03
69	1.14357E-04	-2.46129E-03	-9.83527E-06	0.10670	1.16480E-03	-1.7583
70	-2.26480E-03	7.82197E-06	0.14636	-6.82775E-04	0.54747	-9.62904E-03
71	-3.45279E-04	8.96616E-03	9.39106E-07	-0.37237	1.13113E-03	0.47324
72	-9.93700E-06	1.04588E-04	1.76000E-04	-4.34713E-03	0.24177	5.17262E-03
73	6.78511E-04	-1.54655E-02	1.77930E-05	0.41789	6.78418E-03	4.3116
74	2.23286E-04	-3.27671E-03	-1.06892E-05	0.12143	-2.92921E-03	-2.0241
75	9.79669E-06	-1.99686E-05	2.12319E-03	7.28894E-04	0.34752	-1.48202E-02
76	2.38461E-04	-7.40944E-04	4.48098E-03	-7.36505E-02	1.0729	0.32665
77	2.69449E-04	6.39873E-05	7.75083E-02	2.47239E-03	18.256	-7.69774E-02
78	6.56259E-04	-9.94925E-03	-4.18581E-06	0.38992	-1.44282E-02	-1.2703
79	2.19024E-05	-1.16688E-05	3.03942E-03	5.19470E-04	0.58449	-3.95963E-03
80	-1.14221E-03	1.03337E-02	-3.96937E-06	-0.33192	2.60529E-02	3.3439
81	5.67480E-06	8.13186E-06	5.99877E-04	-2.50324E-04	0.26543	2.13720E-03
82	-1.56197E-02	0.10432	-2.68702E-05	-5.7453	9.39374E-02	20.426
83	-0.11982	7.79405E-03	2.51054E-03	-0.17474	-34.280	1.8958
84	5.72296E-03	-5.30234E-02	1.30573E-04	1.3097	-1.2864	-11.614
85	-3.30136E-04	-1.38791E-05	7.46464E-04	3.23483E-04	-2.71759E-02	-2.86290E-03
86	2.67498E-02	-0.14658	2.70866E-04	3.8280	-1.7996	-34.079
87	-2.00442E-04	1.17459E-05	1.74031E-04	-3.40221E-04	0.13312	1.50999E-03
88	-7.21215E-03	1.52975E-02	-8.15820E-05	-0.41361	0.42531	2.6306
89	0.69429	1.57875E-02	9.11643E-03	-0.36793	-44.876	3.6129
90	-4.12368E-06	-7.41191E-06	4.59005E-04	7.94168E-05	2.42677E-02	-3.50692E-03
91	-2.10900E-03	-3.79940E-03	-2.94589E-05	3.90476E-02	0.15668	-1.7006
92	5.05921E-05	2.24197E-05	7.99316E-05	-6.04611E-04	8.11709E-02	1.29011E-03
93	5.90953E-04	4.85965E-03	1.17404E-05	-0.12968	-5.36403E-02	0.28249
94	-1.80991E-04	-2.33809E-03	8.12907E-05	0.30660	-7.88581E-02	1.8124
95	-1.29855E-06	-3.69764E-06	3.38232E-04	-3.49056E-04	1.24834E-02	-7.66309E-03
96	-1.04291E-04	-4.53665E-04	-1.55430E-06	-4.05471E-02	1.65180E-02	-0.89035
97	-2.31557E-05	-7.21089E-05	-4.57845E-05	1.92429E-03	-6.24077E-02	1.73833E-03
98	-1.17209E-04	-3.15445E-03	-3.01506E-06	8.43015E-02	1.93005E-02	7.74895E-02
99	1.56606E-04	1.83016E-06	1.75834E-03	-8.19174E-04	0.51437	-5.75691E-03
100	7.92969E-06	5.43800E-04	-1.66386E-05	-1.1723	1.97562E-02	-7.7006
101	-4.03081E-04	-1.55335E-02	-4.03777E-04	1.7555	-7.38348E-02	6.2454
102	-5.18837E-06	-5.49723E-06	-2.69821E-04	6.54225E-04	-6.49370E-03	1.23235E-02
103	1.88123E-05	-2.37543E-04	2.40635E-05	2.82831E-02	-6.99569E-03	0.54280
104	5.08532E-02	-7.29438E-04	0.25473	2.79400E-02	-6.8964	0.11706
105	3.59444E-05	2.09765E-03	3.37622E-05	-6.74738E-02	-4.67106E-03	-0.26903
106	-6.83962E-06	1.55942E-04	-1.55515E-05	-5.01288E-03	-4.57273E-02	-1.99924E-02
107	2.72537E-06	2.52920E-04	3.28081E-05	-6.71561E-02	8.79795E-03	-0.63927
108	2.57837E-06	1.59801E-05	-1.40207E-04	-4.24720E-03	-4.87235E-03	-4.03707E-02

109	3.02592E-04	3.10620E-02	-3.45984E-04	1.0664	-0.20252	10.458
110	-1.61259E-05	-2.05364E-03	-1.60369E-05	2.79562E-02	-3.84304E-03	7.14490E-02

E F F E C T I V E M A S S

MODE NO	X-COMPONENT	Y-COMPONENT	Z-COMPONENT	X-ROTATION	Y-ROTATION	Z-ROTATION
1	1.46689E-02	2.34481E+06	1.05991E-05	6.89451E+09	58.555	9.66821E+05
2	2358.6	1.82666E-03	327.57	3.4130	2.77712E+10	273.58
3	9.3003	6.01216E-03	9.80726E+05	33.775	6.96988E+06	4959.9
4	197.34	2.23073E-02	1.40731E+06	112.31	1.35965E+06	44393.
5	0.14805	1433.7	0.37695	21520.	428.38	5.44035E+10
6	3.77651E-06	1.56437E-07	1.59090E-03	1.36671E-03	0.17422	1.53687E-05
7	0.37483	2.11309E+05	1.30834E-02	1.71509E+09	1610.4	1.66931E+09
8	1.74833E-03	1.91641E-07	1.56516E-04	9.40531E-04	33.172	2.31502E-03
9	159.73	1.62129E-03	6.0189	2.5934	6.49221E+09	2.5653
10	2.07714E-02	2435.7	1.30107E-02	3.29776E+07	362.42	5.23479E+09
11	26.446	3.14974E+06	0.26442	1.59662E+10	95914.	9.94739E+10
12	294.48	2.10793E+06	0.79444	1.02975E+10	9.82730E+05	1.48344E+11
13	8.71172E-03	8.59342E-07	4.36316E-04	4.84086E-03	19.279	1.54850E-02
14	674.10	4.07666E+05	0.16598	2.06238E+09	2.27941E+06	4.36735E+09
15	3.44445E+06	157.80	17558.	1.04355E+06	1.15355E+10	4.74831E+06
16	2.72378E+06	74.714	93675.	5.40677E+05	9.20991E+09	2.11755E+06
17	2.28253E-03	3.64662E-07	1.65921E-04	8.57557E-04	8.0694	7.67060E-02
18	15.067	394.58	1.64308E-02	3.50980E+07	48657.	4.18950E+09
19	7.8270	45608.	0.11206	1.19458E+05	36588.	3.03898E+08
20	6.17994E-02	7904.2	6.00109E-02	5.64402E+07	707.14	9.91701E+07
21	2.78857E+06	3.3418	27384.	13452.	1.07930E+10	5.17736E+05
22	4.17500E-03	2.75687E-07	2.46447E-04	2.57316E-04	42.947	1.19376E-02
23	9.3298	9036.4	4.52766E-02	3.08744E+07	65992.	4.14453E+07
24	3344.6	7.97374E-03	50.582	110.45	2.20262E+09	4722.1
25	3.9976	4837.6	0.21428	1.06828E+06	21584.	4.07942E+09
26	2.63742E-03	9.75901E-07	1.02594E-04	2.00371E-04	7.3800	0.14632
27	65.964	4.55683E+05	2.1999	1.32195E+08	5.05237E+05	4.83704E+10
28	24.532	2.09361E+05	8.69768E-04	3.89288E+07	1.70453E+05	3.45076E+09
29	2.00208E-04	4.96670E-06	3.44940E-02	1.82245E-03	21.810	9.67555E-02
30	73.139	0.11848	39167.	32.758	2.82636E+05	17742.
31	74.218	6.78117E+05	3.51847E-02	1.03005E+08	6.23345E+05	3.06854E+09
32	5.96748E-02	693.61	4.90397E-02	2.15720E+05	32.518	1.67772E+09
33	6.62567E-05	5.44771E-07	5.54884E-04	8.71096E-07	41.957	1.14273E-03
34	0.62291	2660.1	8.96176E-02	2.13420E+05	2557.4	3.06319E+09
35	0.86096	2851.1	0.28488	72018.	735.58	5.94773E+09
36	0.12099	452.03	3.08438E-03	3.70094E+05	1400.0	1.52599E+09
37	3.29426E-04	1.15598E-06	1.55384E-03	4.42395E-04	17.419	1.8170
38	0.49027	1098.8	1.01658E-03	96859.	18487.	4.99983E+06
39	7303.3	11.108	60.256	1414.4	2.35519E+09	50013.
40	53887.	75.096	450.63	8614.8	9.22531E+08	3.47345E+05
41	1.39121E-03	27.825	2.76409E-04	10224.	422.50	1.06960E+08
42	2.75950E-03	9.10928E-06	1.72460E-03	8.73843E-04	5.0370	11.624
43	3.59813E-02	0.80041	3.47314E-03	12306.	21.112	1.84627E+07
44	1.56325E-05	6.71423E-08	1.13750E-02	2.72506E-06	247.13	0.17813
45	9.40793E-03	166.31	1.63888E-04	54911.	88.815	920.86
46	1.22212E+05	6.3635	8980.5	6812.9	1.10042E+08	7.01493E+05
47	1029.2	5.31900E-02	17942.	58.626	1.07010E+06	6767.1
48	2.28489E-03	1.66344E-08	4.10334E-03	1.02427E-05	710.02	2.94099E-02
49	0.34026	0.16667	8.29143E-03	4736.3	304.63	4.58673E+06
50	0.26783	3587.2	1.19879E-02	3.88947E+06	183.32	1.10945E+06
51	1.88373E-04	1.96934E-08	4.31060E-02	1.29031E-03	1510.4	0.17251
52	1.08404E-02	3.8786	1.26935E-05	18013.	10.554	41050.
53	4.79573E-02	4417.5	4.06946E-03	3.36007E+06	86.378	1.12910E+06
54	2.78549E-04	1.15292E-08	0.12047	9.60880E-06	9964.7	0.29967
55	1.56876E-03	0.13291	1.53249E-05	2322.7	2.2439	1.54777E+06
56	0.27100	2.17243E-03	10.006	21.552	7.66358E+08	3734.0
57	1.33835E-04	7.62903E-06	5.3768	8.73869E-03	50323.	0.88052
58	5.79806E-03	23.876	7.05527E-06	31619.	8.6589	16771.
59	0.19855	6.08647E-04	4358.5	3.75396E-02	1.51575E+08	900.40
60	5908.8	3.7489	724.73	4708.0	5.08877E+07	5.55829E+05
61	3.40618E-05	5.09574E-07	0.64810	1.62984E-03	19743.	8.93298E-04
62	1.51125E-03	0.50285	1.77621E-04	1702.3	4.9163	8.24930E+05
63	3.44669E-08	3.98246E-10	1.71602E-03	1.64268E-06	59.241	2.34946E-04
64	1.37541E-05	3.59769E-03	4.13302E-07	14.073	9.00047E-03	2005.7
65	1.42089E-05	2.01361E-05	5.64421E-02	3.55008E-02	9263.8	4.94298E-02
66	8.85278E-03	14.602	6.86494E-06	25039.	0.47761	28321.
67	4.87549E-03	3.7949	6.16659E-04	2370.7	721.66	3.15801E+06
68	1.60115E-06	1.20889E-05	0.18880	2.34181E-02	267.35	4.9252
69	2.29973E-03	1.0653	1.70107E-05	2001.9	0.23859	5.43700E+05
70	3.0274	3.61111E-05	12643.	0.27515	1.76900E+05	54.724
71	2.05694E-02	13.871	1.52163E-07	23924.	0.22075	38641.
72	1.70306E-05	1.88663E-03	5.34251E-03	3.2593	10081.	4.6147
73	0.56346	292.74	3.87476E-04	2.13729E+05	56.330	2.27525E+07
74	8.70238E-03	1.8741	1.99439E-05	2573.7	1.4977	7.15130E+05

75	1.67465E-05	6.95766E-05	0.78658	9.27032E-02	21073.	38.324
76	2.97213E-02	0.28695	10.495	2835.2	6.01697E+05	55770.
77	5.18807E-02	2.92577E-03	4292.9	4.3681	2.38167E+08	4234.3
78	7.67621E-02	17.643	3.12288E-06	27099.	37.104	2.87608E+05
79	8.55293E-05	2.42767E-05	1.6471	4.81122E-02	60910.	2.7954
80	0.22703	18.583	2.74184E-06	19172.	118.12	1.94580E+06
81	5.60005E-06	1.14993E-05	6.25772E-02	1.08967E-02	12252.	0.79429
82	70.631	3150.6	2.09024E-04	9.55593E+06	2554.6	1.20788E+08
83	4160.3	17.604	1.8265	8848.3	3.40536E+08	1.04149E+06
84	5.7115	490.28	2.97314E-03	2.99121E+05	2.88583E+05	2.35229E+07
85	1.85911E-02	3.28579E-05	9.50467E-02	1.78494E-02	125.98	1.3981
86	874.33	26254.	8.96482E-02	1.79051E+07	3.95719E+06	1.41907E+09
87	6.88997E-03	2.36598E-05	5.19388E-03	1.98501E-02	3039.2	0.39101
88	8.9245	40.151	1.14194E-03	29352.	31036.	1.18736E+06
89	2.58715E+05	133.77	44.606	72657.	1.08089E+09	7.00572E+06
90	2.97150E-06	9.59985E-06	3.68163E-02	1.10212E-03	102.91	2.1491
91	0.77766	2.5239	1.51730E-04	266.58	4291.9	5.05624E+05
92	4.43964E-04	8.71848E-05	1.10820E-03	6.34065E-02	1142.8	0.28869
93	6.05837E-02	4.0969	2.39120E-05	2917.6	499.15	13844.
94	4.76738E-02	7.9559	9.61722E-03	1.36807E+05	9050.2	4.78058E+06
95	2.74679E-07	2.22720E-06	1.86354E-02	1.98472E-02	25.385	9.5657
96	1.77217E-03	3.35336E-02	3.93621E-07	267.87	44.455	1.29160E+05
97	8.13677E-05	7.89068E-04	3.18108E-04	0.56193	591.04	0.45857
98	2.08471E-03	1.5100	1.37949E-06	1078.4	56.528	911.20
99	5.80359E-07	7.92605E-11	7.31622E-05	1.58794E-05	6.2609	7.84258E-04
100	1.48797E-09	6.99779E-06	6.55109E-09	32.521	9.23609E-03	1403.2
101	9.53276E-03	14.157	9.56569E-03	1.80817E+05	319.86	2.28849E+06
102	4.12385E-06	4.62944E-06	1.11530E-02	6.55685E-02	6.4599	23.265
103	5.42522E-05	8.65007E-03	8.87671E-05	122.63	7.5023	45167.
104	304.51	6.26519E-02	7640.7	91.920	5.60023E+06	1613.4
105	1.70907E-04	0.58205	1.50786E-04	602.24	2.8862	9574.0
106	6.18828E-06	3.21686E-03	3.19928E-05	3.3241	276.60	52.873
107	9.83831E-07	8.47293E-03	1.42571E-04	597.36	10.253	54130.
108	8.80556E-07	3.38242E-05	2.60381E-03	2.3893	3.1444	215.87
109	6.64625E-02	700.36	8.68908E-02	8.25496E+05	29771.	7.93918E+07
110	2.26711E-05	0.36768	2.24217E-05	68.137	1.2876	445.06
TOTAL	9.41863E+06	9.68377E+06	2.62337E+06	3.74057E+10	7.40460E+10	3.91149E+11

THE ANALYSIS HAS BEEN COMPLETED

ANALYSIS COMPLETE
WITH 1 WARNING MESSAGES ON THE DAT FILE

JOB TIME SUMMARY
USER TIME (SEC) = 1.4000
SYSTEM TIME (SEC) = 0.20000
TOTAL CPU TIME (SEC) = 1.6000
WALLCLOCK TIME (SEC) = 2

EIGENVALUE OUTPUT												
	EIGENV.	FREQUENCY	T	G. MASS	HS	HA	VS	VA	TS	TA	ID	Cables
	[Hz]	[RAD/TIME]	[s]	[ton]								
1	0,6466	0,80411	7,81	1 343	X						HS-1	
2	1,8011	1,342	4,68	1 379				X			VA-1	
3	3,6414	1,9082	3,29	746			X				VS-1	
4	6,5982	2,5687	2,45	1 112			X				VS-2	
5	7,3872	2,7179	2,31	1 366		X					HA-1	
6	10,492	3,2391	1,94	132								X
7	11,134	3,3368	1,88	138	X						HS-2	
8	12,827	3,5815	1,75	116								X
9	13,42	3,6633	1,72	1 397				X			VA-2	
10	13,431	3,6648	1,71	124		X					HA-2	
11	16,87	4,1073	1,53	1 169		X						
12	21,714	4,6598	1,35	1 065								
13	26,439	5,1419	1,22	154								X
14	27,003	5,1964	1,21	176	X						HS-3	
15	28,728	5,3599	1,17	2 941								
16	29,509	5,4322	1,16	2 277			X				VS-3	
17	37,261	6,1041	1,03	158								X
18	37,611	6,1328	1,02	191		X					HA-3	
19	38,558	6,2095	1,01	789								
20	42,736	6,5373	0,96	1 083					X		TS-1	
21	52,167	7,2227	0,87	2 092			X					
22	54,904	7,4097	0,85	157								X
23	55,653	7,4601	0,84	157	X							
24	55,918	7,4778	0,84	1 366				X			VA-3	
25	74,2	8,6139	0,73	184		X						
26	74,603	8,6373	0,73	174								X
27	87,286	9,3427	0,67	2 434								
28	96,907	9,8441	0,64	232	X							
29	98,231	9,9112	0,63	171								X
30	99,066	9,9532	0,63	1 371			X					
31	103,21	10,159	0,62	645	X							
32	124,11	11,14	0,56	261		X						
33	124,8	11,171	0,56	188								X
34	126,78	11,26	0,56	718						X		
35	134,06	11,578	0,54	2 013						X		
36	140,8	11,866	0,53	2 725						X	TA-1	
37	154,49	12,429	0,51	178								X
38	154,76	12,44	0,51	179								
39	162,68	12,755	0,49	1 630				X				
40	169,31	13,012	0,48	1 719								
41	183,2	13,535	0,46	2 017								
42	187,03	13,676	0,46	180								X
43	187,24	13,683	0,46	181		X						
44	222,32	14,91	0,42	180								X
45	222,48	14,916	0,42	180	X							

46	249,23	15,787	0,40	2 401								
47	256,52	16,016	0,39	1 266			X					
48	260,17	16,13	0,39	184								X
49	260,29	16,133	0,39	184		X						
50	284,63	16,871	0,37	1 140					X		TS-2	
51	300,36	17,331	0,36	180								X
52	300,42	17,332	0,36	183	X							
53	303,48	17,421	0,36	1 211					X			
54	342,66	18,511	0,34	181								X
55	342,72	18,513	0,34	181		X						
56	383,61	19,586	0,32	917				X				
57	386,76	19,666	0,32	179								X
58	386,82	19,668	0,32	179	X							
59	397,74	19,943	0,32	810				X				
60	404,32	20,108	0,31	2 239			X					
61	432,38	20,794	0,30	179								X
62	432,4	20,794	0,30	179		X						
63	451,47	21,248	0,30	0								X
64	451,47	21,248	0,30	0		X						
65	479,16	21,89	0,29	178								X
66	479,17	21,89	0,29	179	X							
67	498,97	22,338	0,28	611						X	TA-2	
68	526,69	22,95	0,27	177								X
69	526,7	22,95	0,27	177		X						
70	551,99	23,494	0,27	598			X					
71	574,62	23,971	0,26	173	X							
72	574,62	23,971	0,26	173								X
73	584,69	24,18	0,26	1 232		X						
74	622,56	24,951	0,25	171		X						
75	622,56	24,951	0,25	171								X
76	646,04	25,417	0,25	525					X		TA-3x	
77	652,54	25,545	0,25	714			X					
78	670,08	25,886	0,24	179	X							
79	670,11	25,886	0,24	179								X
80	716,81	26,773	0,23	174		X						
81	716,85	26,774	0,23	174								X
82	755,74	27,491	0,23	302					X		TS-3	
83	762,27	27,609	0,23	175				X				
84	762,4	27,612	0,23	169	X							
85	762,76	27,618	0,23	293								X
86	773,92	27,819	0,23	1 234								X
87	806,38	28,397	0,22	171								X
88	806,42	28,398	0,22	171		X						
89	827,75	28,771	0,22	549				X				
90	848,4	29,127	0,22	176								X
91	848,42	29,128	0,22	176	X							
92	888,12	29,801	0,21	174								X
93	888,13	29,801	0,21	174		X						
94	904,89	30,081	0,21	1 388					X			
95	925,19	30,417	0,21	165								X

96	925,19	30,417	0,21	165	X							
97	959,27	30,972	0,20	155								X
98	959,27	30,972	0,20	155		X						
99	970,95	31,16	0,20	0								X
100	970,95	31,16	0,20	0		X						
101	990,11	31,466	0,20	152						X	TA-3	
102	990,11	31,466	0,20	152			X					
103	995,46	31,551	0,20	62	X							
104	1010,7	31,792	0,20	121			X					X
105	1017,4	31,896	0,20	139		X						
106	1017,4	31,896	0,20	139								X
107	1041	32,265	0,19	138	X							
108	1041	32,265	0,19	138								X
109	1050,9	32,417	0,19	751	X							
110	1061,1	32,575	0,19	112		X						